The Analysis Of Telomere Maintenance In The Process Of Cataractogenesis

Savneet Kaur Bains

A thesis submitted for the degree of Doctor of Philosophy

Division of Biosciences

Department of Life Sciences

College of Health and Life Sciences

Brunel University

December 2016

Abstract

Telomeres are structures found at the end of chromosomes, involved in protecting the ends from being recognised as DNA damage. In normal somatic cells telomeres shorten as cells replicate due mainly to the end replication problem, however other mechanisms such as the exonucleolytic activity and oxidative stress are involved.

Telomere length regulation can be affected by the activation of the DNA damage response pathway. These are activated when DNA damaging agents are subjected to DNA. One such agent is ionising radiation (IR). IR has shown to affect the length of telomeres adversely, whereby they shorten at more rapid rates. One interesting area of research is the link between radiation and formation of cataracts. Cataracts are basically the opacity of the lens, which is caused by the changes in the lens cells, and is the leading cause of blindness worldwide. Scientists have found that radiation causes early onset of cataracts.

Given that telomere length regulation is effected due to radiation induction and that radiation causes early onset of cataracts, this study was designed to further understand the link between telomeres and cataractogenesis before and after radiation exposure.

To do this Human Lens Epithelial (HLE) cells and Mouse Bone Marrow cells were used. Telomere length was measured in these cells before and after exposure to radiation, to see the changes in telomere length over a period of time. Furthermore, telomerase activity was measured in HLE cells to see if radiation caused a difference in activity. Alongside this, DNA damage response using the H2AX and TIF assay was examined to see if the cells repaired the damage caused by radiation effectively.

Furthermore, telomere length was measured in bone marrow cells from cataract model mice. The telomere length was measured over the course 24 months in this life-time study (24months).

Our study in the HLE cells has shown an increase in telomere length as the cells age both before and after irradiation. Higher doses of radiation were found to increase telomere length more in these cells. Telomerase activity in HLE cells was shown to decrease as the passage increased. The activity was also found to decrease dose dependently. The DNA damage response mechanisms in HLE cells were found to be normal and repair took place effectively for up to 2Gy of radiation exposure. DNA damage foci were found to go back to normal background amounts after 72hours in both H2AX and TIF analysis.

For the Mouse Bone Marrow cells derived from the life-time study two strains of mice were used; *Ercc2* heterozygous mutant and wild-type. The telomere length in both the mutant and wild-type mice was found to decrease over a period of 24months. Telomere length was found to be longer in the wild-type samples when compared to the heterozygous mutant samples. Finally, telomere length in the female samples of the mouse bone marrow was found to be longer than the male, in both the mutant and wild-type samples.

Publications arising from this thesis

Dalke, Claudia., Neff, Frauke., Bains, Savneet Kaur., Bright, Scott., Bowler, Deborah., Reitmer, Peter., Rößler, Ute., Wagner, Florian., Greiter, Matthias., Unger, Kristian., Braselmann, Herbert., Gomolka, Maria., Hornhardt, Sabine., Kempf, Stefan., Garrett, Lillian., Hölter-Koch, Sabine., Wurst, Wolfgang., Rosemann, Michael., Azimzadeh, Omid., Tapio, Soile., Aubele, Michaela., Theis, Fabian., Hoeschen, Chrisoph., Zitzelsberger, Horst., Slijepcevic, Predrag., Kadhim, Munira., Atkinson, Michael., Kulka, Ulrike., Graw, Jochen. '**Lifetime study in mice after acute low-dose ioninsing radiation: effects on cancer formation, lens opacity, and chromosomal integrity**', (Prepared for PLoS Biology)

Bains, Savneet Kaur., Bright, Scott., Bowler, Deborah., Kadhim, Munira., Slijepcevic, Predrag. '**Effects of radiation on telomere maintenance in association with cataracts**', (In Preparation)

CONTENTS

FIGURE CONTENTS

TABLE CONTENTS

Glossary and Abbreviations

ALT: Alternative telomere lengthening pathway.

Bp: Base pair

BSA: Bovine serum albumin

CHAPS: 3-[(3-Cholamidopropyl)dimethylamminio]-1-propanesulfonate

Control: Models that have no knockouts or mutation, therefore functioning as normal also referred to as wild-type.

DAPI: 4', 6-diamidino-2-phenylindole

DDR: DNA damage response

DMEM: dulbecco's modified eagle's medium.

DMSO: dimethylsulfoxide

DNA: Stands for deoxyribonucleic acid and is the heredity material found in eukaryotic organisms.

DNA damage: mutations and strand breaks due to external and internal causative factors also referred to as exogenous and endogenous.

DSB: Double strand break

Endogenous: Internal factors/ inside the organism that cause DNA damage.

Exogenous: External factors/ outside the organism that cause DNA damage.

FISH: Fluorescence *in situ* hybridisation

FITC: fluorescein isothiocyanate

Flow-FISH: flow cytometric FISH

Genome: This is the whole DNA sequence of an organism.

HeLa: Immortal cancer cell line. HeLa is an abbreviation of Henrietta Lacks.

HLE: Human Lens Epithelial Cells.

HR: Homologous Recombination. DNA damage repair using a template strand.

hTERC: Human telomerase RNA component

hTERT: Human telomerase reverse transcriptase

IR: Ionising radiation

Kb: DNA is made up of bases and kb is the abbreviation of kilo bases. These are 1000 bases.

Ligation: Process through which two strands are joined together using a enzyme called Ligase IV.

LY-R: L5178Y mouse radioresistant lymphoma cells

LY-S: L5178Y mouse radiosensitive cells

Mechanism: Refer to pathways.

Model: Is an organism on which experiments are done to see whether or not, certain mutations or knockouts make an effect on its phenotype.

Mutant /Knockout/Knockdown Models: Model of an organism that has been designed without a particular protein or structure in question during experimentation.

NHEJ: Non Homologous End Joining Process of DNA damage repair involving different proteins and direct ligation of the two broken strands.

Pathways: Processes through which particular changes take place, similar to a mechanism.

PBS: phosphate buffered saline

PD: Population doubling

PNA: peptide nucleis acid

Proteins: a complex made up of different Amino Acids

Q-FISH: Quantitative Fluorescence In-Situ Hybridisation is a telomere measurement method usually done on metaphase cells.

IQ-FISH: Interphase quantitative fluorescence in-situ hybridisation. Telomere length measurement method done on interphase cells.

RPM: revolutions per minute

RT: Room temperature

Senescence: This is the process of growing older therefore showing signs of ageing.

SDS: Sodium chloride sodium citric acid

TBS: tris buffered saline

TRAP assay: telomeric repeat amplification protocol

TRF: terminal restriction fragment

TRF1: telomeric repeat binding factor 1

TRF2: telomeric repeat binding factor 2

TWEEN20: polyxyethylene-sorbitan monolaurate

V(D)J: variable (diversity) joining (recombination)

U20S: An ALT positive osteosarcomas cell line

Wild-type: Original strains with no mutations.

Declaration

I hereby certify that the work done and presented in this thesis is entirely the work of the author unless otherwise specified in the text. The thesis has not been previously submitted to this or any other university.

Signed: 

Date: **05/12/2016**

General Introduction

We are exposed to a number of different carcinogenic reagents on a day to day basis, some of which cause damage in our genome (Lodish et al., 2000). Once the damage is induced a network of mechanisms known as the DNA damage response (DDR) is activated (Mondesert et al., 2015). It has become very important over the years to understand this network as it plays a very important role in the cell survival. It involves the detection, signalling and repair of any induced damage (Jackson and Bartek, 2010).

In recent years telomere maintenance has been linked with the DNA damage response process (Slijepcevic, 2006), (Slijepcevic, 2007), (Lydall, 2009), (d'Adda di Fagagna, Teo and Jackson, 2004). Telomeres not only play a role in DNA damage response but in other processes such as ageing (Slijepcevic, 2007) and carcinogenesis (Blasco, 2005). Therefore, it is important to understand the biology and function of these structures and their interplay with DNA damage response.

Telomeres are TTAGGG tandem repeat sequences (Moyzis et al., 1988), (Blackburn, 1991) found at the end of each chromosome, (Muller, 1938) acting as caps that protect chromosome ends from fusing with other chromosome ends (Griffiths et al., 1999), (de Lange, 2005). Furthermore, telomeres serve to prevent recognition of natural DNA ends as pathological DNA double strand breaks (DSBs) by cellular DNA damage response machinery. As normal somatic cells age telomeres become shorter due to the end replication problem (Watson, 1972) (Olovnikov, 1973), which eventually causes cell senescence.

In cancer cells and germ line cells telomere length is maintained. The most common way through which the maintenance takes place is the enzyme telomerase. It consists of two major subunits; hTERT, a catalytic sub-unit and TERC, a RNA component (Kilian et al., 1997), (Feng et al., 1995), (Greider and Blackburn, 1989), (Espejel et al., 2002). Together with some smaller components, they form a reverse transcriptase-like enzyme which synthesises telomeric DNA.

The aim of this dissertation is to assess the role of telomeres in the process of radiation-induced cataractogenesis. The role of telomeres in this process has not been previously assessed even though some indications in the literature exist that support this notion (Babizhavev and Yegorov, 2010), (Sanders et al., 2011). The lens of the eye is one of the most radiosensitive tissues in the body. Cataracts can be induced by acute doses of <2Gy of low-LET (Linear Energy Transfer) IR and <5Gy of protracted radiation (Ainsbury et al., 2009). A cataract is a lens opacity that obstructs the passage of light, therefore causing reduction in vision (Morris, Fraser and Gray, 2007).

In this literature review the biology of telomeres in light of radiation-induced DNA damage response will be described. Furthermore, relevant aspects of radiation-induced cataractogeneis will be covered.

1.1 Telomere Biology and Telomerase

1.1.1 Telomeres

Telomeres are Guanine rich, TTAGGG tandem repeat sequences (Moyzis et al., 1988) found at the end of each chromosome and act as caps to protect chromosome ends. Telomere as a word is derived from the Greek language, meaning end (“telos”) and part (“meros”). Telomeres were first identified by Muller in 1938 (Muller, 1938), where he thought that these ends were genes that the cell could not lose.

Telomeres prevent chromosomal ends from joining or what is referred to as chromosomal fusions. They also stop chromosome ends from being recognised as DNA DSBs. In terms of molecular structure, telomeres comprise of two loops, the T-loop (telomeric loop) and the D-loop (displacement loop) (Greider, 1999). The T-loop folds away the telomere ends and it is the larger of the two loops (Titia de Lange, 2006).

As seen in Figure 1-1 the loops are formed when the single-stranded 3’ overhang at the end of the chromosome folds onto itself forming the T loop. This creates a displacement in DNA structure when the single strand invades DNA double helix resulting in the formation of the smaller D loop (de Lange, 2005). These loops protect the end of the chromosome from being identified as DNA DSBs. Therefore, this molecular structure plays a very important role in the maintenance of genome integrity (Griffiths et al., 1999).

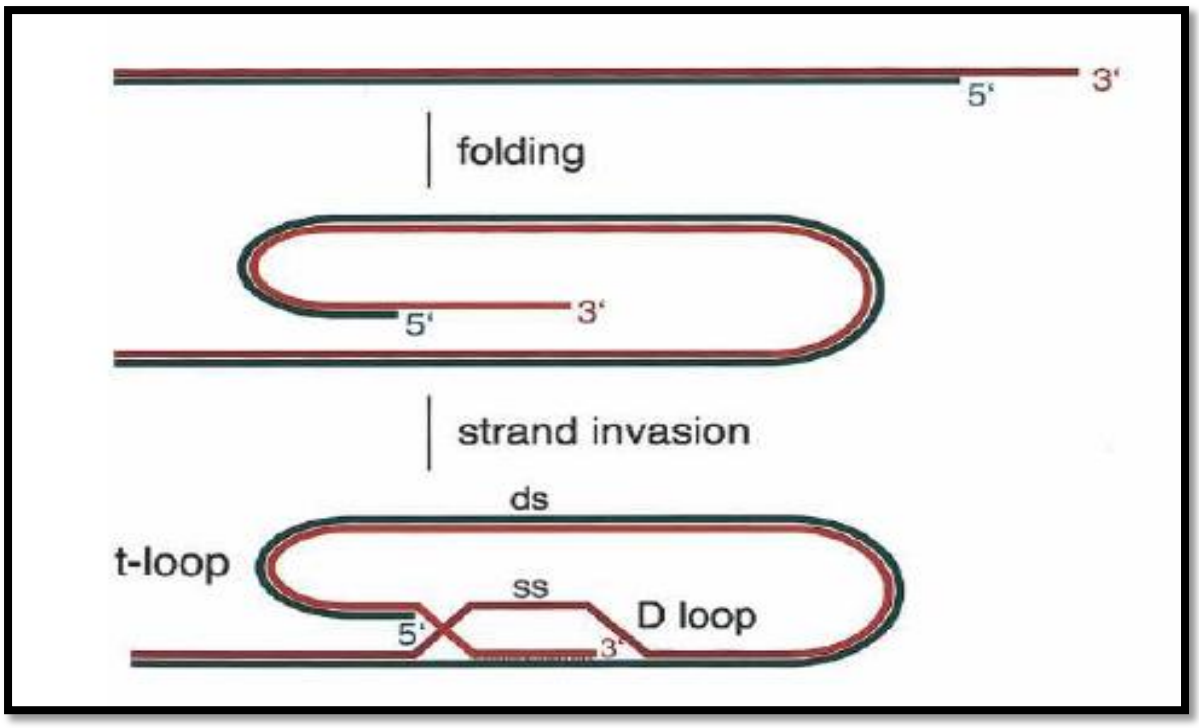

Figure 1-1: Structure of T loop and D loop. This figure shows how the T loop and D loop are formed at the end of chromosomes (telomeres). The telomeric DNA loops back onto itself forming a lariat structure. The 3' G rich strand invades the duplex telomeric repeats, forming a D Loop (displacement loop) (de Lange, 2005).

At the end of each cell cycle, telomere length shortens due to the end replication problem. For DNA to be copied a primer is required by DNA Polymerase to initiate synthesis, therefore when the DNA polymerase gets to the end of the lagging strand from the 5' to 3' end, the end of the 3' end if not copied as the primer is attached here, therefore some bases are lost at this point (Levy et al., 1992) (Lundblad, 1997), this is referred to as the end replication problem (Watson, 1972).

Telomeres range from a length of 2-20kb of double stranded repeats, and can have up to 500 bases of single stranded repeats (Diotti and Loayza, 2011). Human telomeres are found to be around 10kb at birth and shorten progressively with age (de Lange et al., 1990). It was initially thought that telomeres shorten at a rate of 8-

12 base pairs per replication cycle, which is the typical length of an RNA primer (Olovnikov, 1973).

However, later it was shown that telomeres actually shorten at a rate of 50-150 bases per replication (Harley, Futcher and Greider, 1990). This meant that apart from the end replication problem other mechanisms are involved in the shortening of telomeres, oxidative stress and exonucleolytic activity (Makarov, Hirose and Langmore, 1997). This meant that although the 3' end shortened due to the end replication problem the 5' end shortened due to degradation by exonuclease activity (Raymund J Wellinger, 1996) (Makarov, Hirose and Langmore, 1997). This loss takes place to allow the required formation of the t-loop with the 3' overhang of sufficient length (Makarov, Hirose and Langmore, 1997).

Once telomeres shorten it becomes harder for t-loops to form. Thus telomere shortening results in the activation of DNA checkpoint mechanisms (Griffiths et al., 1999) which may further lead to apoptosis, chromosomal fusions or cell cycle arrest (Donate and Blasco, 2011).

For the t-loops and d-loops to form effectively a protein complex known as the Shelterin complex is involved in the maintenance of the molecular telomere structure.

1.1.1.1 *Telomere associated proteins*

The maintenance of the T-loop structure at telomeres is regulated by a set of proteins. In 2005 a protein complex referred to as the Shelterin complex was first proposed (Titia de Lange, 2006). Proteins involved in this complex were discovered over a period of 10 years (de Lange, 2005). The complex protects the telomeres

from fusing with other telomeres, and enables protection against DNA Damage Response (DDR). Shelterin is comprised of six different protein sub-units, POT1, TRF1, TIN2, TPP1, TRF2 and RAP1 these can be seen in Figure 1-2.

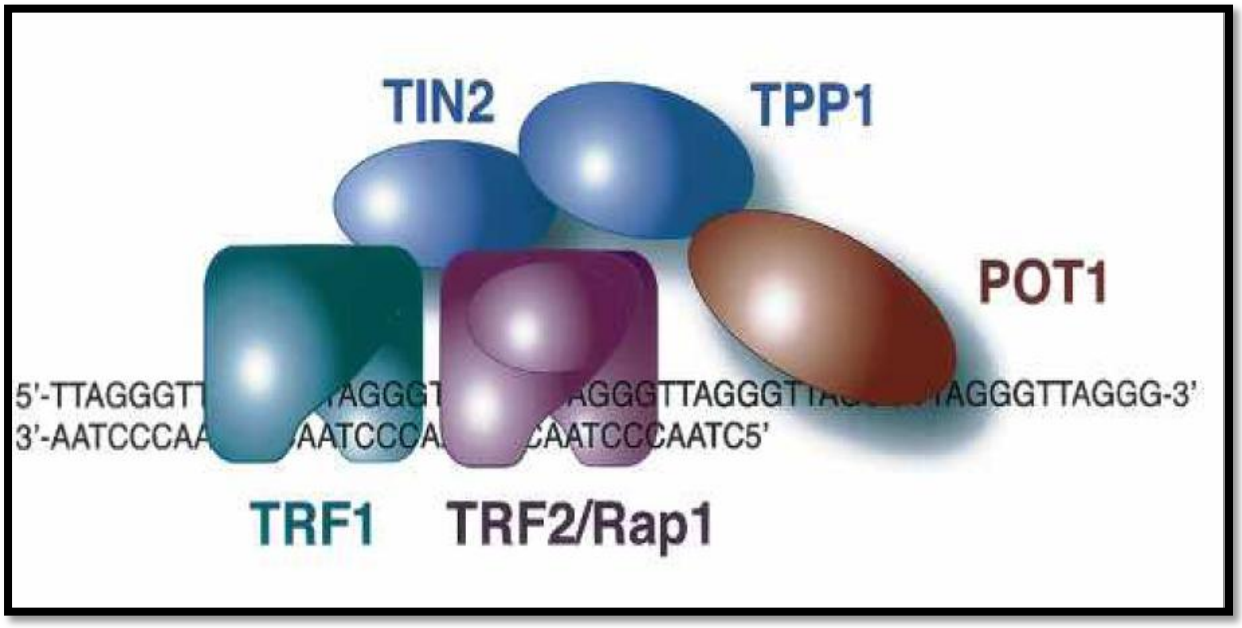

Figure 1-2: Schematic representation of shelterin complex. Figure shows the shelterin complex and all the proteins that it consists of. The figure shows all the links between the telomere strand and the different proteins that are part of the shelterin complex. The TRF1 and TRF2 proteins bind to double stranded DNA while the POT1 protein binds to the single stranded telomeric DNA (de Lange, 2005).

Three subunits directly recognise the telomeric repeat sequence TTAGGG. These are TRF1, TRF2 (Telomere Repeat Factors 1 and 2 respectively) (Broccoli et al., 1997) and POT1 (Protection of Telomere). These three subunits are inter-connected by three other subunits, TIN2 (TRF1 interacting Nuclear Protein 2), TPP1 (tripeptidyl peptidase 1) and RAP1 (Repressor Activator Protein 1) (de Lange, 2005). This complex when put together protects the telomere from being recognised as a DNA DSBs. The collective action of the Shelterin complex stops unwanted DNA repair and also prevents degradation of DNA at the chromosome end.

The six sub-units in Shelterin are linked to each other. TIN2 acts as the link between most of the other protein sub-units. TIN2 recruits the POT1-TPP1 dimer therefore allowing the binding of both POT1 and TPP1 to TRF1 and TRF2 (Frescas and de Lange, 2014) (Sampada and Diego, 2014). TIN2 also links TRF1 and TRF2 (de Lange, 2005).

TRF1 and TRF2 are telomere repeat factors which directly bind to the double stranded telomeric DNA. TRF2 acts as a protection factor for telomeres and is present in 100's of copies per chromosome (de Lange, 2002). TRF2 plays a role in forming the t-loop of the telomere (Griffiths et al., 1999). If TRF2 is silenced in an organism it is noted to cause recognition of telomeres as DNA DSBs (de Lange, 2002) resulting in fused telomeres (van Steensel, Smogorzewska and de Lange, 1998). This then leads to apoptosis through the p53, p21 and Bax pathway (de Lange, 2002).

On the other hand TRF1 is linked to controlling the telomere length (van Steensel and de Lange, 1997) by regulating telomerase. Presence of TRF1 allows telomere shortening to take place and this was shown in tumour-cells HT1080. The results indicated that TRF1 is a suppressor of telomere elongation (van Steensel and de Lange, 1997).

The structures of telomeres have been shown to be influenced by Shelterin to a certain degree (de Lange, 2005). Shelterin is involved in the formation of the t-Loop and how the Shelterin complex is associated to telomeres can clearly be seen in Figure 1-3.

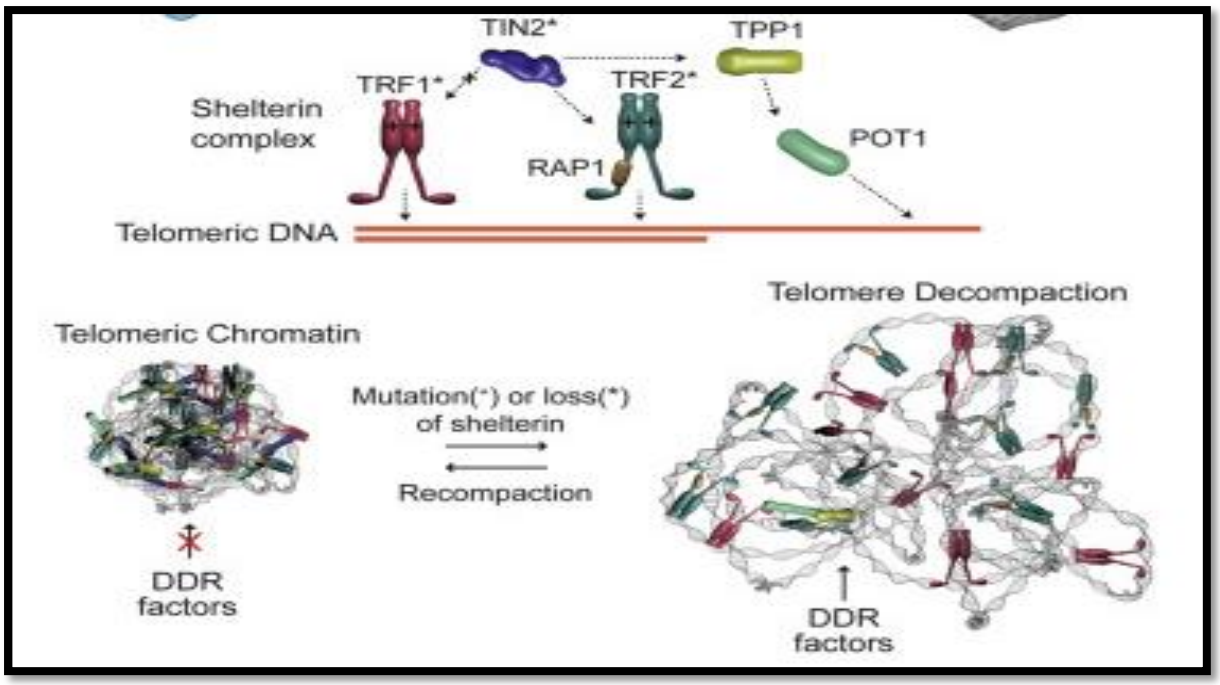

Figure 1-3: Location of shelterin complex at telomere ends. The figure shows in more detail which protein bind to what part of the telomere structure. TRF1 and TRF2 are found at the double stranded telomeric DNA and POT1 is found at the single stranded region of the telomeric DNA. RAP1 is associated with TRF2 while TIN2 binds to both TRF1 and TRF2. TIN2 also binds to TPP1 which binds to POT1. Therefore, TIN2 and TPP1 act as links between the three proteins that are directed binding to the telomeric DNA. The figure also shows how the loss of Shelterin causes the telomere structure to decompact and cause DDR proteins to activate (Bandaria et al., 2016).

It has been seen that the loss of the Shelterin complex causes the loss of the 3' end of the telomere, which further results in activation of the DDR pathway (de Lange, 2005). Shelterin protects telomeres by forming globular structures by remodelling telomeric chromatin. Upon loss of shelterin, telomeres remodel and de-compact up to 10 fold causing DDR proteins to access telomeric end (Bandaria et al., 2016). This is because the t-loop and d-loop structures are lost therefore forming a linear structure, which is recognised as DNA DSB (de Lange, 2002).

Scientists have found that apart from shelterin there are other proteins involved in the maintenance and elongation of telomeres. These include protein called Nbs1

(Nijmegan breakage syndrome 1) and Est1A/SMG6 (de Lange, 2002). The RB-family of proteins have also been found to play a role in telomere maintenance and their loss causes abnormal telomere lengthening (Gonzalo et al., 2005).

Furthermore, research into nucleosomes and how they play a role in the maintenance of genome integrity by interacting with telomeres has been coming to light (Tommerup, Dousmanis and de Lange, 1994). Some studies have suggested as most of the telomeric DNA is packaged in nucleosomes, that the TRF1 proteins bind in the nucleosomal binding sites (Pisano, Galati and Cacchione, 2008).

Given that in most somatic cells telomeres shorten it is important to maintain telomere length in germ line and stem cells, therefore avoiding DDR response in these cells. For this to happen telomeres are maintained using a reverse transcriptase like enzyme, telomerase. This enzyme is absent in somatic cells but is present in both germ-line and stem cells (Wright et al., 1996), (Armanios and Blackburn, 2012). Apart from germ line and stem cells, telomerase is activated in 90% of cancers where it serves to maintain telomere length in the cancer cells, while the other 10% have an Alternative Lengthening Pathway (ALT) activated which is also involved in the elongation of telomeres (Casare and Reddel, 2013).

1.1.2 Telomerase

Telomerase is a specialised reverse transcriptase that synthesis telomeres and was identified in 1985 in Tetrahymena thermophila (Greider and Blackburn, 1985). Telomerase adds telomeric repeats to chromosome ends, using its RNA-based template which is complementary to the TTAGGG sequence (Blackburn, 1991). Telomerase is also referred to as a RNA-dependent DNA polymerase (Cong, Wright and Shay, 2002).

Telomerase is inactive in somatic cells, therefore allowing the end replication problem and exonuclease activity to shorten telomeres, as described in section 1.1.1 of this literature review. However, in stem cells, germ-line cells, lymphocytes and cancer cells (Kim et al., 1994), (Skvortsov et al., 2011) telomerase is active, therefore allowing maintenance of the telomere length in these cells (Cong, Wright and Shay, 2002), (Oeseburg et al., 2010).

The idea of 'telomere healing' was first mentioned by McClintock, where she reported that a broken end does not fuse to other broken ends, therefore calling it a "healed" end (McClintock, 1941). This was shown to take place in young plant embryos shortly after the first zygotic division. She reported that the end is permanently healed, which meant that the "healing" caused a permanent molecular change (Blackburn, 2006). It was later discovered that the telomeres were indeed maintained by some mechanism, in this case telomerase activity (Greider and Blackburn, 1985).

Telomerase comprises of different components hTERT, the catalytic sub-unit (Kilian et al., 1997) and TERC the RNA component (Feng et al., 1995) are considered to be the main subunits which make the telomerase complex. Other than these two components telomerase consists of a number of smaller sub-units. To help telomerase function effectively, there is a telomerase associated protein TEP1. Its function is not very clear, but it has been suggested to play a role in stabilising the telomerase complex (Liu et al., 2000) (Kickhoefer et al., 2001).

Telomerase also has two heat shock proteins, HSP90 and HSP23. The inhibition of HSP90 reduces hTERT expression and decreases telomerase activity (Chiu et al., 2011). Dyskerin is another component in the telomerase complex which binds the

hTERT and TERC subunit, thereby stabilising the telomerase complex (Oeseburg et al., 2010). Dyskerin controls telomerase activity in cancer cells through the regulation of the TERC sub-unit, as it binds to the H/ACA motif of the TERC component, which is involved in the accumulation of TERC (Venteicher et al., 2008).

Dyskerin regulates TERC without effecting hTERT expression. Therefore, when considering the telomerase activity in cancer cells using the expression of hTERT (Montanaro et al., 2008), which is the most commonly used method of calculating telomerase expression this should be taken into consideration.

It should be taken into consideration that the telomerase activity in cancer cells may be lower due to *Dyskerin* even though high levels of *hTERT* are present. Mutations in telomerase genes such as *hTERT*, *TERC* and *Dyskerin* can cause bone marrow failure associated disease known as Dyskeratosis congenita (DC) (Du et al., 2009).

However, from all these telomerase components, two are considered the most important for the enzyme function. hTERT, a catalytic sub-unit which acts as the reverse transcriptase and TERC or TR, a RNA component (Greider and Blackburn, 1989) (Espejel et al., 2002). The RNA subunit which performs as a template for replication, TERC is constantly present in all cells. However, hTERT, the reverse transcriptase and catalytic subunit of telomerase is only present in cells that express telomerase, This suggests that the important component of telomerase is hTERT (Buseman, Wright and Shay, 2012) whereby, introducing *hTERT* to cells lacking telomerase activates telomerase activity in those cells (Shay and Wright, 2011).

When telomere length becomes critically short, the first phase the cells enter is the M1 phase. Here the cell enters telomere-based replicative senescence (Shay and

Wright, 2005). If the cell-cycle checkpoints, pRB/p16 or p53 are inactivated in a cell, then the M1 phase of cellular growth arrest is overcome and the cell enters M2 (crisis stage) (Park et al., 2002). Here, the cells continue to lose telomeres and eventually a wide-spread cell death ensues. Cells that bypass this stage of crisis enter a stage of unlimited proliferation where telomeres are stabilised by fully activated telomerase (Cong, Wright and Shay, 2002).

Therefore, we now know that as a cell continues to divide it reaches what is referred to as the Hayflick limit (Hayflick, 1965), which is usually 50 replications in normal cells. Once this limit is reached the cell enters cellular senescence (Shay and Wright, 2011). However, telomerase activity was found to be present in pre-senescent fibroblast cells. Studies suggested that cells could not enter senescence primarily due to short telomeres, but require something else to trigger senescence (Masutomi et al., 2003). Therefore, it has been suggested that telomere structure and telomerase are regulated together in normal cells and that telomere shortening on its own is unlikely to cause replicative senescence (Masutomi et al., 2003).

Furthermore, when telomerase is not present in a cell the leading strand is usually much longer than the lagging strand. However, when the hTERT is introduced to the cell both the leading and lagging strand are of similar length (Verdun and Karlseder, 2007). As telomeres are crucial in a cell to ensure genomic integrity, experiments, have shown that introduction of telomerase rescues telomere shortening and thus prevents chromosomal fusions (Espejel et al., 2002).

Even in stem cells, although telomerase is present in them, it was found that activity changes in normal stem cells as they age, whereby telomeres shorten however, embryonic stem cells remain constant regardless of age (Shay and Wright, 2011).

Telomerase for many years was the only method of telomere elongation that was known, however in 1995, Roger Reddel's group discovered the Alternative Lengthening Pathway (ALT) (Bryan et al., 1995).

1.1.3 Alternative lengthening of telomeres pathway (ALT)

The Alternative Lengthening of telomeres pathway (ALT) was discovered by Roger Reddel's group in 1995 (Bryan et al., 1995), (Bryan and Reddel, 1997). The same group invented the methodology for accurate measurement of ALT activity (Henson et al., 2009) (Loretta et al., 2012). The ALT pathway is involved in the maintenance and elongation of telomeres in approximately 10% of human cancers. While normal human somatic cells do not normally display detectable ALT activity some studies are showing that ALT and telomerase can coexists (Cerone, Londono-Vallejo and Bacchetti, 2001).

The ALT pathway uses a DNA template to elongate telomeres in comparison to telomerase which uses an RNA template to maintain telomere length (Loretta et al., 2012). For telomeres to be elongated using the ALT pathway, recombination dependent DNA replication is involved. This has been shown conclusively in yeast (McEachern and Haber, 2006), (Grandin and Charbonneau, 2009). Studies have shown that elongation in telomerase-defective yeast depends on the recombination events and the DNA double-strand repair DSB gene *RAD52* (Lundblad and Blackburn, 1993) (McEachern and Haber, 2006). This means that the proteins involved in DNA recombination and repair play a critical role in this pathway. However, there are currently no inhibitors developed for therapeutic use for ALT as there is a lack of knowledge regarding the specific molecules involved in the ALT regulation (Henson et al., 2009).

One of the characteristics of the ALT pathway is the formation of ALT-associated PML bodies (APBs). These are doughnut shaped nuclear structures with ALT specific contents (Henson et al., 2002) including PML (promyelocytic leukaemia) proteins, telomeric DNA, and telomere binding proteins (Yeager et al., 1999). Another marker of ALT cells is the ATRX protein. ATRX is α-thalassemia mental retardation x-linked protein. Experiments done have shown that mutation in ATRX and its binding partner DAXX are involved in the activation of the ALT pathway (Bower et al., 2012) (Lovejoy et al., 2012). ATRX and DAXX have been reported to be involved in the recruitment of histone H3.3 to telomeres (Heaphy et al., 2011). Loss of ATRX/DAXX functions impairs the heterochromatin state at telomeres, possibly due to the reduction in H3.3 incorporation (Heaphy et al., 2011). This results in telomere destabilization and increased HR at telomeres which leads to ALT activation (Heaphy et al., 2011). Loss of ATRX function also results in a DNA damage response and de-repression on telomeric transcription. H3.3 and ATRX/DAXX act in the same pathway to repress ALT (Bower et al., 2012).Experiments were done on telomerase positive and ALT positive cell lines. It was found that the ALT positive cells showed abnormal ATRX (Bower et al., 2012).Many ALT cells lack the G2/M checkpoint therefore continue to proliferate, despite an increased amount of DNA damage both at telomeres and elsewhere in the genome (Lovejoy et al., 2012). ATRX/DAXX may have a role to play in the checkpoint defect as the involvement of chromatin remodelers in the DDR becomes increasingly clear (Lovejoy et al., 2012). Manipulating ATRX/DAXX does not activate the ALT pathway therefore suggesting that a number of other mutations are required for ALT activation (Lovejoy et al., 2012).

In a similar fashion telomeres in humans are elongated by formation of rolling circles, extrachromosomal telomeric repeats and inter-telomeric T-loops, with the presence of homologous recombination (Henson et al., 2002). The telomere length for cells maintained using the ALT pathway can be between 3kb and 50kb with an average length of around 20kb (Murnane et al., 1994), (Bryan et al., 1995), (Henson et al., 2002). The ALT pathway generates unexpectedly large increases in telomere length (Henson et al., 2002). This is because either one of the two mechanisms are used; a linear long telomeric template or a rolling circle (RCA) mechanism (Dunham et al., 2000) (Henson et al., 2002).

In 2009 a marker in ALT positive osteosarcoma patients was detected in their blood (Henson et al., 2009). These markers were named c-circles. They are the telomeric C-strand templates for rolling circle amplification (RCA). A methodology was designed in which the RCA of partially double-stranded C-circles is measured (Bryan et al., 1995), (Bryan and Reddel, 1997). These are now used to detect ALT activity in cells as they show an increase of 1000-folds in ALT positive cells when compared to ALT negative cells (Henson et al., 2009). This therefore becomes the most effective method for detecting ALT activity in mammalian cells.

1.2 DNA Damage response

DNA damage takes place in cells due to a number of different factors. These can be categorised into two sources, endogenous and exogenous. Endogenous sources are ones that cause damage from within the organism such as free radicals. Exogenous ones are sources that cause damage from outside such as ionizing radiation and UV light. The most common type of DNA damage is that which is caused by oxidation, leading to modification of bases in DNA (Evans, 2007).

DDR represents a large network of mechanisms regulated differentially depending on the type of DNA damage or the organism involved. The main focus of this part of the literature review will be DDR due to ionizing radiation.

1.2.1 Radiation

There are a number of different radiation sources that we are exposed to including UV rays (Becker and Wang, 1989), cosmic radiation and even x-rays (Ward, 2000). X-ray radiation is the most common electromagnetic radiation with enough energy to produce ions. It was discovered in 1895 by a German scientist, Wilhelm Conrad Rontgen. Over the course of the years, exposure rates and times have been decreased. This was because scientists noted that high levels of exposure to x-rays caused cellular and molecular damage such as chromosome aberrations and mutations, which eventually led to cell or organismal death (Lodish et al., 2000), (Sansare, Khanna and Karjodkar, 2011).

There are two kinds of radiation sources, IR and non-IR (Slobodan and Peter, 2012). Non-IR does not have enough energy to move an electron from a molecule but has enough to move and/or vibrate atoms. Examples of non-ionizing radiation include UV rays, sound waves, light waves and microwaves. IR, on the other hand, has enough energy to remove electrons from atoms, examples of which include x-rays, gamma rays, alpha and beta rays (Slobodan and Peter, 2012) (Radiation, 2012).

Ionizing radiation usually causes direct or indirect damage to DNA (Desouky, Nan and Zhou, 2015). Direct damage caused by radiation results in the breaking of the DNA backbone, breaking of hydrogen bonds between two bases or damage to bases. In-direct damage is a result of the formation of free radicals therefore causing genomic instability (Kadhim et al., 2013). Radiation directed on water causes water

to lose or gain electrons. Therefore, the water molecule exposed to ionizing radiation will yield following highly reactive radicals: Hydroxyl radical (OH-), hydrogen ion (H+), hydrogen (H^0) or neutral hydroxide (HO^0) (Desouky, Nan and Zhou, 2015). These are highly reactive and harmful free radicals and are harmful as they may cause structural changes in the DNA with a range of consequences (Desouky, Nan and Zhou, 2015).

Direct DNA damage is caused by high charged particles such as alpha and beta particles whereas in-direct damage is caused by low charged particles such as gamma and x-rays. However, low charged particles such as x-rays and gamma rays can also cause direct damage.

Over the course of several decades radiation biologists established the ranges of ionizing radiation dosage depending on health effects in humans or experimental animals as indicated below.

- **Very high** – doses above 15 Gy
- **High** – doses of 5–15 Gy
- **Medium** – doses of 0.5–5 Gy
- **Low** – doses of 0.05–0.5 Gy
- **Very low** – doses below 0.05 Gy

Another parameter that is useful in assessing biological effect of radiation is linear energy transfer or LET. Types of ionizing radiation can be divided into high LET and low LET radiations (Lornax, Folkes and O'Neill, 2013). The high LET particles cannot travel far, as they lose energy as they travel through an object (Lornax, Folkes and O'Neill, 2013). However, low LET particles can penetrate well through objects as

they do not lose as much energy compared to high LET when they travel through an object (Lornax, Folkes and O'Neill, 2013). Figure 1-4 shows how low LET and high LET doses work. Even though they travel differently the dose that is accumulated is the same.

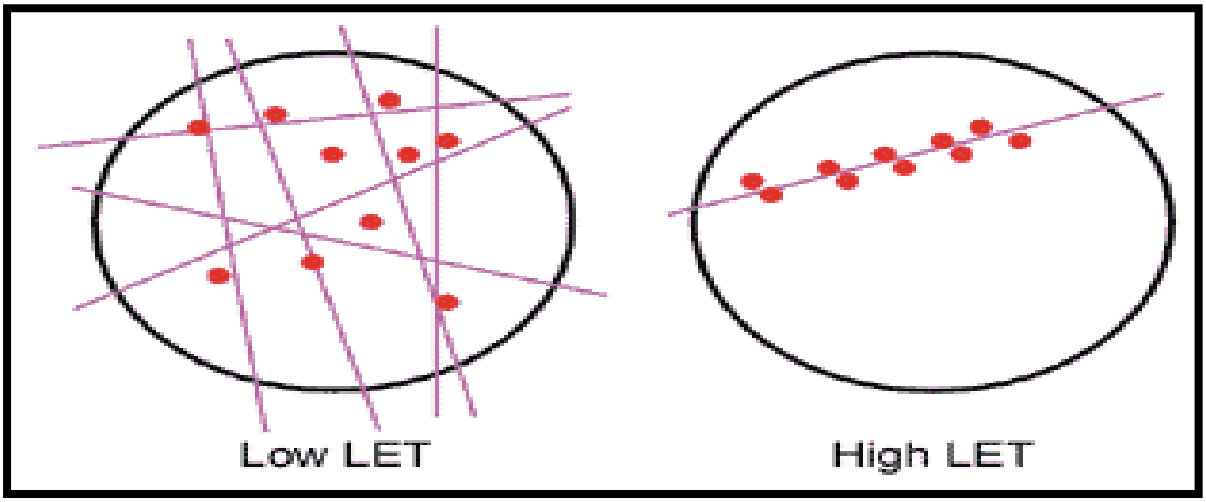

Figure 1-4: Paths of low LET and High LET radiation through a cell. The figure shows how low LET radiation works in comparison to high LET. Low LET radiation works in a more scattered way where as high LET works in a straight line. The figure illustrates that although the two work in a different manner the same total numbers of ionisations are accumulated, therefore presenting the same dose (Radiation, 2007).

According to Health Protection Agency, now Public Health England UK citizens are exposed to an average dose of 0.0027Gy radiation per year, majority of which is from natural background (PHE, 2010). Nuclear factory workers are exposed to up to 0.02Gy of IR. Both these doses fall under the low dose range as suggested by the ICRP (International Commission on Radiological Protection). The ICRP states that low dose radiation is any dose below 0.2Gy, as it is thought that there are no health effects under this dose (Energy, 2012).

For many years radiation biologists have been engaged in investigating the effects of low dose radiation on human health. In recent years, one area that has generated strong interest is how cataracts can be induced by low dose ionizing radiation. Radiation induced cataractogenesis is the main focus of this thesis. Before describing relevant aspects of the processes behind radiation induced cataracts we will first describe mechanisms of radiation-induced DDR.

1.2.2 DNA double strand breaks and detection

The key molecular lesion induced in DNA by ionizing radiation is DSB. As can be seen from Figure 1-5 detection and repair of DNA DSBs is regulated by the ATM (Ataxia telangiectasia mutated) protein pathway. ATM is a signalling molecule targeting a large number of downstream molecules mainly through phosphorylation. It belongs to a group of PIKK (phosphoinositol-3-kinase related kinase) family (Shiloh, 2003). When a DSB occurs ATM autophosphorylates and becomes active. Therefore, it starts to send signals to effector proteins by phosphorylating them, which in turn activate DNA repair proteins, cell cycle arrests proteins and apoptosis. ATM also phosphorylates Artemis in response to IR induced DSBs (Riballo et al., 2004). Artemis is then recruited to these DSB sites where processing takes place before ligation. However, apart from Artemis, damage response proteins such as 53BP1, γ-H2AX and the MRN complex are also phosphorylated and activated by ATM. One of the ATM targets is histone γ-H2AX. The literature review will focus on this histone as it has been used in this thesis to detect DNA DSBs.

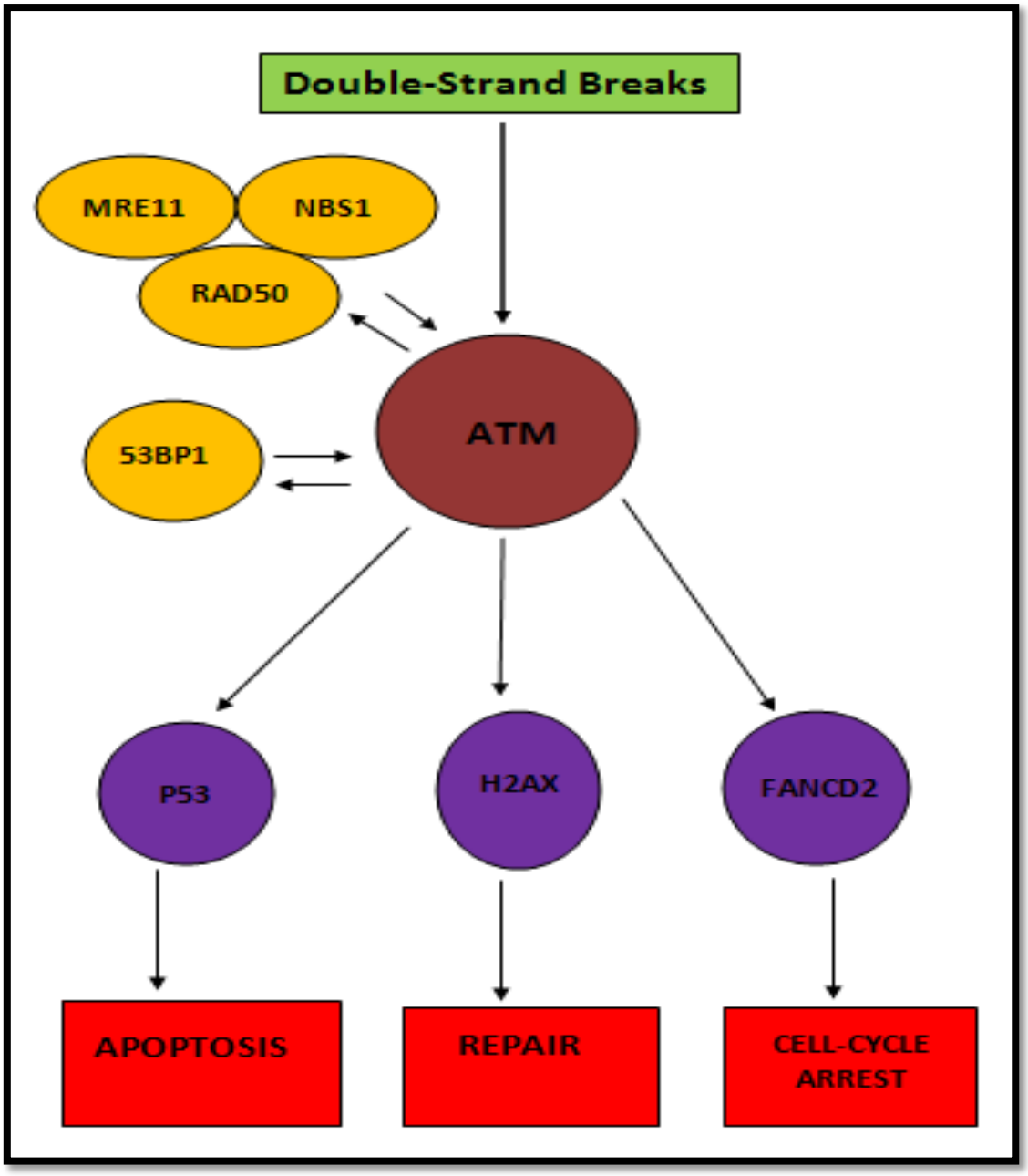

Figure 1-5: Upstream and downstream events after a DSB. The figure shows a schematic image of the upstream and downstream events that take place after a DSB. It can be seen that a number of different pathways can be activated. The outcome of the cell depends on the amount of damage. Therefore, a cell can either repair, undergo apoptosis or enter cell-cycle arrest. Schematic image adapted from (Huen and Chen, 2008) (Jackson and Bartek, 2010).

It is important to be able to detect DNA damage in cells and methods have been developed that allow us to do this. One of the most commonly used DNA damage

markers is an antibody against histone H2AX. This protein gets phosphorylated when DNA is damaged. The phosphorylated form is known as γ-H2AX (Rogakou et al., 1998). The next section will focus on this DNA damage marker. The protocol for detecting γ-H2AX can be adapted to take into account damage at telomeres as well (Taka, Smogorzewska and de Lange, 2003). These are called telomere dysfunction induced foci's (TIFs) (Taka, Smogorzewska and de Lange, 2003).

1.2.2.1 *γ-H2AX*

Chromatin in eukaryotes is formed using nucleosomes, which consist of four histone proteins, H4, H3, H2B and H2A, and 145 base pairs of DNA (Rogakou et al., 1998). The H2A histone protein has three sub-families, one of which is the H2A.X and represents about 2-25% of the H2A histone sub-family. Histones are usually positively charged which allows DNA, which is negatively charged to bind to them tightly.

IR in cells causes the formation of γ components, the most predominant ones being γ-H2AX (Rogakou et al., 1998), which are specifically phosphorylated on residue Serine 139. This can be seen from experiments done by (Celeste et al., 2003), whereby Ser 136 and 139 were mutated and resulted in H2AX not getting phosphorylated, which shows that these sites need to be present for the phosphorylation of H2AX to form γ-H2AX.

The same group of scientists also performed experiments on H2AX double knockout mice to see if H2AX played an important role in the repair pathway. They noted that H2AX was not important for the initial recruiting of the 53BP1 protein but that it was required for the maintenance and steady increase of the 53BP1 protein at DNA damage sites. γ-H2AX therefore, works in the signalling of DSBs and once these are

repaired using the HR or non-homologous repair pathway, γ-H2AX gets de-phosphorylated. However, ATM and H2AX mediated events are early steps in radiation response. They will eventually help activate repair pathways required to repair DNA DSBs.

1.2.3 DSB repair pathways

There are two different strand break repair pathways: non-homologous end-joining (NHEJ) and homologous recombination (HR). During the G1 and G0 phase of the cell cycle NHEJ is pre-dominant it does not require a template strand of DNA to repair the damage. In the S phase and G2 phase of the cell cycle where the sister chromatid is available as a template strand, HR is the dominant repair pathway (Takata et al., 1998).

1.2.3.1 *Non-Homologous End Joining (NHEJ)*

The broken ends are directly ligated together with DNA liagase IV (Pastwa and Blasiak, 2003). From Figure 1-8 it can be seen that the Ku70/80 heterodimer initiates the double strand repair process and that these further recruit DNA-PKcs (Sekiguchi and Ferguson, 2006). Both the Ku heterodimer and DNA-PKcs proteins form a complex named DNA-PK. Artemis is then recruited to the DSB where it cleaves the ends of damaged DNA to prepare for ligation (Davis and Chen, 2013). XRCC4 an x-ray cross-complementing protein 4 bridges the DNA and DNA ligase IV with the help of XLF (Andres et al., 2012). Ligase IV is recruited to the damage where is DSB through a process referred to as ligation (Grawunder et al., 1998).

NHEJ is also part of the immune response and it is used in the process of antibody production (Sekiguchi and Ferguson, 2006). This pathway takes place during the development of B and T lymphocytes (Davis and Chen, 2013).

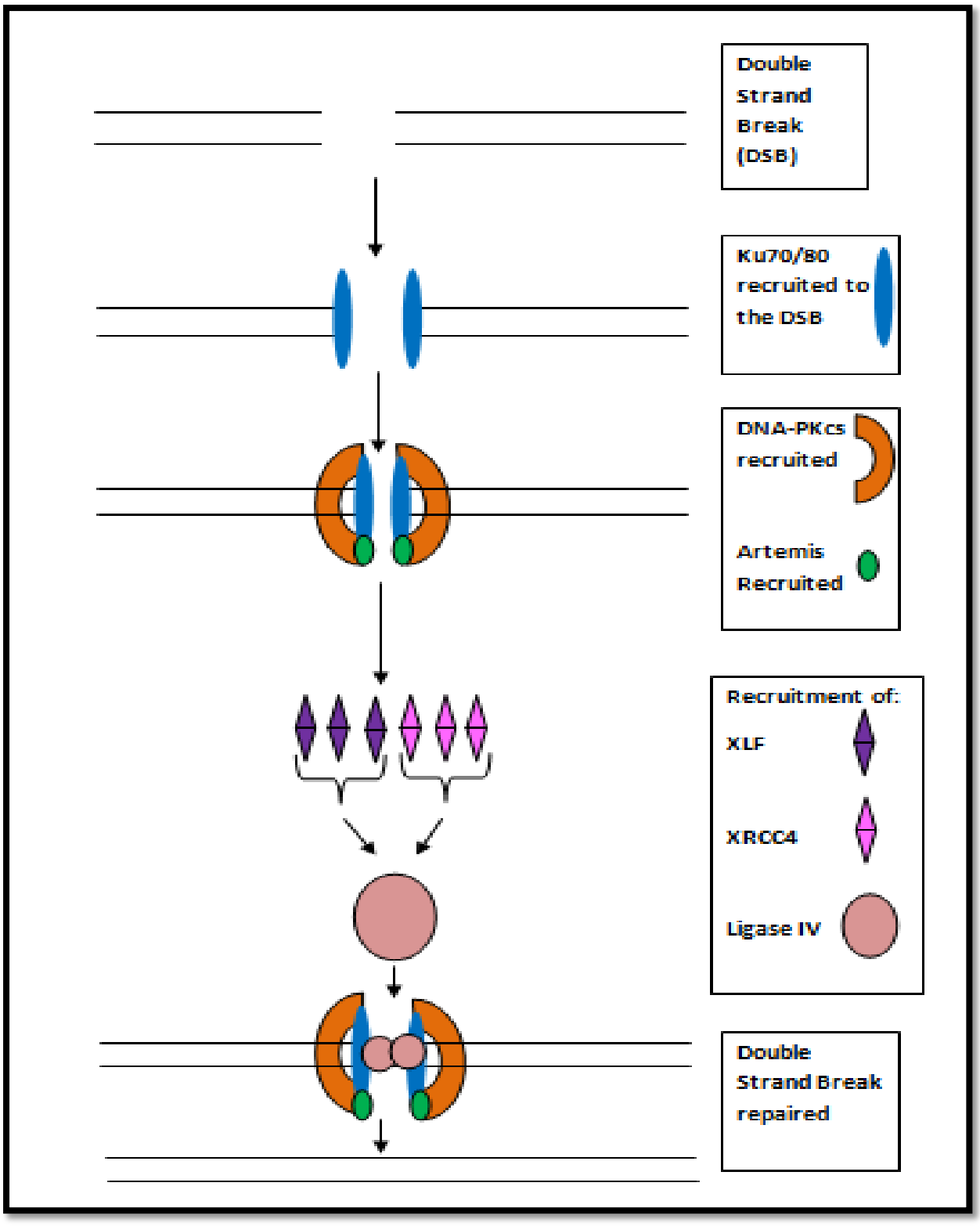

Figure 1-6: Non-Homologous recombination pathway model. The figure shows a schematic image of the NHEJ model of DNA double strand repair. It shows the different protein s involved in the repair process. Schematic image adapted from (Sekiguchi and Ferguson, 2006) (Davis and Chen, 2013).

1.2.3.2 *Homologous recombination (HR)*

The mechanisms behind HR are shown in Figure 1.8. (Pastwa and Blasiak, 2003). When a DSB is detected and the HR pathway is activated, the sections around the 5' end of the DNA are incised and this process is referred to as the re-sectioning process. (Sung and Klein, 2006). Once this is done the overhanging 3' end invades the strand of the sister chromatid of the homologous chromosome for copying to start take place. At this point one of two things can happen, the double-strand break repair pathway or the synthesis-dependent strand annealing pathway (Sung and Klein, 2006). Both these pathways have been illustrated in Figure 1-7.

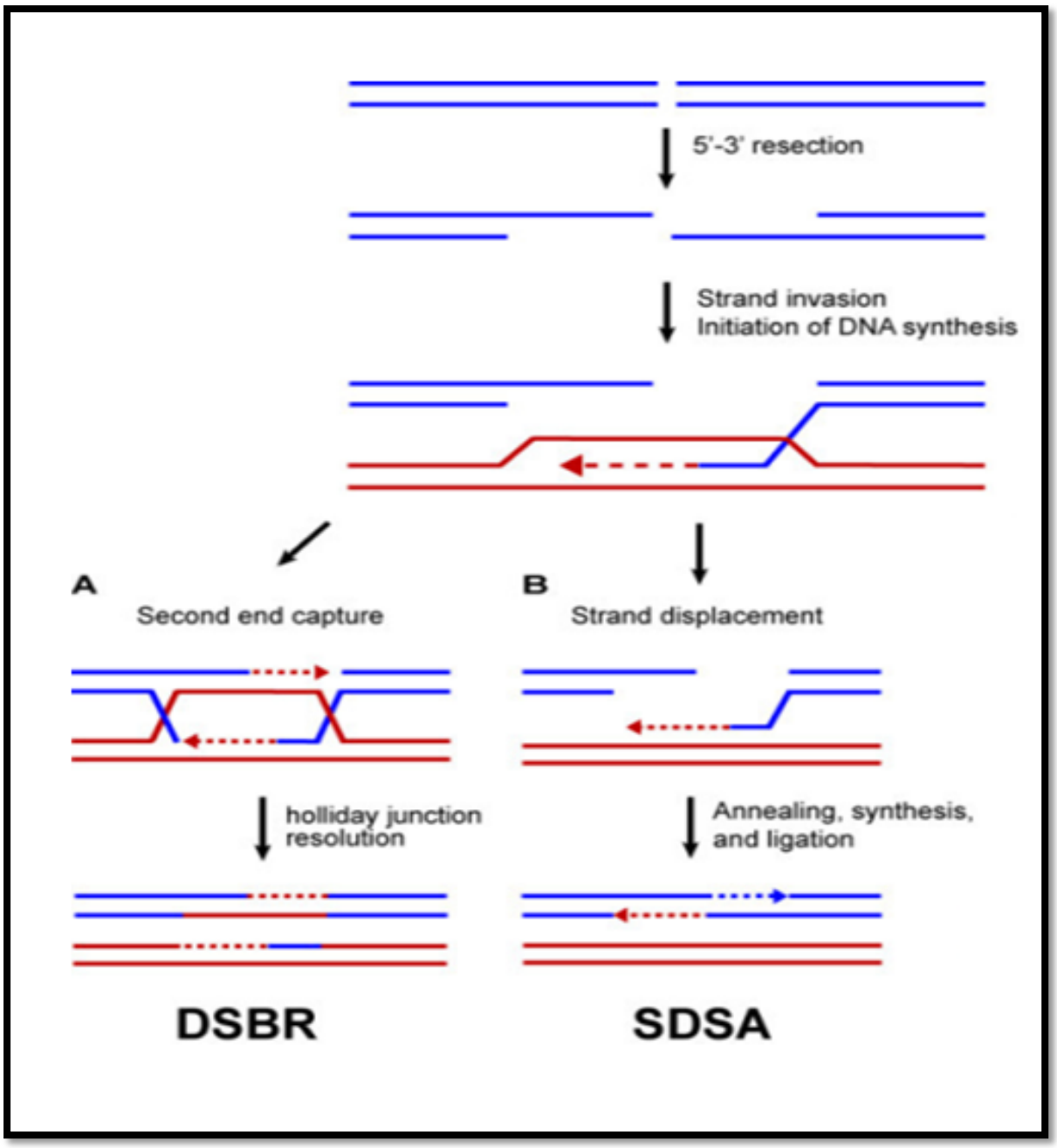

Figure 1-7: Homologous Recombination pathway model, The figure shows the two sub pathways of repair; A) double-strand break repair pathway and B) synthesis-dependent strand annealing pathway. The DSBR pathway causes cross-over whereas the SDSA pathway anneals the strands directly (Barlow and Rothstein, 2010).

The synthesis-dependent strand annealing pathway takes place in meiosis and mitotic cells, the result of this pathway is non-crossover products. This pathway is more dominant in the mitotic pathway (Anderson and Sekelsky, 2010). In this

pathway the 3’ strand is extended by a DNA polymerase. Branch migrations are formed when the 3’ end is extended as it stops between the donor and recipient DNA (Allers and Lichten, 2001). This newly synthesised 3’ end anneals through complementary base pairing with the other 3’ of the damaged chromosome.

For the DSB repair pathway, a Holliday junction is formed with the homologous chromosome being used for repair, therefore forming a double Holliday junction (Krejci et al., 2012). Recombination products are formed from these double Holliday junctions, when single stranded DNA is cut by restriction endonucleases. Depending on how the Holliday junctions are cut, cross-over or non-cross-over products are formed. This pathway is more predominant in meiosis when cross-over takes place (Nelson and Cox, 2004).

For NHEJ a pathway led by Ku proteins is used whereas for HR Rad54 proteins are involved (Takata et al., 1998). To show that the two protein pathways are linked to each other mutant mice were generated (double knock out Rad54 and Ku70). From the analysis done on these mice it was noted that NHEJ was activated during the G1 early phase to S phase, and HR was activated from late S phase to G2 phase of the cell cycle (Takata et al., 1998). The results show that there are more chromosomal aberration in the double mutant mice compared to the single mutants, therefore showing that both pathways play a significant role in double strand repair.

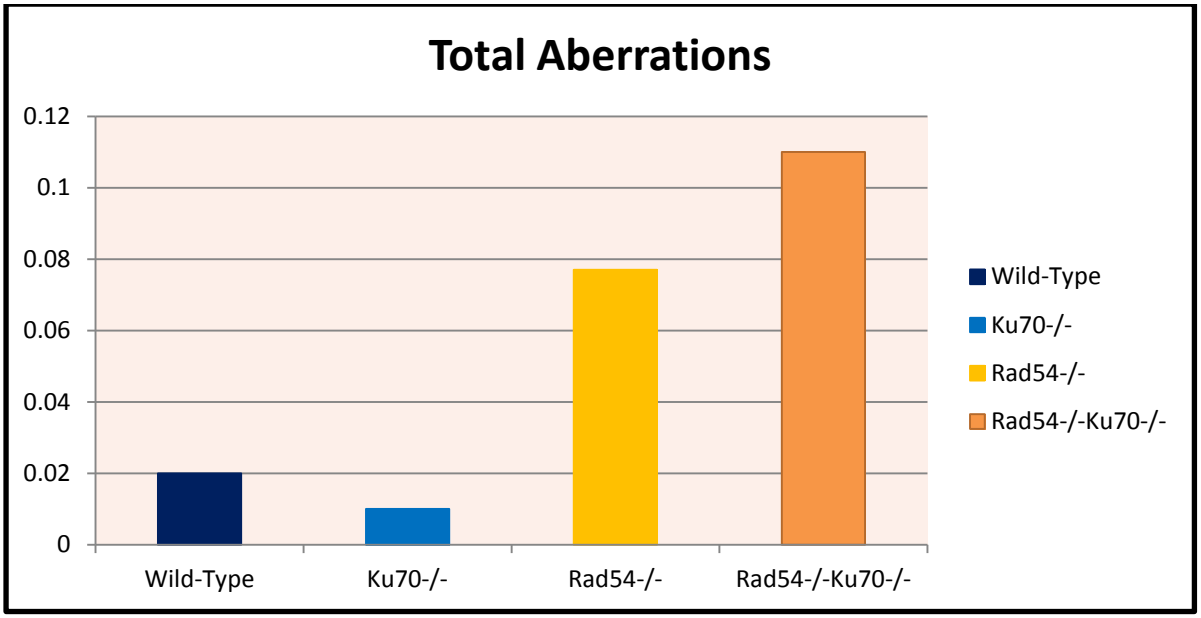

Figure 1-8: Total number of aberrations in mutant and wild-type Ku70/Rad54 models. The figure shows how there are more aberrations in the double knockout KU70/Rad54 model in comparison to the single knock out and wild-type. Data for the graph was extracted from table 1 of (Takata et al., 1998).

From Figure 1-8 it can be seen that the double mutant models have more aberrations compared to the wild-type and Ku mutant models, which clearly shows that the two pathways are very important in maintaining genomic integrity (Takata et al., 1998). It also shows that there is a link between the two as there are fewer aberrations in single mutants compared to the double mutants, this could mean that when one pathway is inactivated the other one kicks in to a certain degree.

Not only have studies been conducted to further understand the proteins involved in DDR but also their association with telomere maintenance has been noted (Lydall, 2009).

1.3 DNA damage response and Telomeres

As discussed in previous sections of this literature review telomeres are DNA sequences protecting chromosome ends from being detected as DNA DSBs. However, as the telomeres become critically short they lose their t-loop and d-loop structures. This exposes their ends, which get recognised as DNA DSBs.

Meta-analysis conducted to understand DDR and the proteins involved showed physiological processing links between the proteins involved in DDR and telomere maintenance. Mouse models designed with knock out or knock down DDR proteins demonstrated changes in telomere structure and/or abnormal chromosomal responses such as chromosomal/telomeric fusions. Some of the main proteins that were experimented included: Ku70/80 (Li et al., 2007), XPF (Zhu et al., 2003) and DNA-PKcs (Espejel et al., 2004). Knock-out models available for these proteins also resulted in mice that were immuno-deficient, aged prematurely and developed cancer. This is because the repair pathways are defective and the dysfunction of the V(D)J recombination pathway results in immunodeficiency. Apart from this, defects in these DDR proteins causes changes to the telomeres. Accelerated telomere shortening, chromosomal end to end fusions, chromosomal aberrations and increased number of TIFs are noted when DDR proteins are defective (Metcalfe et al., 1996), (Samper et al., 2000), (d'Adda di Fagagna, Teo and Jackson, 2004), (Jacobs, 2013)

In humans the deficiency of proteins linked with DDR and telomere maintenance results in immuno-deficiency, aplastic anaemia and changes in highly proliferative tissues (Donate and Blasco, 2011). Diseases linked to loss of these proteins include Dyskeratosis congenital (Shay and Wright, 2004), ataxia telangiectasia (Metcalfe et

al., 1996), Nijmen breakage syndrome (Lijima et al., 2004), Fanconi anemia (Leteurtre et al., 1999), and Xeroderma pigmentosum (Stout and Blasco, 2013), (Slijepcevic, 2007), (O'Sullivan and Karlseder, 2010).

Once telomeres become critically short or after the inhibition of telomere related proteins such as TRF2, ATM becomes phosphorylated. This in turn phosphorylates proteins such as 53BP1, γ-H2AX and the MRN complex (Longhese, 2008). These form TIFs (Takai, Smogorzewska and de Lange, 2003). The activation of the MRN complex at critically short telomeres and at DNA DSBs is illustrated in Figure 1-9. From the figure it can be seen that MRN is one of the first proteins recruited both at DNA DSBs and at critically short telomeres (Lydall, 2009). Apart from the MRN complex, proteins such as the Ku hetero-dimer are also recruited, Figure 1-9.

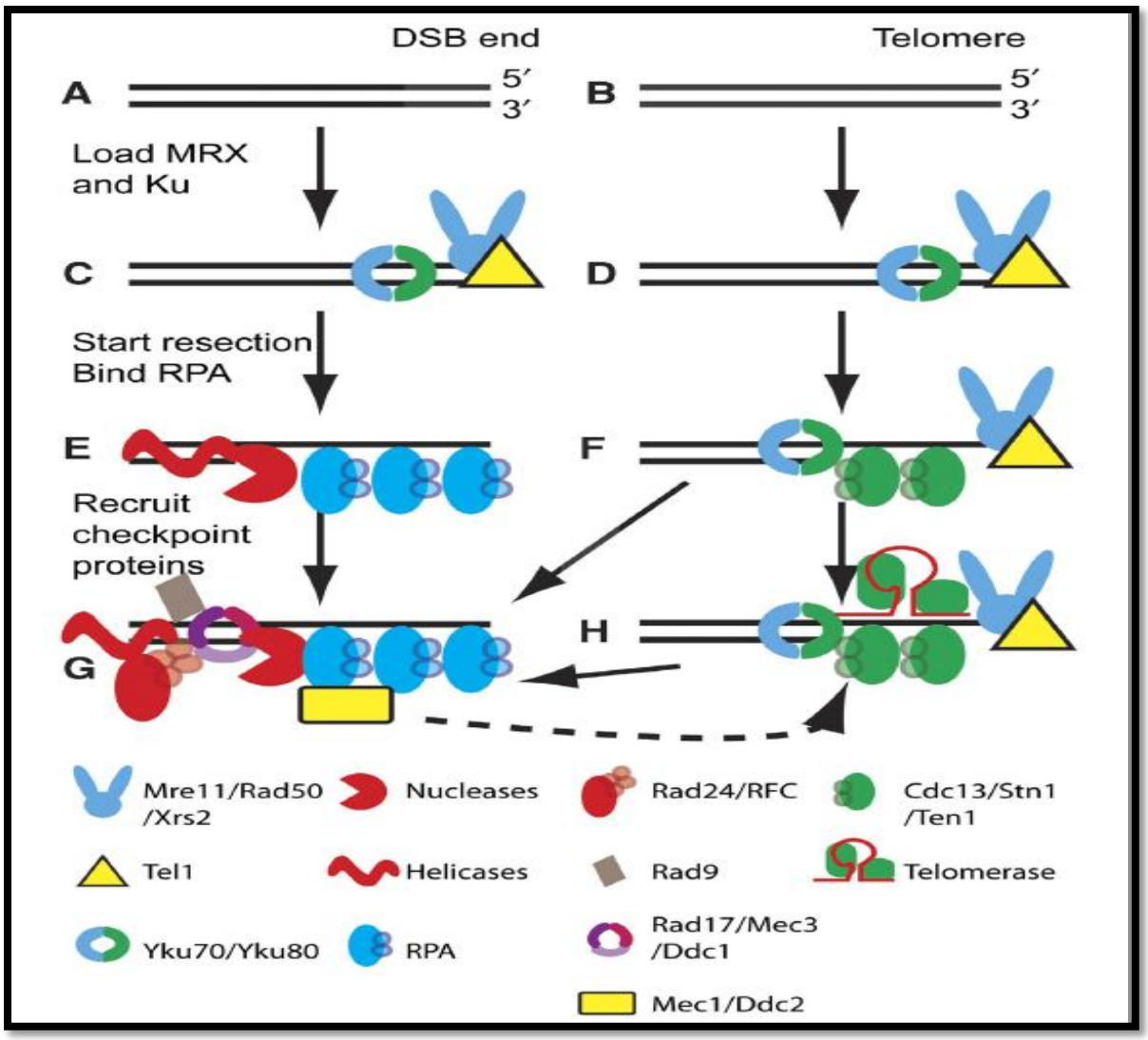

Figure 1-9: Different proteins involved in the maintenance of telomeres and repair of DSBs. The figure shows how similar proteins are involved in both telomere maintenance and DSB's pathway. For example the Mre11/Rad50/Xrs2 proteins are involved in at the start of the double strand breaks detection pathway and at telomere ends (Lydall, 2009).

Another model, Figure 1-10 shows that telomere maintenance is not an independent mechanism but a part of other maintenance pathways, damage processing (I), cell-cycle checkpoint control (II) and apoptosis control (III) (Slijepcevic, 2006). The proteins that are involved are inter-linked to each of these processes illustrated in Figure 1-10.

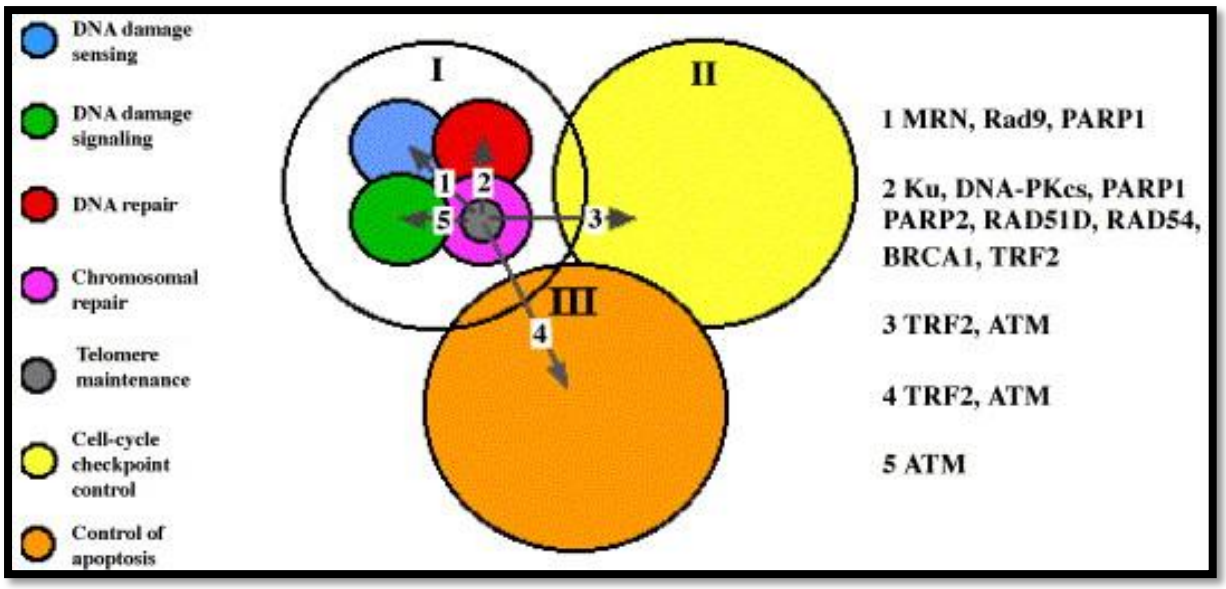

Figure 1-10: Integrative model of telomere maintenance and DDR. The figure shows the proposed integrative model, which links telomere proteins to DDR mechanisms. This figure shows arrows that point out of the telomere maintenance proteins found within the chromosomal proteins pathway towards DNA repair, DNA damage signalling and DNA damage sensing. The arrows also point out to the cell-cycle checkpoint control and control of apoptosis pathways. Therefore, the figure shows that the proteins involved in telomere maintenance are involved in all the other pathways too (Slijepcevic, 2006).

Within the damage processing section there are a number of smaller sub-components such as DNA damage signalling, DNA damage sensing, DNA repair and chromosomal repair (Slijepcevic, 2006). In this integrative model telomere maintenance is part of the chromosomal repair sub-component. Within the telomere maintenance section a number of different proteins are involved. The integrative model shows that these are further associated with all the other sub-components and mechanisms.

Taking the Ku protein as an example, it can be seen that it is involved in interactions with a number of different proteins that are part of the three different pathways mentioned above. Some of its involvements include recruitment to a DSB regardless

of what the sequence is. Ku then silences chromatin (Fisher and Zakian, 2005). Ku interacts with TRF2 at DSB (Ribes-Zamora et al., 2013). This then helps form the t-loop in the telomere and allows the Shelterin proteins to be recruited. This process is referred to as the chromosomal healing process (Slijepcevic, 2006). Ku is also involved in recruiting DNA-PKcs which is involved in the repair pathway. Therefore, the link between these pathways suggests that alternations in any one of them will result in changes to the others (Slijepcevic, 2007).

As discussed earlier in this literature review, activation of the DDR pathway does not only result in damage repair. Apart from repair, damaged DNA can cause a cell to enter premature cell senescence. Here a cell stops dividing before reaching its full replicative potential.

1.3.1 Cell Senescence

Cell senescence is the permanent arrest of cell division. Haylflick in 1965 observed that normal human cells undergo 40 to 60 cell divisions and then enter senescence. This limit of divisions was referred to as the Hayflick limit (Hayflick, 1965).

As mentioned earlier senescence not only takes place due to a cell undergoing its full replicative potential but can also happen prematurely. Some causes of senescence are shown in Figure 1-11. These include oncogene activation, oxidative stress, and DNA replication (Lundberg et al., 2000). DNA replication causes telomere shortening which leads to senescence.

As telomeres shorten in normal somatic cells and become critically short to 5kb-8kb (Henson et al., 2002) the DDR pathway is activated. This causes the cell to enter senescence (Donate and Blasco, 2011). However, in cells where telomere length is

maintained such as embryonic stem cells there is no trigger for senescence, thus allowing unlimited replication (Zeng and Rao, 2007). Apart from telomere shortening, DNA damage can cause a cell to become senescent. When cells are exposed to DNA damage the classical DDR pathway is activated.

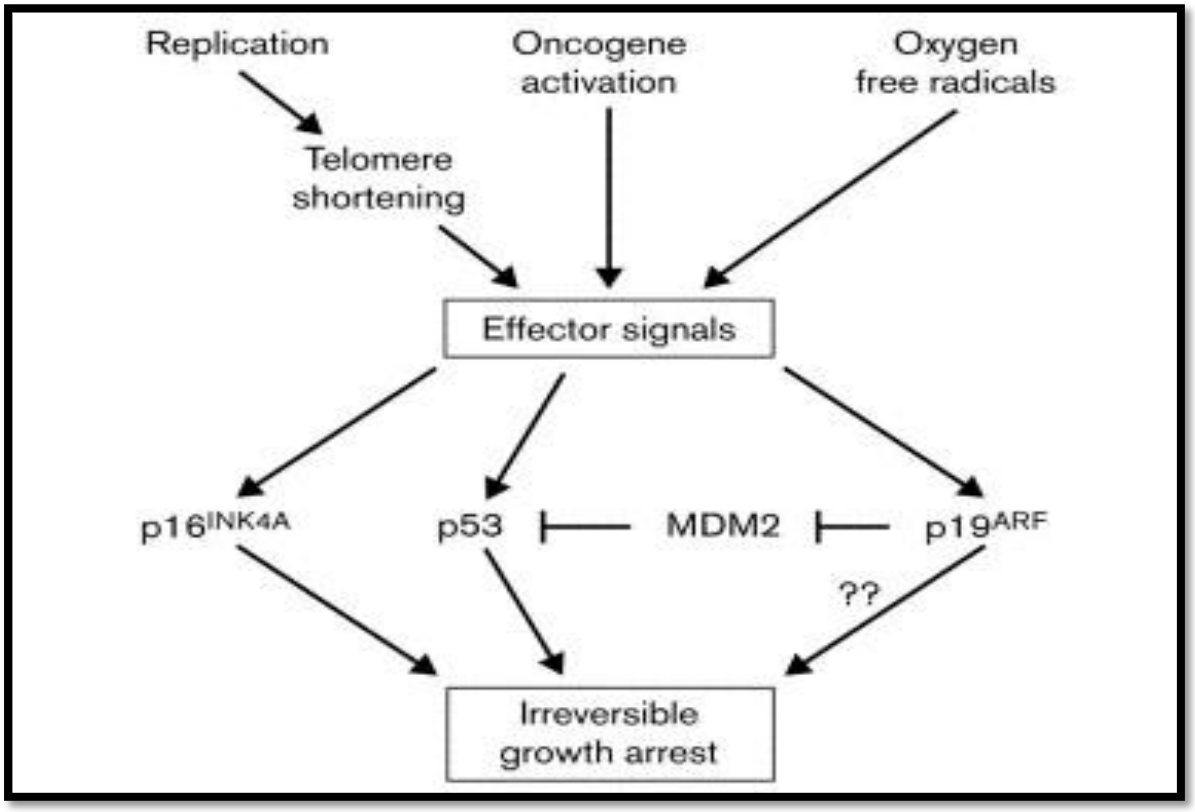

Figure 1-11: Model of proteins involved in senescence. The figure shows the different proteins that are activated in the process of cell senescence. It can be seen that after the effecter signals are activated one of four proteins ($p16^{INK4a}$, P53 or $p19^{ARF}$) are activated which result in irreversible growth (senescence) (Lundberg et al., 2000).

A number of different proteins are involved in cell senescence and are activated depending on the upstream events, Figure 1-11. Before senescence takes place in a cell, mediator proteins such as $p16^{INK4a}$, a tumour suppressor protein are activated (Brookes et al., 2004). As cells undergo cells division, $p16^{INK4a}$ accumulates as they approach senescence (Lundberg et al., 2000). Once $p16^{INK4a}$ accumulates it

activates the pRetiniblastoma (pRb) gene (Kuilman et al., 2010). Rb is a tumour suppressor gene. pRb the tumour suppressor protein is found to enforce permanent cell cycle withdrawal (Thomas et al., 2003). This type of senescence is referred to as oncogene-induced senescence (Kuilman et al., 2010).

Senescent cells display a number of different physiological and cellular characteristics depending on what triggers the cell to undergo senescence. For instance cells that undergo DNA damage will display DNA-SCARS (DNA segments with chromatin alterations reinforcing senescence), examples of which are telomere dysfunction-induced foci (TIF) (Rodier and Campisi, 2011).

Other characteristics that a senescent cell undergoes are shown in Figure 1-12 where the cell releases specific markers such as senescence related β-galactosidase, which is released due to the increase in lysosomal mass. Other characteristics are the increase in the size of the cell and experiments have also shown that chromatin in normal human fibroblast cells show low levels of the protein CENP-A in senescent cells (Maehara, Takahashi and Saitoh, 2010). The reduction in this protein only takes place in cells that are p-53 deficient hence showing that the reduction of this protein protects a cell from tumourigenesis.

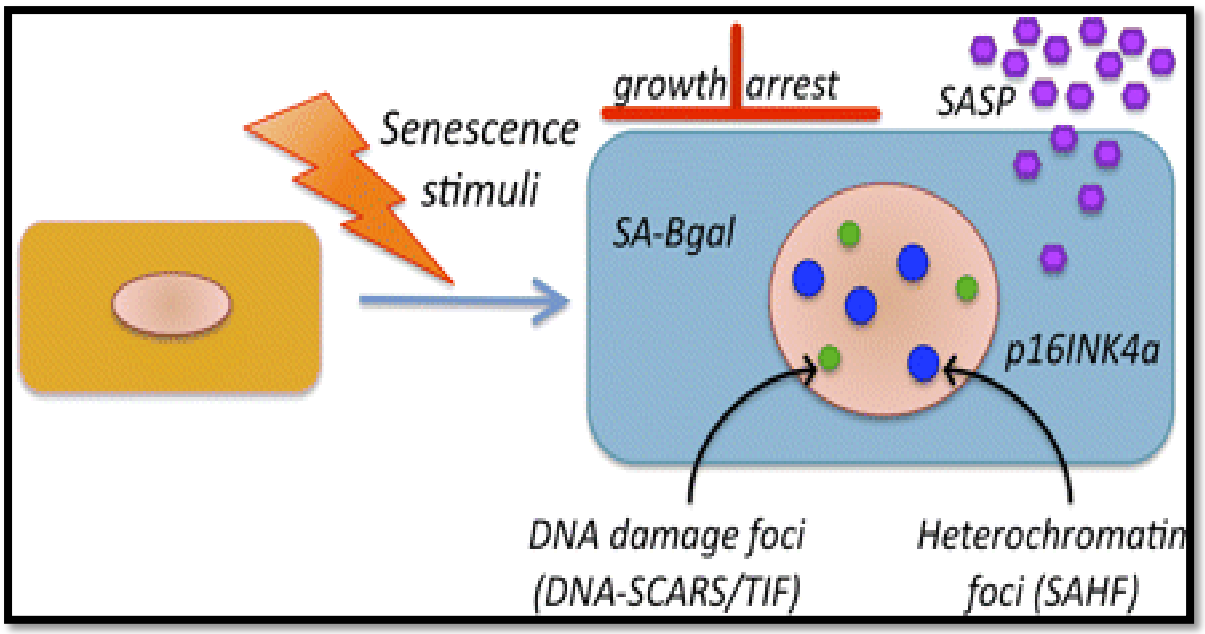

Figure 1-12: M**arkers of a senescent cell.** The figure shows the different markers of senescent cells that are used to detect a senescent cell. The DNA-SCARS are found to increase as the damage in the cell increases (Rodier and Campisi, 2011). Whereas, SAHF increases when oncogenic stress occurs and are present only when genotoxic-induced or replicative senescence occurs (Kosar et al., 2011).

These characteristics further support the “four faces of the cellular senescence model” (Rodier and Campisi, 2011) where senescence increases as different damages in the cell take place. If the damage in the cell is recoverable the cell undergoes repair. Here very little if any markers related to senescence are released. As the damage to the cell increases the DNA-SCARS increase which means definite senescence, which usually results in cell ageing or sometimes immune responses are triggered to get rid of the cell (Rodier and Campisi, 2011).

Different methods can be used to measure the percentage of senescent cells in culture. These methods usually involve the staining of either viable cells or senescent cells in culture. The two main stains that are used to do this are:

a. Ki-67 staining – identifies proliferating cells.
b. Sen-β-Gal staining – which targets senescence-associated β-galactosidase

These markers can sometimes be used alongside each other to get more accurate results. Even though senescence is known to be an irreversible mechanism, in the recent years experiments involving the inactivation of the p53 pathway showed that it is possible for the former senescent cell to re-enter the cell cycle (Kuilman et al., 2010).

1.4 Radiation induced cataractogenesis

The last section of this literature review will focus on the biology of the lens and formation of cataracts. It will further look at the effects of radiation on the lens cells resulting in early onset of cataracts.

1.4.1 Lens Cell Biology

The lens' wet weight is 33% protein which is the reason for its high refraction index. Approximately 90% of these proteins are made of the lens crystallins, alpha, beta and gamma (Michael and Bron, 2011). Other proteins include the transporters, cells communication proteins and enzymes involved in metabolism and protein synthesis. It is thought that membrane rigidity increases in the lens nucleus with age hence causing stiffness (Michael and Bron, 2011)

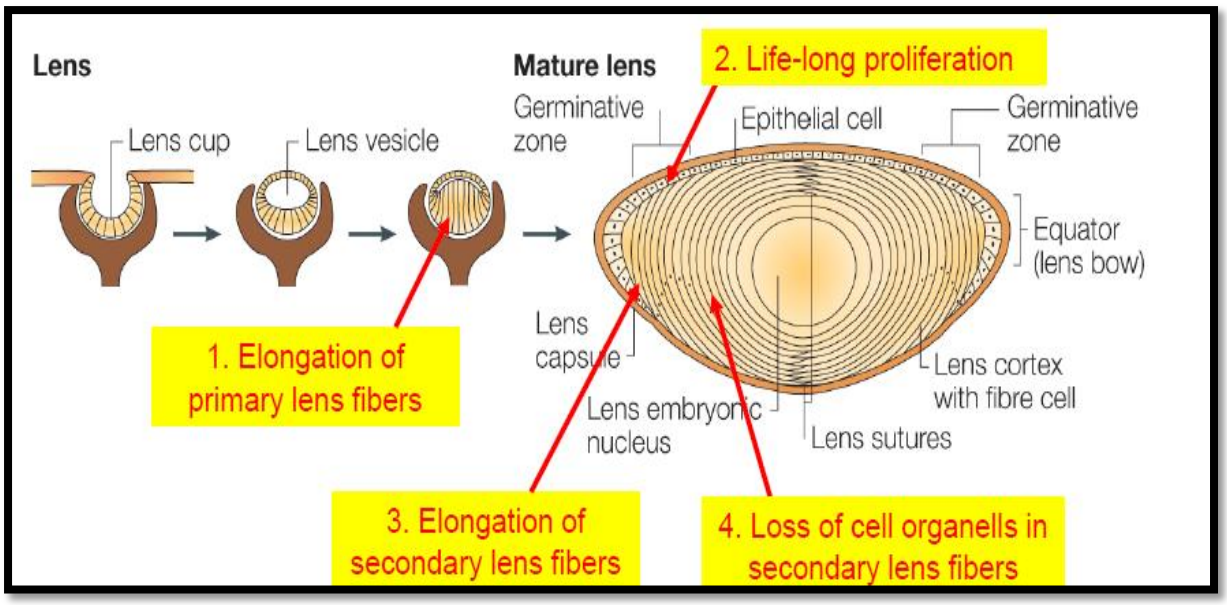

Figure 1-13: Formation of the mature lens. The figure shows how a mature lens cell is formed over time. An elongation in primary lens and secondary lens fibres is noted. Also, as shown by the labels the lens loses its organelles in the secondary fibres. However, the epithelial cells proliferate for life (Graw, 2003).

Lens transparency depends on how the organelles in the lens cells move and the organisation of the proteins inside cells (Bassnettt, Shi and Vrensen, 2011). There is a tendency of cells in the lens to lose their organelles as they move from periphery towards the lens centre as seen in Figure 1-13. The loss of organelles allows the formation of the transparent mass in the middle of the lens through which passes (Graw, 2003).

Two research groups showed that the crystallins have a short-range order, which is an arrangement found typically in the case of glass. This effect is possible because the proteins are packed together and are small in size (Benedek, 1971) (Delaye and Tardieu, 1983). This means that the transparency of the lens is maintained. In the lens cortex, narrow intracellular spaces are found which help with reducing the scattering of light as it moves from the fibre membranes to the cytoplasm (Michael

and Bron, 2011). Radiation causes damage to the dividing cells, which then move to the back of the lens, causing light not to pass through.

Over time the elasticity of the lens changes and the protein structure changes therefore causing light to scatter more. Proteins are exposed to oxidation because antioxidants, such as glutathione, are reduced with age (Giblin, 2000).

1.4.2 Radiation induced Cataracts

Cataracts are basically the mistiness of the lens, which is caused by the changes of the lens cells and their water content. The crystallins in the lens change over time in the lens as the lens ages or when it is exposed to external factors (Moreau and King, 2012). Cataracts are the leading cause of blindness worldwide (Ainsbury et al., 2009).

The risk of cataracts formation can increase due to a number of different risks factors, such as intraocular inflammation, steroid administration, vitreo-retinal surgery and trauma. Mutation in the (CRYBB2 gene), diabetes and radiation can cause early onset of cataracts. Apart from these factors, the risk of cataracts increases naturally due to age. Our interest is radiation induced cataracts.

One of the most radiosensitive tissues in the body is the lens of the eye. Cataracts can be induced by acute doses of <2Gy of low-LET ionizing radiation and <5Gy of protracted radiation (Ainsbury et al., 2009). LET is Linear Energy transfer, which is measured as the loss of energy along the radiation path. Gamma and x-ray are referred to as Low-LET IR sources as they penetrate tissues very easily and do not deposit energy very frequently (Energy, 2012). The formation of cataracts after exposure to high dose radiation can take place as early as two years after exposure.

However, exposure to lower doses of radiation results in longer time required for cataract formation (Chodick et al., 2008).

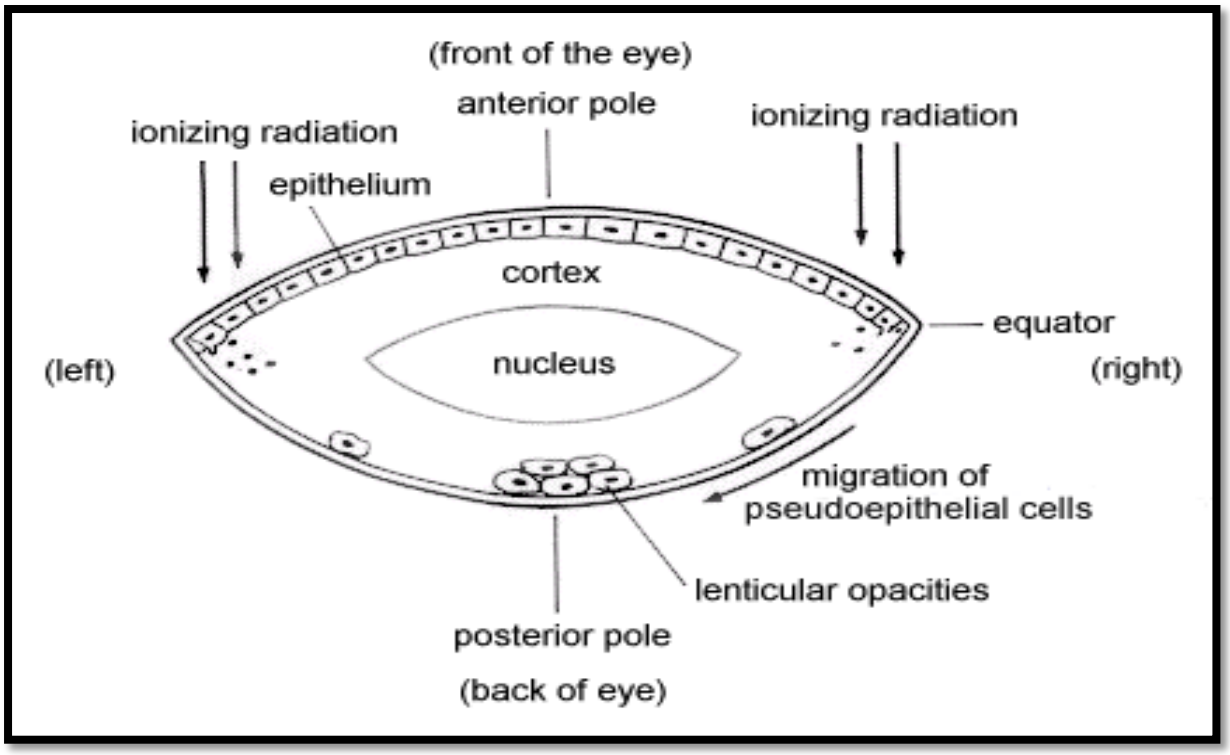

Figure 1-14: Changes in lens after radiation. The figure shows how radiation causes the damaged cells to migrate to the posterior pole of the lens and move to the back of the cells. The damaged cells block light from passing through (Shigematsu, 2013).

Cataracts can form in the posterior, nuclear or cortical of the lens (Figure 1-15). The main cataract formed after IR exposure is the posterior subcapsular cataract (Bouffler S, 2012), but can also form over time due to ageing. For cataracts to form damaged cells have to cover the area of the cataract. For instance, if the cataract is in the posterior region of the lens then an accumulation of damaged cells will be seen in this area.

In studies carried out on Chernobyl workers all three cataracts were noted, but larger numbers of both posterior subcapsular and cortical cataracts were noted compared

to nuclear (Worgul BV, 2007), which are more age related. The formation of cataracts is a long and complex process (Ainsbury Elizabeth, 2016), and the full mechanisms are still not understood (Ainsbury et al., 2009). However, studies have shown that radiation causes formation of senescent markers which are present in the long term which may contribute to the reduced tissue functionality observed (Le et al., 2010). The accumulation of $p16^{INK4a}$ positive senescent cells has also been shown in cells from lens with cataracts (Baker et al., 2011). It has been shown that using a novel transgene *INK-ATTAC* for inducible elimination of $p16^{INK4a}$ – positive senescent cells upon drug (AP20187) administration, can delay or prevent tissue dysfunction and expand life-span of mice (Baker et al., 2016). The study showed that the removal of $p16^{INK4a}$ – positive senescent cells delayed the onset of cataracts in the mouse model used (Baker et al., 2011).

1.5 Aims and Outline of project

The aim of this thesis was to understand the role of telomere maintenance in cataractogenesis. To do this, cells from HLE and mouse bone marrow will be used. The project will be split into three sections:

The first section will analyse telomere biology, telomerase activity and population doubling in HLE cells. Telomere length and telomerase activity will be measured using q-PCR based techniques. This will help understand the role of telomeres in HLE cells and observe any changes over the life-time of these cells in culture.

For the second chapter HLE cells will be exposed to different radiation doses to see if they repair effectively and if an increase in damage is noted over a period of time. Alongside this, analysis of telomere length and telomerase activity after irradiation will be done to see if radiation causes any changes in these cells. This will be done because it is known that cataracts form early due to radiation exposure (Ainsbury et al., 2009). Hence any telomere changes noted in these cells due to radiation exposure will show a link between telomeres and cataract formation.

Lastly, telomere length will be measured in mouse in-vivo models to see if changes are noted in mutant *Errc2* and wild-type mice. The *Ercc2* is a gene involved in the DNA excision repair pathway and is also part of general transcription (Subba, 2007), (Kunze et al., 2015). We will also examine any differences in telomere length between male and female samples, as studies show that females are more likely to get cataracts than males (Courtright and Lewallen, 2009) (Graw et al., 2011). To do this telomere length analysis using IQ-FISH will be used. Telomere length will be measured over a period of 24 months and mice will be exposed to different radiation doses to see if early onset of cataracts is noted.

The work was supported by the DoReMi Network of Excellence grant of the European Atomic Energy Community's 7th Framework Program and was shared with our collaborators Prof. Munira Kadhim in Oxford Brookes University and Prof. Jochen Graw in Helmholtz Centre, Munich, Germany.

Materials and Methods

A number of different materials and methods were used in this project. All of which have been explained in detail in this chapter.

2.1 Cell Lines

Table 2-1 shows a summary of the cell lines used in the project.

Table 2-1: Summary of Cell lines used in the project

Cell Line	Cell Type	Age at Sampling	Sex	Clinically effected	Source
GM08399	Normal Fibroblast	19 Years Old	Female	No	Coriell Cell Repositories
U20S	Human Osteosarcoma Mesnchymal Adherent cells	15 Year Old	Female	Yes	ECCC(European Collection Cell Cultures)
HeLa	Human Cervical Carcinoma, Epithelial Adherent Cells	31 Year Old	Female	Yes	ATTC (American Tissue Culture Collection)
LY-R	Mouse Lymphoma, Normal Radiosensitivity, Lymphoma	Unknown	Unknown	Unknown	Dr Andrzej Wojcik, University of Warszaw, Poland

LY-S	Mouse Lymphoma, Radiosensitive, Lymphoma	Unknown	Unknown	Unknown	Dr Andrzej Wojcik, University of Warszaw, Poland
Donor 1 HLE Cells	Primary Human Lens Epithelial Cells, Adherent Epithelial Cells			No	Caltag Medsystems, ScienCell
Donor 2 HLE Cells	Primary Human Lens Epithelial Cells, Adherent Epithelial Cells			No	Caltag Medsystems
Donor 3 HLE Cells	Primary Human Lens Epithelial Cells, Adherent Epithelial Cells			No	Caltag Medsystems

2.2 Cell Culture

A number of different cell lines were cultured using the aseptic tissue culture technique; details of each are described below:

2.2.1 HeLa (Ovarian Cancer Cell Line) and GM08399 (Normal Human Fibroblast cells)

To culture HeLa and normal human fibroblasts (GM08399), Dulbecco's Modified Eagle's medium (DMEM) (Gibco) is used which is supplemented with 10% Fetal Bovine Serum and 1% Penicillin and Streptomycin. The cells are grown in T25 or T75 flasks which are incubated in a humidified incubator at 37°C with 10% CO_2 concentration.

2.2.2 U2OS (Osteosarcoma cell line)

For the U2OS cell line, McCoy's Medium (Fisher) was used supplemented with 10% FBS and 1% P&S. The cells were incubated in a 37°C humidified incubator with10% CO_2 concentration.

2.2.3 PC3 *h*TERT (Prostatic Adenocarcinoma Cell Line)

The human Prostate cancer cell line PC3 , which stably overexpresses the hTERT cDNA (kind gift from Professor Newbolds group), was cultured using F-12 Nutrient Mixture (Ham) supplemented with 7% FBS, 1% GlutaMAX and 1% P/S... These cells were grown in T25 or T75 flasks and are incubated in a humidified incubator at 37°C with 5% CO^2 concentration.

2.2.4 HLE cells (Primary Human Lens Epithelial Cells)

Epithelial Cell Medium (Caltag Medsystems, Sciencell) with 1% Growth Factors, 1% P&S and 20% FBS. The cells are grown in 2µg/cm^2 poly-lysine coated T75 flasks at

a seeding density of 5000 cells/cm^2. The cells are grown in a 37°C humidified incubator with 5% CO_2.

2.3 Sub-Culturing Cells

2.3.1 Most Adherent cells

Cells were trypsinized with 3 ml of Trypsin EDTA (59418C,Sigma) in a T75 flask and left in the incubator for 3-5 minutes until all the cells detach from the flask. The cells are then collected with equal amounts of media as trypsin added. The cell suspension are transferred to a 15ml tube and centrifuged for 5 minutes at 1500rpm. The supernatant is then aspirated. Cells are then split according to how quick they grow, once they reach 90% confluency. The most commonly used ratio is 1:3, this is done by is re-suspending the cell pellet in 3ml of media. 1ml of this media is then added to a T75 flask containing 15ml of fresh media. The cells are then incubated and the media is changed every 2 days depending on the cell type.

2.3.2 HLE Cells

HLE cells were sub-cultured according to the protocol provided by the company that sold the cells (SC-6550, Caltag Medsystems, ScienceCell; Donor 1 lot no: 5976, Donor 2 lot no: 5971, Donor 3 lot no: 7273)

All the reagents that were used were allowed to warm up to room temperature rather than 37°C as recommended by the supplier. To sub-culture HLE cells in a T75 flask, 3ml of TrypsIn EDTA (0.025% Trypsin + 0.5mM EDTA + 1Mm sodium pyruvate and 10mM HEPES, pH 7.4, ScienceCell, SC-0103) plus 7ml of PBS (Severn Biotech Ltd, 20-74-05) were added to the cells. The flask was then placed in the 37^{o}C incubator for 1-3 minutes to allow the cells to detach from the flask. During the incubation

period 5ml of Fetal Bovine Serum (FBS cat. No 0500) was added to a 50 ml conical centrifuge tube. After 1-3 minutes when the cells rounded off. The trypsin and PBS in the flask were transferred to the 50ml conical centrifuge tube and the flask was incubated for another 1 to 2 minutes in the incubator after which 5ml of TNS (ScienCell, 0113) was added to the flask and the remaining cells were collected. This was then added to the 50ml conical tube. The tube was then centrifuged at 1500rpm for 5 minutes. The pellet was split into three flasks, which were then incubated. The media in the flasks was changed every 2 days.

2.4 Cell Cryopreservation

Cells as per section 2.3 are trypsinised, centrifuged and supernatant is aspirated. Instead of splitting the cells in media they are split into a 1:3 ratio with freezing mixture (90% fetal bovine serum and 10% DMSO). A total of 3ml of freezing down mixture is added to the 15ml tube and 1ml of this is added to 1 cryopreservation tube. This is then kept at -80°C overnight after which it is frozen down in liquid nitrogen.

2.5 DNA Extraction and Precipitation

300μl of digestion buffer plus 15μl of 50mg/ml of protinase K was added to cell pellets harvested from a confluent T75 flask. The eppendorf tube was left at 55^{o}C for 3 hours for digestion.

330μl of phenol (amount needs to be equal to the amount of digestion buffer and protinase K added) and the tube was inverted and vortexed.

After centrifugation at 13000rpm for 10 minutes transfer the aqueous layer to a new eppendorf tube. An equal amount of Chloroform was added to the layer and mixed my inversion for 5 minutes. Centrifuge at 13000rpm for 10 minutes.

Transfer aqueous solution into new eppendorf tube add 10% 3M sodium acetate and 2x volume of ice cold 100% ethanol. Leave at -80ºC for 15minutes centrifuge at 4ºC for 10minutes 13000rpm. Remove supernatant and add 500µl of 70% ethanol and vortex. Centrifuge at 13000rpm for 10 minutes at room temperature and remove the supernatant. Air-dry the pellet. Re-suspend the pellet in 1 x TE Buffer (10mM Tris-Cl and 1mM EDTA) depending on pellet size. Leave at 4ºC and measure DNA concentration next day.

2.6 Protein Extraction

Cells were grown in either a T25 or T75 flask until they are about 90-100% confluent. Cells were then extracted as per section 2.3 of this document, depending on the cell type. Once the cells were trypsinised and centrifuged they were then washed with PBS 3 times. 200µl of lysis buffer or RIPA was added to the cells. Then 10µl of PIX25 was added to each sample and homogenised using a syringe. The contents was then transferred to a 1.5ml eppendorf tube and was centrifuged for 15 minutes at 4°C. The supernatant was then transferred to an eppendorf tube.

Alternatively, protein was extracted using CHAPS buffer for the TRAP assay. 200 µl of CHAPS buffer was added to the samples and homogenised the sample and left on ice for 30 minutes. The samples were then centrifuged and the supernatant was transferred to a new eppendorf tube.

2.7 Protein Concentration measurement using Pierce BCA Protein kit

The concentration of the protein extracted using the two different methods described in section 2.5 of this document were measured using the Pierce BCA extraction kit (Thermo Scientific, 23227).

Firstly, 8 eppendorf tubes with different amounts of Bovine Serum Alumin (BSA) and dH_2O were prepared as per Table 2-2.

Table 2-2: Different amounts of BSA and dH_2O added to eppendorf tubes.

	BSA (Bovine Serum Alumin)	**H_2O**	**Concentration at (µg/ml) protein**	**Concentration of Protein**	**Nano Drop**
A	30 µl	10 µl	1.5	1500	1.500
B	20 µl	20 µl	1.0	1000	1.00
C	20 µl from A	20 µl	0.750	750	0.750
D	20 µl from B	20 µl	0.500	500	0.500
E	20 µl from D	20 µl	0.250	250	0.250
F	20 µl from E	20 µl	0.125	125	0.125
G	10 µl from E	30 µl	0.025	25	0.025
H	0 µl	40 µl		0	0

A standard curve was generated using BCA reagents at a ratio of 1:49 (A:B) and 10µl of the above mentioned (Table 2-2) eppendorf tubes was added to the new eppendorf tubes as per Table 2-3. For the protein samples they were diluted, using

2µl of the protein and 38 µl of dH_2O. From this 10µl was added to the 190 BCA (1:49 A:B).

Table 2-3: The table shows the amount of BCA and amount of solution from Table 2-2 tubes added to the new eppendorf tubes.

Tube numbers		**BCA reagent (A+B)**
1	10µl of tube A	190 µl
2	10µl of tube B	190 µl
3	10µl of tube C	190 µl
4	10µl of tube D	190 µl
5	10µl of tube E	190 µl
6	10µl of tube F	190 µl
7	10µl of tube G	190 µl
8	10µl of tube H	190 µl
P1	10µl of diluted Protein 1	190 µl
P2	10µl of diluted Protein 2	190 µl

These samples were then incubated at 37°C for 30 minutes after which the protein concentration was measured on the nano drop.

2.8 Real-time quantitative PCR Telomeric repeat amplification protocol (RTQ - TRAP) Assay

TRAP assay was used to measure the telomerase activity in different cells using the protocol published in (Wege et al., 2003) and the primers that were used were published in (Kim and Wu, 1997) (ACX (5' – GCGCGGCTTACCCTTACCCTTACCCTAACC - 3') and TS (5' – AATCCGTCGAGCAGAGTT- 3') – both were ordered from Life Technology).

CHAPS buffer (220201-1GM Calbiochem, Millipore) was used to extract protein from cells and 250ng of total protein was used in each assay. The protein concentration was measured using the Thermo Scientific Pierce BCA Protein Assay Kit and was measured on the nano drop. 1X Syber green (4309155 Applied Biosystem PCR Master Mix) was used to stain the products of the reaction therefore giving quantification.

2.8.1 Extraction and measurement of protein

Protein was extracted using 200µl of CHAPS buffer. Each sample was homogenised using a needle syringe. It was ensured that the samples were kept on ice at all times as telomerase is a very sensitive enzyme.

Extracted protein was measured using the Thermo Scientific Pierce BCA Protein Assay Kit as described in section 2.7.

2.8.2 TRAP q-PCR

Once the protein has been extracted and its concentration is measured, the protocol published in (Wege et al., 2003) was used to complete the TRAP assay. The two different primers that were used in this experiment were mentioned in (Kim and Wu, 1997).

Each well used contained a total of 25µl reaction mixture. This mixture consisted of 12.5µl of 1x standard Sybergreen,1µl ACX primer (0.05µg/µl), 1µl TS Primer (0.1µg/µl), 1-4µl (containing 250ng of protein) protein sample depending on the concentration of the protein needed to be added and DEPC water depending on the amount of protein added. Therefore, if 1µl of protein was added to the mixture, 9.5µl of DEPC was added to the mixture. This was calculated as follows. Since the total amount of reaction mixture should be 25µl (total amount) – 15.5 (total of all reagents added including protein) = 9.5µl of DEPC.

In terms of the protein it is important to determine how much needs to be added. This is done by checking the concentration of the protein (section 2.8.1) if the concentration is good then only 1µl of correct 250ng of the protein should be added. Also, it is important to ensure that the amount of protein added is consistent throughout the samples because CHAPS buffer has an effect on PCR activity. Therefore a maximum of 20% RXN volume which means if the total reagents added to each well is 25µl the maximum protein that can be added is (20/100) x 25µl = 5µl

Each 96 well plate should contain an unknown sample, standard curve, non-template control and heat inactivated sample. Each of these were replicated in three wells, so as to give an average at the end.

The unknown sample is the protein extracted from the cell line in question.

The standard curve was generated using PC-3 hTERT cell line (provided by Dr Terry Roberts, Brunel University), which is the positive control for telomerase. The standard curve was made each time an assay was ran. It was generated from serially diluted telomerase positive prostate cell line; PC-3 hTERT extracts (10^8 -10^3).

The non-template control did not contain any protein but had 1µl extra DEPC water. Therefore, the total water for this well was 10.5µl instead of 9.5µl. The extra water should be equal to the amount of protein added to the other samples i.e. if 5µl of protein was added to the unknown samples well then 5µl of water needed to be added to the non-template control.

The heat inactivated sample wells contained 1µl of PC-3 10^5 concentration. The 1 µl was added to the DEPC water (9.5µl) and heated to 85°C for 10 minutes. This solution should then be added to the rest of the reagents i.e. Syber Green, ACX and TS primers. This sample also acts as a control, and should not produce any telomerase activity as the heat kills the reaction.

In the real time PCR machine the reaction mixture should first be incubated a 25°C for 20 minutes to allow the telomerase in the protein extracts to elongate the TS primer by adding TTAGGG repeat sequence. PCR was then started at 95°C for 10 minutes to activate Taq polymerase followed by a two-step PCR amplification of 35 cycles at 95°C for 30s and 60°C for 90s.

2.9 Absolute Telomere Length – Quantitative PCR (aTL q-PCR)

The absolute telomere length protocol was used to measure the average telomere length in cells by extracting their DNA as per (O'Callaghan and Fenech, 2011).

Six different Primers were used which were ordered from Sigma-Aldrich, details of which are in Table 2-4.

Table 2-4: Details of the primers used for aTL q-PCR.

Primer Name	**Primer Sequence**	**Primer Size (bp)**
Telomere Standard	(TTAGGG)4	84
36B4 Standard	CAGCAAGTGGGAAGGTGTAATCCGTCTCCACAGACAAGGCC AGGACTCGTTTGTACCCGTTGATGATAGAATGGG	75
Telo Forward	CGGTTTGTTTGGGTTTGGGTTTGGGTTTGGGTTTGGGTT	>76
Telo Reverse	GGCTTGCCTTACCCTTACCCTTACCCTTACCCTTACCCT	>76
36B4 Forward	CAGCAAGTGGGAAGGTGTAATCC	75
36B4 Reverse	CCCATTCTATCATCAACGGGTACAA	75

The method described in section 2.5 of this thesis were used to extract DNA and a total concentration of 5ng/µl was used per sample. DNA concentration was measured using the nano drop. Power Syber Green (Applied Biosciences, 4367659) was used to get quantification of telomere length.

2.9.1 Telomere length measurement qPCR

DNA was extracted and its concentration was measured using the nano drop.

Once DNA was extracted and its concentration measured the protocol described in (O'Callaghan and Fenech, 2011) was followed to establish telomere length.

In each assay two 96 well plates were prepared, one for the single copy gene, 36B4 (Table 2-5) and the other for the telomere standards (Table 2-6).

Each well in the 36B4 single copy gene contained 10µl of Power Syber Green (Applied Biosystems, 4367659), 1µl of 36B4 forward primer (2µM concentration), 1µl of 36B4 reverse primer (2µM concentration), 6µl of dH_2O and 2µl of standard 36B4 primer at each concentration shown in Table 2-5 (10nM,5nM, 1nM, 0.5nM and 0.1nM). In the sample section of the 36B4 single copy gene 96 well plate, each well contained 10µl of power syber green, 1 µl of 36B4 forward primer (2 µM concentration), 1µl of 36B4 reverse primer (2 µM concentration), 4 µl of dH_2O and 4µl of the DNA (5 ng/µl concentration) sample in question.

In the NTC section of the 96 well plate 10µl of Power Syber Green, 1µl of 36B4 Forward Primer (2µM concentration), 1µl of 36B4 Reverse Primer (2µM concentration) and 8µl of dH_2O.

Table 2-5: All the concentrations of the 36B4 single copy gene.

	1	2	3	4	5	6	7	8	9	10	11	12
A	10nm	10nm	10nm	10nm					Sample 1	Sample 1	Sample 1	Sample 1
B	5nm	5nm	5nm	5nm					Sample 2	Sample 2	Sample 2	Sample 2
C	1nm	1nm	1nm	1nm					Sample 3	Sample 3	Sample 3	Sample 3
D	0.5nm	0.5nm	0.5nm	0.5nm					Sample 4	Sample 4	Sample 4	Sample 4
E	0.1nm	0.1nm	0.1nm	0.1nm								
F												
G												
H									NTC	NTC	NTC	NTC

Each well in the telomere standard contained 10µl of Power Syber Green (Applied Biosystems, 4367659), 1µl of telo forward primer (2µM concentration), 1µl of reverse primer (2µM concentration), 6µl of dH_2O and 2µl of standard Telo primer at each concentration shown in Table 2-6 (50nM, 10nM, 5nM, 1nM, 0.5nM and 0.1nM). In the sample section of the telomere standard 96 well plate, each well contained 10µl of power syber green, 1 µl of telo forward primer (2 µM concentration), 1µl of telo reverse primer (2 µM concentration), 4 µl of dH_2O and 4µl of the DNA (5 ng/µl concentration) sample in question.

In the NTC section of the 96 well plate 10µl of Power Syber Green, 1µl of Telo Forward Primer (2µM concentration), 1µl of telo Reverse Primer (2µM concentration) and 8µl of dH_2O.

Table 2-6: All the concentrations of the Telo genes.

	1	2	3	4	5	6	7	8	9	10	11	12
A	50nm	50nm	50nm	50nm					Sample 1	Sample 1	Sample 1	Sample 1
B	10nm	10nm	10nm	10nm					Sample 2	Sample 2	Sample 2	Sample 2
C	5nm	5nm	5nm	5nm					Sample 3	Sample 3	Sample 3	Sample 3
D	1nm	1nm	1nm	1nm					Sample 4	Sample 4	Sample 4	Sample 4
E	0.5nm	0.5nm	0.5nm	0.5nm								
F	0.1nm	0.1nm	0.1nm	0.1nm								
G												
H									NTC	NTC	NTC	NTC

2.9.2 Telomere Measurement using real time PCR

Each plate was then taken to the real-time PCR machine and incubated as per Table 2-7.

Table 2-7: The different cycles and temperatures used for real time PCR.

	Temperature	**Time**	**Cycles**	
1.	95°C	10 Minutes		
2.	95°C	15 Seconds	40 Cycles	
3.	60°C	1 Minute	40 Cycles	
4.	95°C	15 Seconds		Dissociation Curve
5.	60°C	15 Seconds		Dissociation Curve
6.	95°C	15 Seconds		Dissociation Curve

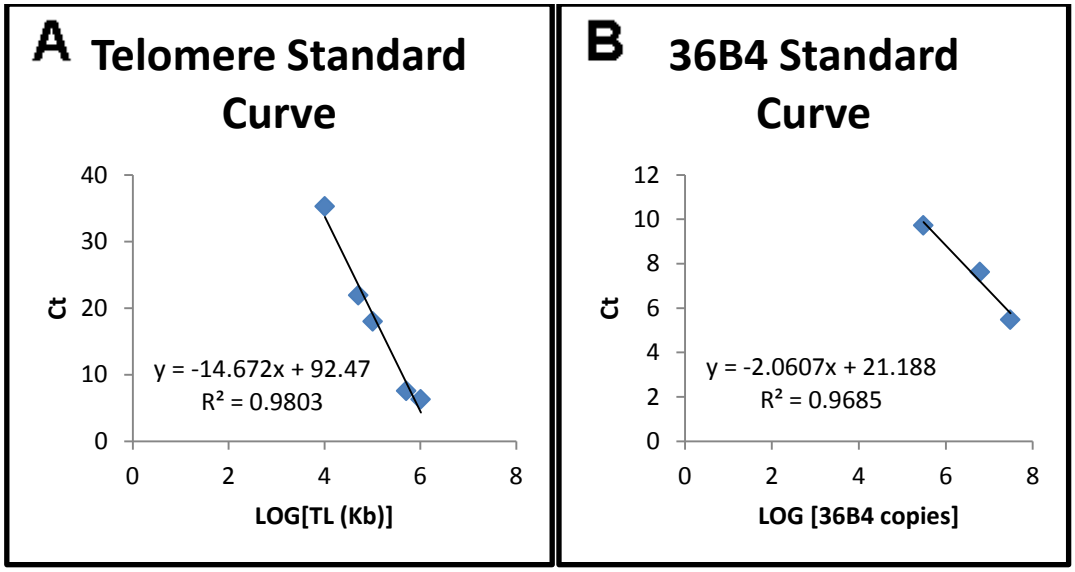

Figure 2-1: Absolute telomere length calculation using standard curve. Ct (cycle threshold) is the number of PCR cycles for which enough SYBR green fluorescence was detected above the background. A) Standard curve for calculating length of telomere sequence per reaction tube: the x-axis represents the amount of telomere sequence in kb per reaction with correlation coefficient of 0.9803. B) Standard curve for calculating genome copies using 36B4 copy number with correlation coefficient of 0.9685.

The standard curves (Figure 2-1) were used to calculate the total telomere length in kb per human diploid genome.

2.10 γ-H2AX and Telomere Dysfunction-Induced Foci (TIF)

γ-H2AX was done as per (Rai and Chang, 2011) methodology. For γ-H2AX repair kinetics and dose response was performed. Six different doses were used to analyse these cells - 0.01Gy, 0.02Gy 0.1Gy, 0.2Gy, 1.0 Gy and 2.0 Gy radiation exposure. The radiation source used for HLE low dose radiation was x-ray whole for all other analysis gamma radiation was used.

The primary antibody for γ-H2AX (Anti-phospho-Histone H2A.X (Ser139), Millipore Cat 05-636) was diluted 1:1000 in blocking buffer. The secondary antibodies, Alexa

Fluor (488 Signal Amplification kit for mouse antibodies Invitrogen A-11054) were each diluted 1:1000 in blocking buffer. 4% Formaldehyde Sigma (F8775) was made in PBS (Severn Biotech Ltd, 20-74-05). Permealising Trition X-100 (Sigma, T8787) solution was made with 100µl Triton X-100 and 50ml dH2O. 1x TBST to wash the slides after antibody incubation was made using 8.8 grams of Sodium Chloride (BDH, 3012375), 0.2 grams Potassium Chloride (BDH, 101984L), 3 grams Tris Base (Fisher Bioreagents BPE152-1) and 500µL Tween 20 (Sigma, P1379) in 1000ml of dH2O at a pH 7.4 (using HCL). 5% Blocking buffer was made using 0.1 grams BSA (Sigma, A2153) in 10ml of 1x TBS (0.242g Tris Base and 0.8g Sodium Chloride in 100ml of dH2O. 70% formamide was made using 70ml Formamide (Fisher, F/1551/PB17), 20ml dH2O and 10 ml of 20x Saline Sodium Citrate (20x SSC buffer), (Sigma, S6639). Washes with TBST and PBS were all done on the shaker.

A 100,000 cells were seeded onto a poly-prep slides in petri dishes using the methodology described in section 2.3 of this document. As per section 2.3 when cells were centrifuged after trypsinization around 100,000 cells were added seeded onto each slide using 1ml medium. The cells were then left in the incubator over-night to settle and attach to the slides.

On the next day an extra 5ml of media was added to the petri dishes containing the slides. If the cells needed radiation they are taken to the radiation bunker and irradiated. The cells were then incubated for 30minutes in the incubator, for the first time point. If repair kinetics was being done then the different slides were left in the incubator for different time points (24 hours, 48hours ad 72 hours) after radiation.

After radiation slides were rinsed in PBS. The slides were then transferred to a coplin jar containing 4% Formaldehyde (Sigma, F8775) in PBS (Severn Biotech Ltd, 20-74-

05) for 15minutes. The slides were then rinsed in PBS and were transferred to a coplin jar containing 100µl of triton X-100 (Sigma, T8787) and 50ml of dH2O for 10 minutes in the fridge. 100µl of 5% BSA blocking buffer was added onto slides, which were covered with parafilm and placed in a dark, damp box for an hour.

A total of 100µl of the diluted primary antibody was then put onto slides and covered with parafilm. The slides were then put in a dark, damp box and incubated for 1 hour at room temperature. The slides were then washed in TBST 3 times for 5 minutes each time. 1µl of the first component of the secondary antibody, Rabbit anti-mouse IgG was diluted in 1000µl of blocking buffer. 100µl of this solution was added onto slides, which were then covered with parafilm and they were incubated in the dark, damp box for 30mins. The slides were then washed with TBST for 5 minutes 2 times. The second component of the secondary antibody was added in the same was as the first component and the slides were incubated for 30 minutes in a dark damp box. The slides were then washed in TBST 3 times for 5 minutes each time and were then fixed in 4%formaldehyde for 10 minutes. The slides were then washed in PBS 3 times for 5 minutes each time. The slides were then dehydrated in ethanol series 70%, 90% and 100% for 2 minutes each. These were then air dried.

At this stage if only γ-H2AX was being done 10µl of Dapi was added after which a coverlip was put on the slide and sealed with clear nail varnish. If TIF was being done then the slides were left in a dark dry place for 24-48 hours after which 20µl of CY-3 telomeric PNA probe was added to them. The slides were then placed on a heating block for 2minutes at 70°C, after which the slides were left in a dark, damp box for 2 hours. The slides were then washed in 70% formamide solution 2 times for 10 minutes and then in PBS 3 times for 5 minutes each. The slides were then

dehydrated in ethanol series 70%, 90% and 100% for 2 minutes each. They were then dehydrated and 10µl of DAPI was added to each slide after which a coverslip was sealed on using clear nail varnish.

The slides were then analysed under the Zeiss Fluorescence microscope equipped with a CCD camera and ISIS (in situ imaging system, metasystems, Altlusshim, Germany).

2.11 IQ-FISH (Interphase Quantitative Fluorescence In-situ Hybridisation)

The slides were aged overnight at 54°C. In the morning they were washed in PBS for 15 minutes to get rid of any impurities, leaving behind specific proteins that were required. The cells were then fixed onto the slide for 2 minutes using 4% formaldehyde (4ml Formaldehyde and 96ml deionised water)

They were then transferred into a coplin jar containing PBS to wash them, and were placed onto the shaker for a total of 15 minutes, changing the PBS in the coplin jar every 5 minutes. After 15 minutes they were washed in 10% pepsin solution at 37°C for 10 minutes. Again, the slides were washed two times in PBS on the shaker for a total of 4 minutes, changing the PBS solution every 2 minutes. After which they were fixed in 4% formaldehyde for 2 minutes not using the shaker.

The slides were then washed in PBS for 5 minutes, three times. After 15 minutes the slides were dehydrated in three different alcohol series, 70% ethanol, 90% ethanol and 100% ethanol for 5 minutes each solution. 1ml of 70% ethanol was added first for 5 minutes the 90% ethanol for another 5 minutes and finally 1ml of 100% ethanol for 5 minutes. These solutions were added to the slides to de-hydrate them. The slides were then air dried.

After air drying them they were ready for hybridisation. 20µl of FITC labelled telomeric probe hybridisation solution was added to each slide and covered them using cover slips. These were left on the heating block for 3 minutes at 70ºC. The slides were then placed in a dark damp container for 2 hours for hybridisation to take place.

After the 2 hours post-hybridisation washes were done, the cover slips on the slides were removed using the 70% formamide solution. The slides were then washed twice in coplin jars containing 70% formamide for 10 minutes each time. While doing this the coplin jars were not placed on the shaker.

The slides were then washed in PBS again, 3 times for 15 minutes, changing PBS every 5 minutes. The alcohol series washes were done again using 70%, 90% and 100% ethanol for 5 minutes each time. They were then air dried and 12ml of Dapi stain was added to each of the slides placing cover slips on them. The cover slips were sealed on the slides and were ready to view under the microscope.

2.11.1 Microscopy

The fluorescence microscope is used to capture images of all the cells. A programme referred to as IP-LAB (smart capture) is used to capture the images in both Dapi, which labels the DNA, in this case chromosomes and fluorescence, in this case FITC was used, which was used to label the telomeres. Interphase cells were captured.

It was important to ensure that the images taken were as sharp as possible so that analysis could be done accurately.

2.11.2 Analysis

To analyses IP-LAB software was used. To analyse using IP-LAB the image needed to be transferred to the software, where it was analysed using segment measurement tools. This calculates the amount of fluorescence present in the cells hence giving the total intensity present in the cell. This number corresponds to the length of telomeres in each one of the cells (Zijlmans et al., 1997). This fluorescence value was then converted to CCFL value as explained in section 5.2 of this thesis.

2.12 Alternative Telomere lengthening Pathway

For this protocol DNA was extracted as described in section 2.5.Once the DNA was extracted and measured using the nano drop. It was diluted in 1M Tris to give a concentration of 30ng.

For the first step of this assay the c-circles were amplified using Φ 29 DNA polymerase (NEB) in a PCR.

Table 2-8: The reaction mix for the C-Circles using PCR.

Stock Concentration	Volume (μl)	Final Concentration
1M DTT	0.8	4nM
10x Φ29 Buffer	2.0	1x conc
10mg/ml BSA	0.4	0.2mg/ml
10% Tween	0.2	0.1%
1mM dNTP (dATP/dTTP/dCTP/dGTP)	0.8	0.1mM
Φ29 DNA Polymerase (10000 U/ml)	1.5	15U
Nuclease-Free Water	4.3	

A total of 10μl of the master mix in Table 2-1 was added to the PCR tube plus 10μl of DNA. The reaction was incubated in the PCR for 8 hours at 30°C followed by 20mins for 65°C. The samples were then stored at -20°C or immediately slot-blotted.

2.12.1 Slot Blotting

Samples were slot-blotted using Amersham Biosciences Slot Blot filtration manifolds. The slot-blot was assembled using 1xnitrocellulose membrane (GE healthcare) and 1x Whatman filter paper which was pre-soaked in 2xSSC. Next the suction unit of the slot-blot was switched on. Samples were diluted in 40μl of 2xSSC, after which

the total volume in the PCR tubes of 60µl was added to the slot blot. Care was taken not to touch the nitrocellulose membrane. The samples were vacuumed for two minutes and laid with 100µl of 2xSSC to wash the remaining samples. The slot-blot was then unassembled and the membrane was allowed to dry. At this point either the membrane was stored at -80°C or if the probe was going to be added immediately the samples were immediately cross-linked using UV cross-linker (GE healthcare) at 1200J twice.

2.12.2 Hybridisation with P32-labelled telomeric probe

2.12.2.1 *Probe preparation*

To prepare the probe the c-rich telomere specific $(CCCTAA)_3$ (Thermo Fisher) oligonucleotides were end-labelled with ATP (γ-32P) (Perking Elmer) using DNA 5' end labelling system (Promega). To do this a stock concentration described in Table 2-9.

Table 2-9: Details of all reagents used for the probe labelling step.

Stock Concentration	**Volume needed (µl)**
Oligonucleotide 100µM	5µl
T4 polynucleotide kinase buffer 10x	1µl
T4 polynucleotide kinase enzyme	1µl
ATP (γ-32P) 3000Ci/mmol 10mCi/ml	3µl

Total volumes of 10µl of the reagents listed in Table 2-9 were incubated at 37°C for 10 minutes in a water bath. To stop the reaction 1µl of 0.5m EDTA was added to the

reaction, after which 40μl of saline TE (STE) buffer were added to the above 10μl probe buffer.

2.12.2.2 *Purification of p32 probe*

The newly prepared probe was washed to remove any unbound nucleotide or probe using column base chromatography (Perkin Elmer). The resin was re-suspended by vortexing for a few seconds. The bottom cap of the column was twisted and spun down to remove solutions from the resin at 735xg for 1 minute.

Immediately the probe mix samples (50μl in total volume) were added to the resin before the resin bed dried up. The column was then placed into a new clean 1.5ml eppendorf collection tube and the column was spun down for 2 minutes at 735xg. The purified probe was then stored at -20°C.

2.12.2.3 *Hybridisation*

The nitrocellulose membrane containing the slot-blotted cc assay amplified samples were placed in a glass hybridisation bottle and incubated at 10,l of pre-warmed hybridisation buffer (PerfectHyb Plus, Sigma- Aldrich) at 37°C for 15mins. This blocked the unspecific binding. Lastly, the freshly prepared C-rich telomeric probe labelled with P32 was added to the hybridisation bottle and allowed to hybridise overnight at 37°C.

The next morning the membrane was rinsed with high stingency wash buffer, which contained 0.5xSSC and 0.1% SDS at 37°C. This was done three times while shaking the whole time. After the membrane was washed it was wrapped in a hybridisation bag and exposed overnight onto x-ray film in the dark. The exposed x-ray film was

then developed using automated system (Xograph) and images were scanned for analysis.

2.12.3 Image analysis of CC assay

The x-ray films containing the developed images of the CC assay were scanned and the ImageJ software (NIH) was used to analyse the slot-blot pixel intensity. Then Microsoft Excel was used to analyse the data and generate the mean CC activity for each samples which corresponded to the ALT activity in the samples.

2.13 Statistical Analysis

I used Excel 2010 and GraphPad Prism 6 software to analyse my data for all statistics presented in sections 3.2 and 4.2. However, the statistical analyses in section 5.2 were done by our German collaborators (Prof. Jochen Graw's team) as uniform analyses were required for the paper that has been prepared for publication.

RESULTS

Analysis of telomere length and telomerase activity in Human Lens Epithelial Cells in association with cataracts

3.1 Introduction

From the time of Muller's discovery of the telomeres (Muller, 1938) to present day telomere biology has come a long way. Telomeres have become extremely important structures for studies and have been associated with a number of different processes in an organism. These include ageing and carcinogenesis; studies also show that progression of cancers can be lowered or raised by variations caused genetically in telomere maintenance (Blackburn, Epel and Lin, 2015)

In germ line cells and majority of cancers telomere length is maintained using an enzyme called telomerase. Telomerase is a reverse transcriptase enzyme made up of two mains sub-units. The two subunits are TERC and hTERT. The RNA component of the enzyme is TERC and the reverse transcriptase subunit is hTERT. TERC is present in all cell lines. However, the functional part of the telomerase complex is hTERT which is not present in all cell lines. For telomerase to be activated in a cell it is important for hTERT to be present. To analyse telomerase activity, percentage of hTERT present is measured in cells (Kim and Wu, 1997) (Wege et al., 2003).

In cancer cells telomere length is maintained either by the telomerase activity or by the ALT mechanism. If maintained by telomerase activity, telomere length is under 10kb and if maintained by the ALT pathway telomere length can vary between 3kb to over 50kb (Henson et al., 2002).

When cells divide to a point that telomeres become critically short, they enter senescence. Once cells enter telomere-initiated senescence DNA damage response proteins are activated. If these proteins are not activated the cell continues to enter S phase of the cell cycle (d'Adda di Fagagna, 2003). A number of studies in the last decade have shown that cells can re-enter the cell cycle after entering senescence. It is important to note that expression of hTERT in mammary epithelial cells and keratinocytes maintains telomere length, however does not allow these cells to bypass senescence. For cells to bypass senescence they require additional activation of signalling pathways (Lundberg et al., 2000).

One such study carried out on keratinocytes, shows an accumulation of reactive oxygen species, which have the ability to start off a mutagenic response in senescent cells. These studies show that the reactive oxygen species could be contributing to tumourgenesis, after senescence (Gosselin et al., 2009). Experiments conducted showed that senescence and the connected oxidative stress in epithelial cells could be tumour promoting.

Another kind of senescence is one through an activating mutation of the oncogene or inactivation of a tumour suppressor gene. This is referred to as oncogene induced senescence (Chandeck and Mooi, 2010). A study conducted in epithelial cells showed that cells bypass this senescence which triggers carcinogenesis. The study was conducted in the mammary epithelial cells. It showed that due to genomic instability in heterozygous mutant BRCA1 mammary cells they entered senescence prematurely. This type of senescence is termed haploinsufficiency-induced senescence (HIS) (Sedic et al., 2015). The evading of this pathway is thought to be involved in early onset of breast cancer in individuals with *BRCA1* mutations. The

cells that bypass HIS are shown to have increased telomere erosion and DNA damage but the exact mechanism effecting telomere maintenance is unknown (Sedic et al., 2015).

Therefore, it is not necessarily true that if cells enter senescence they stop to divide. They can re-enter the cell cycle and can be a cause of disease, in the case of the above mentioned examples; carcinogenesis is triggered.

However, carcinogenesis is not the only disease mechanism of interest in research today. Understanding the process of cataractogenesis, for example, is important because it represents the leading cause of blindness (47.9%) according to the World Health Organisation (Organisation, 2016). Cataract is typically an age related disorder which forms over a period of time and the chances of getting cataracts increases with age (Graw et al., 2011). Factors contributing to this include: genetic disposition, radiation exposure and even smoking (Graw, 2003). Hence, it is typically an age related disorder but not absolutely. Moreover, it is not a matter of whether the cataracts will form but when. It is not an all or nothing situation, rather an earlier onset than a later onset, as described in the KORA eye study (Graw et al., 2011).

Recently, a lot of research has been directed into understanding the structure of the lens and the changes that take place when cataracts form. These studies are conducted both at a structural and at a molecular level, as the aetiology of cataracts is still ambiguous (Ainsbury et al., 2009).

To determine whether telomere length and telomerase activity play a role in cataractogenesis, HLE cells from different donors were used. Having a number of cell donors means being able to look at the genetic disposition of cataracts in relation

to telomere function. For each of the experiments, cells from three different Donors were used. These were labelled as Donor 1, Donor 2 and Donor 3. All cells for the three donors were bought from Caltag Medsystems (SC-6550).

3.2 Results

3.2.1 Summary of methodologies available for telomere length measurement

As discussed in both the introduction of this chapter and the main introduction of this thesis, telomeres play an important role in an organism. Understanding the changes in their length is essential as their shortening leads to a number of different problems, like cancer, premature ageing and even obesity (Tzanetakou et al., 2011).

This means that measuring telomere length accurately is vital. There are a number of different techniques available to measure telomere length. Therefore it is of the essence to decide which methodology is appropriate to use for any given experiment. For this chapter we analysed the advantages and disadvantages of the available methodologies, to decide which one would suit best the analysis of HLE cells.

3.2.1.1 *Southern Blot*

Southern Blot was the first technique that was developed to measure telomere length in humans (Allshire, Dempster and Hastie, 1989). The method was designed to give the average length of the telomeres in the cell. It was noted that telomeres did not comprise solely of TTAGGG repeat signals but other sub-telomeric signals, which include TTGGGG and TTTAGGG signals (Allshire, Dempster and Hastie, 1989). This technique is considered to be accurate enough to give an average

telomere length. However there are concerns as it measures sub-telomeric signals as well.

It was noted that even though these sub-telomeric signals are part of the telomere, they do not change in number of repeats as the telomere shortens, due to the end replication problem. The length of the telomere is determined by how many TTAGGG repeats there are present in the chromosome and these are the only sequences that decrease in number as the telomere shortens.

This method gives the average length of the telomeres in a cell using terminal restriction fragments (TRFs) (Kimura et al., 2010). To measure the telomeres, DNA is extracted from the cell line in question and restriction enzymes are used to cut it in the appropriate areas. Specially designed labelled oligonucleotide probes, which target telomere sequences, are also used for hybridisation with the TRFs. The amount of hybridisation between the telomeric signals and probes is calculated giving the average number of telomeres present in the cell (Allshire, Dempster and Hastie, 1989).

The method is time consuming and requires large amounts of DNA (Cawthon, 2002). Telomeres cannot be measured in some cell lines using this method as they are not within the detection boundaries of this approach, examples of these are mouse cell lines (Slijepcevic, 2001). It is useful to be able to measure telomeres in mouse cell lines as many knock down and knock out experiments are done on mouse models. This method is better for measuring shorter telomeres.

3.2.1.2 *Fluorescence In-Situ Hybridisation (FISH)*

FISH, Fluorescence In-Situ Hybridisation, is a very commonly used cytogenetic method which is used to detect specific DNA sequences in the genome. In the direct method of labelling the probe contains nucleotides which contain a fluorophore whereas in the indirect method a nucleotide containing a hapten is used. There are three main ways of labelling these include: PCR, Nick translation and random primed labelling (Speicher and Carter, 2005).

Q-FISH stands for Quantitative Fluorescence In-Situ Hybridisation (Volpi and Bridger, 2008). It was first used to measure mouse telomeres in 1997 (Zijlmans et al., 1997). This immediately solved the problem faced when using the southern blotting method as mouse telomeres cannot be measured using that method. Furthermore, Q-FISH does not measure average telomere length but measures individual telomere length in a cell which none of the other methods is capable of doing.

In this method, cells are extracted and fixed to a slide using standard FISH procedures. The cells require arresting at metaphase and this is done using a chemical known as colcemid (Zijlmans et al., 1997). Fluorescently labelled Peptide Nucleic Acid probes (PNA) made of the CCCTAA sequence, complementary to telomeres are used (Zijlmans et al., 1997). In PNA probes the backbone is made up of peptides instead of phosphodiester backbone as found in DNA (Ray and Norden, 2000). These PNA probes have higher hybridisation percentage compared to RNA and DNA probes. This is because the PNA backbone has no charge whereas RNA and DNA backbone is usually negatively charged. This charge causes repulsion during hybridisation. The fluorescence intensity is measured using TFL-TELO, a

software readily available on the internet. The fluorescence intensity corresponds to the telomere length in the cell (Zijlmans et al., 1997).

Q-FISH is capable of analysing telomeres as short as 200 base pairs (McIIrath et al., 2001). Unlike Southern blotting, Q-FISH can measure individual telomere length. However, the major disadvantage of Q-FISH is that it is very time consuming due to the chromosome preparation step where cells need to be arrested at metaphase, and also because it takes long to analyse the cells. This means that it is difficult to analyse many cells at one particular time (Derradji et al., 2005). Within Q-FISH, techniques such as STELA are used to measure single telomeres (Volpi and Bridger, 2008).

To solve the problem of time consuming analysis in Q-FISH another technique within it was developed, Flow-FISH (Rufer et al., 1998). In this technique same principles as Q-FISH are used, but the telomere length is measured as an average length per cell, and many cells can be analysed in a short period. To perform this measurement a flow-cytometer is required, which is a very expensive piece of equipment. The major disadvantages of this technique are its cost to run and that it only produces average telomere length.

The Q-FISH methods used to measure telomeres have certain problems, to overcome some of the problems a new method was developed, Interphase Q-FISH. This method is considered to be accurate compared to southern blotting, faster than Q-FISH and less expensive then Flow-FISH. This methodology was designed in Dr Predrag Slijepcevic's lab.

3.2.1.3 *Absolute telomere length qualitative PCR (aTL q-PCR)*

Q-PCR is a more accurate method compared to southern blotting and uses specifically designed primers that target telomeres (Cawthon, 2002). The main disadvantages of this methodology are the long preparation time, need of accuracy while preparing plates and it is expensive in comparison to IQ-FISH. Two different primers are used for this methodology, a single copy gene 36B4 and telomere gene (O'Callaghan and Fenech, 2011). The single copy gene acts as the reference gene in this case and the telomere length is used to measure the length in each sample against this single copy gene. It acts as the reference gene. This methodology is sensitive and reliable hence is the one used more often in studies these days.

All the methodologies discussed above were considered for this chapter. It was decided after analysing the advantages and disadvantages of each technique, summary of which is shown in (Table 3-1) that aTL q-PCR is the right method to use for HLE cells. It is most accurate method at present, because the results give telomere length directly in kilobases/diploid genome based on the power of q-PCR approach. The telomere length is given as an average of all the cells which is appropriate for this study.

Table 3-1: Comparison of telomere length measurement methods.

Methodology	Advantages	Disadvantages
Southern Blot	• First technique developed for telomere analysis • Average Telomere length analysed	• Measures sub-telomeric signals also • Time consuming • Cannot measure some telomeres as they are not in range
FLOW FISH	• The speed and the power of	• Expensive • Only average telomeres analysed
FISH	• Accurate • Faster than most methods • Can measure very short telomeres down to 200 bp.	• Average telomere length
Q-PCR	• More accurate than the other techniques because of the power of q-PCR	• Expensive • Time consuming

3.2.2 Optimisation of aTL q-PCR

Therefore, a fairly new methodology, that is q-PCR based approach to measure telomere length, aTL q-PCR (O'Callaghan and Fenech, 2011), was used in this chapter. It has not been used in Dr Predrag Slijepcevic's lab before. Therefore optimisation was required.

To start off with, DNA was extracted from U2OS, HeLa and GM08399 cell lines and stored at -20^{o}C. Once the DNA was extracted the protocol established by (O'Callaghan and Fenech, 2011) was used. Detailed methodology for this purpose has been described in section 2.9 of this thesis.

For this first experiment, primer concentration for standard curves was established for each primer, the telomere binding primer and the primer specific for the 36B4 gene, which is a house keeping single copy gene (Table 3-2). This was important as

the data from serial dilutions was used to generate the standard curve. Different dilutions were used for both primers ranging in concentration between 0.1nM to 50nM (Table 3-2). It was noted at the end of this run that no ct value was gathered for the 50nM concentration of the 36B4 single copy gene (Table 3-2). This is most likely because the concentration was too high.

Table 3-2: Data generated from the serial dilution for both 36B4 and Telo Primer. The left part of the table shows the results from the 36B Primer and the right part shows the results from the Telo primer. The Ct value corresponding to each concentration has been presented.

36B4 Primer Conc nM	Copies of SCG	Log of [36B4 copies]	Ct	Telo Primer Conc nM	TL in Kb	Log [TL in KB]	Ct
50	30625000	7.486076		50	5092000	6.706888	8.048856
10	6125000	6.787106	6.905877	10	1018400	6.007918	12.09023
5	3062500	6.486076	7.488753	5	509200	5.706888	16.31865
1	612500	5.787106	9.752463	1	101840	5.007918	24.52293
0.5	306250	5.486076	10.95019	0.5	50920	4.706888	29.14665
0.1	61250	4.787106	13.53233	0.1	10184	4.007918	36.85155

Therefore, for the rest of the experiments the concentration of 0.1nM to 10nM was used for the single copy gene and 0.1nM to 50nM for the telomere primer. The standard curves for these concentrations are presented in (Figure 3-1).

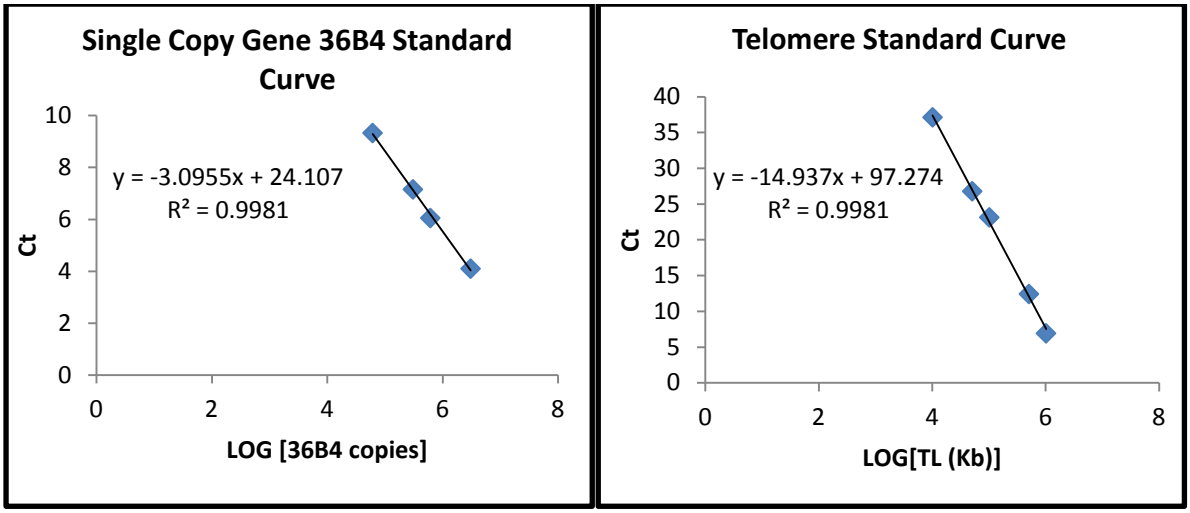

Figure 3-1: Standard curves for aTL q-PCR. Figure shows an example of the generated standard curved while optimising the aTL q-PCR protocol. A) Standard curve for calculating genome copies using 36B4 copy number with correlation coefficient of 0.9981. B) Standard curve for calculating length of telomere sequence per reaction tube: the x-axis represents the amount of telomere sequence in kb per reaction with correlation coefficient of 0.9981.

An example for the amplification results for telomere measurement using q-PCR have been presented in (Figure 3-2). This shows all amplification that took place in each well.

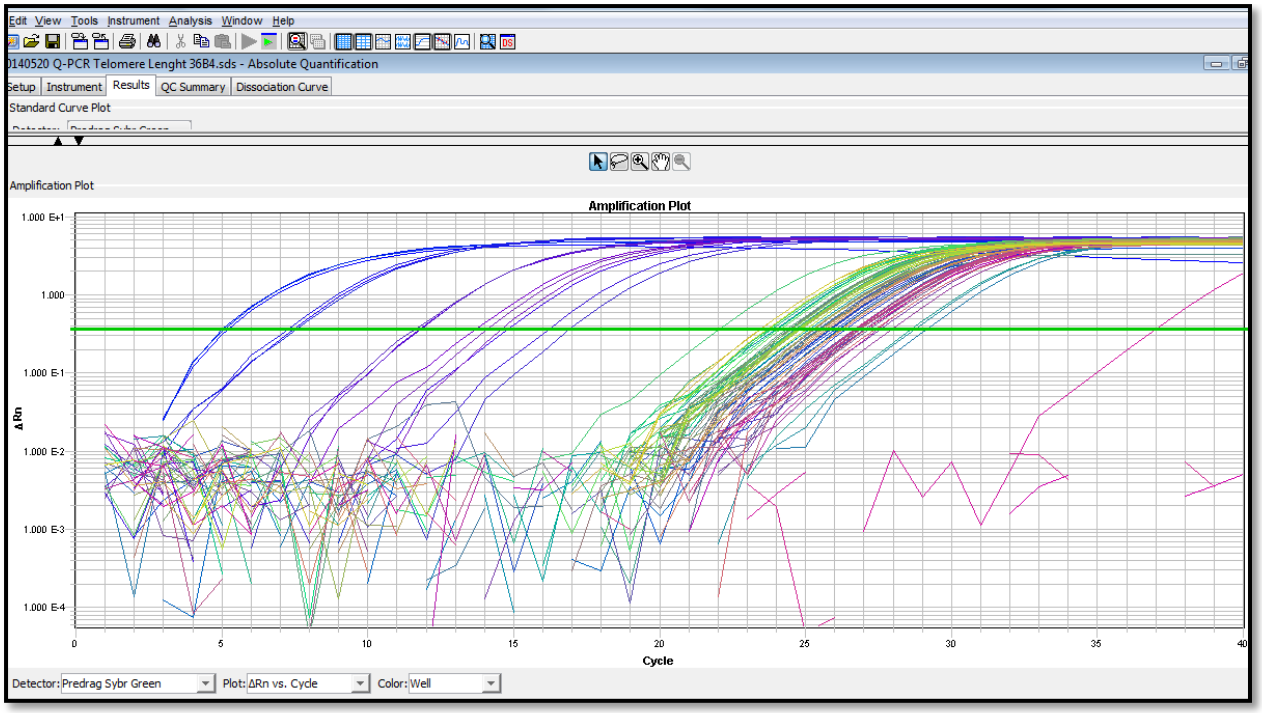

Figure 3-2: Example of **plotted amplification for aTL q-PCR assay.** An example of plotted amplification of results from a q-PCR run for telomere length analysis. The results shows the amplification for each sample run in the plate.

For the telomere length measurement protocol a dissociation curve was generated at the end of the PCR run. This curve shows any primer dimers and the accuracy of the run. An example of this is presented in (Figure 3-3).

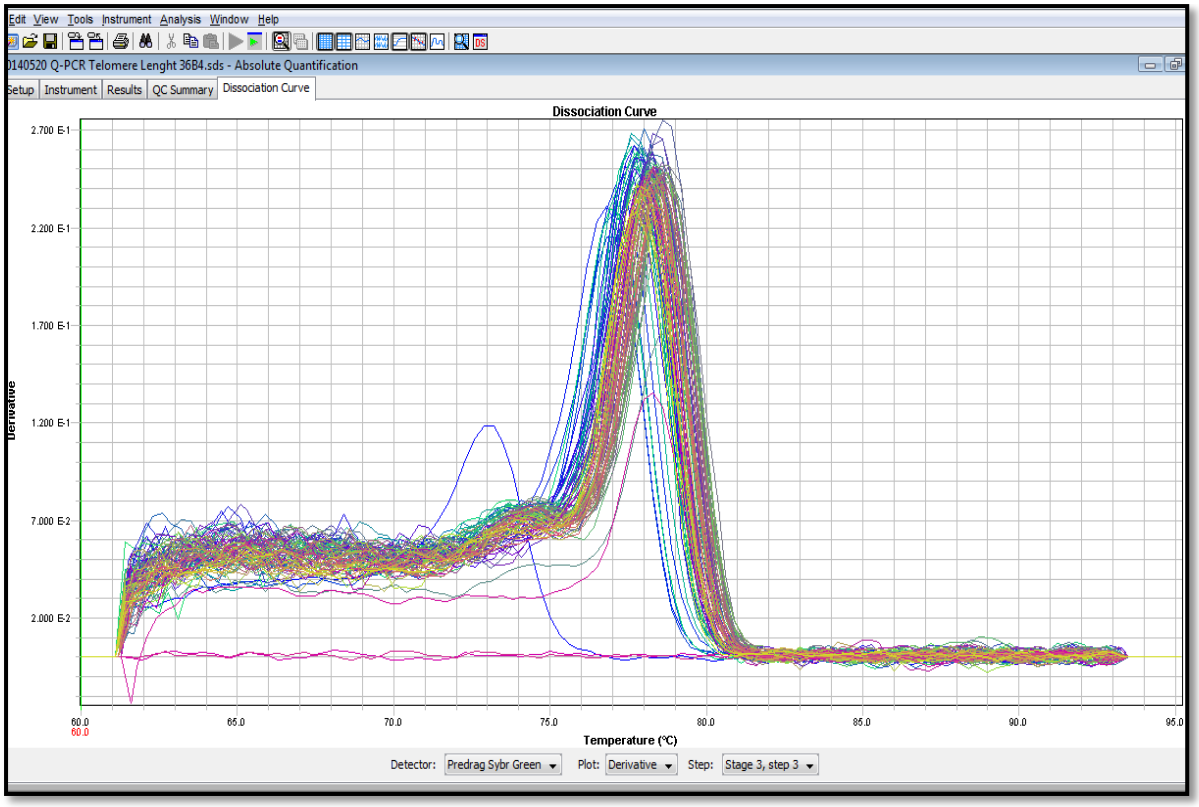

Figure 3-3: Example of dissociation curve. An example of a dissociation curve for the telomere length measurement assay. Any primer dimers can be noted here. The curve needs to show one peak per sample as seen in this figure. This shows that there is only one product per sample ran.

The results from this section were compared to previous results from a study conducted in Dr Predrag Slijepcevic's lab, while establishing IQ-FISH. In the study telomere length was measured in HeLa and U2OS cells. The IQ-FISH results showed 60% greater telomere length in U2OS cells compared to HeLa cells (Dr Maryan Ojani PhD thesis). Telomere length in human primary cell lines has been measured and estimated previously to be in the region of 5kb – 15kb (Samassekou et al., 2010).

To establish if my results are in line with previously published results, telomere length was measured by aTL qPCR in GM08399, U2OS and HeLa cell lines. Results of the analysis are presented in (Figure 3-4). From previous studies it is known that

U2OS cells have long telomeres maintained by the ALT pathway (Jegou et al., 2009). HeLa cells have much shorter telomeres than U2OS cells, which is in line with published work, showing longer telomeres in ALT positive cells compared to telomerase positive cells (Cerone, Londono-Vallejo and Bacchetti, 2001). Primary human cell lines, such as GM08399, are expected to show telomere length longer than HeLa but shorter than U2OS cells. Therefore, a trend of long telomeres for U2OS, medium length for GM08399 and shortest telomere length for HeLa should be observed. It can be seen from (Figure 3-4) that this pattern was observed. Therefore, we can conclude that the optimization of the aTL qPCR protocol including primer concentration establishment has worked appropriately.

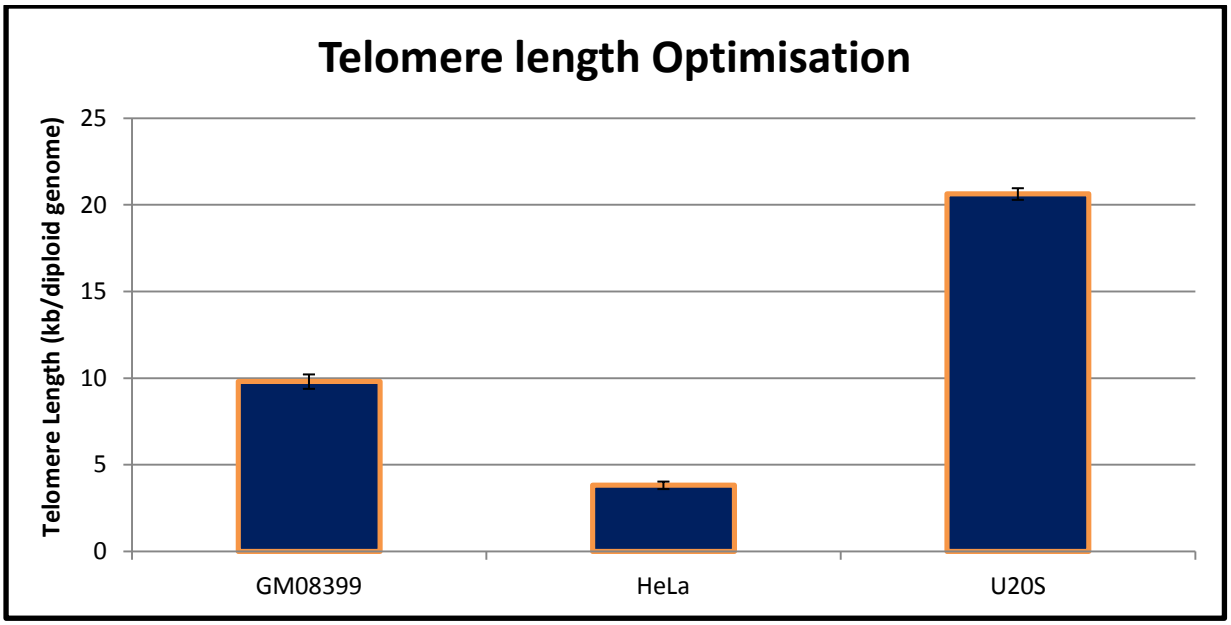

Figure 3-4: Telomere length optimisation. Telomere length measurement in GM08399, HeLa and U2OS cells. Data represents average of three runs. The results show longest telomere length in U20S cells, followed by GM08399 and the shortest telomeres are noted in HeLa cells. Error Bars represent S.E.M.

Once the accuracy of the protocol was determined it was important to establish if it can be used to measure small changes in telomere length. To do this telomere

length was measured in the primary fibroblast cell line, GM08399, over a period of several passages. Results of this analysis are shown in (Figure 3-5). The results show a decrease in telomere length as the cells age. A difference of 9.47kb/haploid genome was noted in these cells between passage 6 and passage 20. This showed that the method is not only accurate but also sensitive in measuring telomere length changes over time in a single cell line.

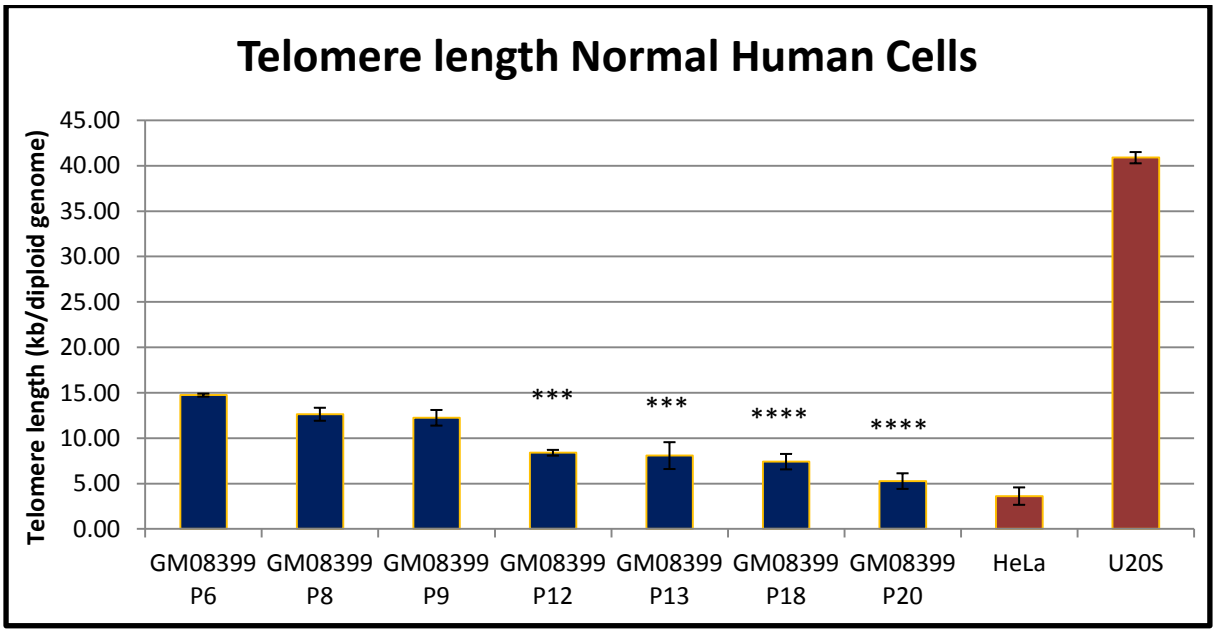

Figure 3-5: Telomere length measurement in GM08399 cells. The figure shows telomere length in different GM08399 passages (blue bars). A decreasing trend of telomeres is noted in GM08399 samples as passage increases. Telomere length in control samples, HeLa and U2OS (red bars). Error bars represent S.E.M. (*** P<0.001, **** P<0.0001)

Having established the working aTL q-PCR protocol for telomere length measurement and having demonstrated its accuracy on primary human fibroblasts which showed expected rate of telomere shortening with time, we were satisfied that the protocol is suitable for measuring telomere length in HLE cells from three different donors.

3.2.3 Telomere length measurement in HLE cells

The aim of the experiments with HLE cells was to assess the effect of radiation on telomere length and telomerase activity in association with lens opacity. All radiation experiment results are presented in next chapter. Here, we will present results of telomere length analysis and telomerase activity in non-irradiated samples. These results essentially constitute control samples for radiation experiments presented in next chapter (referred to as SHAM irradiated samples). The HLE cells were collected and irradiated with our project collaborators at Oxford Brookes University. The cells were processed for DNA and protein extraction at Brunel University. Samples for both the telomere length measurements and telomerase activity were collected as control non-irradiated samples at the same time when collection was done in the case of irradiated samples 30mins post irradiation. Thereafter, the cells were incubated at 37^{o}C and left to become confluent. Cells were harvested after each passage until cells stopped growing. Cells collected post-confluence and in each subsequent passage are referred to as the delayed samples.

Telomere length was analysed after each passage starting from P5 in each of the Donor's cells. For each run of aTL q-PCR three control cell lines were also analysed for telomere length, U2OS, HeLa and GM08399.

The results of the analysis for cells from Donor 1 are shown in (Figure 3-6). Interestingly, we did not see the expected trend of telomere shortening with passage number as in the case of control fibroblast cells (Figure 3-5). Instead, we observed telomere length increases with the passage time. The increase in telomere length amounted to a total of 11.86 kb/diploid genome when cells in P5 delayed and P8 Delayed were compared or 8.02 kb/diploid genome when cells in P5 30mins and P8

Delayed were compared. We observed the difference between the P5 30mins sample and the P5 Delayed sample. However, this difference was not significant (Figure 3-6). This difference was noted and can be due to the difference in confluency of cells when DNA was extracted.

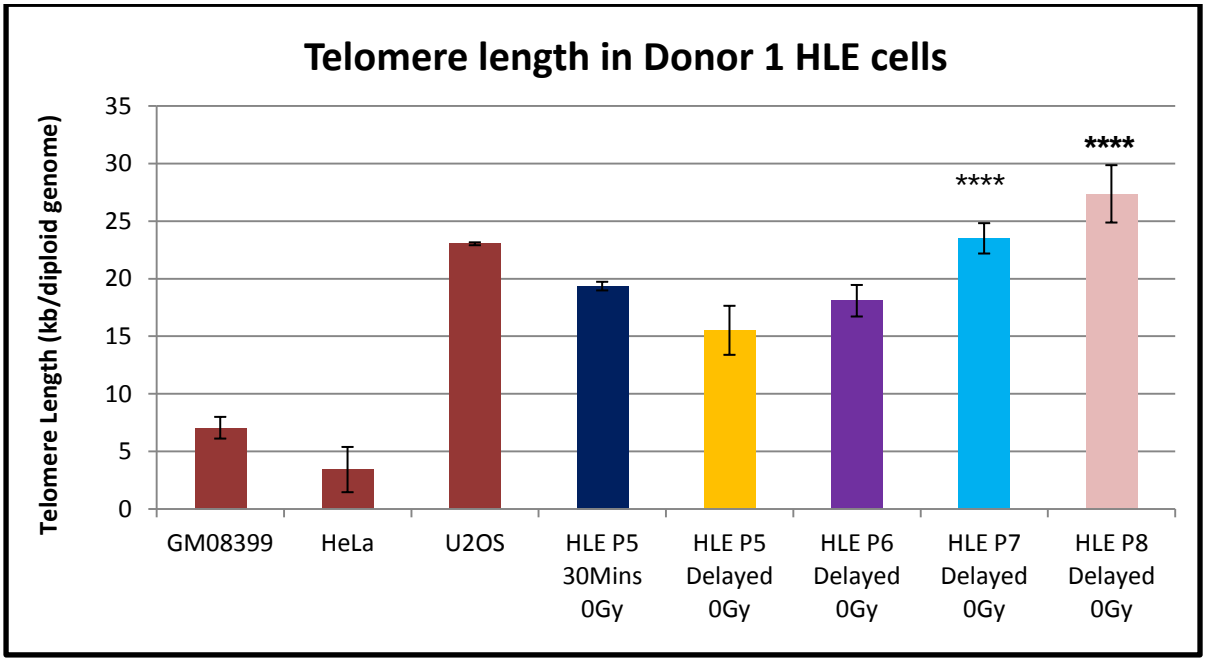

Figure 3-6: Telomere length in HLE Donor 1 cells. Figure shows telomere length in different passages in HLE donor 1 cells. An increase in telomere length is noted in the cells as the passage increases. Blue bar represents HLE donor 1 cells 30mins after radiation and yellow, purple, light blue and pink bars represent delayed donor 3 cells at different passages. Red bars represent controls. Error bars represent S.E.M. (**** P< 0.0001)

The results for HLE cells from Donor 2 are shown in (Figure 3-7). We observed the same trend as in (Figure 3-6). It is important to mention that the Donor 2 cells grew poorly and could not grow beyond P6. The calculated increase in telomere length was 3.22 kb/diploid genome when comparing the P5 delayed sample against the P6 delayed sample. The difference between P5 30mins and P6 delayed sample amounted to 4.74 kb/diploid genome.

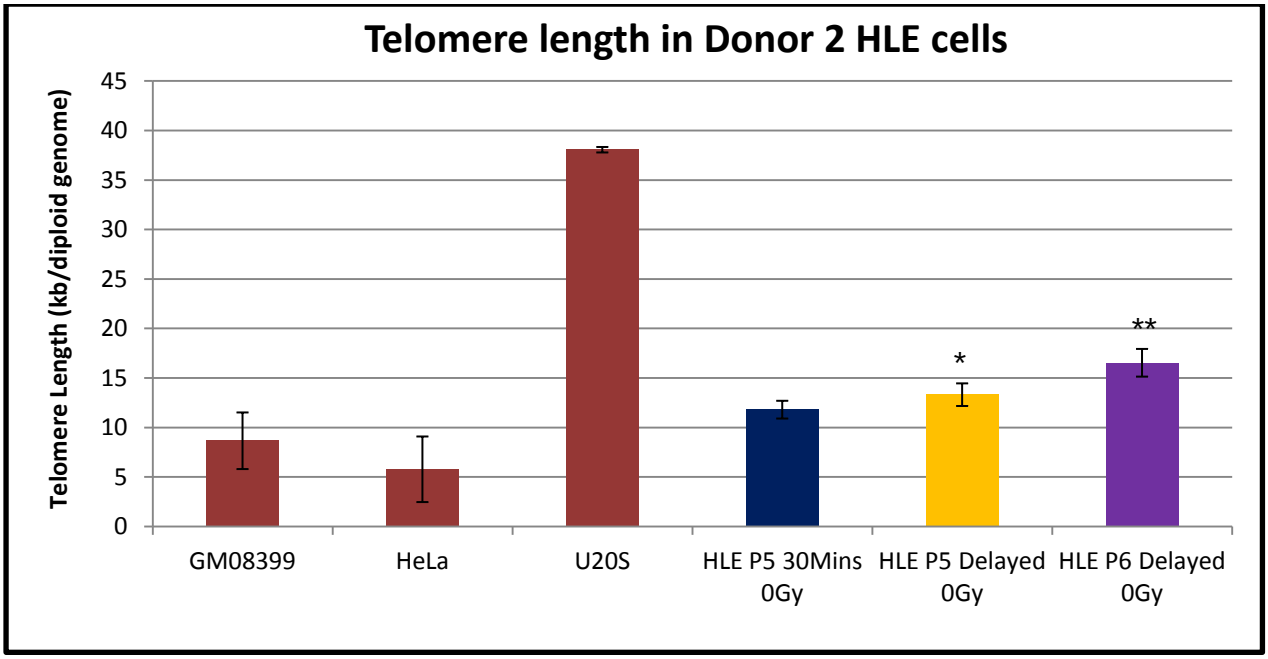

Figure 3-7: Telomere length in HLE Donor 2 cells. Figure shows telomere length in different passages in HLE donor 2 cells. An increase in telomere length is noted in the cells as the passage increases. Blue bar represents HLE donor 2 cells 30mins after radiation and yellow and purple bars represent delayed donor 3 cells. Red bars represent controls. Error bars represent S.E.M. (* $P<0.05$; ** $P<0.01$)

The result of telomere length analysis for Donor 3 HLE cells is shown in Figure 3-8. In contrast to HLE cells from Donors 1 and 2, HLE cells from Donor 3 did not grow at all beyond passage 5. We observed a difference between P5 30 mins and P5 Delayed samples. This difference can be explained due to the difference in confluency of cells in each flask. We found that the flask containing the P5 delayed sample compared to the P5 30mins was more confluent, suggesting that the flask had undergone a number of more population doublings.

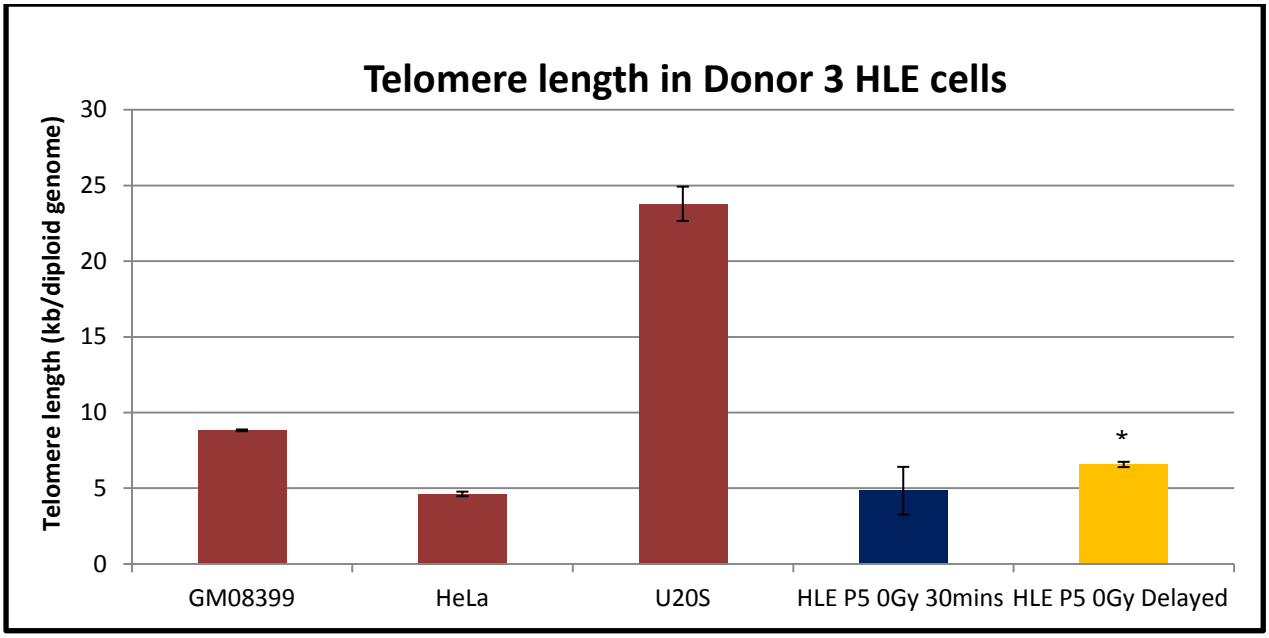

Figure 3-8: Telomere length in HLE Donor 3 cells. Figure shows telomere length in different passages in HLE donor 3 cells. An increase in telomere length is noted in the cells as the passage increases. Blue bar represents HLE donor 3 cells 30mins after radiation and yellow bars represent delayed donor 3 cells. Red bars represent controls. Error bars represent S.E.M. (* P <0.05)

3.2.4 Population Doublings

To establish the rate of telomere changes relative to population doublings we counted cells in each passage to establish the number of population doublings per passage. Cells were grown at a recommended density of 5000 cells/cm^2. The cells were incubated until confluent and at each passage split and grown again. At each point of splitting the cells were counted and seeded at a 5000 cells/cm^2 density. Population doubling was counted using the formula; $\{Population\ doubling = \left(\frac{\log N1}{Log\ 2}\right) - \left(\frac{Log\ N0}{Log\ 2}\right)\}$, where *N1* is the final count of cells and *N0* is the initial count of cells.

We received the cells from our collaborators at different passages. As can be seen from (Table 3-3) each HLE sample grew for different periods of times. Cells from

Donor 1 grew for the longest period of time and had a cumulative population doubling of 6.46. Cells from Donor 2 grew for three passages and had a cumulative population doubling of 4.52. Finally, cells from Donor 3 were received from our collaborators at P5 and only grew for another passage. Cells from Donor 3 had a cumulative population doubling of 1.33.

Table 3-3: Details of population doubling per passage in HLE cells from all three Donor cells.

Passage	Donor 1	Donor 2	Donor 3
P4-P5	2.66	2.98	
P5-P6	1.92	1.42	1.12
P6-P7	1.49	0.11	0.21
P7-P8	0.39		

Furthermore to compare the telomere length in the HLE donor cells we grew normal fibroblast, GM08399 cells. The population doubling for these normal fibroblast cells have been presented in (Table 3-4). A cumulative population doubling of 77.36 was observed in these cells over a period of 14 passages. These results are in line with those presented by Dr Erik Cabuy in Dr Predrag Slijepcevic's lab where these same cells were used for his thesis. He found a total of 22.1 population doublings in 5 passages.

Table 3-4: Details of population doubling per passage in GM08399 cells.

Passage	GM08399
P6-P7	6.87
P7-P8	5.15
P8-P9	6.65
P9-10	6.97
P10-P11	5.77
P11-P12	6.58
P12-P13	5.46
P13-P14	5.11
P14-P15	5.98
P15-P16	5.88
P16-P17	5.79
P17-P18	5.99
P18-P19	3.37
P19-P20	1.79

To calculate the rate of telomere length change per population doubling we used the results of telomere length measurements from (Figure 3-5 - Figure 3-8) which are then summarized in (Table 3-5, normal fibroblasts) and (Table 3-6, HLE cells).

Table 3-5: Telomere length and population doubling information for GM08399 cells. The telomere length has been presented in kb/diploid genome and bases of DNA. The table also shows figures of cumulative population doubling for GM08399 cells over a period of P6 to P20.

Passages	Telomere length kb/diploid genome	Telomere length Bases
P6	14.75	14750
P8	12.64	12640
P9	12.25	12250
P12	8.4	8400
P13	8.08	8080
P18	7.42	7420
P20	5.28	5280
Total	68.82	68820
Difference Telomere length bases		**9470**
Cumulative population Doubling		**77.36**

Table 3-6: Telomere length and population doubling information for HLE Cells. The table shows telomere length in all three donors both in kb/diploid genome and in bases of DNA. The table also presents the cumulative population doubling of each donor.

Passage	Donor 1 Kb/diploid genome	Donor 2 Kb/diploid genome	Donor 3 Kb/diploid genome
P5	19.36	11.8	4.83
P5 Delayed	15.32	13.32	6.57
P6	18.09	16.54	
P7	23.51		
P8	27.38		
Total	103.66	41.66	11.4
Total Bases	103660	41660	11400
Difference Telomere length Bases	**8020**	**4740**	**1740**
Cumulative Population Doubling	**6.46**	**4.52**	**1.33**

To calculate the rate of telomere length per population doubling, cumulative population doubling was divided by the number of base pair changes for each cell line (Figure 3-9). For GM08399 cells, a loss of 122.42 bases per population doubling was observed. The results for GM08399 cells is within the range of telomere loss expected in normal cells, where telomeres are lost at a rate of 40 to 200 bases per cell division (Henson et al., 2002).

These results are also in line with results from an earlier PhD student in our laboratory (Dr Erik Cabuy), where he showed telomere shortening in GM08399 cells at a rate of 97.7 bases per population doubling when measured with southern blot and 93.4 bases when measured with flow-FISH. This on its own shows that the methodology used in this section was optimised well and worked effectively to measure telomeres.

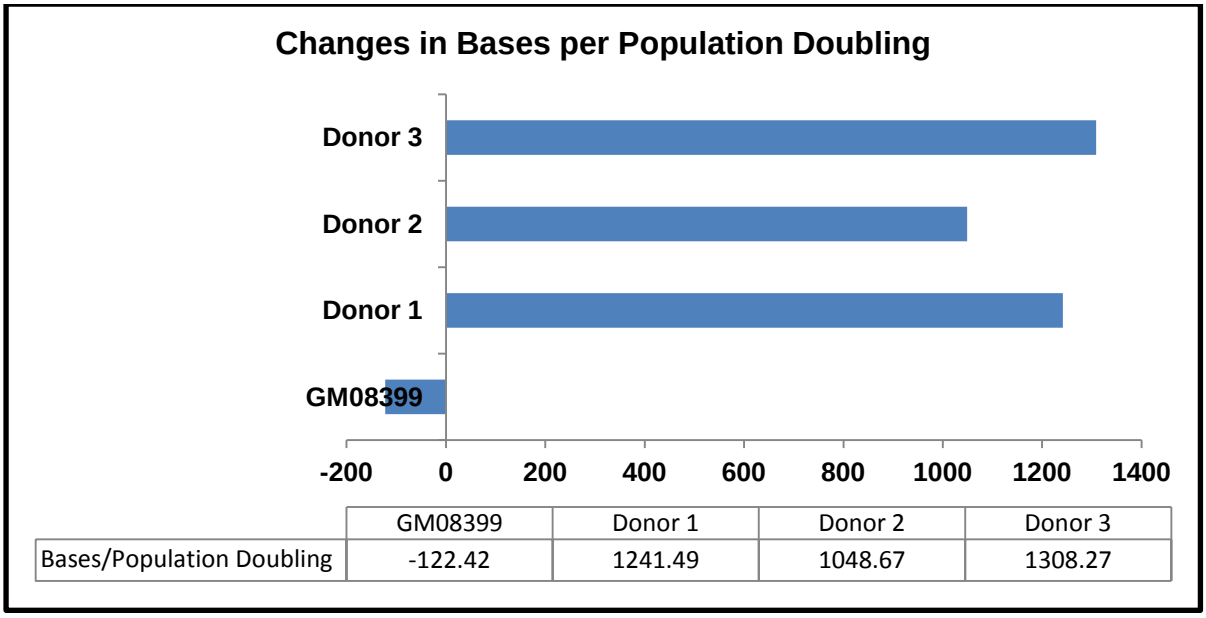

	GM08399	Donor 1	Donor 2	Donor 3
Bases/Population Doubling	-122.42	1241.49	1048.67	1308.27

Figure 3-9: Rate of telomere length change per population doubling. Figure shows the rate of telomeric base changes per population doubling in GM08399 and HLE cells. For GM08399 cells, a loss of telomere length can be observed whereas for HLE cells a gain in telomere length can be observed per population doubling.

3.2.5 Telomerase activity in Human Lens Epithelial Cells

Next, we wanted to probe the causes of telomere length increase in HLE cells with population doublings. Telomere length in human cells is maintained either by telomerase or the ALT pathway. We started with monitoring telomerase activity. As controls, we used the MCF-7 cell line (positive control) and the U2OS cell line as negative control (Cerone, Londono-Vallejo and Bacchetti, 2001) (Perrem et al., 2001).

For telomerase activity analysis a q-PCR based assay, TRAP was used. TRAP stands for Telomeric Repeat Amplification Protocol. For this two primers were used: a ACX primer; which is the reverse primer and TS primer, which is the telomerase substrate. For protein extraction we used CHAPS buffer as described earlier (Wege et al., 2003).

The telomerase positive prostate cancer cell line, PC3 hTERT, was used to generate a standard curve (Figure 3-10). PC3 hTERT cells were serially diluted at a concentration between 10^3 -10^6.

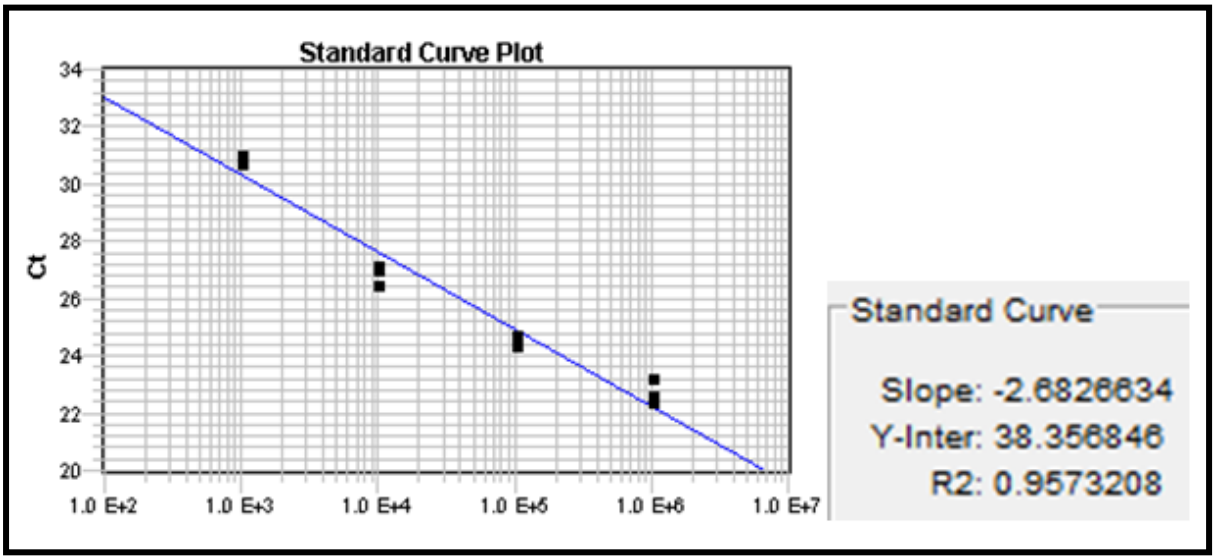

Figure 3-10: Standard curve for TRAP assay. The standard curve generated from serially diluted PC3 hTERT cells at a concentration of 10^3 - 10^6. This standard curve was used to get the concentration of the unknown samples.

PC3 hTERT cells were also used as the 100% telomerase positive control, against which telomerase activity in all other cell lines was measured.

It can be seen from (Figure 3-11) that telomerase activity is present in non-irradiated HLE cells from all three Donors. It can also be seen that the telomerase activity decreases as the passages increase and at P6 telomerase activity is very low, close to insignificant when compared against GM08399 cells which are used as our negative control. It can also be seen that telomerase activity in normal human cells is very low as expected.

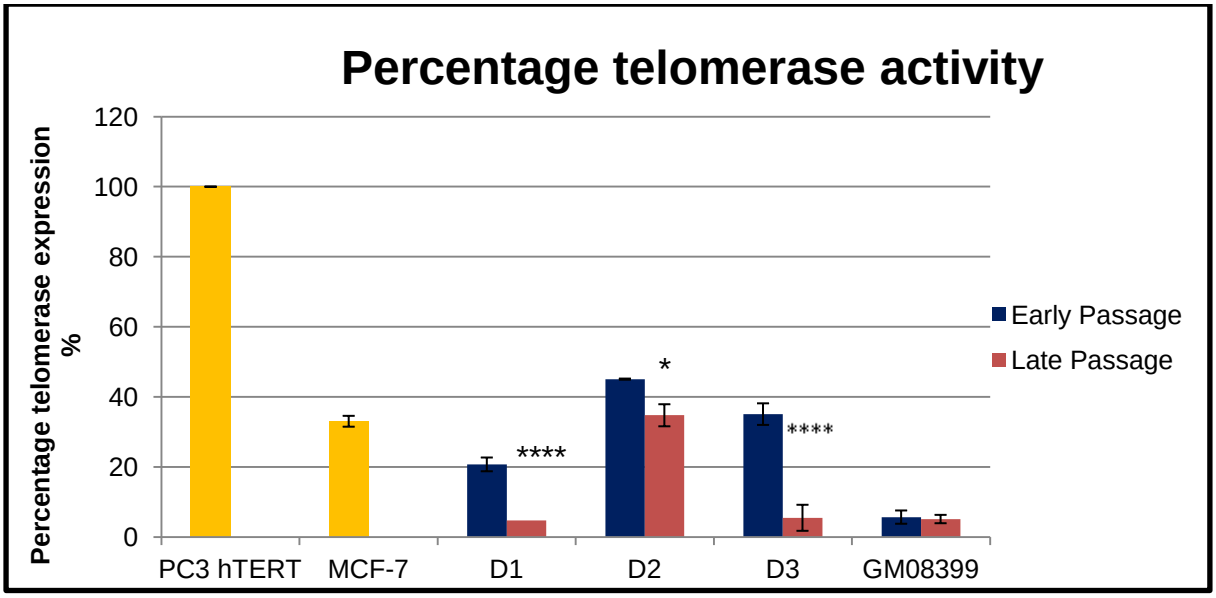

Figure 3-11: Telomerase activity in HLE cells. Figure shows the telomerase activity at different passages in the three different Donor's cells [D1 (Donor 1), D2 (Donor 2), D3 (Donor 3)] and in GM0899. The figure shows results at an early passage and a late passage. Blue bars represent early passages. Red bars represent late passages. Yellow bars represent controls. Error bars represent S.E.M. (* P>0.05; **** P>0.0001)

3.2.6 ALT c-cirlce assay

We also wanted to identify whether the ALT pathway may contribute to observed increase in telomere length with population doubling in HLE cells. Previous research on Friedreich ataxia fibroblasts has shown a presence of long telomeres in the absence of telomerase, and markers of ALT, PML bodies suggesting that there could be an involvement of ALT-like mechanism hence resulting in long telomeres (Virmouni et al., 2015). Therefore, it was decided to identify if ALT played a role in the increase in telomere length as telomerase decreased in HLE cells. The assay that identifies the ALT activity unequivocally is called the C-circle assay (Loretta et al., 2012). For the assay we used three different control cell lines. HeLa, a telomerase positive cell line and a human fibroblast cell line, GM08399, were used

as negative controls. The U2OS was used as the positive control cell line (Jegou et al., 2009).

We first needed to establish the right amount of DNA concentration to use for the assay. To do this 5 different concentrations of U2OS DNA were used, 50ng, 40ng, 30ng, 20ng and 10ng (Figure 3-12). These concentrations served for the establishment of the calibration curve.

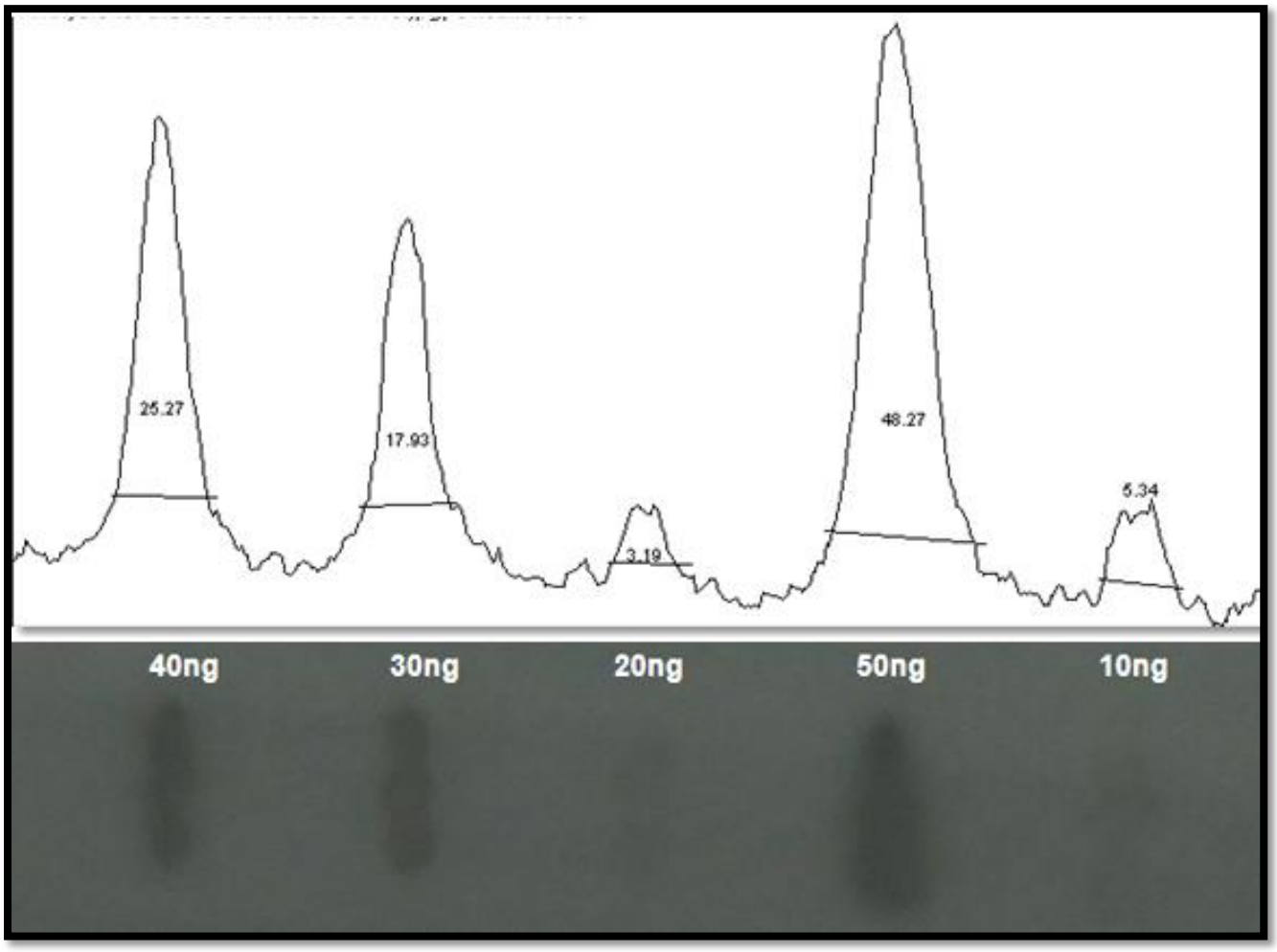

Figure 3-12: Calibration curve from ALT c-circle assay. The figure shows the results of the different U2OS concentrations. This was used to generate a calibration curve. The peaks represent results of analysis done on the film using the ImageJ software.

The results showed that three of the concentrations produced good bands: 50ng, 40ng and 30ng. Therefore, the smallest amount of DNA required was used as HLE cells are expensive and were only available in small quantities to us.

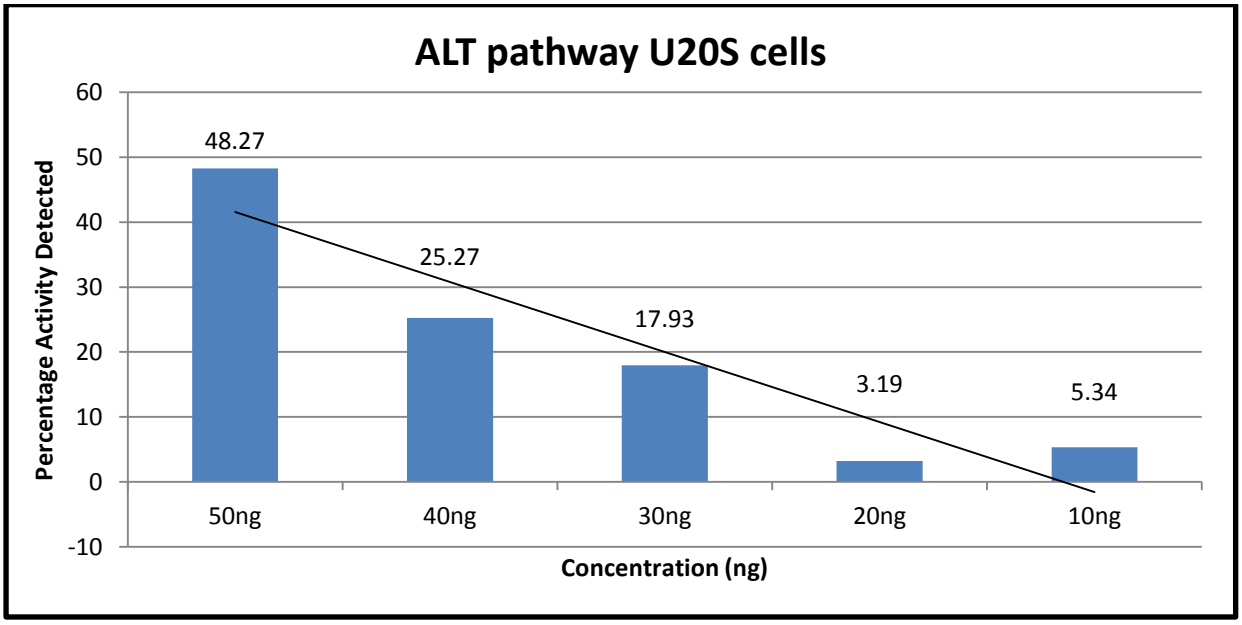

Figure 3-13: Calibration curve for ALT pathway. The figure shows the results represented in Figure 3-12 as a graph. The results from Figure 3-12 were used to generate a graph representing U2OS intensity as ALT percentage. This was done using different DNA concentrations of U20S.

Results were used to plot a linear regression line shown in (Figure 3-13). For the actual experiment with HLE cells all the samples were ran together with the controls (GM08399, HeLa and U2OS). This experiment was repeated twice to ensure results were consistent. Alongside the control two concentrations of HLE 30mins D3 2Gy were ran 10ng and 50ng. The HLE sample used for different concentrations used was selected as more DNA was available for this sample. This was done to ensure that changing concentrations in these samples would not affect results.

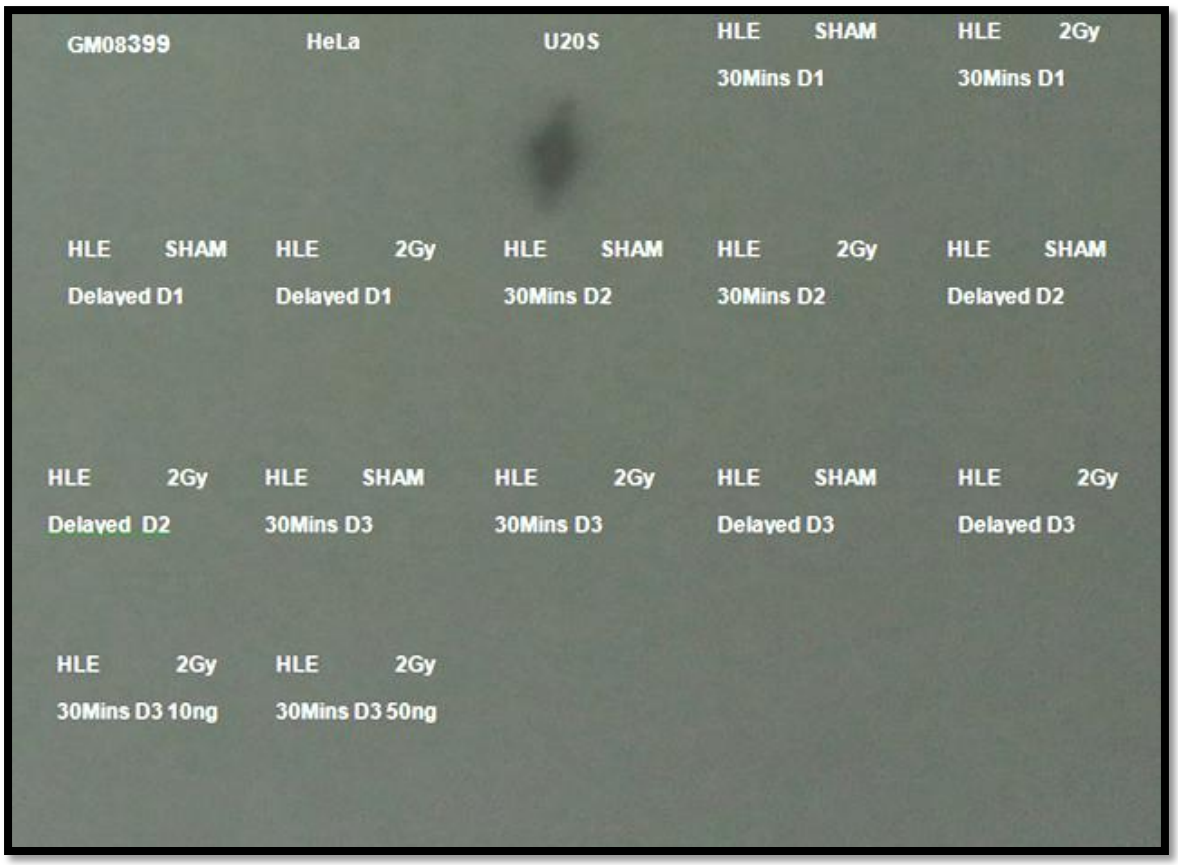

Figure 3-14: X-RAY film with results of ALT c-circle assay. The figure is a photograph of the x-ray film which was generated from the ALT activity assay. The results show positive c-circles (ALT activity) in only U2OS (positive control) and no activity in the HLE donor cells or HeLa and GM08399 (negative control samples).

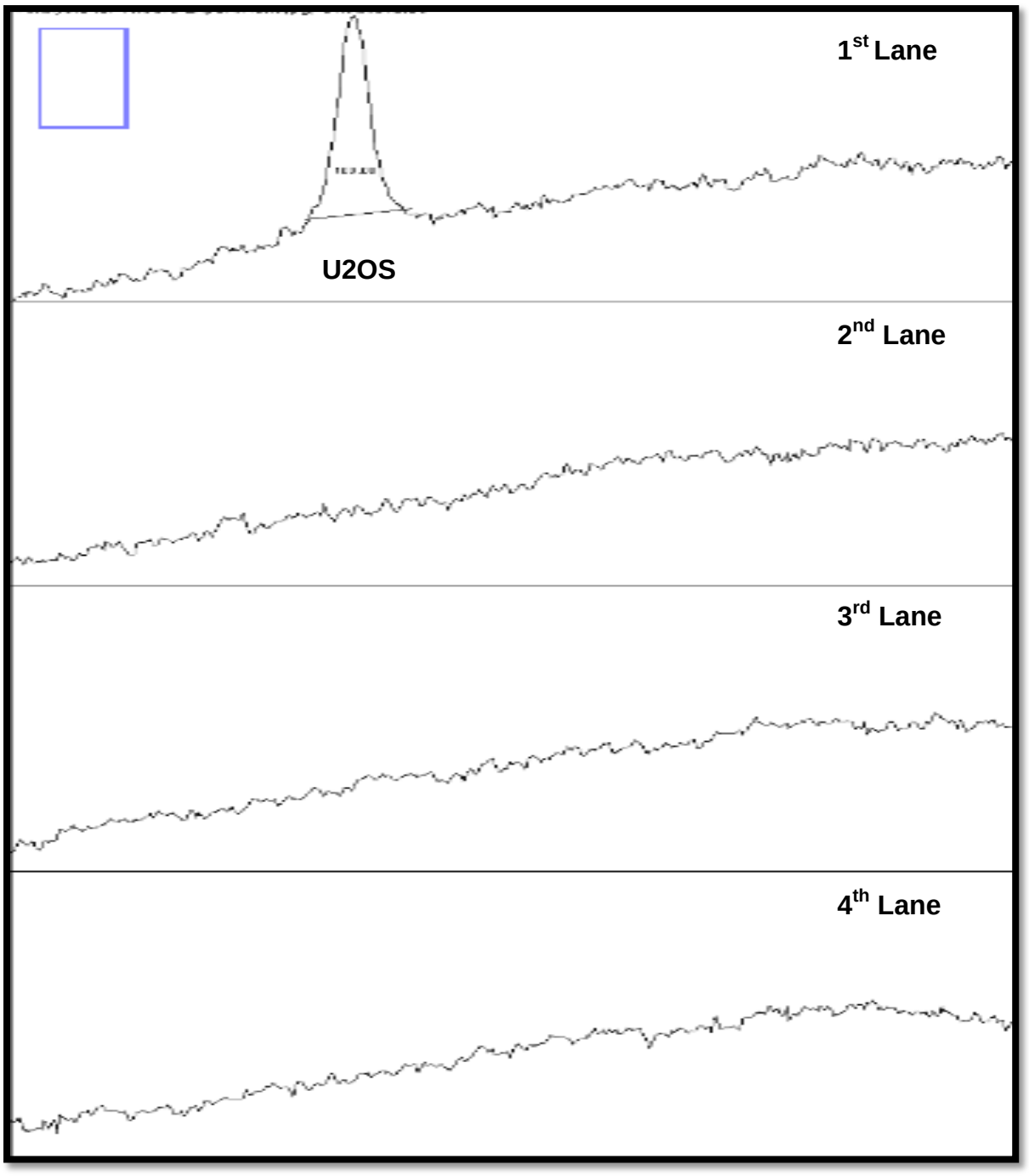

Figure 3-15: ImageJ analysis of x-ray film. Figure represents the ImageJ analysis of the x-ray film shown in Figure 3-14. The analysis of the x-ray film shows clearly a peak at U20S cells and none in the controls (GM08399 and HeLa) and HLE donor cells.

When analysis of the film with the HLE samples was done using the imageJ software only one peak in the whole film was noted, the peak associated with the U2OS sample (Figure 3-15).

The results (Figure 3-14) and (Figure 3-15) showed that there was no ALT activity in the HLE cells even in the sample that was increased in concentration. The control samples GM08399 and HeLa cells also showed no ALT activity. However, activity was noted in the positive control U2OS.

3.3 Discussion

Our first and foremost aim for this chapter was to establish the aTL q-PCR methodology (O'Callaghan and Fenech, 2011) in our laboratory. Having shown the efficiency and accuracy of this methodology (Figure 3-4 - Figure 3-5) we went ahead and measured the telomere length in HLE cells from different donors.

Results indicated that telomere length in HLE cells in comparison to normal human cells behave differently. The telomere length in normal human fibroblasts decreases as the passages increase (Figure 3-5), which is in line with previous studies (Allsopp et al., 1992), (Ouellette et al., 2000), (Ning et al., 2003), (Shammas, 2011). However, in HLE cells this phenomenon was not observed. Instead we found that telomere length increased with passage time or population doubling [Donor 1 HLE cells (Figure 3-6), Donor 2 HLE cells (Figure 3-7), Donor 3 HLE cells (Figure 3-8)].

To the best of my knowledge this has not been observed in HLE cells previously. Actually, results on telomere length analysis in HLE cells are non-existent. The other relevant source of information comes from canine studies. Analysis on canine lens epithelial cells has shown a decrease in telomere length with propagation of cells in culture (Babizhayev and Yegorov, 2014).

However, there is a simple potential explanation for the observed increase in telomere length. All HLE cells used are cells obtained from lens cells of embryos, gestation weeks 20-24 (Caltag Medsystems). Previous studies on telomerase activity have shown that telomerase switches on very early in development and its activity is still present 16-20 weeks into gestation (Wright et al., 1996), (Wright et al., 2001). Therefore, we cannot rule out that the presence of telomerase activity and telomere lengthening in these cells could be solely because they are embryonic cells. Even

though they are older than the reported age at which telomerase has been detected previously (Wright et al., 1996).

In line with this possibility TRAP assay showed presence of telomerase activity in HLE cells (Figure 3-11). Telomerase activity has not been detected in HLE cells previously (Huang et al., 2005) and is not expected to be observed at high levels in normal somatic cells (Kim et al., 1994). Other groups investigating lens cells have shown telomerase expression in canine lens cells (Colitz, Davidson and McGahan, 1999). Other studies have shown that some primary pre-senescent human fibroblasts express low telomerase activity (Masutomi et al., 2003). However, what is striking in our results is an extremely high level of telomerase activity in HLE cells which is the same as the level observed in the human breast carcinoma cell line MCF7, and far above the level observed in a normal fibroblast cell line (Figure 3-11).

However, telomerase activity goes down in subsequent passages possibly in line with its natural switch off during the embryonic development. It is also important to stress that there is no good correlation between telomere length and telomerase activity in later passages. For example, the rate of telomere length change in cells from each donor increased with cell propagation in vitro in spite of telomerase activity going down from early to late passage cells (Figure 3-11). In donor 1 cells, telomere length after one passage increased by 2.57kb/diploid genome (Figure 3-6). An increase of 3.22kb/diploid genome for donor 2 cells was observed (Figure 3-7). Finally a total increase of 1.74kb/diploid genome in donor 3 cells was noted (Figure 3-8).It is possible that the initially robust telomerase activity was enough to sustain the increase in telomere length observed.

However, there is a possibility that the observed increase in telomere length may be due to ALT activity. To further investigate why this telomere length increase, experiments to observe ALT activity were done. Studies have shown that telomerase and ALT can co-exist in human cells (Cerone, Londono-Vallejo and Bacchetti, 2001) (Perrem et al., 2001). Interestingly, research from Dr Slijepcevic's group indicates that even primary human fibroblasts might express an ALT-like activity (Virmouni et al., 2015).

Roger Reddel and his group did experiments where they generated a mouse model with a DNA tag. This DNA tag was inserted in a single telomere and they observed that the tag was copied in the somatic tissues but not in the germ line tissues, proposing that ALT also occurs in somatic mouse tissue (Neumann et al., 2013).

Given that ALT plays an important role in normal cell telomere maintenance, we decided to analyse the ALT pathway to see if it was activated in HLE cells. Also, the rate of telomere length increase observed in cells from HLE donors is more reminiscent of ALT-like activity: large increase of up to 20kb/diploid genome. This length is more in line with cells that maintain their telomeres by the ALT pathway, as seen with the U2OS cell line, length varies between 3kb and 50kb (Henson et al., 2002). However, once we ran the ALT assay we found that there was no ALT activity in any of the HLE cell donors (Figure 3-14). No activity was found in HeLa and GM08399 samples as well, which were used as negative controls. Activity was noted in our positive control of U2OS (Figure 3-12) (Figure 3-14).

This meant that even though telomerase was decreasing in the cells as passages increased (Figure 3-11), the amount present was possibly sufficient to keep telomere length increasing (Figure 3-6 Figure 3-7 Figure 3-8). Alongside this, to further

understand the characteristics of HLE cells our collaborators at Oxford Brookes conducted additional experiments. Their experiments involved analysis of ROS activity and cell viability data unpublished (personal communication with Dr Scott Bright, Mrs Deborah Bowler and Prof. Munira Kadhim). This was done because it is understood that the main features of human cataractogenesis include the presence of senescence lens cells and accelerated oxidative stress-induced DNA damage (Babizhayev and Yegorov, 2014).

For the ROS activity in Donor 2, our collaborators found, 2 Hours after SHAM radiation that cells showed 15000 H_2DCFDA (general oxidative stress indicator) fluorescence units. This decreased to 11000 after 24 hours and further down to 400 H_2DCFDA fluorescence units, several population doublings later.

In Donor 3 samples they showed that ROS activity, 2 Hours post SHAM radiation, started at 26000 H_2DCFDA fluorescence units and went down to 17000 24 hours after. This then increased to 20000 H_2DCFDA fluorescence units as the cells divided over a period of several population doublings.

These results suggest that in the case of ROS activity, the natural oxidative stress present in Donor 3 samples is greater than that in Donor 2 samples.

For cell viability they showed that there is a decrease in normal cells 24 hours after SHAM irradiating them. They found that cell viability using the reduction of alamar blue as a measure of viability decreased from approximately 50000 to 37000 after 24hours in Donor 2 samples. It further decreased to 21000 several population doublings later.

However, in Donor 3 samples it was noted that this change was less. The initial count 2 hours after SHAM radiation was 45000 which decreased to 44000, 24 hours later. After several population doublings this amount decreased to 37000.

This shows that as the cells are ageing in culture the cell viability is decreasing for both Donor 2 and Donor 3.

These results show that the higher the oxidative stress levels in these cells the greater their ability to survive. This can be seen from Donor 3 cells where ROS activity is higher than that in Donor 2 cells. However, the cell survival rates are greater in Donor 3 than in Donor 2. This could potentially be because once the cells stop growing i.e.: enter senescence; a mechanism may kick in resembling a mechanism shown to be operational in keratinocytes, where pre-transformed cells emerge in cultures after senescence (Gosselin et al., 2009). Similarly, a bypass of the oncogene induced senescence is shown to occur in mammary epithelial cells (Sedic et al., 2015).

Our collaborators in Germany ran a separate study (KORA study) to understand the genetic differences/ similarities which are associated with cataractogenesis (Graw et al., 2011). In the KORA study it was illustrated that there is genetic involvement in cataract development. They showed two polymorphic markers that were significantly associated with cataracts *GJAB* and *CRYBB3* (Graw et al., 2011).

Furthermore, to understand the genetic differences in cells from all three donors the rate of telomere loss was analysed. As discussed earlier the rate of telomere loss is different in the cells from all the donors. Therefore, it can also be linked to genetic

variation. The least increase of telomere length was noted for donor 3 cells and greatest for donor 2 cells.

Studies conducted on telomere length and also telomerase activity in different individuals has shown that there can be genetic variations. These variations can result in a number of different outcomes. One such study linked telomeres to higher risks of breast cancer (Shen et al., 2010). Another study was conducted to understand human longevity and healthy aging. The study showed that there is a hTERT haplotype associated with longer telomeres, which result in exceptional longevity (Atzmon et al., 2010).

The results from our work and that of our Oxford Brookes collaborators can help understand whether or not cataract formation can also be genetically determined. As seen in Donor 2 it is more likely that this donor will get cataracts at an early stage as the cells are unable to undergo stress compared to Donor 3 cells where they can survive under harsher conditions; in this case higher oxidative stress. Also, the telomere length increase is greater in Donor 2 cells in comparison to Donor 3 cells, therefore it could mean that Donor 2 is more inclined to get cataracts compared to both Donor 3 and Donor 1. However, it is important to be cautious here as the HLE cells we used were embryonic in origin.

Therefore, the variance in telomere length from each individual's cells might also be linked to cataracts, whereby the greater the increase in telomere length the higher the chances of cataracts.

Effects of Radiation on Telomere length and telomerase activity in Human Lens Epithelial Cells in association with cataracts

4.1 Introduction

The lens of the eye is known to be one of the most radiosensitive tissues in the body (Hamada Nobuyuki, 2016). Cataracts are known to form due to a number of reasons, including genetic predisposition, aging, smoking and even radiation (Graw et al., 2011). Radiation induced cataracts form in the posterior part of the lens epithelial cell, however very little is currently known about the mechanism of cataractogenesis (Ainsbury et al., 2009) (Ainsbury et al., 2016). However, it is known that an acute dose of less than 2.0Gy and a fractionated dose of 5.0Gy, of Low LET IR can cause cataracts (Chodick et al., 2008).

A number of different studies have been conducted to see the chances of early onset of cataracts due to radiation exposure. One interesting study was conducted on US radiologists – where they followed the radiobiologists for a period of 20 years (Chodick et al., 2008). They found that cataracts increased as the frequency of x-ray exposure by the individual increased. There was also an early onset of cataracts in people who had been exposed to other types of radiation such as UV light due to sun exposure (Chodick et al., 2008).

It was also found in rabbit lens cells that radiation caused changes in the molecular weight of the crystalline and changes to the backbone of the protein (Mohamed and Saad, 2011). Therefore, the effects of radiation on the lens cells are an important field of study, to further understand the reasons for cataract formation.

The KORA study conducted in Germany showed that females had higher chances of getting cataracts compared to males (Graw et al., 2011), results of which were in line with studies conducted previously (Klein, Klein and Lee, 1998).

In 1895 x-ray radiation was discovered by Roentgen. Two years subsequent to the discovery of x-ray, Chalupecky suggested that cataracts could be caused by radiation (Merriam and Worgul, 1983).

Studies have also shown that UV causes changes in telomeres. Telomeres shorten faster in fibroblast exposed to UVA radiation than in control cells (Ma et al., 2012). Furthermore, individuals who show sensitivity to ionizing radiation show accelerated telomere shortening (Metcalfe et al., 1996). Telomeres act as hallmarks of radio-sensitivity (Goytisolo et al., 2000). DNA damage at telomeres is potentially irreparable (Fumagalli et al., 2012). Experiments done on human fibroblasts showed that cells did not repair some damage even after four months post 20Gy irradiation (Fumagalli et al., 2012). The study suggested that the damage that was irreparable was found at genomic loci, in this case telomeres (Fumagalli et al., 2012). They found that the number of DDR foci that was not repaired actually increased in numbers at telomeres (Fumagalli et al., 2012). They also showed that the telomere length was not relevant to cell entering senescence and that cells underwent senescence even with long telomeres (Fumagalli et al., 2012). This is due to a defect in the NHEJ pathway (Fumagalli et al., 2012). However, it has been shown that even though telomeres may not shorten due to the defects in NHEJ, HR can cause telomere shortening to take place which may still be a mechanism (Fumagalli et al., 2012).

It is known that a long telomere is able to make stronger telomere cap. However, this is not always the case. Telomeres do not have to become critically short for them to be recognised as damaged DNA. In some cases they lose their protective ability while they are long due to loss of certain genes and proteins. One such study shows the loss of TRF2 causes telomeres to unmask and fuse to each other without additional shortening (Karlseder et al., 1999) (Smogorzewska et al., 2002). When telomeres lose their T-loop structure genomic instability takes place (O'Sullivan and Karlseder, 2010) and over a period of time it can lead to carcinogenesis (Ayouaz et al., 2008).

It is therefore important to understand if once irradiated, telomeres repair effectively in the HLE cells, or if they cause long term genomic instability, hence causing cataracts. To do this, assays for detecting DNA damage will be used, to see if repair kinetics is effective in these cells (Rogakou et al., 1998) (Rai and Chang, 2011).

Therefore, for this section the main aim was to see if radiation caused any changes to the telomere length or function once HLE cells were irradiated, hence causing early onset of cataracts.

4.2 Results

The basic characteristics of the HLE cells from all three donors were presented in the previous chapter. To further understand the process of cataractogenesis it was decided to examine the changes in HLE cells after irradiation. A range of doses were selected. These ranged from low doses of 0.001Gy to high doses of 2.0Gy.

Cells were subjected to a low dose of 0.001Gy, which is set as the annual low-LET background radiation dose, that typical radiation workers are exposed to. Alongside this, 0.001Gy is a typical diagnostic x-ray dose used in hospitals. Apart from 0.001Gy, hospitals use a typical dose of 0.01Gy for abdominal CT scans, which was selected as the third dose for this study. For the next dose, 0.02Gy was selected which has been suggested as the limit for clinical interventions by the “International Commission On Radiation Protection” (ICRP). However, 0.1Gy is used as the upper limit for diagnostics and was also selected for this section of research. Lastly, high doses of 1.0 Gy and 2.0 Gy were selected as positive controls (the dose of 2.0 Gy is known to induce cataracts). Cells were also subjected to SHAM irradiation which acted as negative controls.

Irradiation of cells was performed using a 250kV x-ray set at the Gray institute for Radiation Oncology and Biology, Oxford University.

This chapter investigates the changes in telomerase activity, telomere length and DNA damage response in HLE Cells after exposure to x-ray radiation. As per the results in section 3.2 cells were bought from Caltag Medsystems, and were collected from our collaborators in Oxford Brookes in flasks.

4.2.1 Telomere length

First and foremost for this section, telomere length in the cells from each donor was measured. The aTL q-PCR protocol established in section 3.2 was used. The same concentrations of primers, the same control cell lines (GM08399, HeLa, U2OS) and the same settings for q-PCR run were used as established in the previous section, 3.2.

4.2.1.1 *Donor 1*

Figure 4-1 shows the telomere length in HLE Donor 1 cells 30mins after x-ray irradiation. Telomere length differences were not noted in most doses apart from two, 0.01Gy and 1Gy.

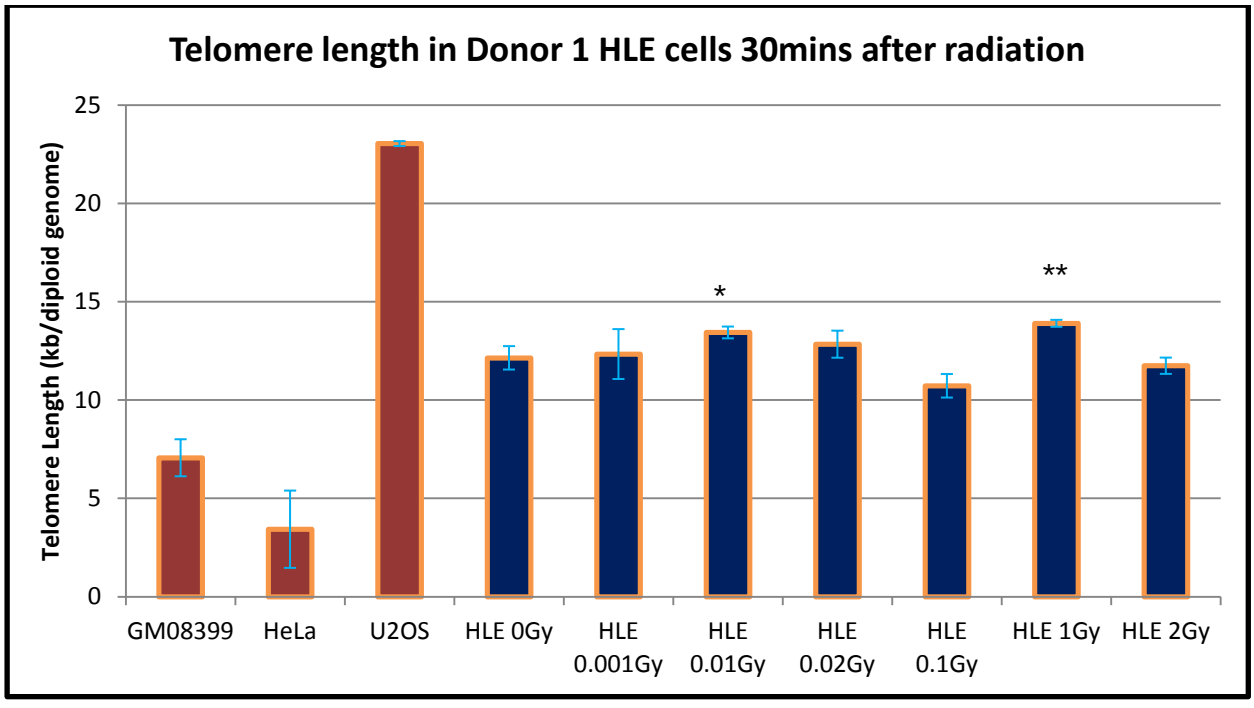

Figure 4-1: Telomere length in HLE cells, 30mins after x-ray radiation. The figure represents the telomere length in HLE donor 1 cells. A significant increase in telomere length is noted in HLE donor 1 cells after 0.01Gy and 1.0Gy of x-ray radiation. Red bars represent control samples and blue samples represent HLE donor 1 cells. Error bars represent S.E.M. (* P<0.05, ** P<0.01)

The highest increase in telomere length is noted after 1.0Gy of radiation exposure where telomere length increases by 1.75 kb/diploid genome when compared to control 0Gy.

Furthermore, a study on telomere length in delayed samples was carried out. The cells were irradiated and left to become confluent in the incubator. Cells were harvested after every passage and were left to grow until the flasks became confluent. The results for Donor 1 cells are shown below in Figure 4-2, Figure 4-3, and Figure 4-4. The results represented for 0Gy (SHAM irradiated samples are results previously represented in section 3.2 . These results have been used to compare the non-irradiated and irradiated samples and experiments were ran together to avoid discrepancy in results.

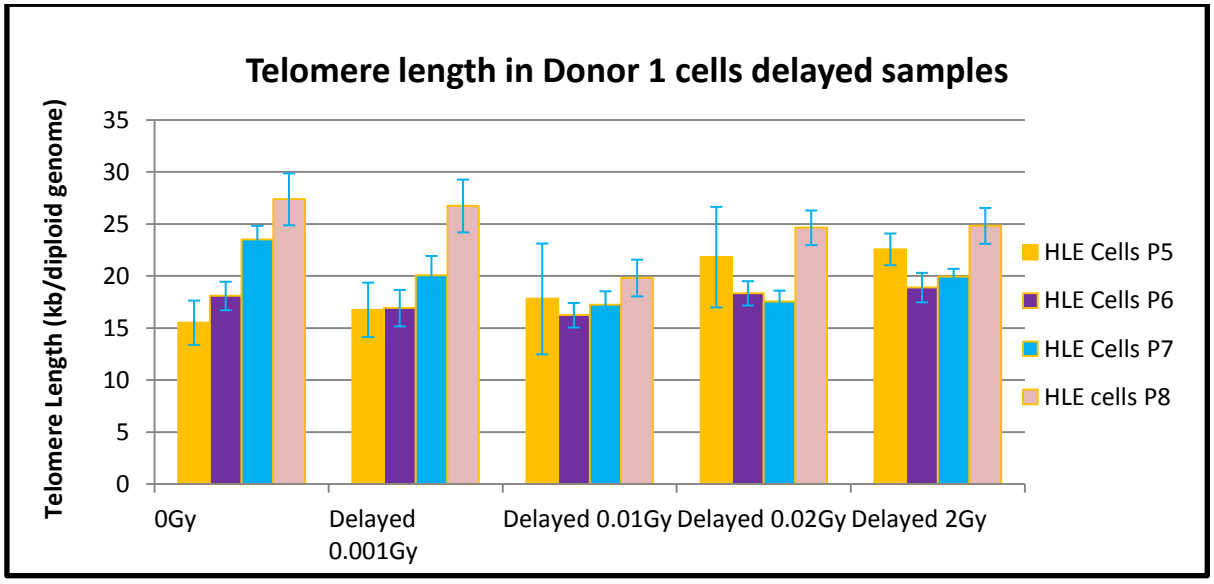

Figure 4-2: Telomere length results in donor 1 HLE cells. The figure represents the combined results of the telomere length analysis in HLE cells from Donor 1 after x-ray radiation. The different colours represent different passages. The yellow bar represents P5 cells. The purple bar represents P6 cells. The light blue bar represents P7 cells. The pink bar represents P8 cells. Error bars represent S.E.M.

To analyse the data properly Figure 4-2 was split into smaller graphs. Figure 4-3 shows dose dependent changes in the delayed Donor 1 HLE cells at different passages. It can be seen that there are significant differences at P5, P7 and P8 relative to SHAM irradiated cells. In Passage 5 it can be seen that there is a significant increase in telomere length after 2.0Gy of radiation. However, in both passage 7 and 8 there is no difference at higher doses but at lower doses, where telomere length has decreased. There is no clear explanation as to why this decrease is noted at these doses as the general conclusion so far is that telomere length increases in these cells (Figure 3-6 Figure 3-7 Figure 3-8).

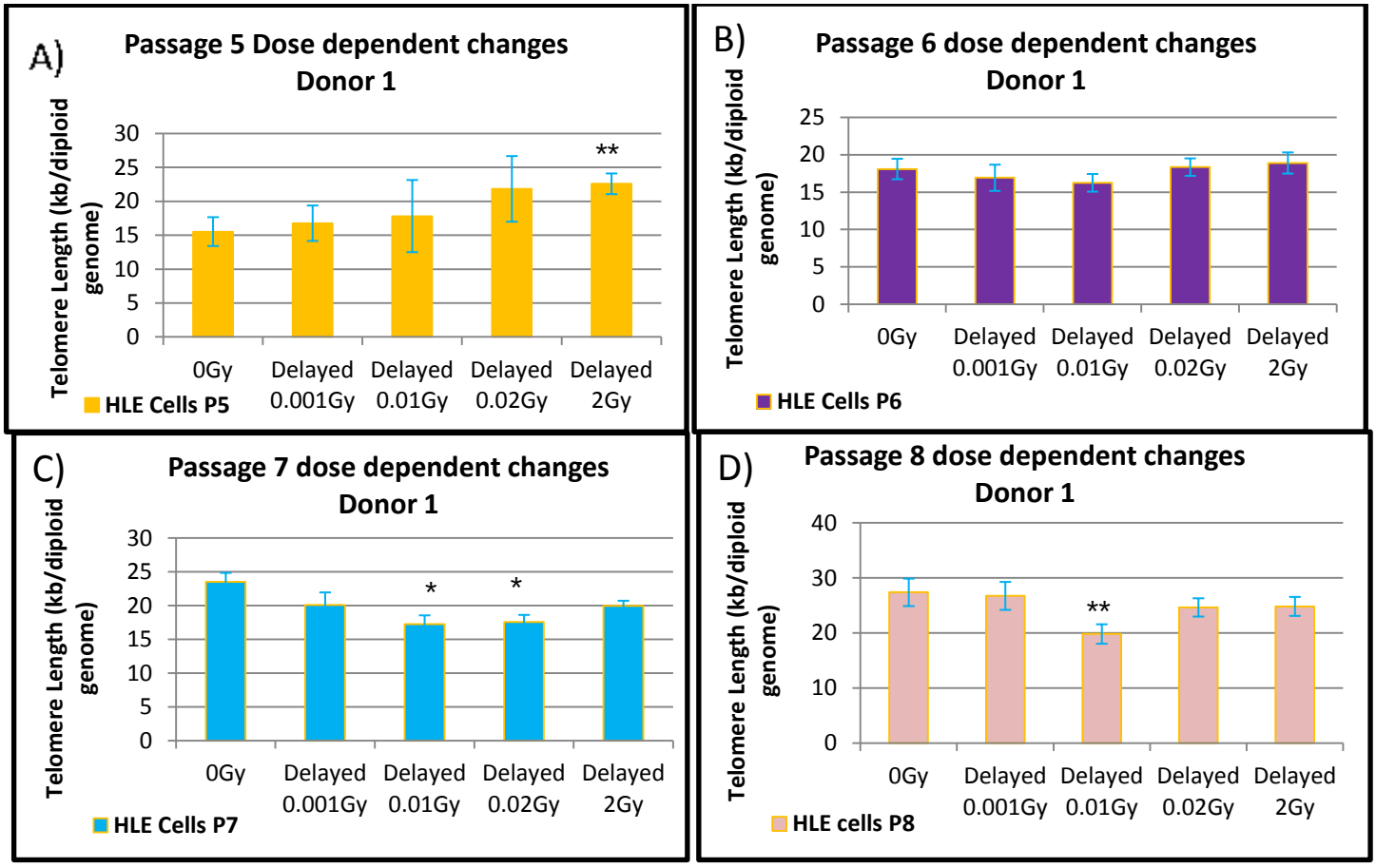

Figure 4-3: Telomere length at different passage numbers in Donor 1 HLE cells. A) Dose dependent comparison of telomere length in P5 cells. An increase in telomere length is noted after 2.0Gy of radiation. B) Dose dependent comparison of telomere length in P6 cells. No significant changes are noted in these cells. C) Dose dependent comparison of telomere length in P7 cells. Significant changes noted in cells irradiated with 0.01Gy and 0.02Gy of x-ray radiation. D) Dose dependent comparison of telomere length in P8 cells. Significant change noted in cells irradiated with 0.01Gy of x-ray radiation. Error bars represent S.E.M. (* P<0.5, ** P<0.01)

Another graph was generated from the data presented in Figure 4-2. Figure 4-4 shows telomere length in non-irradiated samples and irradiated delayed samples. Here telomere length in each dose was analysed over a period of 4 passages. This was done to understand telomere length changes at each dose, at different passages. A significant difference was not noted in all doses. However an increase was noted in 0Gy, 0.001Gy and 2.0Gy. In these doses an increase was noted in telomere length in later passages.

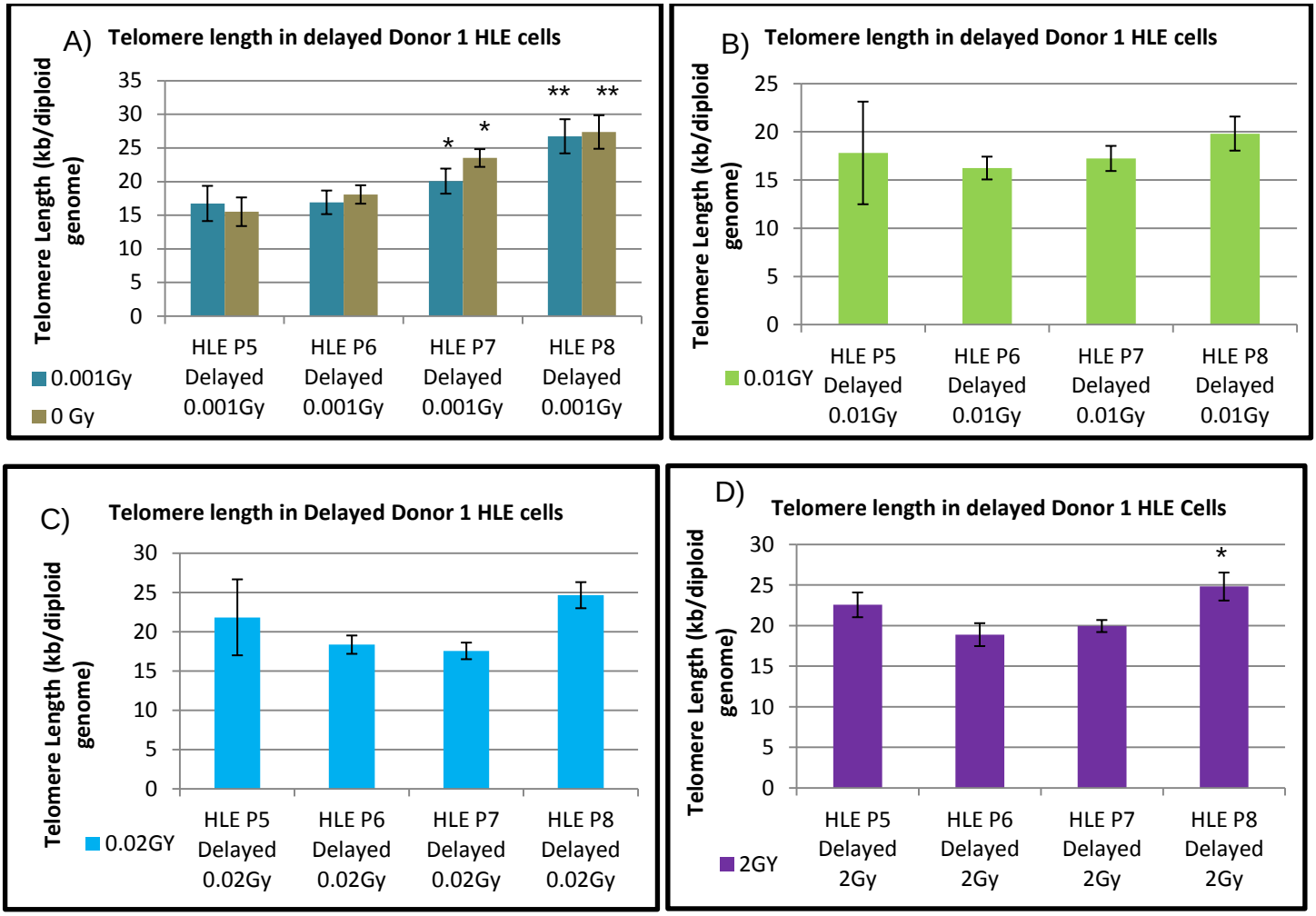

Figure 4-4: Telomere length in HLE Donor 1 cells as passage increases. Graphs A)-D) present data from x-ray irradiated samples 0.001Gy, 0.01Gy, 0.02Gy and 2.0Gy respectively. The results show that there is a significant increase in telomere length at P7 and P8 in 0Gy (dark blue bars) and 0.001Gy (brown bars) after x-ray irradiated samples in donor 1 cells. No significant changes are noted in 0.01Gy (light green bars) and 0.02Gy (light blue bars) after x-ray radiation in Donor 1 cells as passage increase. Lastly, significant Increase in telomere length is noted in P8 cells when compared to P5 cells, 2.0Gy after radiation (purple bars). Error bars represent S.E.M. (* P<0.5, ** P<0.01)

4.2.1.2 *Donor 2*

For Donor 2 cells 30mins after radiation exposure we were only able to analyse data on 0Gy and 2.0Gy as these are the only samples that were available. The telomere length in Donor 2 cells showed a similar trend to that of Donor 1 cells after 30mins post radiation exposure. No significant difference was noted in telomere length dose dependently.

As seen in the Figure 4-5 there is an increase of 0.81kb/diploid genome from the 2.0Gy sample, 12.61 kb/diploid genome in comparison to the 0Gy, 11.80 kb/diploid genome. This shows that although there is no significant change in the telomere length an increase in the length is noted.

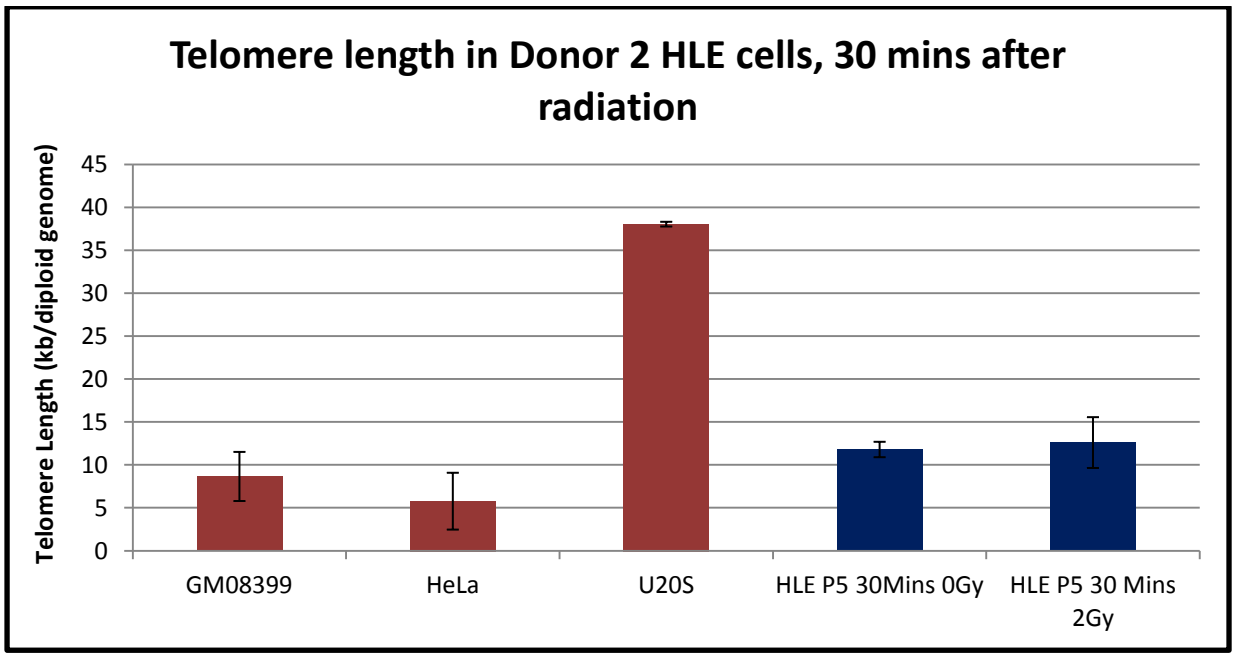

Figure 4-5: Telomere length 30mins after radiation in Donor 2 HLE cells. No significant dose dependent changes are noted in HLE Donor 2 cells 30minutes after x-ray radiation. Red bars represent controls and blue bars represent HLE donor 2 cells. Error bars represent S.E.M.

Results of all the Donor 2 delayed samples have been represented in Figure 4-6. Analysis of the delayed samples showed a significant increase in telomere length as the passage number increased. The cells grew for two passages after radiation, which is what was analysed. When compared to the non-irradiated samples the increase in telomere length was higher in the irradiated samples in comparison to the non-irradiated samples. The P7 delayed 2.0Gy irradiated cells had 33.94kb/diploid genome and the 30mins after radiation had 12.61kb/diploid. This is an increase of 21.33kb/diploid genome. This is also the case with all the other irradiated samples where the increase of kb/diploid genome ranged from 0.80 to 2.78. The highest increase was noted after 2.0Gy of radiation.

Apart from a significant increase as the cells aged, a significant dose dependent telomere length increase was noted in the later passage, P6. An increase of 17.4 kb/diploid genome after 2.0Gy radiation was noted.

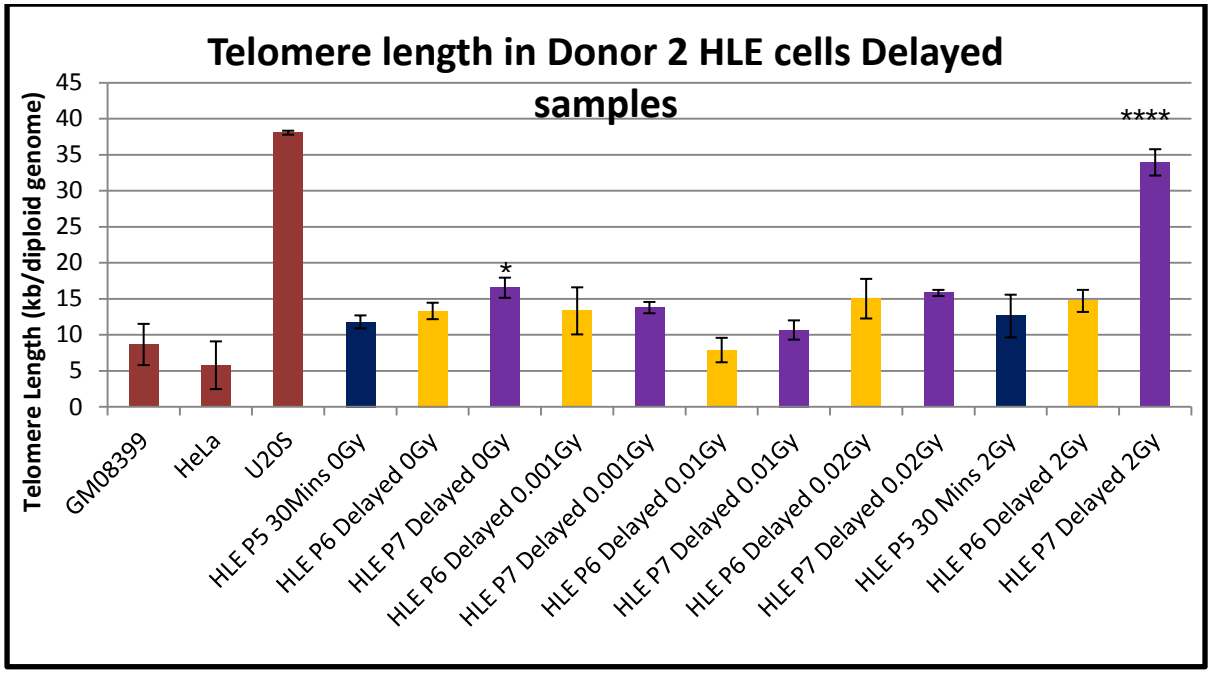

Figure 4-6: Telomere length in delayed HLE Donor 2 cells. A significant increase is noted in P7 cells after SHAM radiation when compared to P5 SHAM irradiated cells. A significant increase in telomere length is also noted in 2.0Gy after x-ray radiation P7 cells when compared to P5 cells after 2.0Gy of x-ray radiation. The blue bars show telomere length in Donor 2 HLE cells 30 mins after radiation. The yellow and purple bars show telomere length in delayed samples. The red bars represent controls. Error bars represent S.E.M. (**** P<0.0001).

4.2.1.3 *Donor 3*

In Donor 3 cells telomere length was measured 30mins after radiation, (Figure 4-7). Results show significant increase in telomere length dose dependently. These results are more in line with results from Donor 2, just that in the case of Donor 3 a significant increase is noted rather than just a trend.

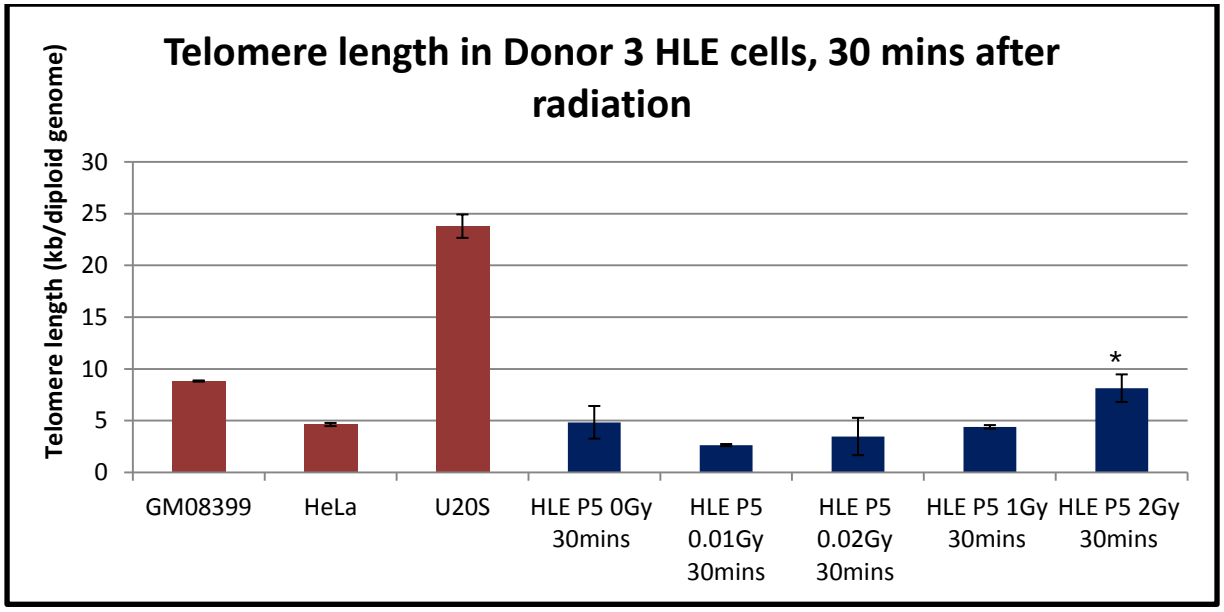

Figure 4-7: Telomere length 30mins after x-ray radiation in Donor 3 HLE cells. The figure shows the results of dose dependent comparison of telomere length in Donor 3 HLE cells. A significant increase in telomere length is noted 2.0Gy after x-ray radiation when compared to SHAM (0Gy) irradiated cells. The red bar represents controls and the blue bar represents HLE donor 3 samples. Error bars represent S.E.M. (* $P<0.05$)

In the delayed Donor 3 cells, a significant dose dependent increase was noted in the later passages especially after 0.02Gy of radiation. In the cells of this Donor the significant increase was noted in the lower doses as well.

Alongside, a dose dependent increase, a significant increase at each dose was noted as the passages increased in culture i.e.: telomere length increased significantly from P5 to P6 where the cells stopped growing in culture.

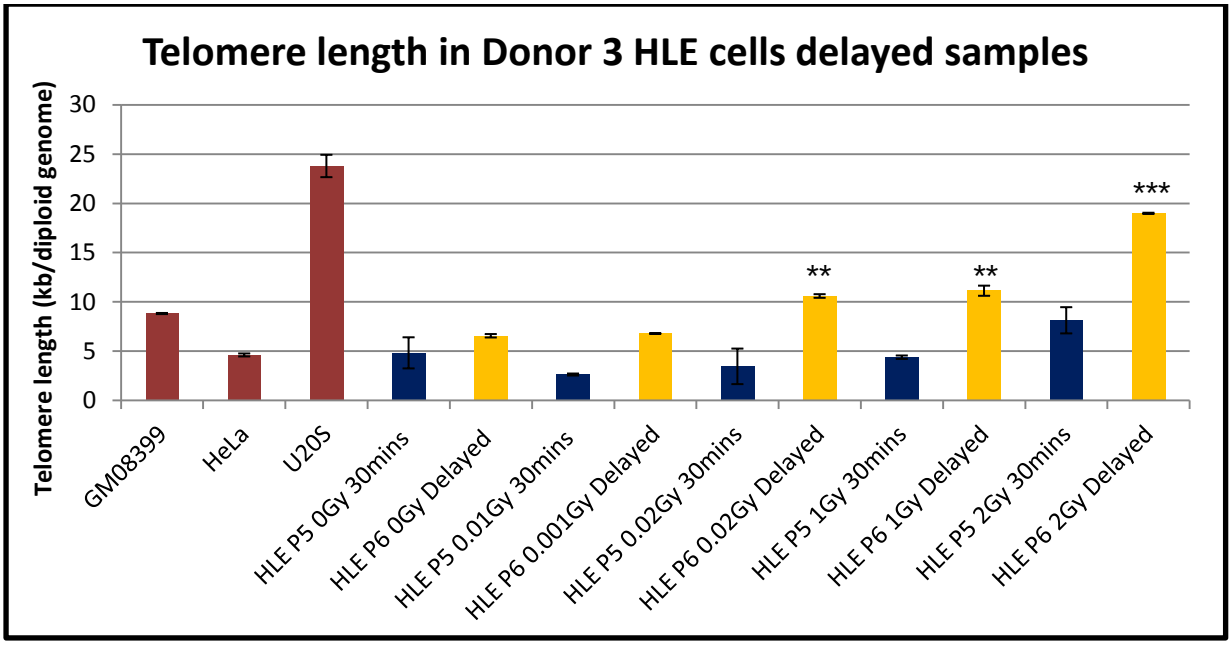

Figure 4-8: Telomere length in delayed HLE Donor 3 cells. A significant increase is noted in delayed 0.02Gy, 1.0Gy and 2.0Gy samples when compared to the 30mins after x-ray irradiation samples. The blue bars shows telomere length in Donor 3 HLE cells 30 mins after radiation and the yellow bars show telomere length in delayed samples. The red bars represent controls. Error bars represent S.E.M. (** P<0.01, *** P<0.001)

To sum up the findings of telomere length after radiation in all three cell donors, a change in telomere length is noted in some samples due to radiation. The increase is more apparent and significant in Donor 3 cell samples in comparison to the others. The difference in telomere length is noted more at the higher doses of 1.0Gy and 2.0Gy however, in Donor 3 cells a significant increase was noted at 0.02Gy when the results were compared to non-irradiated samples.

4.2.2 Telomerase activity

Next telomerase activity was measured in all three Donors before and after irradiating the cells.

Telomerase activity in HLE cells was measured using the q-PCR TRAP methodology. A number of different cell lines whose telomerase activity was known were used; PC3 hTERT, MCF-7 GM08399 as controls. As PC3 hTERT cells have hTERT activated they were used as 100% telomerase activity. MCF-7 is a breast cancer cell line and it is known that telomerase is activated in these cells, therefore these were used as the positive control and GM08399 are normal human fibroblasts which were used as negative controls.

The results in Figure 4-9 show telomerase activity present in HLE Donor 1 cells. It can be seen that telomerase activity decreases dose dependently. Whereby, 2.0Gy has 5.49% of telomerase activity compared to 20.73% of activity at 0Gy.

It can also be seen that telomerase activity decreases as the passages increase in these cell lines. This can be seen from P5 0Gy cells which have 20.73% of activity and P6 have 4.76% of activity. This is in line with the results represented in Figure 3-11 in section 3.2.5 of this thesis.

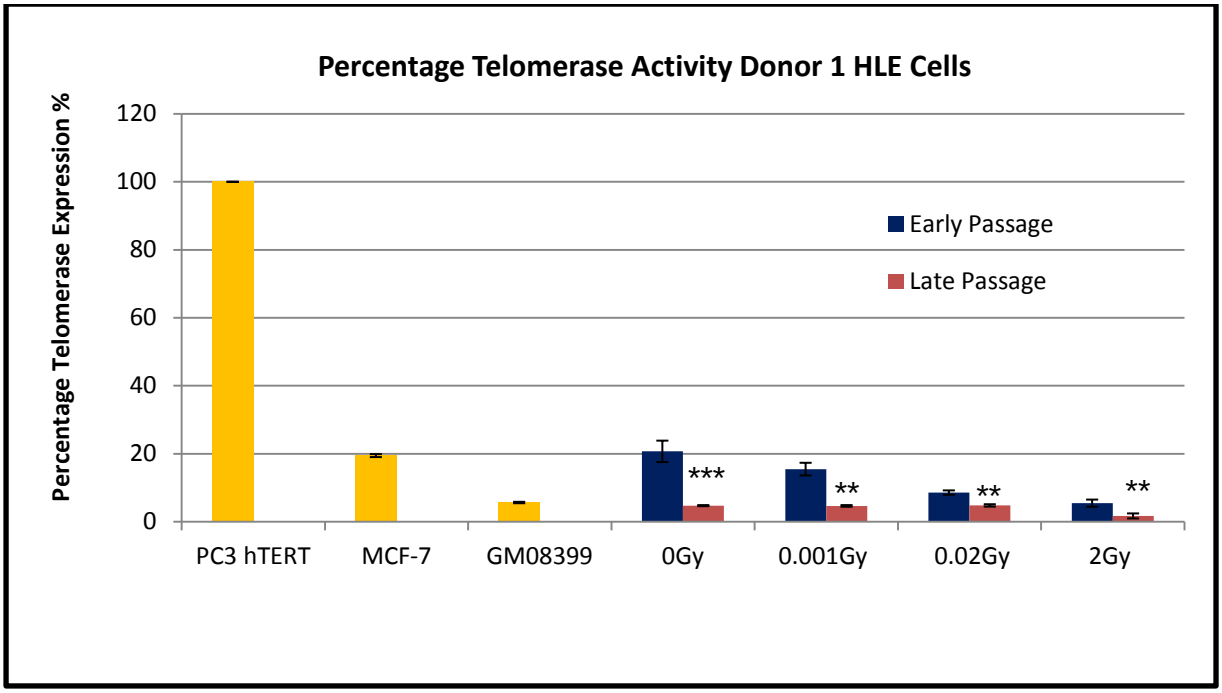

Figure 4-9: Telomerase activity in Donor 1 HLE cells. The PC3 hTERT cells were used as 100% telomerase activity reference point and all other cell lines were calculated against them. Positive control MCF-7 cells show telomerase activity and negative control GM08399 cells show insignificant amounts of telomerase activity. The Donor 1 HLE cells show a significant amount of telomerase activity in the early passages which decreases dose dependently. A significant decrease is also noted when early and late passages are compared at all radiation doses. Telomerase activity decreases significantly in late passages when compared to early passages. The yellow bars represent controls. The blue bars represent early passages. The red bars represent late passages. Error bars represent S.E.M. (* P<0.05, ** P<0.01, *** P<0.001)

The experiment was repeated on Donor 2 cells where cells were irradiated and grown for a period of time until they stopped growing, results of which have been presented in Figure 4-10. For Donor 2, similar results as those observed in Donor 1 were noted. Telomerase activity decreased dose dependently in both P5 and P6. The activity at 0Gy is 45.06% and at 2.0Gy it is 12.51 in passage 5 cells. This decrease is also seen in P6 cells where telomerase activity decreases from 34.75% at 0Gy to 10.67% after 2.0Gy of radiation.

Figure 4-10 also shows a decrease in telomerase activity as the cells age this can be seen in all the different doses.

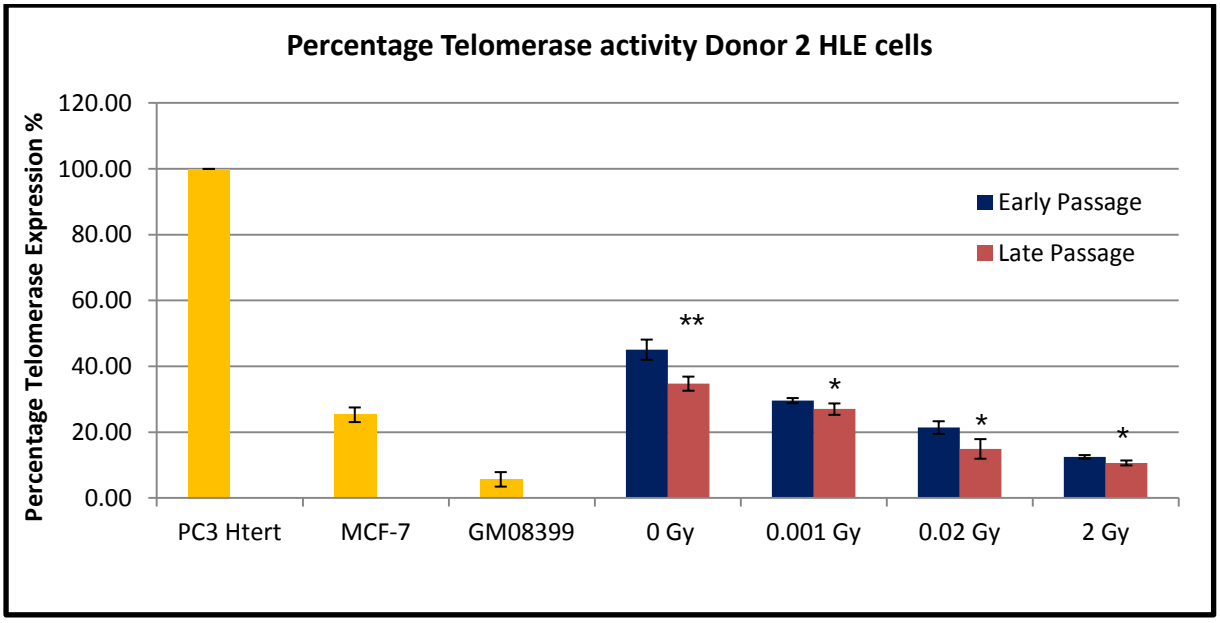

Figure 4-10: Telomerase activity in Donor 2 HLE cells. The PC3 hTERT cells were used as 100% telomerase activity reference point and all other cell lines were calculated against them. Positive control MCF-7 cells show telomerase activity and negative control GM08399 cells show insignificant amounts of telomerase activity. The Donor 2 HLE cells show a significant amount of telomerase activity in the early passages which decreases dose dependently. A significant decrease is also noted when early and late passages are compared at all radiation doses. Telomerase activity decreases significantly in late passages when compared to early passages. The yellow bars represent controls. The blue bars represent early passages. The red bars represent late passages. Error bars represent S.E.M. (* P<0.05, **P<0.01)

For Donor 3 samples, telomerase activity is seen to decrease as cells age and also, dose dependently. The results for this Donor cells are consistent with the results from the other two Donors; Donor 1 and Donor 2.

The telomerase activity is decreasing significantly from P5 to P6 at all doses. The activity is at 35.08% in the non-irradiated sample at P5 and goes down to 5.48% at

passage 6. This is the same for the irradiated 2.0Gy samples where the activity decreases to 1.75% from 8.25%. There is a dose dependent decrease of 26.83% from 0Gy to 2.0Gy in P5 cells and 3.73% in P6 cells.

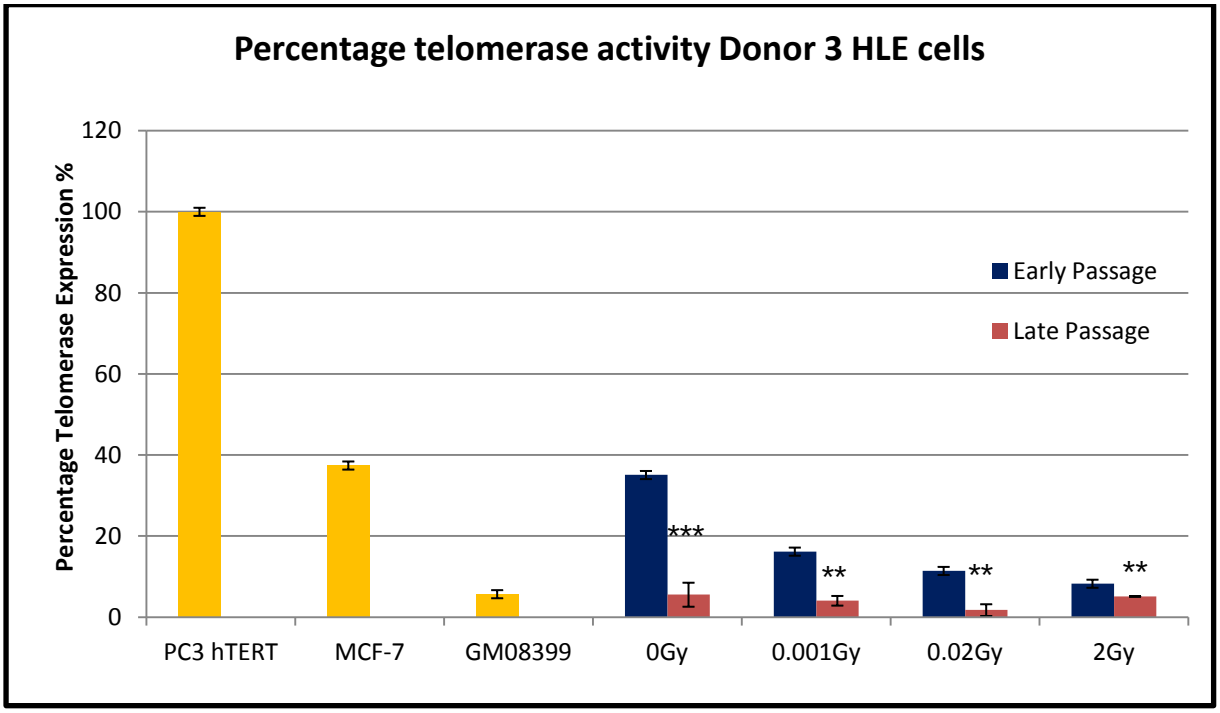

Figure 4-11: Telomerase activity in Donor 3 HLE cells. The PC3 hTERT cells were used as 100% telomerase activity reference point and all other cell lines were calculated against them. Positive control MCF-7 cells show telomerase activity and negative control GM08399 cells show insignificant amounts of telomerase activity. The Donor 3 HLE cells show a significant amount of telomerase activity in the early passages which decreases dose dependently. A significant decrease is also noted when early and late passages are compared at all radiation doses. Telomerase activity decreases significantly in late passages when compared to early passages. The yellow bars represent controls. The blue bars represent early passages. The red bars represent late passages. Error bars represent S.E.M. (** P<0.01, *** P<0.001)

To summarize the results for telomerase activity, telomerase activity in irradiated samples decreases dose dependently. Analyses also show that percentage telomerase activity also decreases as the cells age. This decrease is highest in the

non-irradiated samples and decreases in the irradiated samples. This is apparent for all three donors.

Donor 1 samples show 4.36 fold decrease at 0Gy and 3.16 fold decrease at 2.0Gy between the earlier passage and later passage. Donor 2 samples show a 1.30 fold decrease from P5 to P6 in at 0Gy and 1.17 fold decrease at 2.0Gy. For Donor 3 non-irradiated samples the decrease in percentage telomerase activity is 6.4 folds whereas the decrease in the 2.0Gy sample is 4.7 folds.

This shows that there is differences in the percentage change in telomerase activity between the donors. Donor 3 shows the greatest change in comparison to Donor 1 and Donor 2. Donor 2 cells show the least percentage decrease in telomerase activity.

4.2.3 DDR

To assess the DDR in these cells the γ-H2AX assay was used. The assay was used to measure both the repair kinetics of DNA damage in these cells and the DNA damage dose response. As mentioned above 7 different doses were used, ranging from 0Gy to 2.0Gy.

For the dose response study we measured γ-H2AX in the irradiated cells 30 mins after radiation. Cells were seeded in our collaborators lab in Oxford Brookes, on Poly-L-Lysine coated slides. The cells were incubated overnight and irradiated the next morning after which they were left in the incubator until the 30mins after radiation time point was reached.

4.2.4 H2AX Dose Response

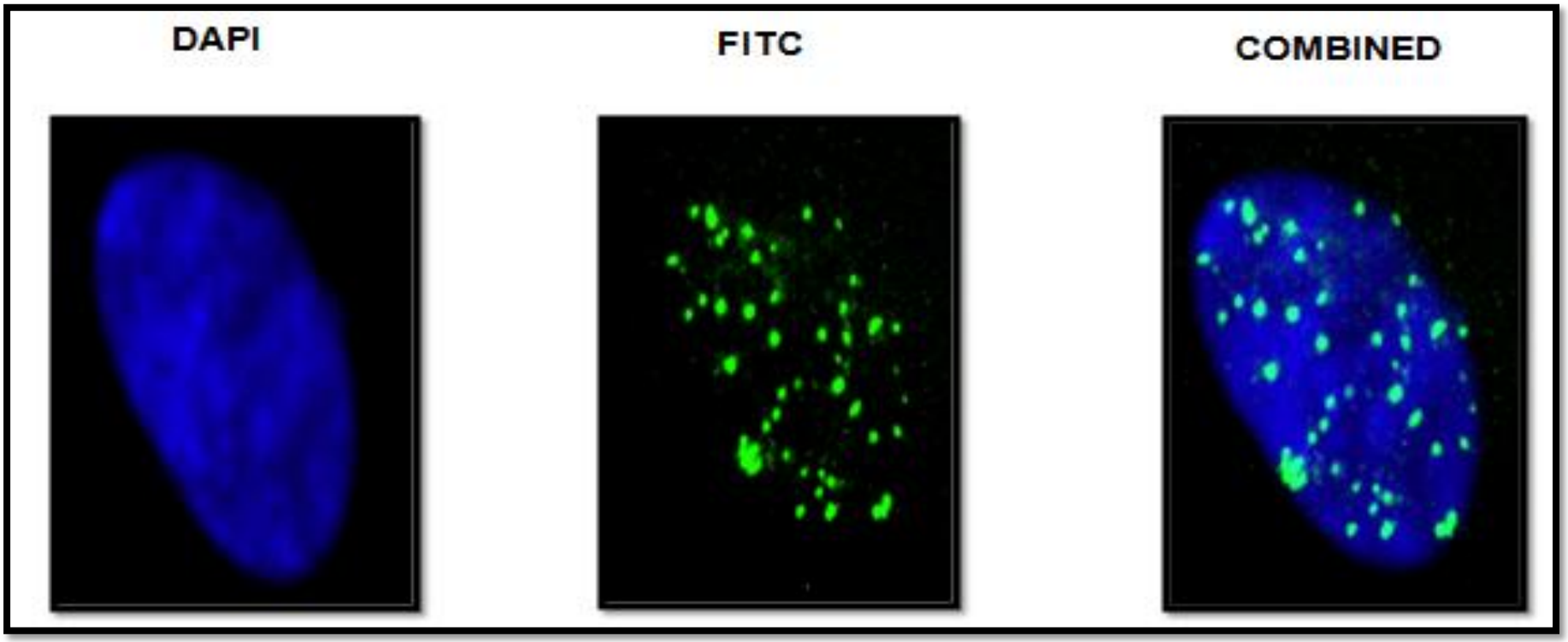

Figure 4-12: γ-H2AX foci in HLE Donor 3 cell. The figure shows an image of an irradiated HLE D3 cell at 2.0Gy. The image shows the number of γ-H2AX foci found in these cells after 2.0Gy of irradiation. Each green spot represents one γ-H2AX foci. The image has been divided into three channels. The first one represents the DAPI image of the cell. This shows all the DNA contents in the cell. The second image shows the FITC channel of the microscope. This shows all the γ-H2AX foci in the cell. The third image shows the combined image of the FITC and DAPI image.

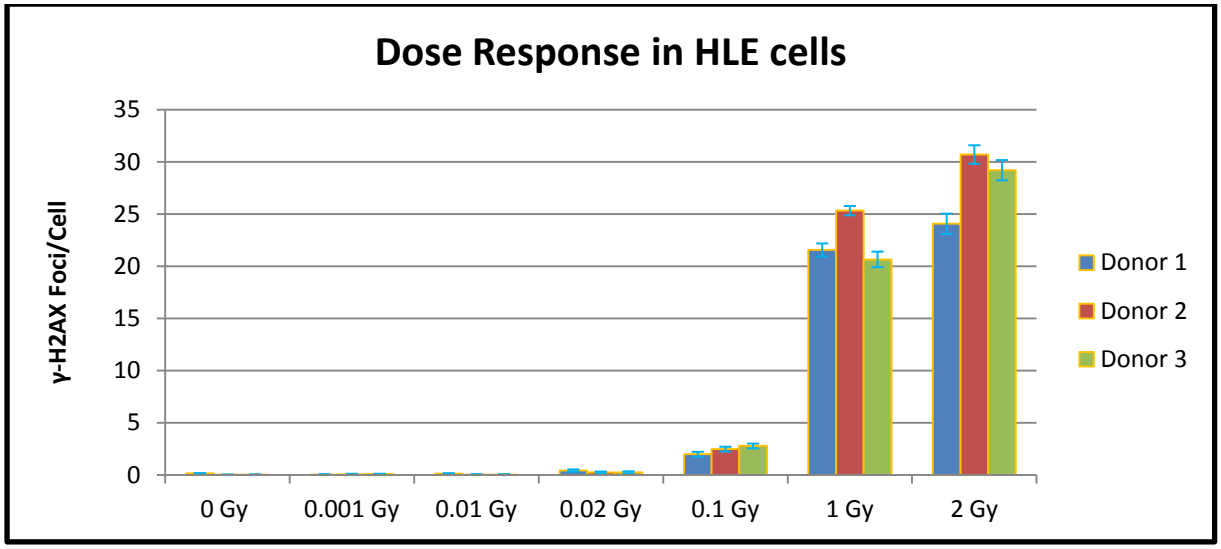

Figure 4-13: γ-H2AX dose response in HLE donor cells. The graph shows the number of γ-H2AX foci after 30mins of radiation in all three Donors. The blue bar shows the number of γ-H2AX foci in Donor 1 cells, Red bar shows Donor 2 cells and green bar shows Donor 3 cells. It can be seen that the first change in DNA damage is seen at 0.02Gy for all three Donors. The significant results were compared using a TTEST analysis and the results were compared to 0Gy of radiation. Error bars represent S.E.M.

It can be seen from Figure 4-13 that there is a dose dependent increase in number of γ-H2AX foci in cells from all three Donors, the number of γ-H2AX foci increase significantly after 0.02Gy of radiation in all three Donors.

4.2.5 H2AX Repair Kinetics

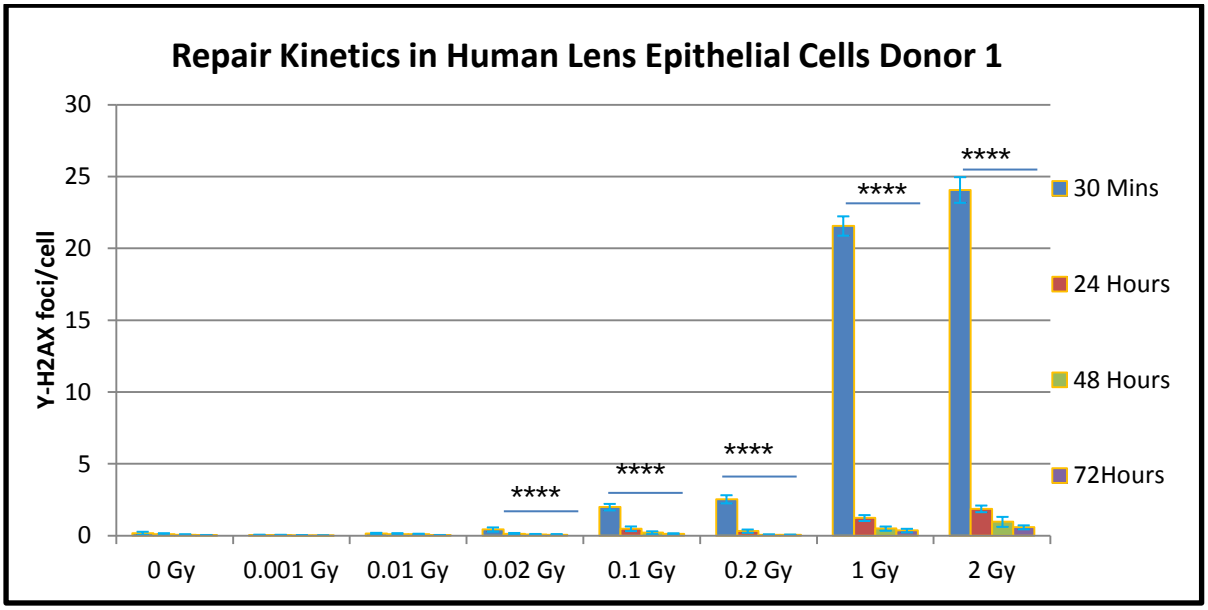

Figure 4-14: γ-H2AX repair Kinetics of Donor 1 HLE cells. The figure shows the graph representing repair kinetics in Donor 1 HLE cells at different doses. The results show a significant decrease in number of γ-H2AX foci after 72hours after x-ray radiation. Therefore, the results show clear repair kinetics in the cells for up to 2.0Gy of x-ray radiation. The blue bar shows the number of γ-H2AX foci in the cells 30mins after radiation; the red bar shows 24hours, Green Bar 48 hours and Purple Bar 72hours after cells were irradiated. Error bars represent S.E.M. (**** P<0.0001)

Figure 4-14 shows the repair kinetics in HLE Donor 1 cells. The graph shows effective repair in the cells up to 2.0Gy of radiation where it can be seen at 30mins after radiation there is 24.07 γ-H2AX foci and after 72 hours there are 0.59 γ-H2AX foci. This shows clearly that the damage that was caused by the x-ray radiation has been repaired effectively.

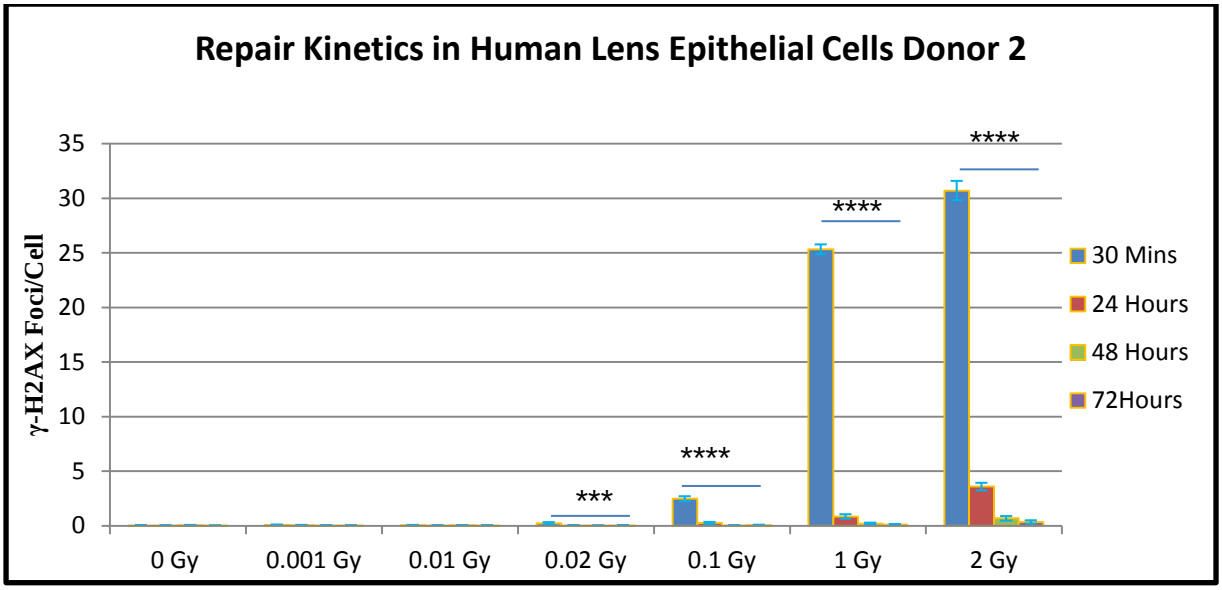

Figure 4-15: γ-H2AX repair Kinetics of Donor 2 HLE cells. The figure shows the graph representing repair kinetics in Donor 2 HLE cells at different doses. The results show a significant decrease in number of γ-H2AX foci after 72hours after x-ray radiation. Therefore, the results show clear repair kinetics in the cells for up to 2.0Gy of x-ray radiation. The blue bar shows the number of γ-H2AX foci in the cells 30mins after radiation; the red bar shows 24hours, Green Bar 48 hours and Purple Bar 72hours after cells were irradiated. Error bars represent S.E.M. (*** P<0.001, **** P< 0.0001)

Figure 4-15 shows the repair kinetics in HLE Donor 2 cells. The graph shows effective repair in the cells up to 2.0Gy of radiation where it can be seen at 30mins after radiation there is 30.71 γ-H2AX foci and after 72 hours there are 0.36γ-H2AX foci. This shows clearly that the damage that was caused by the x-ray radiation has been repaired effectively.

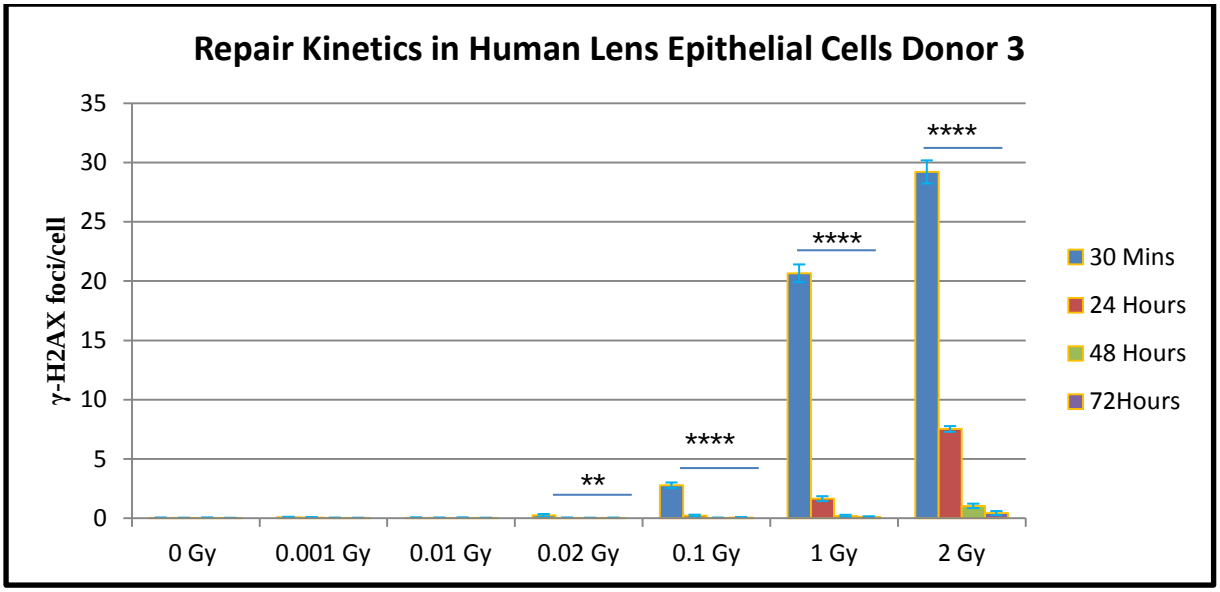

Figure 4-16: γ-H2AX repair Kinetics of Donor 3 HLE cells. The figure shows the graph representing repair kinetics in Donor 3 HLE cells at different doses. The results show a significant decrease in number of γ-H2AX foci after 72hours after x-ray radiation. Therefore, the results show clear repair kinetics in the cells for up to 2.0Gy of x-ray radiation. The blue bar shows the number of γ-H2AX foci in the cells 30mins after radiation; the red bar shows 24hours, Green Bar 48 hours and Purple Bar 72hours after cells were irradiated. Error bars represent S.E.M. (** P<0.01, *** P<0.001, **** P<0.0001)

Figure 4-16 shows the repair kinetics in HLE Donor 3 cells. The graph shows effective repair in the cells up to 2.0Gy of radiation where it can be seen at 30mins after radiation there is 29.21 γ-H2AX foci and after 72 hours there are 0.45 γ-H2AX foci. This shows clearly that the damage that was caused by the x-ray radiation has been repaired effectively.

4.2.6 TIF Dose Response

Given that the cells available were limited we decided to use the cells that were most sensitive to analyse the dose dependent changes and repair kinetics of TIFs in HLE cells. Our collaborators at Oxford Brookes ran experiments and determined that Donor 3 was the most sensitive Donor, we therefore used this Donor to analyse the TIF's present in these cells.

Each TIF was counted as one overlapping H2AX foci at telomere, which is represented as a yellow spot, example of which is presented in Figure 4-17. Given that the microscope used for the analysis was not a confocal microscope, it was important to ensure that the number of TIFs analysed were a true value. To ensure this, controls were used. Non-irradiated (SHAM irradiated 0Gy) samples of the cell line (Donor 3 HLE cells) acted as controls. These gave the number of TIFs before x-ray radiation therefore, the number of TIFs measured after x-ray radiation were taken as a true value of number of TIFs.

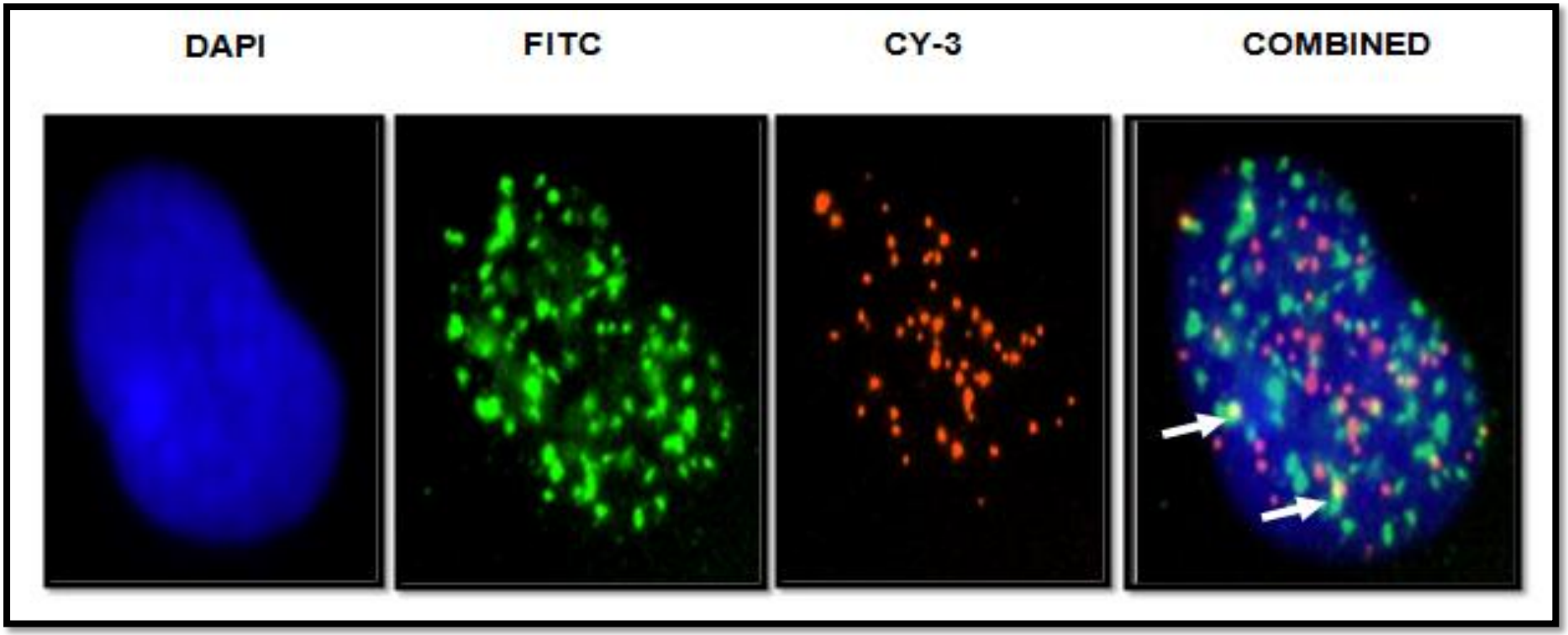

Figure 4-17: An image representing a HLE Donor 3 cell for TIF analysis 2.0Gy after x-ray radiation. Each image represents different filters used in the microscope. The first one from the left is a DAPI image of the cell analysed. This image shows the overall DNA in the cells. The second image is a FITC representation of the cell. This shows all the DNA damage Foci in the cell (γ-H2AX foci). The third image is the CY-3 filter and these are the telomeres in the cell. The last image shows a combination of all three images together and it can be seen where the white arrows are pointing that there are yellow spots. These show overlapping of the FITC and CY-3 staining. This represents TIF – these are DNA damage foci at telomeres.

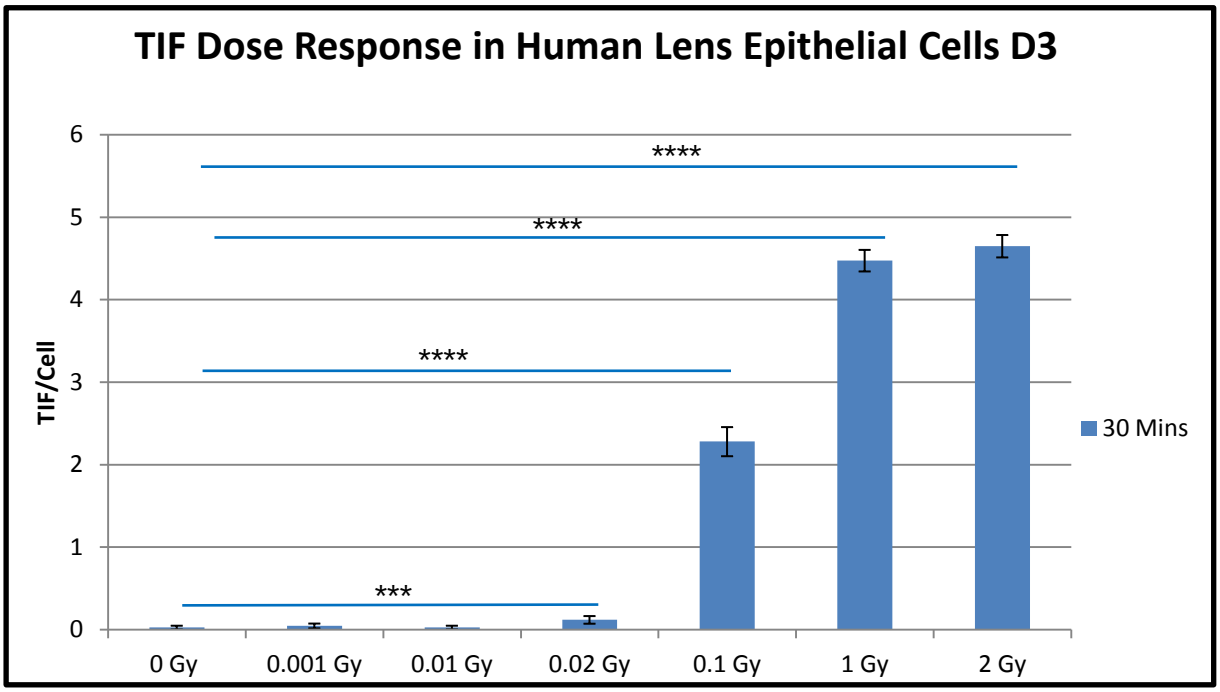

Figure 4-18: TIF dose response of Donor 3 HLE cells at different doses. The results show a significant increase in number of TIF's 0.02Gy after x-ray radiation. A significant dose dependent increase is noted after 0.02Gy of x-ray radiation. This repair is noted for up to 2.0Gy after x-ray radiation. The blue bar shows the number of TIF in the cells 30mins after radiation. Error bars represent S.E.M. (*** P<0.001, **** P<0.0001)

A dose dependent increase was seen of 0.05 TIF/cell at 0.001Gy of radiation to 4.65 TIF/cell after 2.0Gy of radiation. This is an increase of 4.62 foci per cell post irradiation when compared to the control. Significant increases in TIF/cells were noted only after 0.02Gy of radiation. The results for 0.001Gy and 0.01Gy were similar to the ones observed at 0Gy and no significant changes were noted.

4.2.7 TIF Repair Kinetics

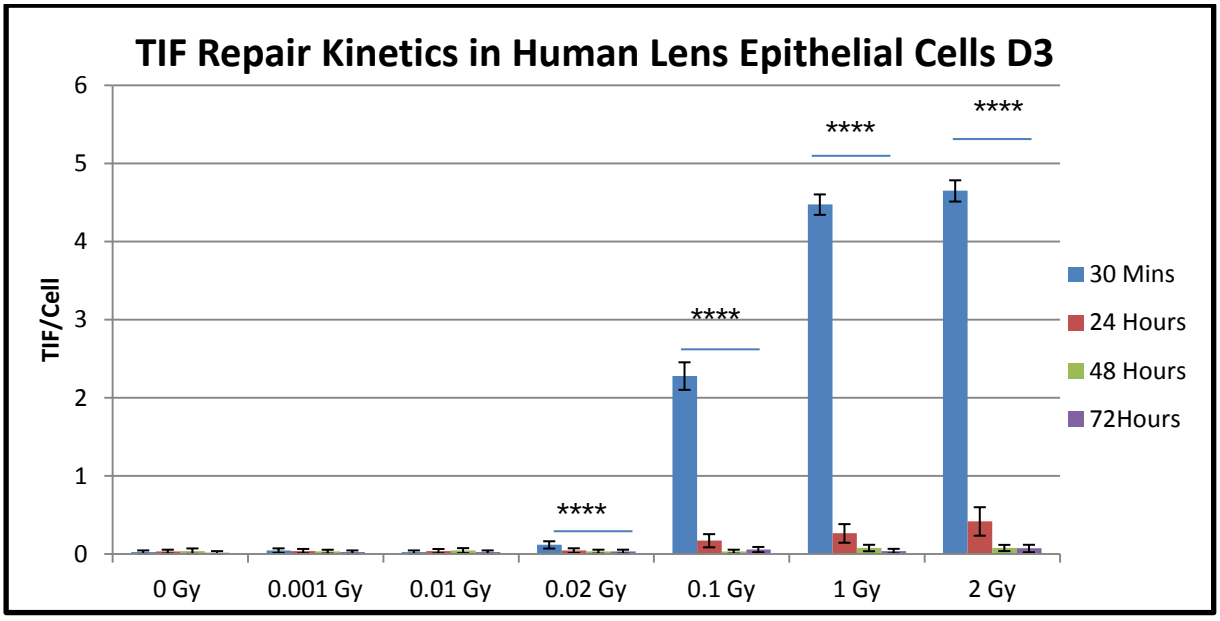

Figure 4-19: TIF repair kinetics of Donor 3 HLE cells at different doses. It can be seen that TIF's are repaired effectively 72hours after radiation, for up to 2.0Gy of x-ray radiation. The blue bar shows the number of TIF in the cells 30mins after radiation; the red bar shows 24hours, Green Bar 48 hours and Purple Bar 72hours after cells were irradiated. Error bars represent S.E.M. (**** P<0.0001)

The repair kinetics for TIF's in these cells is normal for up to 2.0Gy of radiation as seen in Figure 4-19. DNA damage at telomeres decreases from 4.65 to 0.07 foci after 72 hours, of 2.0Gy irradiation. The 0.07 foci per cell is close to the 0.04 noted in 0Gy of radiation. This can be seen for all three doses that show a significant increase in TIF's 30mins after radiation exposure; 0.02Gy, 0.1Gy, 1.0Gy and 2.0Gy. TIF's per cell decrease to similar number to background TIFs after 72 hours post exposure.

4.3 Discussion

Telomere length in normal cells decreases as the cell ages (Harley, Futcher and Greider, 1990) (Allsopp et al., 1992) (Shammas, 2011) due to the end replication problem and exonucleolytic activity (Watson, 1972) (Olovnikov, 1973) (Makarov, Hirose and Langmore, 1997). However, both section 3.2 and 4.2 of this thesis show that telomere length in HLE cells increases as the passages in culture increase.

Furthermore, the investigations in this chapter have revealed that the effects of radiation on HLE cells results in longer telomeres at higher doses as the passages increase (Figure 4-3 Figure 4-6 Figure 4-8).

It is known that cataracts form at doses of 2.0Gy (Ainsbury et al., 2009), (Chodick et al., 2008) and from this chapter it can be seen evidently in Donor 2 (Figure 4-5 Figure 4-6) and Donor 3 (Figure 4-7 Figure 4-8) that there is an increase in telomere length, after radiation, in both the 30mins after radiation and in the delayed samples after higher doses of exposure. This change is not significantly different in Donor 1, and could be due to genetic differences in this donor.

To the best of my knowledge there are no studies conducted on HLE cells in the context of telomere length and cataractogenesis after irradiation. The study conducted in this chapter shows that telomere length is affected more so in the higher doses than in the low (Figure 4-4 Figure 4-6 Figure 4-8).

However, telomere length analyses were conducted on victims exposed to IR during the Chernobyl nuclear power plant accident (Reste et al., 2014). The studies showed that in victims who developed cataracts, telomere length shortened approximately 23 years after victims were exposed to IR. The victims of this accident did not receive doses that exceeded over 1.0Gy of IR (Reste et al., 2014). We have to take into

consideration that the results from this study were conducted on victim blood leukocytes and not directly in the lens cells. Therefore, it cannot be concluded whether the telomere length in the lens cells with cataracts had shorter or longer telomeres and were affected to radiation.

Furthermore, telomerase activity before and after irradiating HLE cells in all three donors was examined (Figure 4-9 Figure 4-10 Figure 4-11). There is telomerase activity in normal HLE cells; this is in line with published data (Colitz, Davidson and McGahan, 1999) where they show telomerase activity in canine Lens epithelial cells. We find that telomerase activity decreases dose dependently (Figure 4-9 Figure 4-10 Figure 4-11) which is also in line with activity measured in canine lens cells (Colitz, Davidson and McGahan, 1999).

This however, is not normal for other cell types, where previous studies have shown increase in telomerase activity after exposure to IR (Milanovic et al., 2006). Studies have also shown that the activity increases dose dependently (Leteurte et al., 1997). This however does not seem to be the case for Lens epithelial cells as activity both in our HLE donor cells and previous studies have shown decrease. There is no clear reasoning behind why telomerase activity in these cells decreases dose dependently, however for our HLE cells it could be because they are embryonic cells.

To understand whether the decrease in telomerase activity and increase in telomere length causes any detrimental damage to a cell before and after radiation, DDR analyses were done.

The DDRs; H2AX and TIF were analysed in all three donors (Figure 4-13 - Figure 4-19). Dose dependent increases were noted in cells from all three donors. A significant difference was noted after 0.02Gy of exposure. The repair kinetics for

these cells was normal for up to 2.0Gy of irradiation ((Figure 4-13 - Figure 4-19). Therefore, no long term effects of radiation were noted in cells from all three donors.

The results from both this chapter and the previous chapter show that there is an increase in telomere length and a decrease in telomerase activity in HLE cells in culture. These results can be compared to a study that was conducted in Human Mammary Epithelial Cells (HMEC's) where telomerase activity decreased as these cells aged in culture but a change in telomere length was not noted (Sputova et al., 2013). Therefore, it would be important to see if these same changes are noted in cells in-vivo as they might be different to those noted in culture.

The results from section 3.2 and 4.2 show that there are several differences between each donor demonstrating that genotype is important in the response of the lens to radiation.

The conclusion of this chapter is that telomere length increases significantly at higher doses. However, no significant changes are seen at lower doses. This is in line with previous research where cataracts have been shown to form at higher doses of 2.0Gy (Ainsbury et al., 2009), (Chodick et al., 2008).

Analysis of telomere length in mouse cataract model in life-time study

5.1 Introduction

Cataract is typically an age related disorder which forms over a period of time (Graw, 2003) (Ainsbury et al., 2009) (Ainsbury et al., 2016). Moreover, it is not a matter of whether the cataracts will form but when (Graw, 2003). Factors contributing to this include: genetic disposition, radiation exposure (Ainsbury et al., 2016) and even smoking. Hence, it is typically an age related disorder but not absolutely.

Several studies have been conducted to further understand radiation induced cataracts. The threshold dose for the development of cataracts is 2.0Gy (Ainsbury et al., 2009). However, some studies in this area have shown that doses of 0.5Gy can result in radiation-induced cataracts (Kleiman et al., 2007).

Telomere length is an important marker of ageing. Telomeres have shown to shorten as a cell divides due to the end replication problem (Watson, 1972) (Olovnikov, 1973) and exonucleolytic activity (Makarov, Hirose and Langmore, 1997). Furthermore when telomeres become critically short the cell enters senescence (Herbig et al., 2004) and scientists use short telomeres as markers of cellular senescence (Bernadotte, Mikhelson and Spivak, 2016). Therefore, telomeres play important roles in the study of many diseases, including cancer. Interestingly studies have also linked telomere length to cataracts (Babizhayev and Yegorov, 2014).

To understand better the development of cataracts studies have been conducted in a number of different mammals, canine (Colitz, Davidson and McGahan, 1999) (Babizhayev and Yegorov, 2014) and mouse (Kunze et al., 2015) (Graw et al., 2015) being examples of a couple.

Mouse models with a defect in the *Ercc2* gene have shown postnatal development of cortical cataracts (Graw et al., 2015). *Ercc2* is also referred to as *XPD* (Kunze et al., 2015). The *Ercc2* gene is involved in the excision repair pathway, which is important to repair a number of different DNA lesions such as interstrand adducts and base methylations (Subba, 2007).

Other than this, there are epidemiology studies which suggest that there is an increased risk of cataract formation with polymorphisms in *XPD* (Padma et al., 2011). One study has shown that not only does this gene cause problems with the NER (Nucleotide excision repair) repair pathway but a mutation has been linked to cataracts where homozygous Xpd^{G602D} mice show opacities in the eye (Kunze et al., 2015). It is known that the *Ercc2* gene is involved in both general transcription and DNA damage repair (Kunze et al., 2015).

The damage repair pathway that this gene is involved in is referred to as the NER pathway. NER pathway is involved in the repair through two sub pathways, global genome NER (GG-NER) and transcription-coupled NER (TC-NER) pathway (Marteijn et al., 2014). The GG-NER pathway is involved in repair throughout the genome in transcribed and un-transcribed DNA (Spivak, 2015). However, TC-NER is involved in repair at transcriptionally active parts of the genome (Spivak, 2015). NER works faster in the transcriptionally active regions of the genome. Here a whole damaged section of DNA strand containing a damaged nucleotide is replaced using the intact strand as a template (Sancar and Tang, 1993). Defects in the NER pathway can lead genetic diseases such as Xeroderma pigmentosum (XP), which results in UV light sensitivity. One form of DNA lesion caused by UV light is pyrimidine dimers. These can also be found at telomeres after exposure to UV light. NER is present at

telomeres, and repair of these dimmers through this pathway is effective (Jia, Chengtao and Chai, 2015). However, repair at telomeres with NER reduces with age (Jia, Chengtao and Chai, 2015).

Furthermore, studies in human subjects, showed a relationship between lens transparency and telomere length in lymphocytes (Sanders et al., 2011) and leukocytes (Reste et al., 2014). Furthermore telomeres have been noted to be determinants of radiation sensitivity in mice (Goytisolo et al., 2000).

Given this information we collaborated with Prof Jochen Graw and Dr Claudia Dalke, from Helmholtz Zentrum Munich Germany. Prof Graw and his team conducted a life-time study on heterozygous *ERCC2* mutant mice to understand the relationship between radiation and cataracts. Doses below the 2.0Gy threshold dose were used to see if lower doses caused early onset of cataracts. Therefore, for this section of the project low doses below 0.5Gy were used to see the effects on cataract formation. Very little is known about the effects of low dose radiation on cataract formation.

A heterozygous mutant *ERCC2* model was used as it is known that the homozygous *ERCC2* mutant results in early onset of cataracts. Therefore, the heterozygous mutant model is pre-disposed to cataracts hence exposure to radiation would be a second hit showing if radiation causes early onset of cataracts.

For our part of the study bone marrow samples from these heterozygous mutant mice were analysed for telomere length. We used these samples to link telomere length differences to see if telomere length linked to cataractogenesis as has been done in previous studies using lymphocytes and leukocytes (Sanders et al., 2011) (Reste et al., 2014).

5.2 Results

For this section of the thesis telomere length was measured in bone marrow samples from a cataract mouse model. The bone marrow samples were received from Prof Jochen Graw's lab. His team had recessive *Ercc2* mutation mice. These were on the background of a C3H strain (suffering from a recessive retinal degeneration caused by a mutation in the *Pde6b* gene (Pittler and Baehr, 1991). Prof. Graw's team crossed homozygous male mutants (homozygous female mutants are sterile) with female C57BL/6J mice resulting in virtually healthy heterozygous *Ercc2* mutants. These mice were also heterozygous for the two parental strains (F1 hybrids). Correspondingly, the wild-type controls are crossed in a similar way (wild-type male C3H x wild-type female C57BL/6J).

The initial plan for this section was to investigate telomere length in both bone marrow and mouse lens epithelial cells. However, the mouse lens epithelial cells did not ship well from Germany to Prof. Munira Kadhim's lab, our Oxford Brookes University project collaborators. The lens epithelial cells received did not grow in culture. Therefore, enough cells were not obtained to enable telomere length measurements. Hence, telomere length was only measured in the bone marrow samples.

A different method of telomere length measurement was used for this section. Cells were shared between our lab and Prof. Munira Kadhim's team, who used them for chromosomal aberration analysis. The amount of bone marrow cells were not enough to split for chromosomal aberration analysis and DNA extraction, for aTL q-PCR. Instead, a methodology established in Dr Predrag Slijepcevic's lab, interphase Q-

FISH (IQ-FISH) was used. This required cells in fixative which could be used for both our work and that of Prof. Munira Kadhim's team.

The methodology used for this section was developed by Dr Predrag Slijepcevic's research group in collaboration with Digital scientific (Sway, 2010) as used to measure the telomere length in 2013. The methodology uses the IP-LAB software to measure the fluorescence intensity in the cells, where the strength of the fluorescence intensity is proportional to the telomere length. Detailed description of this methodology is found in section 2.11 of this thesis. Examples of images analysed are shown in Figure 5-1.

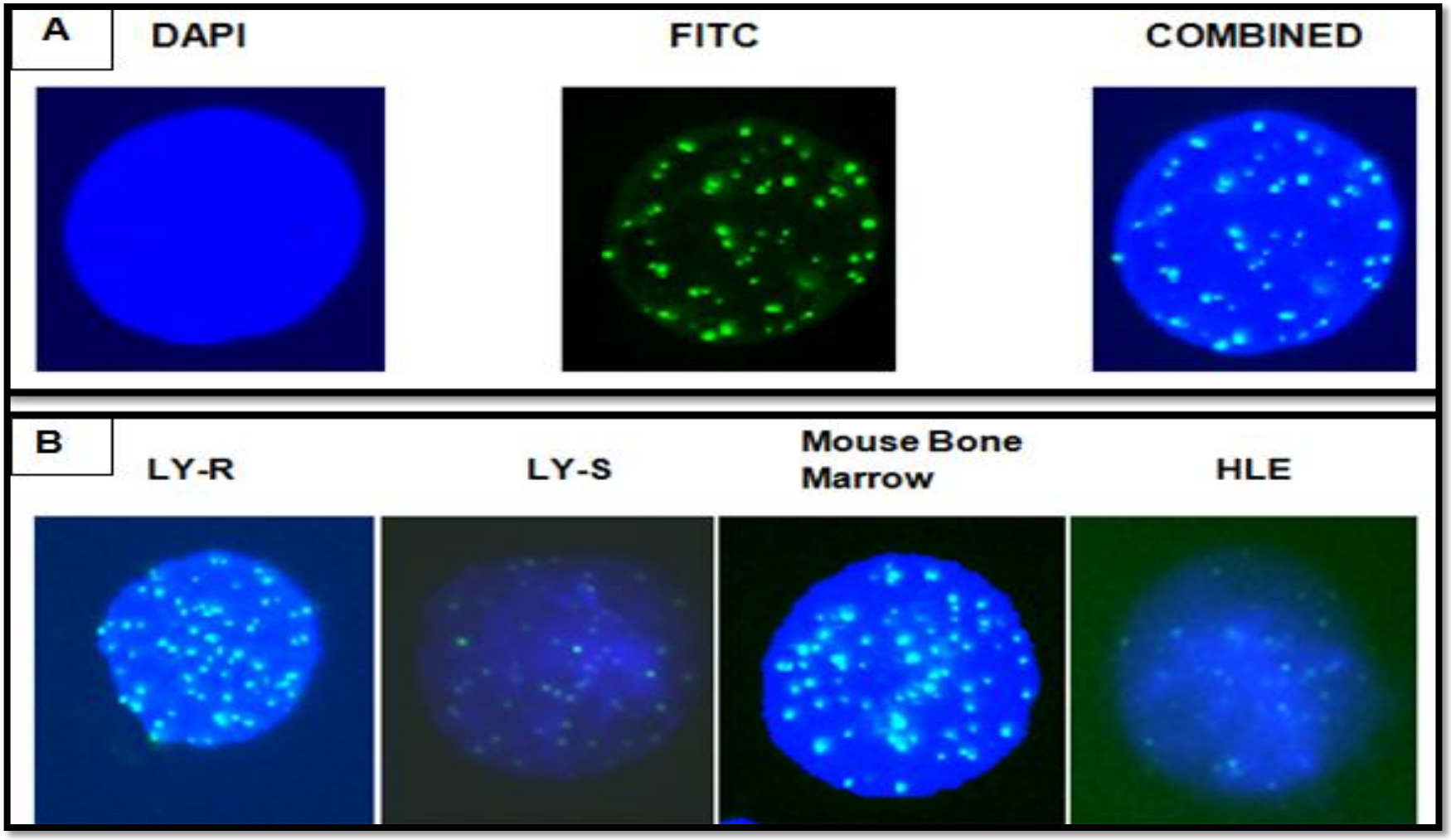

Figure 5-1: Microscopic IQ-FISH cell images: A) Cell line divided into three rows, DAPI filter (DNA), FITC filter (telomeres) and combined image. Combined image corresponds to the analysed sample, where fluorescence signal is proportional to the telomere length. B) Examples of different cell lines to show difference in fluorescence intensity.

For each experiment, two cell lines LY-R (L5178Y radioresistant) and LY-S (L5178Y-S radiosensitive) were used alongside the sample in question as calibration standards. It is known from previous work that the telomere length for LY-R cells is around 48kb and that of LY-S cells is around 7kb (McIlrath et al., 2001). During analysis using the IP-LAB software 25 images are taken of the sample in question and 25 of both LY-R and LY-S. The analyses were done in triplicate. Therefore a total of 75 cells is analysed per sample. The average fluorescence obtained from these 75 cells is then converted to CCFL (corrected calibrated Fluorescence). The CCFL value is calculated to eliminate the changes in telomere fluorescence intensity. This change is observed due to the changes in bulb intensity which changes every time the microscope is switched on during the triplicate analysis.

To obtain the CCFL value 25 cells from LY-R and 25 cells from LY-S are measured. This is done at 5 different times. The average of these 5 analyses is kept for future analysis. These values give historic average fluorescence for LY-R and LY-S and are referred to as the fluorescence for LY-R (FL_{LY-R}) and fluorescence for LY-S (FL_{LY-S}).

Each time a new experiment is done IQ-FISH is performed on a new LY-R and LY-S slide alongside the new samples. In the case of this chapter, mouse bone marrow samples are the new samples in question. Telomere length in 25 LY-R cells and LY-S cells is measured, this is referred to as the experimental fluorescence value (Experimental Fluorescence of LY-R ($FL_{LY-R(exp)}$) and Experimental fluorescence of LY-S ($FL_{LY-S(exp)}$)). Alongside the 25 LY-R and 25 LY-S cells, a total of 25 cells from the samples in question are measured (mouse bone marrow sample).

For each of the calibration standard cell lines correction factors (CF) are calculated. For the LY-R cell line CF1 values are calculated by using the formula ($CF1 = FL_{LY-R}/FL_{LY-R(exp)}$) and for the LY-S cell line CF2 values are calculated using the formula ($CF2 = FL_{LY-S}/FL_{LY-S(exp)}$).

The results from CF1 and CF2 are then averaged. This value gives the final correction factor (CF). To get the CCFL value, the CF value is multiplied by the average fluorescence value of the sample under investigation (FL_x).

The formulas for each step are shown below:

1. $CF1 = FL_{LY-R}/FL_{LY-R(exp)}$ **2. $CF2 = FL_{LY-S}/FL_{LY-S(exp)}$** **3. $CCFL = CF \times FL_x$**

The determined CCFL is graphically plotted and analysed to examine the telomere length differences in each of the samples being investigated.

A total of 320 samples were obtained from the life-time study conducted on cataract model mice. Prof. Jochen's team irradiated and maintained the mice for a total of 24 months. Whole body irradiation (^{60}Co) was done on 10 week old male and female mice (Figure 5-2). The doses used were 0Gy, 0.063Gy, 0.125Gy and 0.5Gy at a dose rate of 0.063Gy/min (Figure 5-2).

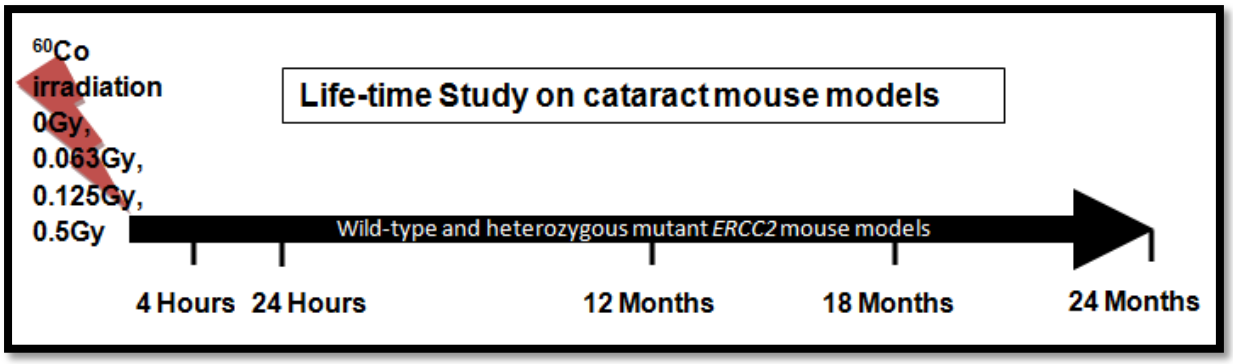

Figure 5-2: Time-line of the project. Illustration of the life-time study showing the different time points when mice were sacrificed. Mice were exposed to radiation at 10 weeks of age.

The mice were monitored over a period of 24 months. Every month the lens transparency was checked using a Scheimpflug camera. A Scheimpflug camera is a top end camera that is used in medicine to look at opacity of the lens. Examples of Scheimpflug images of the lens are shown in Figure 5-3. Figure 5-3 represents female wild-type and heterozygous mutant *ERCC2* lens cells, 4 hours after radiation and 24 hours after radiation (control and 0.5Gy) mice. The densitometer shows that there is a slight percentage increase in opacity of the lens 24 months after radiation. However, this change is not clinically significant, as can be seen from the opacity of the lens images.

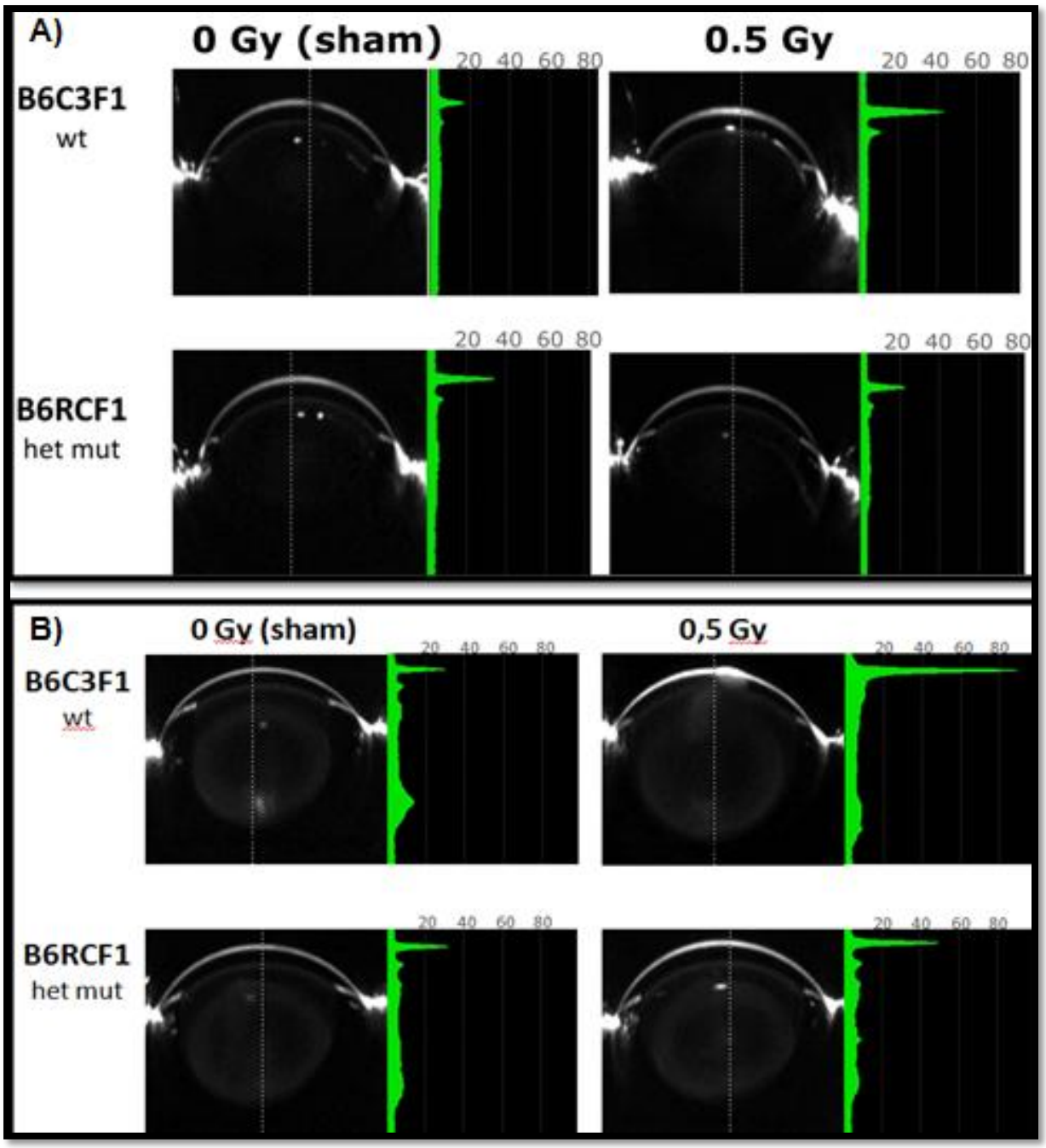

Figure 5-3: Example of Scheimpflug images. Scheimpflug images of mouse lens cells taken by Prof. Jochen Graw's team on a monthly basis. A) The lens Scheimpflug images 4 hours after radiation in female mice. B) The lens Scheimpflug images 24months after radiation in female mice. The lens is in the centre while the cornea is at the top. The shiny areas on the left and right sides are hairy skin. The green densitometer represents the percentage opacity of the lens measured at the dotted line. The peaks (from top to bottom) represent the reflections at the cornea and the surface of the lens.

Mice were sacrificed at 4 hours, 24 hours, 12 months, 18 months and 24 months after irradiation for chromosomal analysis and telomere length measurement (Figure 5-2).

During shipping, 5 of these samples did not have bone marrows in them. This was due to damage to tubes during shipping and mice dying before reaching certain time-points. The samples were divided into smaller workable groups to make analysis easier.

5.2.1 Telomere length in non-irradiated mouse bone marrow samples

We started with measuring telomere length in non-irradiated samples. The result of these analyses is shown in Figure 5-4.

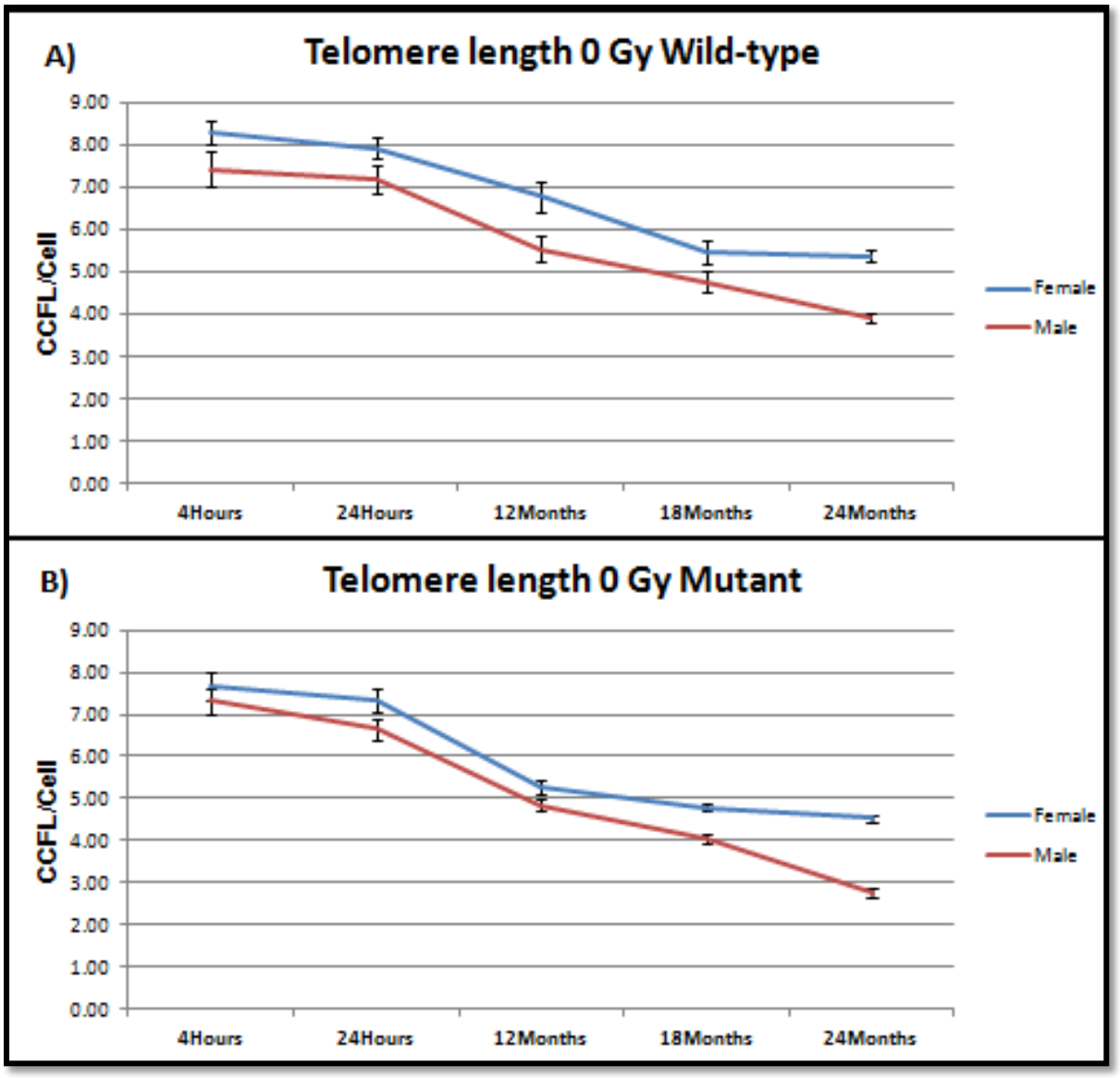

Figure 5-4: Telomere length in mutant and wild-type non-irradiated mice. The red bar represents the male samples and the blue bars represent the female samples. A) Telomere length in wild-type mice. Male samples have shorter telomeres compared to female samples. B) Telomere length in mutant mice. Male samples have shorter telomeres compared to female samples. Both graphs show telomere length decrease 24months later when compared against 4hours. The error bars represent S.E.M

It can be seen from Figure 1-4 that telomere length in both mutant and wild-type samples decreases over the period of 24 months. Additionally, there is a difference in telomere length between female and male samples throughout the monitoring period in both mutant and wild-type samples (for the result of statistical analysis section 5.2.7.

5.2.2 Telomere length in wild-type mouse bone marrow samples after irradiation

Next, we measured telomere length in samples from irradiated wild-type mice. Results of these analyses are presented in Figure 5-5.

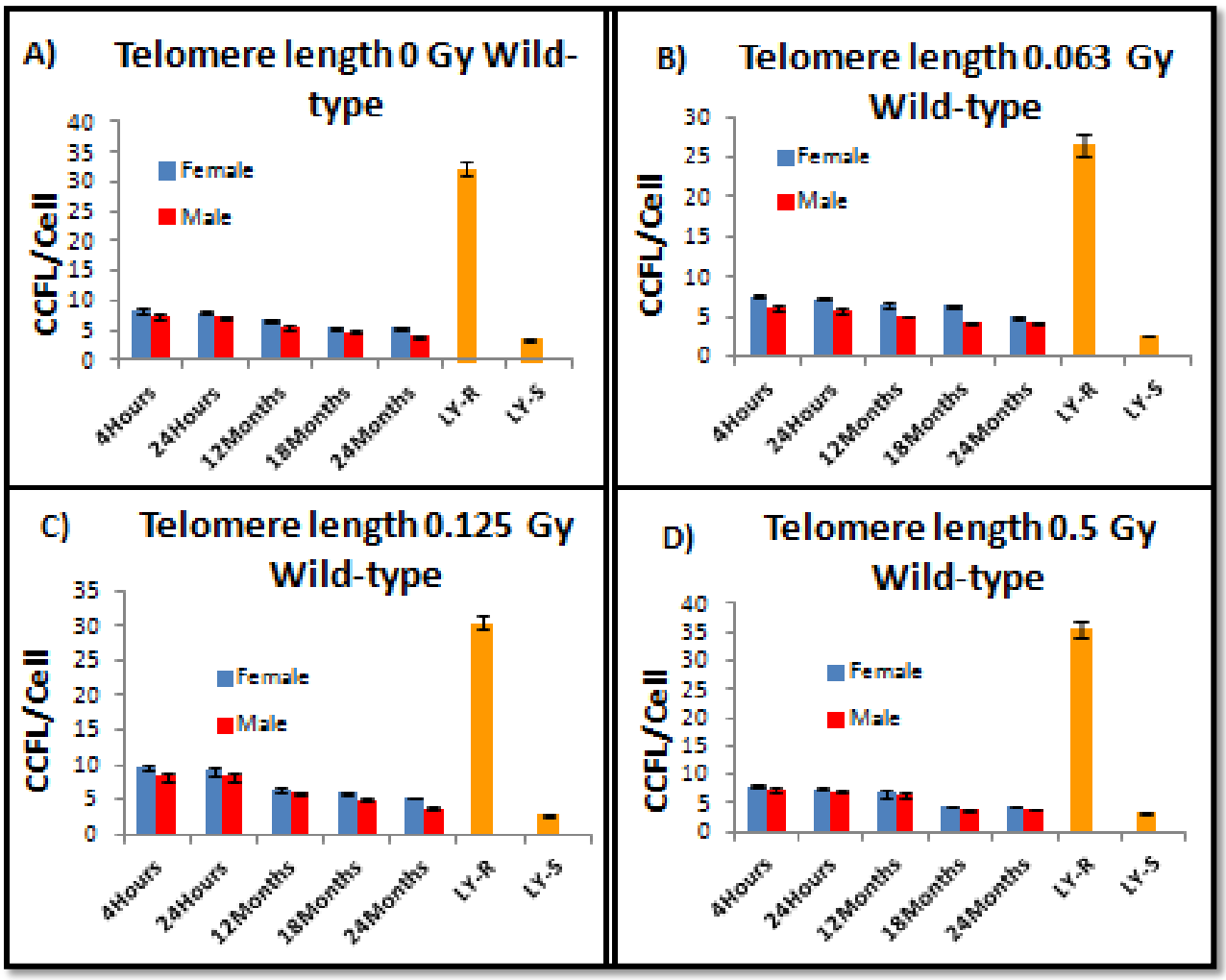

Figure 5-5: Telomere length in irradiated wild-type samples. A) Telomere length in control non-irradiated samples. B) Telomere length after 0.063Gy of irradiation. C) Telomere length after 0.125Gy of irradiation. D) Telomere length after 0.5Gy of irradiation. All four graphs show telomere length decrease in cells when measured after 24months when compared to samples from 4hours after radiation. The blue bars represent data in female samples and the red represents data in the male samples. The orange bars represent calibration standards. The error bars represent S.E.M.

The results in Figure 5-5 show that telomere length in wild-type samples decreases over the period of 24 months. The male samples show shorter telomeres in comparison to the female samples, as seen in the non-irradiated samples (Figure 5-4).

5.2.3 Telomere length in mutant mouse bone marrow samples after irradiation

Furthermore, telomere length analyses were conducted on mutant irradiated samples. The results of this have been shown in Figure 5-6.

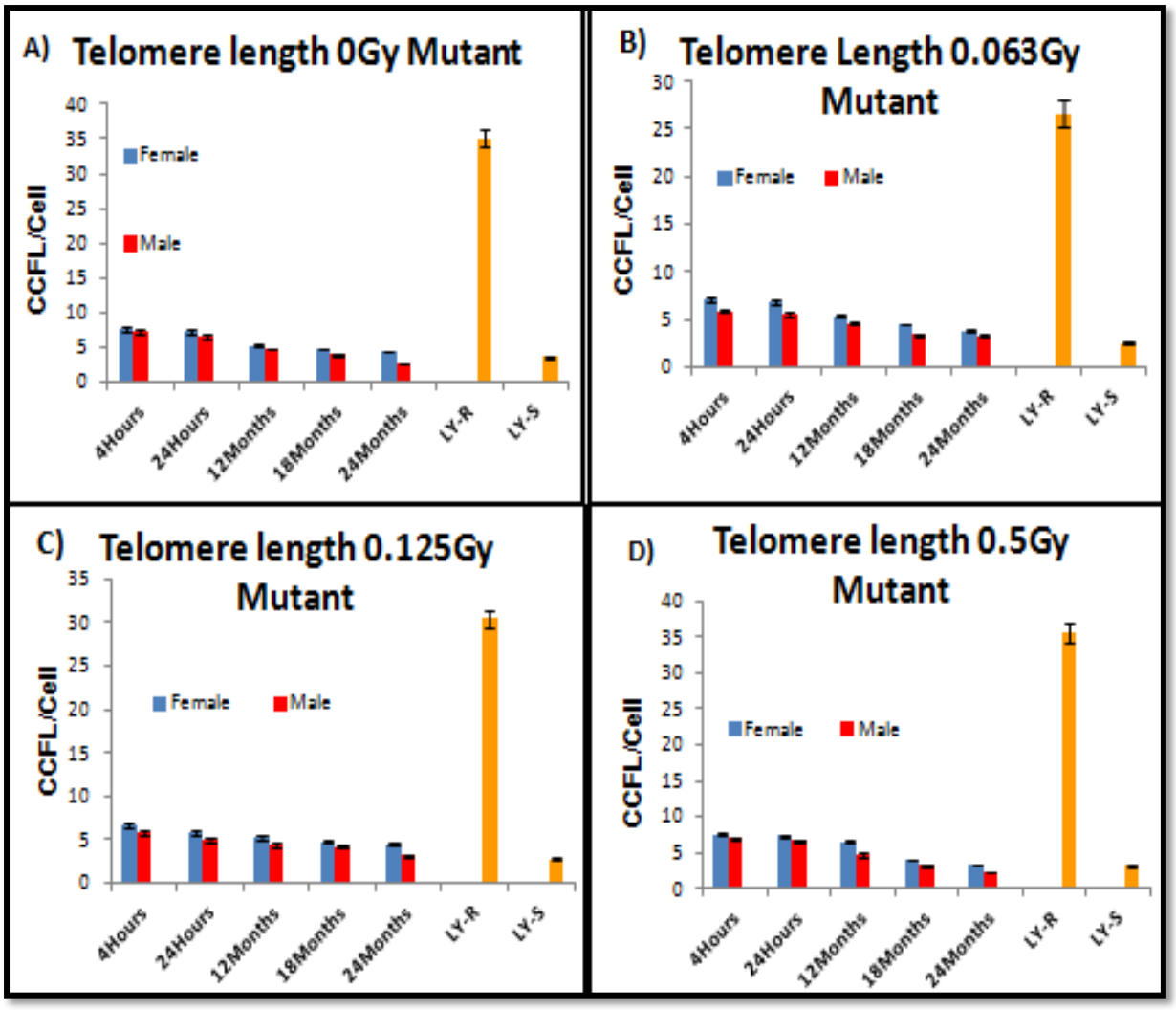

Figure 5-6: Telomere length in irradiated mutant samples. A) Telomere length in control non-irradiated samples. B) Telomere length after 0.063Gy of irradiation. C) Telomere length after 0.125Gy of irradiation. D) Telomere length after 0.5Gy of irradiation. All four graphs show telomere length decrease 24months later when compared to 4 hours after irradiation. The blue bars represent data in female samples and the red represents data in the male samples. The orange bars represent calibration standards. The error bars represent S.E.M.

The results show an overall telomere length decrease over a period of 24 months. This trend is similar to the one noted in wild-type irradiated samples (Figure 5-5). It can be seen that female samples like in the wild-type irradiated samples (Figure 5-5) is longer than the male samples.

5.2.4 Dose dependent comparison of telomere length in mice bone marrow samples

Given that from section 5.2.2 and 5.2.3 dose dependent changes were unable to be determined, analyses were done on wild-type and mutant samples to understand this better.

5.2.4.1 *Wild-type*

The results of the dose dependent changes in wild-type samples have been presented in Figure 5-7.

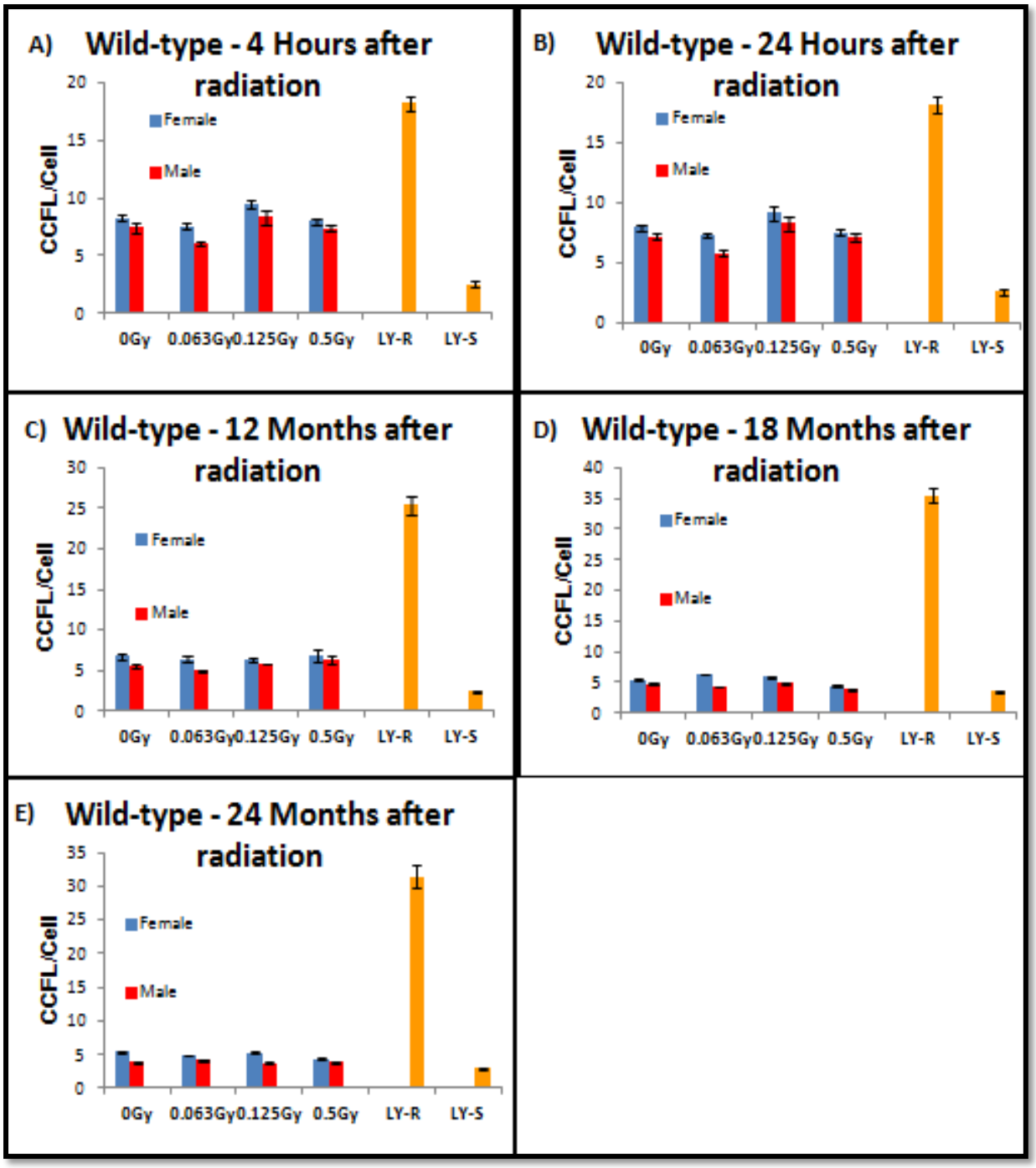

Figure 5-7: Telomere length comparison at different radiation doses in wild-type mice. A) All samples 4 hours after irradiation. B) All samples 24 hours after irradiation. C) All samples 12 months after irradiation. D) All samples 18 months after irradiation. E) All samples 24 months after irradiation. All five graphs show no dose dependent changes in telomere length. The red bars show male samples and the blue bars show female samples. The orange bars represent calibration standards. The error bars represent S.E.M.

Like with all the previous results, the telomere length in the female mice samples is longer than that of the male samples. The results of wild-type samples showed no dose dependent changes in telomere length at any time points (Figure 5-7). Statistical analysis have been presented in section 5.2.7.

5.2.4.2 *Mutant*

The results of the dose dependent telomere length changes in mutant samples have been presented in Figure 5-8.

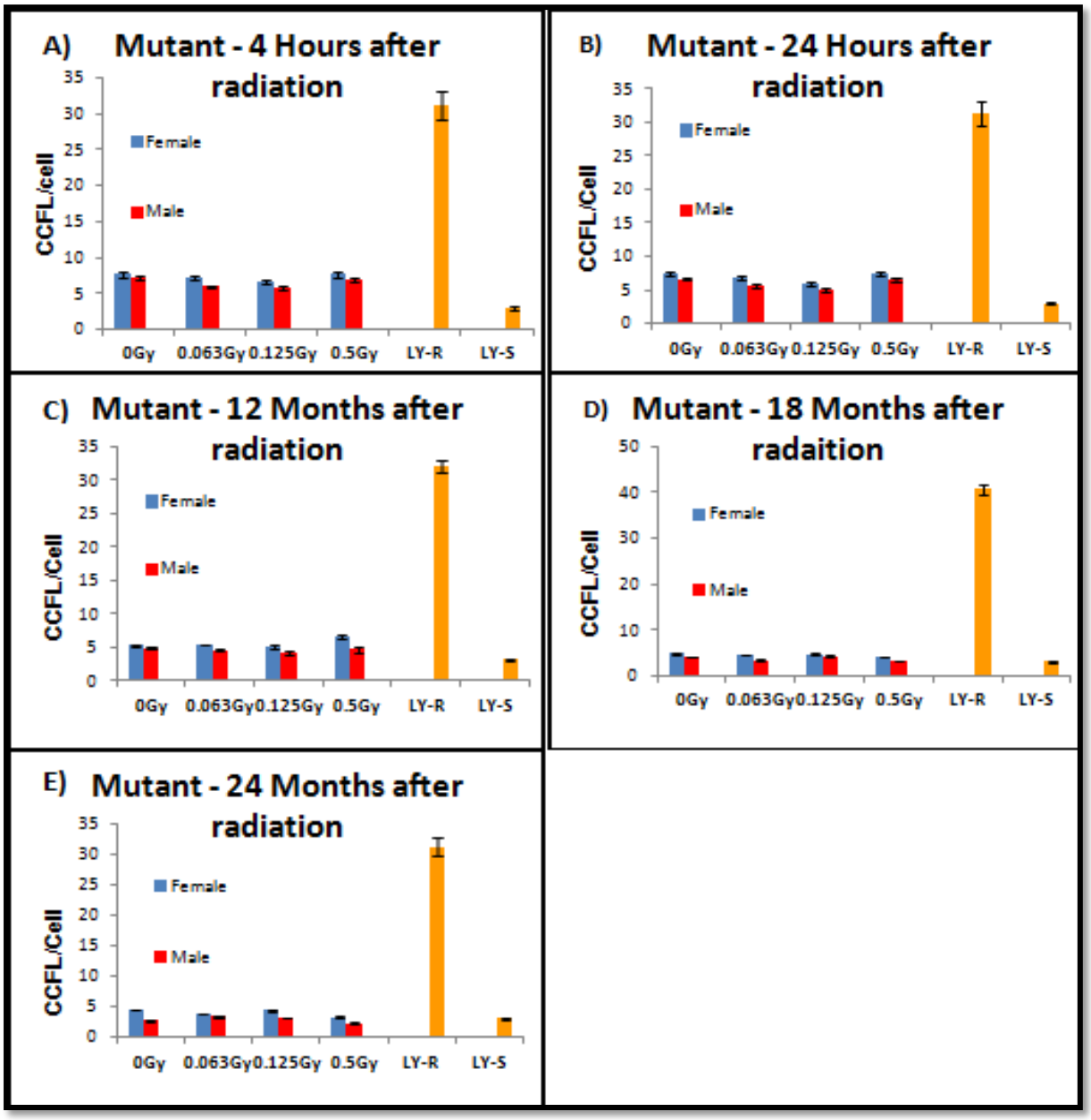

Figure 5-8: Telomere length comparison at different radiation doses in mutant mice. A) All samples 4 hours after irradiation. B) All samples 24 hours after irradiation. C) All samples 12 months after irradiation. D) All samples 18 months after irradiation. E) All samples 24 months after irradiation. All five graphs show no dose dependent changes in telomere length. The red bars show male samples and the blue bars show female samples. The orange bars represent calibration standards. The error bars represent S.E.M.

There are no statistical (section 5.2.7) dose dependent changes noted in the mutant samples (Figure 5-8) just like in the wild-type samples (Figure 5-7). The only

changes seen in this sample are the ones shown in male samples when compared to female samples.

5.2.5 Comparison of telomere length of mice bone marrow in mutant and wild-type samples

Having established that the telomere length in bone marrow samples shortened over a period of 24 months, both in non-irradiated (Figure 5-4) and irradiated (Figure 5-5 - Figure 5-6) samples and that there were no dose dependent changes (Figure 5-7 - Figure 5-8), telomere length analyses on mutant and wild-type samples were done.

5.2.5.1 *Female*

Once it was determined that there were no dose dependent changes in the samples. Analyses were done on female bone marrow samples to see if there was a difference in mutant and wild-type samples. The results in Figure 5-9 show these results.

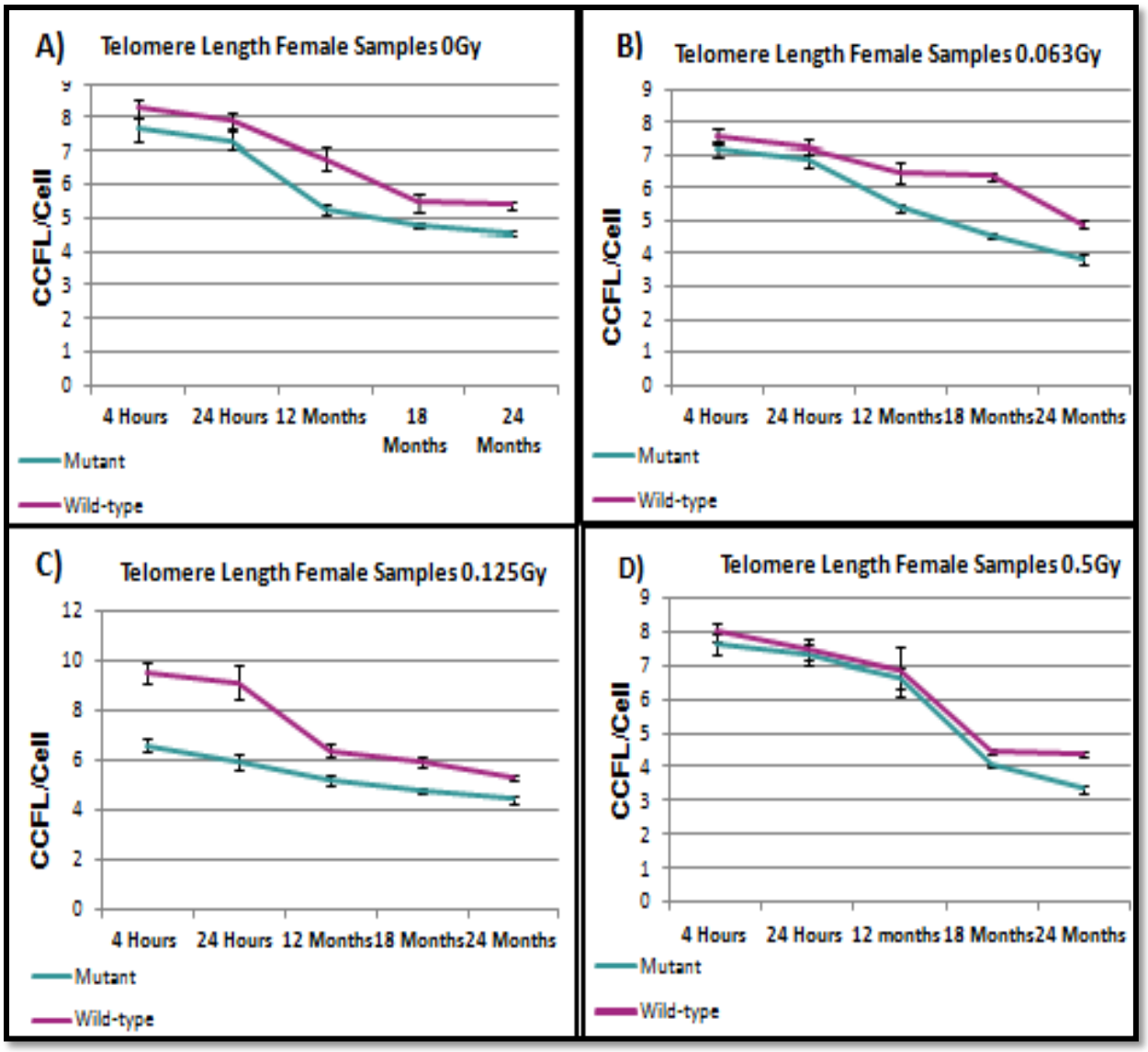

Figure 5-9: W**ild-type and mutant telomere length in female samples.** A) Telomere length in control samples. B) Telomere length 0.063Gy after irradiation C) Telomere length 0.125Gy after irradiation D) Telomere length 0.5Gy after irradiation. All four graphs show shorter telomeres in mutant samples when compared to wild-type samples. The pink lines show wild-type samples and the green line shows mutant samples. Error bars represent S.E.M.

The results show that there are shorter telomeres in mutant samples when compared to wild-type samples. These changes are statistically significant (section 5.2.7).

5.2.5.2 *Male*

Telomere length was then measured in the male samples to see if the mutant mice had shorter telomeres than wild-type samples as noted in the female samples. The results of this have been presented in Figure 5-10.

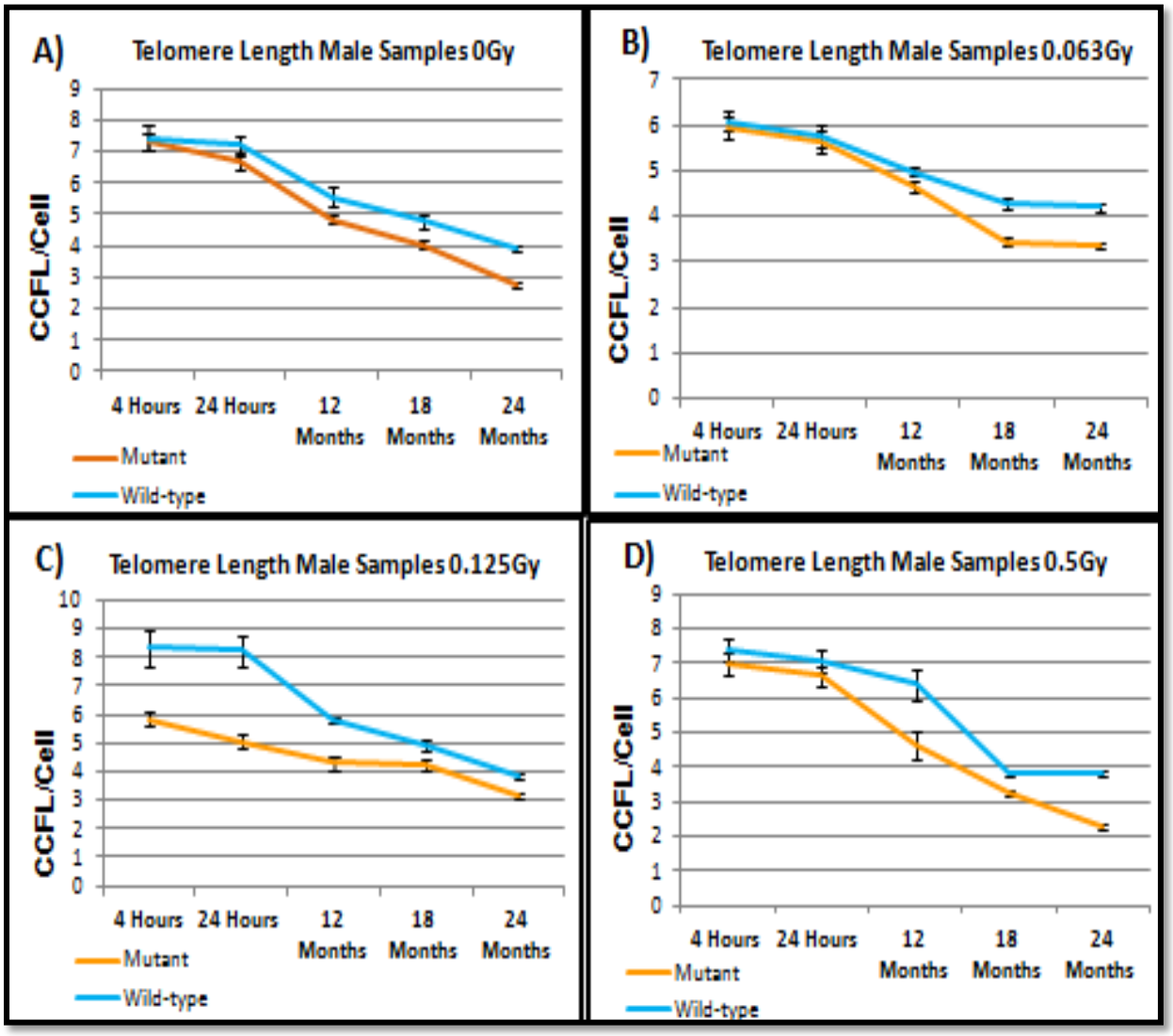

Figure 5-10: Wild-type and mutant telomere length in male samples. A) Telomere length in control samples. B) Telomere length 0.063Gy after irradiation C) Telomere length 0.125Gy after irradiation D) Telomere length 0.5Gy after irradiation. All four graphs show shorter telomeres in mutant samples when compared to wild-type samples. The blue lines show wild-type samples and the orange line shows mutant samples. Error bars represent S.E.M.

The results show similar results to those presented in Figure 5-9, female samples. The mutant samples in the male mice also show shorter telomeres when compared to the wild-type samples. These are statistically significant (section 5.2.7).

5.2.6 Rate of telomere length difference over 24 months

Having analysed the dose dependent changes and changes over time in mice the rate of telomere change was calculated and presented in Table 5-1. This was calculated by taking the CCFL value of each group at 24 hours and subtracting it at 4 hours. The greatest telomere length difference was noted in mutant samples apart from at 0.125Gy where wild-type samples show a higher rate of change (Table 5-1).

Table 5-1: Represents the telomere differences 24 months after radiation. It also represents the difference in telomere length at each given dose, in both wild-type and mutant mice.

Differences in telomere length (4 hours to 24months)				
	0GY	**0.063Gy**	**0.125Gy**	**0.5Gy**
Mutant Female	3.13	3.30	2.17	4.29
Wild-type Female	2.89	2.68	4.21	3.60
Mutant Male	4.55	2.60	2.67	4.70
Wild-type Male	3.52	1.90	4.50	3.55

5.2.7 Statistical Analysis

The statistics on our data was done by our German collaborators as they wanted uniform statistics for the publication. The statistical analysis of all the telomere results showed that there was no significant dose dependent change (p=0.261). However, statistically female samples were longer than male samples (p<0.001). It was also found that there was a significant difference between wild-type and mutant samples where telomeres were longer in wild-type compared to mutant (p<0.0001). The statistical analysis have been presented in Table 5-2.

Table 5-2: Statistical analysis done on all the mouse bone marrow samples.

	Adjusted Means	95% CI
0 Gy	5.87	5.52; 6.23
0.063 Gy	5.43	5.08; 5.78
0.125 Gy	5.87	5.51; 6.22
0.5 Gy	5.68	5.32; 6.03
females	6.21	5.96; 6.46
males	5.22	4.97; 5.47
mutants	5.21	4.96; 5.46
wild types	6.22	5.97; 6.47

For the analysis of the telomere lengths a linear regression model with the classification variables dose group, gender, genotype and all of their interaction terms where used. Based on this model adjusted means and the corresponding confidence intervals were derived.

For the P-values shown in this chapter the F-test was used. For group differences the F-test obtained from the linear regression model was applied. P values less than 0.05 were considered as

statistically significant. All analyses were done by the statistical software package SAS Version 9.3.

5.2.8 Chromosomal Aberrations

Our collaborators, Prof. Munira Kadhim and her team at Oxford Brookes University analysed the number of chromosomal aberrations that were found in the mouse bone marrow samples. These results were obtained from them and have been presented in Figure 5-11.

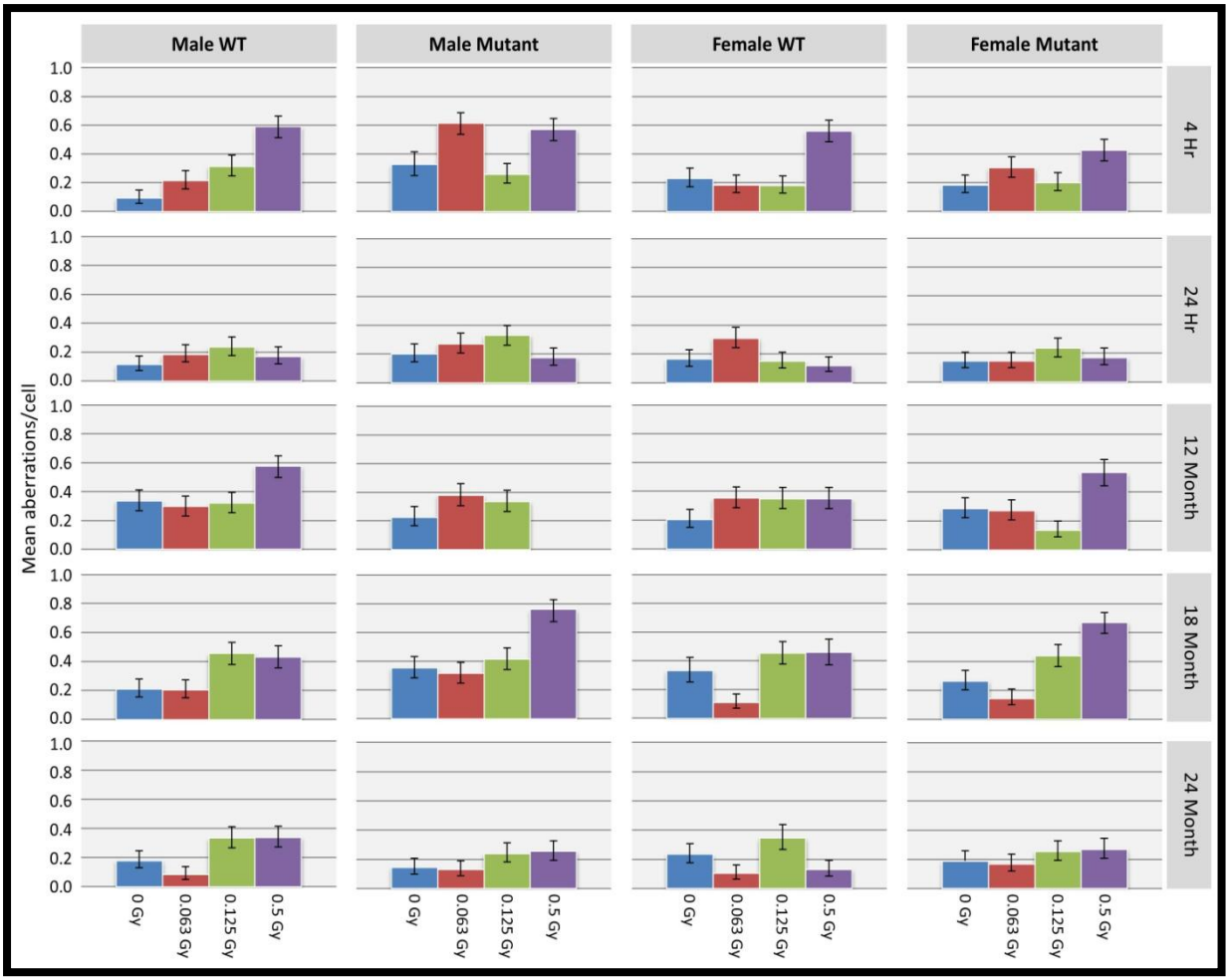

Figure 5-11: Chromosomal aberrations in mouse bone marrow samples. Figure shows graph representing results from our Oxford Brookes collaborators. Chromosomal aberrations were counted in all the samples using 50 metaphases. An average per cell for each group has been presented in this figure. The Blue bars represent data in the non-irradiated samples; the red bars represent data 0.063Gy after radiation, green bars 0.125Gy after radiation and purple bars 0.5Gy after radiation.

The results were analysed in 50 metaphases after Giemsa staining. An overall statistically significant dose-response relationship was observed for most of the samples, exceptions of which were seen in; male wild types at 24 hrs (p= 0.058), male mutants at 24 hrs (p=0.0153), male mutants at 12 months (p=0.024), male mutants at 24 months (p=0.0161), female wild types at 12 months (p=0.0195); female mutants at 24 hrs (p=0.1112) and female mutants at 24 months (p=0.0907).

These statistics show that the mutant groups were more affected than the wild-type groups, where a dose dependent change was not noted.

5.2.9 Lens Opacities

Our project collaborators in Munich, Germany, Pof. Jochen Graw and his team examined the lens opacities on a monthly basis on the mice models whose bone marrow was used to measure telomere length. The results were obtained from his team and have been presented in Figure 5-12.

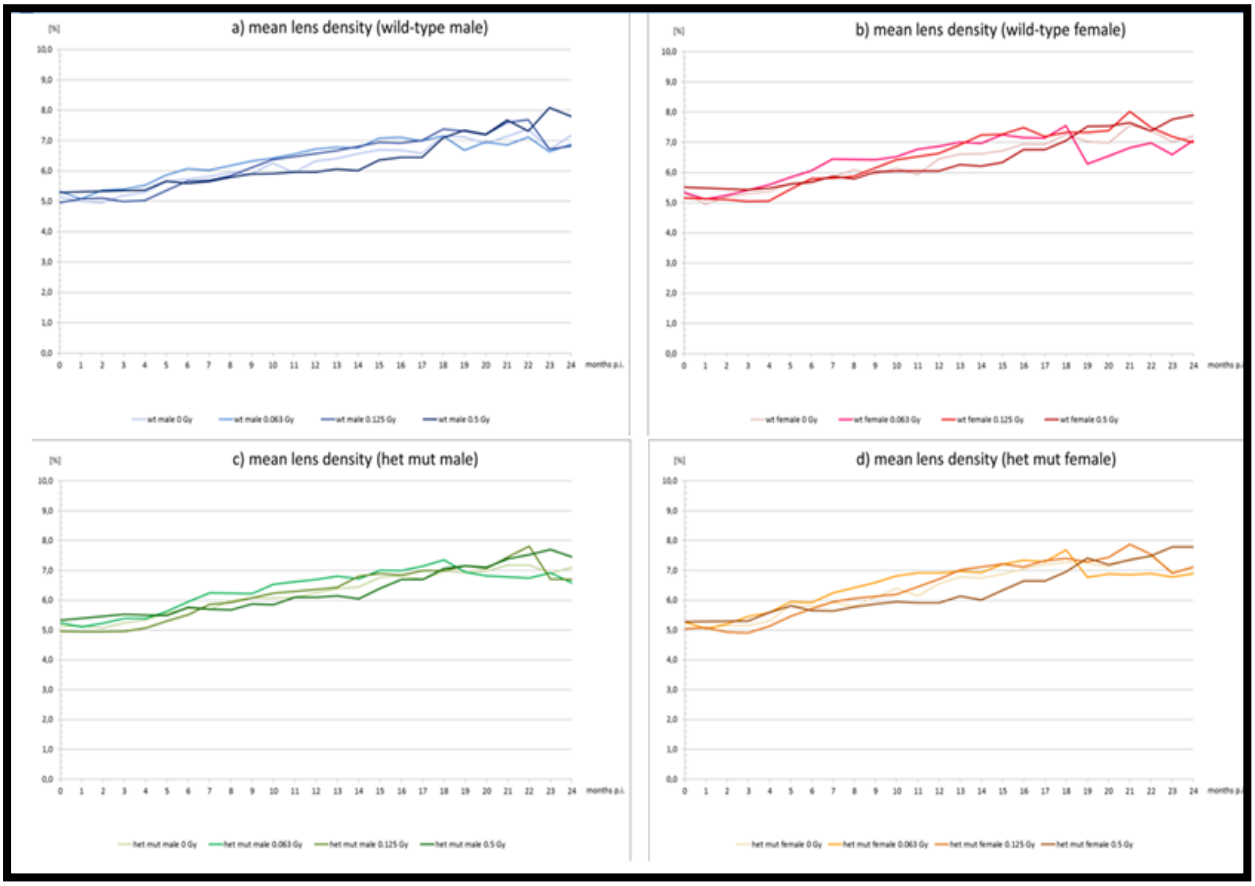

Figure 5-12: Lens density of mouse lens. Figure represents graphs of the data from our Munich collaborators, showing the lens opacities of the mice determined using a Scheimpflug camera. Graph A) represents the lens opacity in wild-type males, B) in wild-type female, C) mutant male and D) female. Each graph shows results for all four radiation doses used; 0, 0.063, 0.125 and 0.5Gy.

The results showed that there are no significant differences in the lens opacities due to radiation. Although a trend of increasing opacities can be seen as the mice age, the radiation induced to the mice does not show a significant increase in the opacities noted. The highest radiation 0.5Gy, leads to an increase in lens opacity however this is clinically insignificant.

They found that there were slight but significant differences between females and males, however no differences were observed between the mutant and wild-type samples.

Furthermore, they found that age made a difference to the lens density where it was 5.1-5.5% at the time of irradiation and increased to 7.5-7.9% 24months post-irradiation in all the groups.

The results of this section are now prepared for publication which includes other results done in the study by collaborators including overall survival, body weight and even pathological findings. The work was supported at least in part by the DoReMi Network of Excellence grant agreement n° 249689 of the European Atomic Energy Community's 7th Framework Program.

5.3 Discussion

The aim of this section was to understand the link between telomeres and cataractogenesis in-vivo. This was a collaborative study with Prof Jochen Graw, Helmholtz centre, Munich, Germany and Prof Munira Kadhim, Oxford Brookes University. Telomeres in bone marrow samples were measured in our lab, chromosomal aberrations in Prof. Munira Kadhim's and lens opacities in Prof. Jochen Graw's lab. The combination of these results helped understand the link between DNA damage repair and telomere length in association with cataractogenesis.

The results did not show a direct correlation between the lens transparency of the mice (Figure 5-12) and the telomere length in the bone marrow samples (Figure 5-4 - Figure 5-10) of these mice. There was no early onset of cataracts due to radiation. Nonetheless significant conclusions were obtained.

For telomere length analysis, it was found that the telomere length in female samples was longer than in male samples. These results were in line with results from previous studies (Cherif et al., 2003) (Peter Möller, 2009). Results are supported by previous studies based on comparisons made in the kidney, pancreas, liver and lung of rats (Cherif et al., 2003). The other study was conducted in human lymphocytes samples where longer telomeres were found in females when compared to males (Peter Möller, 2009). They also found that telomere length shortening was faster in males when compared to female samples (Peter Möller, 2009).

The telomere length in both the irradiated and non-irradiated samples decreased over a period of 24 months (Figure 5-4). These results are in line with telomere

shortening in normal cell. Telomeres shorten in normal cells as they age (Harley, Futcher and Greider, 1990) (Allsopp et al., 1992) (Shammas, 2011).

Our study also show, telomere length in the mutant samples was shorter at every time point when compared to the wild-type samples (Figure 5-9 Figure 5-10). This was the case for both the male (Figure 5-10) and female (Figure 5-9) samples. A possible explanation for this outcome is the missing repair gene in the mutant samples. The mutation in the *Ercc2* gene could have affected the telomere length in the next generation of mice, which were used in this study. Yuri Dubrovah's lab has shown that offspring of irradiated parental mice show effects of radiation (Safeer K Mughal, 2012). Therefore, it is interesting to see that there are changes in telomere length in the heterozygous mice in our study.

The lens opacity data showed a significant difference between the male and female samples (Figure 5-12), this data is in line with previously published data, which showed that females are more likely to get cataracts compared to males (Klein, Klein and Lee, 1998), (Courtright and Lewallen, 2009), (Graw et al., 2011). The Scheimpflug camera images showed no difference in lens density between the mutant and wild-type samples (Figure 5-12). Finally the results of this study showed no dose-dependent changes in lens opacities (Figure 5-12). However, a slight increase in lens opacity was noted both at 0.063 and 0.5Gy after radiation (Figure 5-12). However, no significant clinical implications can be made with this small change. The biggest lens opacity change was noted between the early mice and the 24 months after mice (Figure 5-12). Age showed a significant increase in the density of lens, when imaged with the Scheimpflug camera.

With the results for the chromosomal aberrations an increase in the number of aberrations was noted 4 hours after radiation, this reduced down significantly to background levels in all the samples in the 24 months analysis (Figure 5-11). There was a dose dependent increase in the number of aberrations in these mice (Figure 5-11). However, it was noted that this was not the case for many of the mutant male time points and one of the female mutant times (Figure 5-11). Our collaborators are at this moment unable to say why this is the case.

Although there was no correlation between cataract formation and telomere length due to the heterozygous *Ercc2* gene mutation, the telomere length decreased with age. It is known that cataracts form over time too. This was even seen in the Scheimpflug camera images, lens density increased as the sample age increased.

It was also observed that telomeres did not change dose-dependently and our collaborators did not find any changes in the transparency of the lens dose dependently either. Therefore, telomere length can be linked to the formation of cataracts due to age. However a conclusive link between telomeres and early onset of cataracts was not observed in this study.

General Discussion

In this thesis we have assessed the changes that take place in telomere length in association with the formation of cataracts due to radiation. Our study was conducted both in-vivo, in bone marrow samples from mouse models and in culture using primary HLE cells. Our results have revealed some previously unknown facts about telomere length and telomerase activity in HLE cells.

The study found that telomere length increased in the cells from all three donors as the passages increased in culture.

This is not in line with previous known facts, where normal cells are shown to have shorter telomeres as they age (Jiang, Ju and Rudolph, 2007), (Shammas, 2011). One possible explanation for this increase in telomere length in HLE cells is that the cells used for this study are embryonic cells gestation weeks 20-24 (Caltag Medsystems). Therefore, the telomeres in these cells could possibly behave differently when comparing them to normal human fibroblasts. However, there is a study that has been conducted on normal human fibroblasts which shows that the length of telomere does not affect whether the cell ages (Fumagalli et al., 2012). This suggests that although previously it was believed that short telomeres indicate ageing in a cell, that this may not be the case and that long telomeres can also result in early onset of ageing (Fumagalli et al., 2012). However, the study suggests that the amount of damage at telomeres may still be used as a marker of ageing. It has been seen in this experiment that the amount of unrepaired damage increases at telomeres. We however, in our study have found that the TIFs (damage at telomeres) in HLE donor 3 cells repair effectively for up to 2.0Gy of radiation (Figure

4-19). This however, is a low dose when compared to the dose used in the study which used 20Gy (Fumagalli et al., 2012).

To the best of my knowledge there are no studies conducted directly on HLE cells studying telomere length. However, one group has designed a drug (N-acetylcarninosine), which reduces the rate at which telomeres shorten. They have concluded that this helps prevent the formation of cataracts. Also stating that telomeres decrease in length as cells age in the HLE cells, therefore causing premature senescence (Babizhavev and Yegorov, 2010). However, the studies conducted by the group and used to understand cataracts in humans were actually done in canine, feline and murine mammals (Colitz, Davidson and McGahan, 1999) (Babizhayev and Yegorov, 2015). Therefore, it is unknown if telomeres like in these three mammals decreases in humans too.

Other studies have shown that premature senescence can take place in keratinocytes when in culture without post-mitotic fibroblast feeder cells (Darbro, Schneider and Klingelhutz, 2005). They found that $p16^{INK4a}$ accumulates in these cells regardless of the telomere length (Darbro, Schneider and Klingelhutz, 2005), and that as the passages increase in culture, expression of p16 increases steadily too (Natarajan et al., 2003). Therefore, it can be that that the HLE cells used in this thesis may have undergone premature senescence in culture even though the telomeres were maintained in length, more so due to the short replicative lifespan of these cells in-vitro. However, this may not be the case in in-vivo models.

Apart from telomeres increasing as the cell passages increased, changes in telomere length were noted due to radiation. The study showed that no significant

changes were noted at lower doses. However, telomere length increases were noted at higher doses (2.0Gy).

It was also noted that there were genetic differences in the cells from each donor. Therefore, suggesting that genetics plays a big role in the formation of cataracts as previous studies have shown (Graw et al., 2011).

The study presented in this thesis also found that telomerase activity decreases dose dependently in HLE cells, as the passages in culture increased. Telomerase activity is known to decrease dose dependently in canine lens cells (Colitz, Davidson and McGahan, 1999).

Given that telomerase activity decreases and telomere length increases in cells from all three donors the ALT pathway was investigated. Here it was found that HLE cells did not present ALT activity. Therefore, the increase in telomere length was solely due to the amount of telomerase activity present which was unexpectedly high in HLE cells.

It will be interesting to analyse telomere length, telomerase activity and DNA damage in these cells after exposing them to protracted radiation doses; i.e.: exposing the same cells to different radiation doses throughout their lifetime in the incubator, maybe after each passage. This could show changes in all three factors examined, as they might not be able to repair from the constant radiation exposure. This will help show clear cut links between the three factors and cataractogenesis. Alongside this, increasing the amount of radiation doses used to those shown in (Fumagalli et al., 2012) would be beneficial. This would show if repair takes place at telomeres even after higher amounts of radiation. Even though the paper has stated that 2Gy of

radiation showed similar amounts of DDR foci at telomeres after 30days post radiation it would be interesting to see if similar results are seen in HLE cells.

It would have also been interesting to measure lens opacities in these cells where telomere studies were being conducted. However, this is difficult as cells are not readily available.

Therefore, to cover this aspect we collaborated with Prof. Jochen Graw to study telomere length and relate it to lens opacities in-vivo. Using a mouse model, analysis of telomere length and lens opacities was possible in the same organism. However, as the lens cells for the mouse were not easy to transport it was difficult to analyse telomere length directly in the lens. Hence bone marrow samples were used. This was found as an appropriate approach as previously lymphocytes and leukocytes have been used to show a link between telomere length and lens transparency (Sanders et al., 2011) (Reste et al., 2014).

Given that some previous studies have suggested that doses as low as 0.5Gy can result in early onset of cataracts (Kleiman et al., 2007), the in-vivo lifetime study was designed to analyse changes at these low doses.

In our study we found that there were no significant changes in the lens opacities (work done by Prof. Jochen Graw's team) caused due to radiation. Although some changes were noted at 0.5Gy irradiation, these were not found to be clinically significant. Therefore, the study concluded that although in the past the lens was considered to be the most radio-sensitive tissue in the body (Ainsbury et al., 2009) our study shows that it is not.

Telomere length studies conducted on the bone marrow samples from these mice showed that there was a decrease in telomere length as the bone marrow cells aged. This is in line with telomere length studies as seen in normal cells (Allsopp et al., 1992), (Ouellette et al., 2000), (Ning et al., 2003), (Shammas, 2011).

However, no dose dependent changes were noted in these cells.

Telomere length was significantly higher in both the female and wild-type samples when compared to the male and mutant samples. The difference in telomere length between male and female samples has previously been shown in rats (Cherif et al., 2003), where females have longer telomeres. Other studies have shown that females are more likely to get cataracts compared to males (Klein, Klein and Lee, 1998) (Courtright and Lewallen, 2009) (Graw et al., 2011). Therefore, the results of this part of the study can be used to show that telomeres can be linked to cataractogenesis, as telomere length in females being different to males corresponds to differences in cataract formation. This was also noted in the lens opacities in the mice used in this study where females had earlier lens opacities to males.

To better understand the link between telomeres and cataractogenesis in mice, homozygous mutant mouse models should have been used. As it is known that there is an early onset of cataracts in these models to be control strains. Apart from this telomere length should be measured directly in the lens of the mouse samples to see if there are changes noted as cataracts form.

Alongside this, a higher dose as a control should also be used to see if 2Gy of radiation in the mutant samples shows an increase in cataract formation. This would

have been the positive control as it is known that acute doses of 2Gy causes early onset of cataracts (Ainsbury et al., 2009) (Ainsbury Elizabeth, 2016).

The study therefore concludes that when analysing the results closely a small link between telomere length and cataractogenesis can be seen. This link however is not clear at present but further studies discussed in this section and the next (section 7, Future Work) will help give a conclusion to this link.

Future Work

The results of the work presented in this thesis opened at least a couple of interesting avenues for future research. The first one is to look at the changes that will take place to telomere length, telomerase activity and DNA damage responses (both in the chromosomes and at telomeres), after exposing the cells to protracted or fractionated radiation rather than acute radiation. This would show if the cells still behave in the same way as they do after exposure to acute radiation.

To do this, cells will have to be grown as have been done in this study; they will be cultured and harvested after each passage. However, instead of just being irradiated once they would be irradiated after each passage either by the same amount of radiation dose as at the becoming or by diving that one dose into smaller fractions. To elaborate, if 2Gy of radiation is being used, the cells will be exposed to 2Gy of radiation at each passage until they stop growing. Alternatively, the cells can be left in the incubator and exposed to fractions of this dose. For instance, if the cells grow for 8 passages then at each passage instead of 2Gy, 0.25Gy will be used.

This would help to show if the cells repair as effectively after exposure to radiation of this kind as they did with the acute irradiations. It will also help understand more if the changes in telomeres are directly linked to the formation of cataracts.

The second one is to look at the presence of shelterin complex proteins in cells where cataracts are present. This can be done by analysing the presence of TRF2 which is usually the protein of choice when examining shelterin interaction. To analyse this interaction, cells from all three donors should be left in the incubator as done in this project and analysed at each passage for changes in the amount of

TRF2 present. If TRF2 does not show an increase, other proteins part of the shelterin complex should be measured. This is because as telomeres increase the amount of shelterin increases too, therefore it would be interesting to see if in lens cells from cataract patients these proteins are part of the proteins that cause cloudiness. It is already known that the crystalline proteins in the lens change as the lens becomes cloudy, leading to cataracts. Therefore, it will be interesting to see if other proteins involved in this change are shelterin proteins.

Finally, the link between cataracts and telomeres needs to be studied further. The in-vivo study conducted on mice should be conducted in the lens of the cell. Telomere length should be measured directly in the lens of the mouse to see if any changes are noted as the mouse ages and due to radiation.

To further investigate the correlation, the use of a homozygous mutant model, where cataract formation has been known to take place is suggested. As our collaborators did not find early onset of cataracts in these heterozygous mutant models the correlation between telomeres and cataracts was not seen.

It would further be interesting to examine the mice with protracted doses of radiation to see if this makes a difference to the formation of cataracts as the low doses used in this study did not show any significant differences in lens opacity. It would be interesting to see if the mice would react differently to the irradiation as the mice ages or in the next generations of the mutant mice.

Other studies have shown that telomeres decrease as the mice age, so it would be interesting to see if the shorter telomere mice are more sensitive to radiation as shown by Maria A Blasco. They show that fifth generation mice with short telomeres are more sensitive to irradiation and are hypersensitive to cumulative doses of

gamma rays (Goytisolo Fermin, 2000). This could mean that results from protracted radiation in terms of cataractogenesis could also be different to those of acute radiation.

The study therefore concludes that although there is no concrete evidence that telomeres are directly linked to the formation of cataracts, some evidence of changes in telomere length are noted in the lens of the eye, both due to ageing and radiation. Therefore, further studies as suggested in this section will help make conclusive the link between telomeres and cataractogenesis.

References

Ainsbury, E., Barnard, S., Bright, S., Dlake, C., Jarrin, M., Kunze, S., Tanner, R., Dynlacht, J., Quinlan, R., Graw, J., Kadhim, M. and Hamada, N. (2016) 'Ionising radiation induced cataracts: Recent biological and mechanistic developments and perspectives for future research', *Mutation research-reviews in mutation research*.

Ainsbury, E., Bouffler, S.D., Dorr, W., Graw, J., Muirhead, C.R., Edwards, A.A. and Cooper, J. (2009) 'Radiation cataractogenesis: a review of recent studies', *Radiation Research*, vol. 172, no. 1, July, pp. 1-9.

Allers, T. and Lichten, M. (2001) 'Differential timing and control of noncrossover and crossover recombination during meiosis', *Cell*, vol. 106, no. 1, July, pp. 47-57.

Allshire, R.C., Dempster, M. and Hastie, N.D. (1989) 'Human telomeres contain at least three types of G-rich repeat distributed non-randomly', *Nucleic Acids Research*, vol. 17, no. 12, June, pp. 4611-4627.

Allsopp, R.C., Vaziri, H., Patterson, C., Goldstein, S., Younglai, E.V., Futcher, A.B., Greider, C.W. and Harley, C.B. (1992) 'Telomere length predicts replicative capacity of human fibroblasts', *Proc Natl Acad Sci*, vol. 89, July, pp. 10114-10118.

Anderson, S. and Sekelsky, J. (2010) 'Meiotic versus mitotic recombination: two different routes for double-strand break repair: the different functions of meiotic versus mitotic DSB repair are reflected in different pathway usage and different outcomes', *Bioassays*, vol. 32, no. 12, December, pp. 1058-1066.

Andres, S.N., Vergnes, A., Ristic, D., Wyman, C., Modesti, M. and Junop, M. (2012) 'A human XRCC4-XLF complex bridges DNA', *Nucleic Acids Research*, vol. 40, no. 4, February, pp. 1868-1878.

Armanios, M. and Blackburn, E.H. (2012) 'The telomere syndromes', *Nat Rev Genet*, vol. 13, no. 10, September, pp. 693-704.

Atzmon, Cho, Cawthon, Budagov, Katz, Yang, Siegel, Bergman, Huffman, Schechter, Wright, Shay, Barzilai, Govindaraju and Suh. (2010) 'Genetic variation in human telomerase is associated with telomere length in Ashkenazi centenarians', *PNAS*, vol. 107, January, pp. 1710-1717.

Ayouaz, A., Raynaud, C., Heride, C., Revaud, D. and Sabatier, L. (2008) 'Telomere: Hallmarks of radiosensitivity', *Biochimie*, vol. 90, pp. 60-72.

Babizhavev, M. and Yegorov, Y. (2010) 'Telomere attrition in lens epithelial cells - a target for N-acetylcarnosine therapy', *Front biosciences (Landmark ed)*, vol. 1, no. 15, June, pp. 934-956.

Babizhayev, M.A. and Yegorov, Y.E. (2014) 'Biomarkers of Oxidative Stress and Cataract. Novel Drug Delivery Therapeutic Strategies Targeting Telomere Reduction and the Expression of Telomerase Activity in the Lens Epithelial Cells with N-Acetylcarnosine Lubricant Eye Drops: Anti-Cataract ', *Current Drug Delivery*, vol. 11, no. 1, pp. 24-61.

Babizhayev, M.A. and Yegorov, Y.E. (2015) 'Telomere attrition in Human lens epithelial cells assocaited with oxidative stress provide a new therapeutic target for the treatment, dissolving and prevention of cataracrs with n-acetylcarnosine lubricant eye drops. ', *Bentham Science*, vol. 10, June, p. 82.129.

Baker, D., Childs, B., Durik, M., Wijers, M., Sieben, C., Zhong, J., Saltness, R., Jehanathan, K., Verzosa, G., Pezeshki, A., Khazaie, K., Miller, J. and van Deursen,

J. (2016) 'Naturally occuring p16INK4a-positive cells shorten healthy lifespan', *Nature*, vol. 530, February, pp. 184-204.

Baker, D., Wijshake, T., Tchonoa, T., LeBrasseur, N., Childs, B., Van de Sluis, B., Kirkland, J. and van Deursen, J. (2011) 'Clearance of p16INK4a- positive senescent cells delays ageing-associated disorders', *Nature*, vol. 479, no. 7372, October, pp. 232-236.

Bandaria, J., Qin, P., Berk, V., Cu, S. and Yilsiz, A. (2016) 'Shelterin protects chromosome ends by compacting telomeric chromatin', *Cell*, vol. 164, no. 4, February, pp. 735-746.

Barlow, J.H. and Rothstein, R. (2010) 'Timing is everything: cell cycle control of Rad52', *Cell Division*, vol. 5, no. 7, February, pp. 1-8.

Bassnettt, S., Shi, Y. and Vrensen, G. (2011) 'Biological glass: structural determinants of eye lens transparency', *Philos Trans R Soc Lond B Biol Sci*, vol. 366, no. 1568, April, pp. 1250-1264.

Becker, M. and Wang, Z. (1989) 'Origin of ultraviolet damage in DNA', *J Mol Biol*, vol. 210, no. 3, December, pp. 429-438.

Benedek, G. (1971) 'Theory of transparency of the eye', *Appl Opt*, vol. 10, no. 3, March, pp. 459-473.

Bernadotte, A., Mikhelson, V. and Spivak, I. (2016) 'Markers of cellular senescence. Telomere shortening as a marker of cellular senescence', *Aging*, vol. 8, no. 1, January, pp. 3-11.

Blackburn, E.H. (1991) 'Structure and function of telomeres', *Nature*, vol. 350, April, pp. 569-573.

Blackburn, E. (2006) 'A history of telomere biology', in Titia de Lange, V.L.E.B. (ed.) *Telomeres*, Second Edition edition, Cold Spring Harbour Laboratory Press.

Blackburn, E., Epel, E. and Lin, J. (2015) 'Human telomere biology: A contributory and interactive factor in aging, disease risks and protection', *Science*, vol. 350, no. 6265, pp. 1193-1198.

Blasco, M.A. (2005) 'Telomere and human disease: ageing, cancer and beyond', *Nature reviews Genetics*, vol. 6, August, pp. 611-622.

Blasco, M.A., Lee, H.-W., Hande, M.P., Samper, E., Lansdorp, P.M., Depinho, R.A. and Greider, C.W. (1997) 'Telomere shortening and tumour formation by mouse cells lacking telomerase RNA', *Cell*, vol. 91, October, pp. 25-34.

Bonwell, C.C. and Eison, J.A. (1991) *Active Learning: Creating Excitement in the classroom*, Washington DC: Clearinghouse on Higher Education.

Bouffler S, A.E.G.P.H.J. (2012) 'Radiation-induced cataracts: the Health Protection Agency's response to the ICRP statement on tissue reactions and recommendation on the dose limit for the eye lens.', *J Radiol Pro*, vol. 32, no. 4, December, pp. 479-488.

Bower, K., Napier, C.E., Cole, S.L., Dagg, R.A., Lau, L.M.S., Duncan, E.L., Moy, E.L. and Reddel, R.R. (2012) 'Loss of Wild-Type ATRX Expression in Somatic Cell hybrids segregates with activation of alternative lengthening of telomeres', *PLOS*, vol. 7, no. 11, November, pp. 1-10.

Broccoli, D., Smogorzewska, A., Chong, L. and de Lange, T. (1997) 'Human telomeres contain two distinct Myb-related proteins, TRF1 and TRF2.', *Nat Genet*, vol. 17, no. 2, Oct, pp. 231-235.

Brookes, S., Rowe, J., Gutierres Del Arroyo, A., Bond, J. and Peters, G. (2004) 'Contribution of p16(INK4a) to replicative senescence of human fibroblasts', *Exp Cell Res*, vol. 298, no. 2, August, pp. 549-559.

Bryan, T.M., Englezou, A., Gupt, J., Bacchetti, S. and Reddell, R. (1995) 'Telomere elongation in immortal human cells without detectable telomerase activity', *The EMBO journal*, vol. 14, no. 17, pp. 4240-4248.

Bryan, T.M. and Reddel, R. (1997) 'Telomere dynamics and telomerase activity in in vitro immortalised human cells', *Eur J Cancer*, vol. 33, no. 5, April, pp. 767-773.

Buseman, C.M., Wright, W.E. and Shay, J. (2012) 'Is telomerase a viable target in cancer?', *Mutat Res*, vol. 730, February, pp. 90-97.

Casare, A.J. and Reddel, R.R. (2013) *Alternative Lengthening of Telomeres in Mammalian Cells*, Madame Curie Biosceinces Database.

Cawthon, R.M. (2002) 'Telomere measurement by quantitative PCR', *Nucleic Acids Research*, vol. 30, no. 10, May.

Celeste, A., Fernandez-Capetillo, O., Kruhlak, M., Pilch, D., Staudt, D., Lee, A., Bonner, R., Bonner, W. and Nussenzweig, A. (2003) 'Histone H2AX phosphorylation is dispensable for the initial recognition of DNA breaks', *Nature Cell Biology*, vol. 5, no. 7, July, pp. 675-679.

Cerone, M.A., Londono-Vallejo, J.A. and Bacchetti, S. (2001) 'Telomere maintenance by telomerase and by recombination can coexist in human cells', *Human Molecular Genetics*, vol. 10, no. 18, pp. 1945-1952.

Cesare, A.J. and Reddel, R.R. (2008) 'Telomere uncapping and alternative lengthening of telomeres', *Mechanisms of Ageing and development*, vol. 129, no. 1-2, pp. 99-108.

Chandeck, C. and Mooi, W. (2010) 'Oncogene-induced cellular senescence.', *Advances in Anatomic Pathology*, vol. 17, no. 1, pp. 42-48.

Cherif, H., Tarry, J.L., Ozanne, S. and Hales, C. (2003) 'Ageing and telomeres: a study into organ- and gender-specific telomere shortening', *Nucelic Acids Res*, vol. 31, no. 5, March, pp. 1576-1583.

Chiu, W., Shen, S., Yang, L., Chow, J., Wu, C. and Chen, Y. (2011) 'Inhibition of HSP90-dependent telomerase activity in amyloid β-induced apoptosis of cerebral endothelial cells', *J Cell Physiol*, vol. 226, no. 8, August, pp. 2041-2051.

Chodick, G., Bekiroglu, N., Hauptmann, M., Alexander, B.H., Freedman, D.M., Doodt, M.M., Cheund, L.C., Simon, S.L., Weinstock, R.M., Bouville, A. and Sigurdson, A.J. (2008) 'Risk of Cataract after exposure to low dose of ionising radiation: A 20 year Prospective Cohort study among US Radiologic Technologists', *American Journal Of Epidemiology*, vol. 168, no. 620-631.

Clout, C.S.N.J. (1999) 'Structure of the crystallins', *Eye*, vol. 13, pp. 395-402.

Colitz, C.M.H., Davidson, M.G. and McGahan, M.C. (1999) 'Telomerase activity in lens epithelial cells of normal and cataractous lenses', *Exp. Eye Res.*, vol. 69, pp. 641-649.

Cong, Y.-S., Wright, W.E. and Shay, J.W. (2002) 'Human telomerase and its regulation', *Microbiology Mol Bio Rev*, vol. 66, no. 3, September, pp. 407-425.

Courtright, P. and Lewallen, S. (2009) 'Why are we addressing gender issues in vision loss?', *Community eye health*, vol. 22, no. 70, June, pp. 17-19.

d'Adda di Fagagna, R.P.M.C.-F.L.F.H.C.P.V.Z.T.S.G.C.N.J.S. (2003) 'A DNA damage checkpoint response in telomere-initiated senescence', *Nature*, vol. 426, no. 6963, pp. 194-198.

d'Adda di Fagagna, F., Teo, S.-H. and Jackson, S.p. (2004) 'Functional links between telomeres and proteins of the DNA-damage response', *Genes and Development*, vol. 18, pp. 1781-1799.

Darbro, B., Schneider, G. and Klingelhutz, A. (2005) 'Co-regulation of p16INK4a and migratory genes in culture conditions that lead to premature senescence in human keratinocytes', *J Inves Dermatol*, vol. 125, no. 3, September, pp. 499-509.

Davis, A.J. and Chen, D.J. (2013) 'DNA double strand break repair via non-homologous end-joining', *Translational cancer research*, vol. 2, no. 3, June, pp. 130-143.

de Lange, T. (2002) 'Protection of mammalian telomeres', *Oncogene*, vol. 21, pp. 532-540.

de Lange, T. (2005) 'Shelterin: the protein complex that shapes and safeguards human telomeres', *Genes and Development*, vol. 19, no. 18, September, pp. 2100-2110.

de Lange Titia, V.L.B.E. (2006) *Telomeres*, 2nd edition, New York: Cold Spring Harbor.

de Lange, T., Shiue, L., Myers, R.M., Cox, R.M., Naylor, S.L., Killery, A. and Varmus, H. (1990) 'Structure and variability of human chromosome ends', *Mol Cell Biol*, vol. 10, no. 2, February, pp. 518-527.

Delaye, M. and Tardieu, A. (1983) 'Short-range order of crystallin proteins accounts for eye lens transparency', *Nature*, vol. 302, March, pp. 415-417.

Derradji, H., Bekaert, S., Oostveldt, P.V. and Baatout, S. (2005) 'Comparison of different protocols for telomere length estimation by combination of Quantitative Fluorescence In Situ Hybridisation (Q-FISH) and Flow Cytometry in human cancer cell lines', *Anticancer research*, vol. 25, no. 2A, March, pp. 1039-1050.

Desouky, O., Nan, D. and Zhou, G. (2015) 'Targeted and non-targeted effects of ionising radaition', *Journal of Radiation Research and Applied Sciences*, vol. 8, no. 2, April, pp. 247-254.

Diotti, R. and Loayza, D. (2011) 'Shelterin complex and associated factors at human telomeres', *Nucleus*, vol. 2, no. 2, March, pp. 119-135.

Donate, L.E. and Blasco, M.A. (2011) 'Telomeres in cancer and ageing', *Philosophical transactions of the royal society*, vol. 366, pp. 76-84.

Dunham, M., Nermann, A., Fasching, C. and Reddel, R. (2000) 'Telomere maintenance by recombination in human cells', *Nat Genetics*, vol. 26, no. 4, December, pp. 447-450.

Du, H., Pumbo, E., Ivanovich, J., An, P., Maziarz, R., Reiss, U., Chirnomas, D., Shimamura, A., Vlachos, A., Lipton, J., Goyal, R., Goldman, F., Wilson, D., Mason, P. and Bessler, M. (2009) 'TERC and TERT gene mutations in patients with bone marrow failure and the significance of telomere length measurements', *Blood*, vol. 113, pp. 309-316.

Energy, U.S.D.o. (2012) *Low Dose Radiation Research Program*, October, [Online], Available: http://lowdose.energy.gov/faqs.aspx#07.

Espejel, S., Franco, S., Sgura, A., Gae, D., Bailey, S.M., Taccioli, G.E. and Blasco, M.A. (2002) 'Functional interaction between DNA-PKcs and telomerase in telomere length maintenance', *The Embo Journal*, vol. 21, no. 22, November, pp. 6275-6287.

Espejel, S., Martin, M., Klatt, P., Martin-Caballero, J., Flores, J.M. and Blasco, M.A. (2004) 'Shorter telomeres, accelerated ageing and increased lymphoma in DNA-PKcs-deficient mice', *EMBO reports*, vol. 5, no. 5, May, pp. 503-509.

Evans, J.T.C. (2007) *NEB expressions Spring DNA damage - the major cause of missing pieces from the DNA puzzle*, [Online], Available: https://www.neb.com/tools-and-resources/feature-articles/dna-damage-the-major-cause-of-missing-pieces-from-the-dna-puzzle.

Fan, Q., Zhang, F., Barrett, B., Ren, K. and Andreassen, P.R. (2009) 'A role for monoubiquitinated FANCD2 at telomeres in ALT cells', *Nucleic Acids Research*, vol. 37, no. 6, January, pp. 1740-1754.

Feng, J., Funk, W., Wang, S., Weinrich, S., Avilion, A., Chiu, C., Adams, R., Chang, E., Allsopp, R. and Yu, J. (1995) 'The RNA component of human telomerase', *Science*, vol. 269, no. 5228, September, pp. 1236-1241.

Fermin A Goytisolo, E.S.J.M.-C.P.F.E.H.J.M.F.S.D.B.M.A.B. (2000) 'Short telomeres result in organismal hypersensitivity to ionising radiation in mammals', *J Exp Med*, vol. 192, no. 11, December, pp. 1625-1636.

Fisher, T.S. and Zakian, V.A. (2005) 'Ku: A multifunctional protein involved in telomere maintenance', *DNA repair*, vol. 4, April, pp. 1215-1226.

Fleming, N. and Baume, D. (2006) 'Learning Style Again: VARKing up the right tree!', *Educational Developments, SEDA Ltd*, vol. 7, no. 4, November, pp. 4-7.

Frescas, D. and de Lange, T. (2014) 'Binding of TPP1 protein to TIN2 protein is required for POT1a,b protein-mediated telomere protection', *J Biol Chem*, vol. 289, no. 35, August, pp. 24180-24187.

Fumagalli, M., Rossiello, F., Clerici, M., Barozzi, S., Cittaro, D., Kaplunov, J.M., Bucci, G., Dobreva, M., Matti, V., Beausejour, C.M., Herbig, U., Longhese, M.P. and d'Adda di Fagagna, F. (2012) 'Telomeric DNA damage is irreparable and causes persistent DNA-damage-response activation', *Nature Cell Biology*, vol. 14, February, pp. 355-365.

Giblin, F. (2000) 'Gluthathione: a vital lens antioxidant', *J Ocul Pharmacol Ther*, vol. 16, no. 2, April, pp. 121-135.

Gonzalo, S., García-Cao, M., Fraga, M., Schotta, G., Peters, A., Cotter, S., Eguía, R., Dean, D., Esteller, M., Jenuwein, T. and Blasco, M. (2005) 'Role of the RB1 family in stabilizing histone methylation at constitutive heterochromatin', *Nat Cell Biol*, vol. 7, no. 4, April, pp. 420-428.

Gosselin, K., Martien, S., Pourtier, A., Vercamer, C., Ostoich, P., Morat, L., Sabatier, L., Duprez, L., T'Kint de Roodenbeke, C., Gilson, E., Malaquin, N., Wernert, N.,

Slijepcevic, P., Ashtari, M., Chelli, F., Deruy, E., Vandenbunder, B., De Launoit, Y. and Abbadie, C. (2009) 'Senescence-Associated Oxidative DNA Damage Promotes the Generation of Neoplastic Cells', *Cancer Research*, vol. 69, no. 20, pp. 7917-7925.

Goytisolo, F., Samper, E., Martin-Caballero, J., Finnon, P., Herrera, E., Flores, J., Bouffler, S. and Blasco, M. (2000) 'Short telomeres result in organismal hypersensitivity to ionising radiation in mammals', *J Exp Med*, vol. 192, no. 11, December, pp. 1625-1636.

Grandin, N. and Charbonneau, M. (2009) 'elomerase- and Rad52-independent immortalization of budding yeast by an inherited-long-telomere pathway of telomeric repeat amplification.', *Mol Cell Biol*, vol. 29, no. 4, February, pp. 968-985.

Graw, J. (2003) 'The genetic and molecular basis of congenital eye defects', *Nature Reviews*, vol. 4, pp. 876-888.

Graw, J., Kunze, S., Dalke, C., Fuchs, H., Klaften, M., Sabrautzki, S. and Hrabe de Angelis, M. (2015) 'Mutation in the ERCC2 gene of the mouse causes cataracts', *Acta Ophthalmologica*, vol. 93, no. S255, September.

Grawunder, U., Zimmer, D., Fugmann, S., Schwarz, K. and Lieber, M. (1998) 'DNA Ligase IV is essential for V(D)J recombination and DNA double-strand break repair in human precurdor lymphocytes', *Mol Cell*, vol. 2, no. 4, October, pp. 477-484.

Graw, J., Welzl, G., Ahmad, N., Klopp, N., Heier, M., Wulff, A., Heinrich, J., Döring, A., Karrasch, S., Nowak, D., Schulz, H., Rathmann, W., Illig, T., Peters, A., Holle, R., Meisinger, C. and Wichmann, H. (2011) 'The KORA Eye Study: a population-based

study on eye diseases in Southern Germany (KORA F4).', *Investigative opthalmology & visual science*, vol. 52, no. 10, pp. 7778-7786.

Greider, C.W. (1999) 'Telomeres do D-Loop - T-Loop', *Cell*, vol. 97, May, pp. 419-422.

Greider, C.W. and Blackburn, E.H. (1985) 'Identification of a specific Telomere terminal transferase activity in Tetraymena Extracts', *Cell*, vol. 43, December, pp. 405-413.

Greider, C.W. and Blackburn, E. (1989) 'A telomeric sequence in the RNA Tetrahymena telomerase required for telomere repeat synthesis', *Nature*, vol. 337, January, pp. 331-337.

Griffiths, J.D., Comeau, L., Rosenfield, S., Stansel, R.M., Bianchi, A., Moss, H. and Lange, T.d. (1999) 'Mammalian telomeres end in a large duplex loop', *Cell*, vol. 97, May, pp. 503-514.

Gutierrez-Enriquez, S. and Hall, J. (2003) 'Use of the cytokinesis-block micronucleus assay to measure radiation-induced chromosome damage in lymphoblastoid cell lines', *Mutation Research*, vol. 535, pp. 1-13.

Hamada Nobuyuki, S.T. (2016) 'Cataractogenesis following high-LET radiation exposure', pp. 1-55.

Harley, C.B., Futcher, A.B. and Greider, C.W. (1990) 'Telomeres shorten during ageing of human fibroblasts', *Nature*, vol. 345, no. 6274, pp. 458-460.

Hayflick, L. (1965) 'The Limited in vitro lifetime of human diploid cell strains', *Experimental cell research*, vol. 37, no. 3, March, pp. 614-636.

Heaphy, Wilde, d., Jiao, Klein, Edil, Shi, Bettegowda, Rodriguez, Eberhart, Hebbar, Offerhaus, McLendon, Rasheed, He, Yan, Bigner, Oba-Shinjo, Kazue, Marie, Riggins et al. (2011) 'Altered telomeres in tumours with ATRX and DAXX mutations', *Science NIH public access* , vol. 333, no. 6041, July, pp. 1-4.

Henson, J.D., Cao, Y., Huschtscha, L.I., Chang, A.C., Au, A.Y.M., Pickett, H.A. and Reddel, R.R. (2009) 'DNA C-circels are specific and quantifiable markers of alternative-lengthening-of-telomeres activity', *Nature Biotechnology*, vol. 27, no. 12, December, pp. 1181-1186.

Henson, J., Neumann, A.A., Yeager, T.R. and Reddel, R.R. (2002) 'Alternative lengthening of telomeres in mammalian cells', *Oncogene*, vol. 21, no. 4, January, pp. 598-610.

Herbig, U., Jobling, W., Chen, B., Chen, D. and Sedivy, J. (2004) 'Telomere shortening triggers senescence of human cells through a pathway involving ATM, p53 and p21 but not p16INK4a', *Molecular Cell*, vol. 14, no. 4, May, pp. 501-513.

Huang, X., Wang, J., Liu, J., Feng, H., Liu, W., Yan, Q., Liu, Y., Sun, S., Deng, M., Gong, L., Y, L. and Li, D. (2005) 'hTERT extends proliferative lifespan and prevents oxidative stress-induced apoptosis in human lens epithelial cells', *Invest Ophthalmol Vis Sci*, vol. 46, no. 7, July, pp. 2503-2513.

Huen, M.S. and Chen, J. (2008) 'The DNA damage response pathways: at the crossroad of protein modifications', *Cell Research* , vol. 18, December, pp. 8-16.

ICRP, U.S.D.o.E. (2012) *Low Dose Radiation Research Program*, October, [Online], Available: http://lowdose.energy.gov/faqs.aspx#07.

Jackson, S.P. and Bartek, J. (2010) 'The DNA-damage response in human biology and disease', *Nature*, vol. 461, no. 7267, October, pp. 1071-1078.

Jacobs, J.J.L. (2013) 'Loss of telomere protection: consuquences and oppertunities', *Front Oncol*, vol. 3, no. 88, April, pp. 1-7.

Jegou, T., Chung, I., Heuvelman, G., Wachsmuth, M., Gorisch, S., Greulich-Bode, K., Boukamp, P., Lichter, P. and Rippe, K. (2009) 'Dynamics of telomeres and promyelocytic leukemia nuclear bodies in a telomerase-negative human cell line', *Molcular Biology of the cell*, vol. 20, no. 7, pp. 2070-2082.

Jeremy D Henson, A.A.N.T.R.Y.R.R.R. (2002) 'Alternative lengthening of telomeres in mammalian cells', *Oncogene*, vol. 21, pp. 598-610.

Jia, P., Chengtao, H. and Chai, W. (2015) 'DNA excision repair at telomeres', *DNA repair*, vol. 36, December, pp. 137-145.

Jiang, H., Ju, Z. and Rudolph, K. (2007) 'Telomere shortening and ageing', *Z Gerontol Geriatr*, vol. 40, no. 5, October, pp. 314-324.

Kadhim, M., Salomaa, S., Wright, E., Hildebrandt, G., Belyakov, O.V., Prise, K.M. and Little, M.P. (2013) 'Non-targeted effects of ionizing radiation–implications for low dose risk', *Mutation Research*, vol. 752, no. 1, July, pp. 84-98.

Karlseder, J., Broccoli, D., Dai, Y., Hardy, S. and de Lange, T. (1999) 'p53 and ATM-dependent apoptosis induced by telomeres lacking TRF2', *Science*, vol. 283, no. 5406, February, pp. 1321-1325.

Kickhoefer, V., Liu, Y., Kong, L., Snow, B., Stewart, P., Harrington, L. and Romea, L. (2001) 'The Telomerase/Vault-Associated Protein Tep1 Is Required for Vault RNA

Stability and Its Association with the Vault Particle', *Journal of Cell Biology*, vol. 152, no. 1, January, pp. 157-164.

Kilian, A., Bowtell, D., Abud, H., Hime, G., Venter, D., Keese, P., Duncan, E., Reddel, R. and Jefferson, R. (1997) 'Isolation of a candidate human telomerase catalytic subunit gene, which reveals complex splicing patterns in different cell types', *Human Mol Genetics*, vol. 6, no. 12, November, pp. 2011-2019.

Kim, N., Piatyszek, M., Prowse, K., Harley, C., West, M., Ho, P., Coviello, G., Wright, W., Weinrich, S. and Shay, J. (1994) 'Specific association of human telomerase activity with immortal cells and cancer.', *Science*, vol. 266, no. 5193, December, pp. 2011-2015.

Kimura, M., Stone, R.C., Hunt, S.C., Skurnick, J., Lu, X., Cao, X., Harley, C.B. and Aviv, A. (2010) 'Measurement of telomere length by the southern blot analysis of terminal restriction fragment lengths', *Nature protocols*, vol. 5, no. 9, September, pp. 1596-1607.

Kim, N.W. and Wu, F. (1997) 'Advances in quantification and charaterization of telomerase activity by the telomeric repeat amplification protocol (TRAP)', *Nucleic Acids Research*, vol. 25, no. 13, May, pp. 2595 - 2597.

Kleiman, N., David, J., Elliston, C., Hopkins, K., Smilenov, L., Brenner, D., Worgul, B., Hall, E. and Lieberman, H. (2007) 'Mrad9 and atm haploinsufficiency ehnace spontaneous and X-ray-induced catarctogenesis in mice', *Radiation Res*, vol. 168, no. 5, November, pp. 567-573.

Klein, B., Klein, R. and Lee, K. (1998) 'Incidence of age-related cataract: the Beaver Dam Eye Study', *Arch Opthalmology*, vol. 116, no. 2, pp. 219-225.

Knowles, M.S., Holton, E.F. and Swanson, R.A. (2005) *The Adult Learner: The definitive classic in adult education and human resource development*, Elsevier.

Kosar, M., Bartkova, J., Hubackova, S., Hodny, Z., Lukas, J. and Bartek, J. (2011) 'Senescence-associated heterochromatin foci are dispensable for cellular senescence, occur in a cell type- and insult-dependent manner and follow expression of p16(ink4a).', *Cell Cycle*, vol. 10, no. 3, February, pp. 457-468.

Krejci, L., Altmannova, V., Spirek, M. and Zhao, X. (2012) 'Homologous recombination and its regulation', *Nucleic Acids Research*, vol. 40, no. 13, July, pp. 5795-5818.

Kuilman, T., Michaloglou, C., Moor, W.J. and Peeper, D.S. (2010) 'The Essence of senescence', *Genes and Development*, vol. 24, pp. 2463-2479.

Kunkel, T.A. and Erie, D.A. (2005) 'DNA mismatch repair', *Biochemistry*, vol. 74, no. 10, July, pp. 681-71.

Kunze, S., Claudia, D., Helmut, F., Marrhias, K., Ute, R., Sabine, H., Maria, G., Oliver, P., Sibylle, S., Ulkrike, K., Hrabe de Angelis, M. and Graw, J. (2015) 'New mutation in the mouse xpd/ercc2 gene leads to recessive cataracts', *Plos One*, vol. 10, no. 5, May, pp. 1-16.

Le, O., Rodier, F., Fontaine, F., Coppe, J.-P., Campisi, J., DeGregori, J., Laverdiere, C., Kokta, V., Haddad, E. and Beausejour, C.M. (2010) 'Ionising radaition-induced long-term expression of senescencemarkers in mice is independent of p53 and immune status', *Ageing Cell*, vol. 9, no. 3, June, pp. 398-409.

Leteurte, F., Li, X., Gluckman, E. and Carosella, E. (1997) 'Telomerase activity during the cell cycle and in gamma-irradiated hematopoietic cells', *Leukemia*, vol. 11, no. 10, October, pp. 1681-1689.

Leteurtre, F., Li, X., Guardiola, P., Le Roux, G., Sergère, J., Richard, P., Carosella, E. and Gluckman, E. (1999) 'Accelerated telomere shortening and telomerase activation in Fanconi's anaemia', *Br J Haematol*, vol. 105, no. 4, June, pp. 883-893.

Levy, M., Allsopp, R., Futcher, A., Greider, C. and Harley, C. (1992) 'Telomere end-replication problem and cell aging', *Journal of Molecular Biology*, vol. 225, no. 4, June, pp. 951-960.

Lijima, K., Komatsu, K., Matsuura, S. and Tauchi, H. (2004) 'The Nigmegen breakage syndrome gene and its role in genome instability', *Chromosoma*, vol. 113, no. 2, September, pp. 53-61.

Liu, Y., Bryan, E., Snow, M., Hande, P., Baerlocher, G., Kickhoefer, V., Yeung, D., Wakeham, A., Itie, A., Siderovski, D., Lansdorp, P., Robinson, M. and Harrington, L. (2000) 'Telomerase-Associated Protein TEP1 Is Not Essential for Telomerase Activity or Telomere Length Maintenance In Vivo', *Molecular and Cellular Biology*, vol. 20, no. 21, November, pp. 8178-8184.

Li, H., Vogel, H., Holcomb, V.B., Gu, Y. and Hasty, P. (2007) 'Deletion of Ku70, Ku80 or both causes early aging without substantially increased cancer', *Molecular and cellular biology*, vol. 27, no. 23, December, pp. 8205-8214.

Lodish, H., Berk, A., Zipursky, S.L., Matsudaira, P., Baltimore, D. and Darnell, J. (2000) 'DNA Damage and Repair and Their Role in Carcinogenesis', in Freeman, W.H. (ed.) *Molecular Cell Biology*, 4th edition, New York: W H Freeman.

Longhese, M.P. (2008) 'DNA damage response at functional and dysfunctional telomeres', *Genes and Development*, vol. 22, pp. 125-140.

Loretta, L., Rebecca, D., Jeremy, H., Amy, A., Janice, R. and Roger, R. (2012) 'Detecton of alternative lengthening of telomeres by telomere quantitaitve PCR', *Nucleic Acids*, vol. 10, August, pp. 1-9.

Lornax, M.E., Folkes, L.K. and O'Neill, P. (2013) 'Biological Consequences of Radiation-induced DNA Damage: Relevance to Radiotherapy', *Clinical Oncology*, vol. 25, no. 10, October, pp. 578-585.

Lovejoy, Li, Reisenweber, Thongthip, Bruno, Lange, d., De, Petrini, Sung, Jasin, Rosenbluh, Zwang, Weir, Hatton, Ivanova, Macconaill, Hanna, Hahn, Lue, Reddel et al. (2012) 'Loss od ATRX, genome instability, and an altered DNA damage response are hallmarks of the alternative lengthening of telomeres pathway', *PLOS genetics*, vol. 8, no. 7, July, pp. 1-16.

Lundberg, A.S., Hahn, W.C., Gupta, P. and Weinberg, R.A. (2000) 'Genes involved in senescence and immortalization', *Current Opinion in Cell Biology*, vol. 12, no. 6, December, pp. 705-709.

Lundblad, V. (1997) 'The end replication problem: More than one solution', *Nature Medicine*, vol. 3, no. 11, pp. 1198-1199.

Lundblad, V. and Blackburn, E. (1993) 'An alternative pathway for yeast telomere maintenance rescues est1- senescence', *Cell*, vol. 73, no. 2, April, pp. 347-360.

Lydall, D. (2009) 'Taming the tiger by the tail: modulation of DNA damage responses by telomeres', *The Embo Journal*, vol. 28, July, pp. 2174-2187.

Maehara, K., Takahashi, K. and Saitoh, S. (2010) 'CENP-A reduction induces a p53-Dependent cellular senescence response to protect cells from executing defective

Makarov, V.L., Hirose, Y. and Langmore, J.P. (1997) 'Long G Tails at Both Ends of Human Chromosomes Suggest a C Strand Degradation Mechanism for Telomere Shortening', *Cell*, vol. 88, no. 5, pp. 657-666.

Ma, H.-M., Liu, W., Zhang, P. and Yuan, X.-Y. (2012) 'Human skin fibroblast telomeres are shortened after ultraviolet irradiation', *The journal of international medical research*, vol. 40, pp. 1871-1877.

Marteijn, J.A., Lans, H., Vermeulen, W. and Hoeijmakers, J.H.J. (2014) 'Understanding nucleotide excision repair and its roles in cancer and ageing', *Nature reviews molecular biology*, vol. 15, June, pp. 465-481.

Masutomi, K., Yu, E., Khurts, S., Ben-Porath, I., Currier, J., Metz, G., Brooks, M., Kaneko, S., Murakami, S., DeCaprio, J., Weinberg, R., Stewart, S. and Hahn, W. (2003) 'Telomerase maintains telomere structure in normal human cells.', *Cell*, vol. 114, no. 2, July, pp. 241-253.

McClintock, B. (1941) 'The stability of broken ends of chromosomes in Zea Mays', *Genetics*, vol. 26, March, pp. 234-282.

McEachern, M. and Haber, J. (2006) 'Break-induced replication and recombinational telomere elongation in yeast', *Annu Rev Biochem*, vol. 75, pp. 111-135.

McIlrath, J., Bouffler, S.D., Samper, E., Cuthbert, A., Wojcik, A., Szumiel, I., Bryant, P.E., Riches, A.C., Thompson, A., Blasco, M.A. and Slijepcevic, R.F.N.a.P. (2001) 'Telomere Length Abnormalities in Mammalian Radiosensitive Cells', *Cancer Research*, vol. 61, February, pp. 912-915.

Merriam, G.R. and Worgul, B. (1983) 'Experimental radiation cataract - its clinical relevance', *Acad Med*, vol. 59, no. 4, pp. 372-392.

Metcalfe, J., Parkhill, J., Campbell, L., Stacey, M., Biggs, P., Byrd, P. and Taylor, A. (1996) 'Accelerated telomere shortening in ataxia telangiectasia', *Nat Genet*, vol. 13, no. 3, July, pp. 350-353.

Meyerson, M., Counter, C.M., Eaton, E.N., Ellisen, L.W., Steiner, P., Caddie, S.D., Ziaugra, L., Beijersbergen, R.L., Davidoff, M.J., Liu, Q., Bacchetti, S., Haber, D.A. and Weinberg, R.A. (1997) 'hEST2, the putative human telomerase catalytic subunit gene is up-regulated in tumour cells and during immportalization', *Cell*, vol. 90, August, pp. 785-795.

Michael, R. and Bron, A. (2011) 'The ageing lens and cataracts: a model of normal and pathological ageing', *Philosophical transacyions of the royal society*, vol. 366, pp. 1278-1292.

Milanovic, D., Maier, P., Wenz, F. and Herskind, C. (2006) 'Changes in telomerase activity after irradiation of human peripheral blood mononuclear cells (PBMC) in vitro', *Radiation Protection Dosimetry*, vol. 122, no. 1-4, December, p. 173.

Mohamed, A.E. and Saad, M.E. (2011) 'Effect of infrared radaition on the lens', *Indian Journal of Ophthalmology*, vol. 59, no. 2, Mar-Apr, pp. 97-101.

Möller, P., Mayer, S., Mattfeldt, T., Müller, K., Wiegand, P. and Brüderlein, S. (2009) 'Sex-related differences in length and erosiion dynamics of human telomeres favour females', *Aging (Albany NY)*, vol. 1, no. 8, August, pp. 733-739.

Mondesert, O., Frongia, C., Clayton, O., Boizeau, M.-L., Lobjois, V. and Ducommun, B. (2015) 'Monitoring the Activation of the DNA Damage Response Pathway in a 3D Spheroid Model', *PLoS One*, vol. 10, no. 7, July.

Montanaro, L., Calienni, M., Ceccarelli, C., Santini, D., Taffurelli, M., Pileri, S., Treré, D. and Derenzini, M. (2008) 'Relationship between dyskerin expression and telomerase activity in human breast cancer', *Cell Oncology*, vol. 30, no. 6, pp. 483-490.

Moreau, K.L. and King, J.A. (2012) 'Protein misfolding and aggregation in cataract disease and prospects for prevention', *Trend Mol Med*, vol. 18, no. 5, May, pp. 273-282.

Morris, D., Fraser, S.G. and Gray, C. (2007) 'Cataract surgery and quality of life implications', *Clinical Interv Aging*, vol. 2, no. 1, March, pp. 105-108.

Moyzis, R.K., Buckingham, J.M., Cram, L.S., Dani, M., Deaven, L.L., Jones, M.D., Meyne, J., Ratliff, R.L. and Wu, J.R. (1988) 'A highly conserved repetitive DNA sequence, (TTAGGG)n, present at the telomeres of human chromosomes.', *Proceedings of the national academy of sciences of the united states of America*, vol. 85, no. 18, September, pp. 6622-6626.

Mughal, S.K., Myazin, A.E., Zhavoronkov, L.P., Rubanovich, A.V. and Dubrova, Y.E. (2012) 'The dose and dose-rate effects of paternal irradiation on transgenerational instability in mice: a radiotherapy connection', *Plos One*, vol. 7, no. 7, July, pp. 1-5.

Muller, H.J. (1938) 'The remaking of chromosomes', *The collecting net*, vol. 13, no. 117, September, pp. 181-195.

Murnane, J., Sabatier, L., Marder, B. and Morgan, W. (1994) 'Telomere dynamics in an immortal human cell line', *EMBO Journal*, vol. 13, no. 20, October, pp. 4953-4963.

Natarajan, E., Saeb, M., Crum, C., Woo, S., McKee, P. and Rheinwald, J. (2003) 'Co-Expression of p16INK4a and Laminin 5 gamma2 by microinvasive and superficial squamous cell carcinomas in vivo and by migrating wound and senescent keratinocytes in culture', *American journal od pathology*, vol. 163, no. 2, August, pp. 477-491.

Nelson, D.L. and Cox, M.M. (2004) 'Lehninger Principles of Biochemistry', in Nelson David L, C.M.M. *Principles of Biochemistry*, 4th edition, Freeman.

Neumann, A., Watson, C., Noble, J., Pickett, H., Tam, P. and Reddel, R. (2013) 'Alternative lengthening of terlomeres in normal mammalian somatic cells', *Genes and Development*, vol. 27, pp. 18-23.

Ning, Y., Xu, J.-f., Li, Y., Chavez, L., Riethman, H.C., Lansdorp, P.M. and Weng, N.-p. (2003) 'Telomere length and the expression of natural telomeric genes in human fibroblasts', *Human Molecular Genetics*, vol. 12, no. 11, pp. 1329-1336.

Noordzij JG, V.N.v.d.B.M.v.V.L.d.B.-V.S.W.W.V.J.W.C.d.G.R.Z.M.v.G.D.v.D.J. (2003) 'Radiosensitive SCID patients with Artemis gene mutations show a complete B-cell differentiation arrest at the pre-B-cell receptor checkpoint in bone marrow.', *Blood*, vol. 101, no. 4, February, pp. 1446-1452.

O'Callaghan, N.J. and Fenech, M. (2011) 'A quantitative PCR method for measuring absolute telomere length', *Biological Procedures Online*, vol. 13, no. 3.

Oeseburg, H., de Boer, R., van Gilst, W. and van der Harst, P. (2010) 'Telomere biology in healthy aging and disease', *Pflugers Arch*, vol. 459, no. 2, January, pp. 259-268.

Olovnikov, A.M. (1973) 'A theory of marginotomy: The incomplete copying of template margin in enzymic synthesis of polynucleotides and biological significance of the phenomenon', *Jornal of Theoretical Biology*, vol. 41, no. 1, September, pp. 181-190.

Organisation, W.H. (2016) *World Health Organisation*, [Online], Available: http://www.who.int/blindness/causes/en/ [2016].

O'Sullivan, R.J. and Karlseder, J. (2010) 'Telomeres: Protecting chromosomes against genome instability', *Nature Reviews Molecular Cells Biology*, vol. 11, March, pp. 171-181.

Ouellette, M.M., Liao, M., Herbert, B.-S., Johnson, M., Holt, S.E., Liss, H.S., Shay, J.W. and Wright, W.E. (2000) 'Subsenescent Telomere Lengths in Fibroblasts Immortalized by Limiting Amounts of Telomerase', *The journal of biological chemistry*, vol. 276, no. 14, April, pp. 10072-10076.

Padma, G., Mamata, M., Reddy, K., Ravi, K. and Padma, T. (2011) 'Polymorphisms in two DNA repair genes (XPD and XRCC1) - association with age related cataracts', *Molecular vision biology and genetics in vision research*, vol. 17, January, pp. 127-133.

Park, J., Kim, B., Han, Y. and Park, I. (2002) 'The effect of telomerase expression on the escape from M2 crisis in virus-transformed human retinal pigment epthelial cells', *Exp Mol Med*, vol. 34, no. 2, May, pp. 107-113.

Pastwa, E. and Blasiak, J. (2003) 'Non-Homologous DNA end joining', *Acta Biochimica Polonica*, vol. 50, no. 4, December, pp. 891-908.

Perrem, K., Colgin, L.M., Neumann, A.A., Yeager, T.R. and Reddel, R.R. (2001) 'Coexistence of Alternative lengthening of telomeres and telomerase in hTERT-tranfected GM847 cells', *Molecular and Cellular Biology*, vol. 21, no. 12, pp. 3862-3875.

PHE, (.H.E. (2010) *Radiation Protection Services*, [Online], Available: https://www.phe-protectionservices.org.uk/radiationandyou/; https://www.phe-protectionservices.org.uk/cms/assets/gfx/content/resource_3595csc0e8517b1f.pdf.

Pisano, S., Galati, A. and Cacchione, S. (2008) 'Telomeric nucleosomes: Forgotten players at chromosome ends', *Cellular and Molecular Life Sciences*, vol. 65, pp. 3553-3563.

Pittler, S. and Baehr, W. (1991) 'Identification of a nonsense mutation in the rod photorecepter cGMP phosphodiesterase beta-subunit gene of the rd mouse', *Proceedings of the national academy of sciences of the united states of America*, vol. 88, no. 19, October, pp. 8322-8326.

Radiation, e.r.f. (2007) *Radiation effects research foundation*, [Online], Available: http://www.rerf.jp/radefx/basickno_e/radcell.htm.

Radiation, P. (2012) *Radiation Protection - Australian Governemnt - Australian Radiation Protection and Nuclear Safety Agency*, 13 January, [Online], Available: http://www.arpansa.gov.au/radiationprotection/basics/ion_nonion.cfm.

Rai, R. and Chang, S. (2011) *Probing the Telomerase Damage Response*, 735th edition, Spinger Science+Business Media.

Raymund J Wellinger, K.E.P.L.V.A.Z. (1996) 'Evidence for a new step in telomere maintenance', *Cell*, vol. 85, pp. 423-433.

Ray, A. and Norden, B. (2000) 'Peptide nucleic acid (PNA): its medical and biotechnical applications and promise for the future', *The FASEB journal*, vol. 14, no. 9, June, pp. 1041-1060.

Reste, J., Zvigule, G., Zvagule, T., Kurjabe, N., Eglite, M., Gabruseva, N., Berzina, D., Plonis, J. and Miklasevics, E. (2014) 'Telomere length in Chernobyl accident receovery workers in the late period after the disaster', *Journal of Radiation Research*, vol. 55, June, pp. 1089-1100.

Riballo, E., Kohne, M., Rief, N., Doherty, A., Smith, G., Reico, M., Reis, C., Dahm, K., Fricke, A., Krempler, A., Parker, A., Jackson, S., Gennery, A., Jeggo, P. and Lobrich, M. (2004) 'A pathway of doublestrandbreak rejoining dependent upon ATM, Artemis, and proteins locating togamma-H2AX Foci', *Cell*, vol. 16, December, pp. 715-724.

Ribes-Zamora, A., Indiviglio, S.M., Mihalek, I., Williams, C.L. and Bertuch, A.A. (2013) 'TRF2 interactions with Ku heterotetramerization interface gives indight into c-NHEJ prevention at human telomeres', *Cell Rep*, vol. 5, no. 1, October, pp. 194-206.

Rodier, F. and Campisi, J. (2011) 'Four faces of cellular senescence', *JCB*, vol. 192, no. 4, February, pp. 547-556.

Rogakou, E.P., Pilch, D.R., Orr, A.H., Ivanova, V.S. and Bonner, W.M. (1998) 'DNA Double-stranded Breaks Induce Histone H2AX Phosphorylation on Serine 139', *The journal of Biological Chemistry*, vol. 273, no. 10, March, pp. 5858-5868.

Rubtsova, M.P., Vasilkova, D.P., Malyavko, A.N., Naraikina, Y.V., Zvereva, M.I. and Dontsova, O.A. (2012) 'Telomere Lengthening and other functions of Telomerase', *Acta Nature*, vol. 4, no. 2, April, pp. 44-61.

Rufer, N., Dragowska, W., Thornbury, G., Roosnek, E. and Lansdorp, P.M. (1998) 'Telomere length dynamics in human lymphocyte subpopulations measured by flow cytometry', *Nature Biotechnology*, vol. 16, no. 8, August, pp. 743-747.

Samassekou, Gadji, Drouin and Yan (2010) 'Sizing the ends: normal length of human telomeres', *Ann Anat*, vol. 192, no. 5, September, pp. 248-291.

Sampada, K. and Diego, L. (2014) 'Shelterin complex in telomere protection: recent insights and pathological significance', *Cell Health and Cytoskeleton*, vol. 6, September, pp. 11-26.

Samper, E., Goytisolo, F., Slijepcevic, P., van Buul, P. and Blasco, M. (2000) 'Mammalian Ku86 protein prevents telomeric fusions independently of the length of TTAGGG repeats and the G-strand overhang', *EMBO Rep*, vol. 1, no. 3, September, pp. 244 -252.

Sancar, A. and Tang, M.-S. (1993) 'Nucleotide Excision Repair', *Photochemistry and Photobiology*, vol. 57, no. 5, May, pp. 905-921.

Sanders, J.L., Iannaccone, A., Boudreau, R.M., Conley, Y.P., Opresko, P.L., Hsueh, W.-C., Cummings, S.R., Cawthon, R.M., Harris, T.B., Nalls, M.A., Kritchevsky, S.B. and Newman, A.B. (2011) 'The association of Cataracts with Leukocyte Telomere length in older adults: Defining a New Marker of Aging', *J Gerontol A Biol Sci Med Sci*, vol. 66A, no. 6, June, pp. 639-645.

Sansare, K., Khanna, V. and Karjodkar, F. (2011) 'Early victims of x-rays: a tribute and current perception', *Journal of head and neck imaging*, vol. 40, no. 2, February, pp. 123-125.

Sedic, M., Skibinski, A., Brown, N., Gallardo, M., Mulligan, P., Martinez, P., Keller, P.J., Glover, E., Richardson, A.L., Cowan, J., Toland, A.E., Ravichandran, K., Riethman, H., Naber, S.P., Naar, A.M., Blasco, M.A., Hinds, P.W. and Kuperwasser, C. (2015) 'Haploinsufficiency for BRCA1 leads to cell-type specific genomic instability and premature senescence', *Nature Communications*, vol. 6, no. 7505, pp. DOI: 10.1038/ncomms8505.

Sekiguchi, J.M. and Ferguson, D.O. (2006) 'DNA Double-Strand Break Repair: A Relentless Hunt Uncovers New Prey', *Cell*, vol. 124, January, pp. 260-262.

Shammas, M.A. (2011) 'Telomeres, lifestyle, cancer and aging', *Curre Opin Nutr Metab Care*, vol. 14, no. 1, January, pp. 28-34.

Shay, J. and Wright, W.E. (2004) 'Telomeres in dyskeratosis congenita', *Nature Genetics*, vol. 36, pp. 437-438.

Shay, J.W. and Wright, W.E. (2005) 'Senescence and immortalization: role of telomeres and telomerase', *Carcinogenesis*, vol. 26, no. 5, October, pp. 867-874.

Shay, J.W. and Wright, W.E. (2011) 'Role of telomeres and telomerase in cancer', *Semin Cancer Biology*, vol. 21, no. 6, December, pp. 349-353.

Shen, Gammon, Wu, Terry, Wang, Bradshaw, Teitelbaum, Neugut and Santella. (2010) 'Multiple genetic variants in telomere pathway genes and breast cancer risk', *Cancer Epidemiol Biomarkers Prev*, vol. 19, no. 1, January, pp. 219-228.

Shigematsu, I. (2013) *The effects of A-Bomb radaition on the human body*, 2nd edition, Bunkodo Co., Ltd.

Shiloh, Y. (2003) 'ATM and related protein kinases: Safeguarding genome integrity', *Nat Rev Cancer*, vol. 3, no. 3, March, pp. 155-168.

Skvortsov, D., Zvereva, M., Shpanchenko, O. and Dontsova, O. (2011) 'Assays for detection of telomerase activity', *ActaNature*, vol. 3, no. 1, March, pp. 48-68.

Slijepcevic, P. (2001) 'Telomere length measurement by Q-FISH', *Methods in cell science*, vol. 23, pp. 17-22.

Slijepcevic, P. (2006) 'The role of DNA damage response proteins at telomeres - an "integrative" model', *DNA Repair - Elsevier*, vol. 5, no. 11, November, pp. 1300-1304.

Slijepcevic, P. (2007) 'DNA damage response, telomere maintenance and ageing in light of the integratice model', *Mechanisms of Ageing*, vol. 129, November, pp. 11-16.

Slobodan, R. and Peter, G.F. (2012) 'Summary of Information on the Effects of Ionizing and Non-ionizing Radiation on Cytochrome P450 and Other Drug Metabolizing Enzymes and Transporters', *Curr Drug Metab*, vol. 13, no. 6, July, pp. 787-814.

Smogorzewska, A., Karlseder, J., Holtgreve-Grez, H., Jauch, A. and de Lange, T. (2002) 'DNA ligase IV-dependent NHEJ of deportected mammalian telomeres in G1 and G2', *Current Biology*, vol. 12, October, pp. 1635-1644.

Speicher, M.R. and Carter, N.P. (2005) 'The new cytogenetics: Blurring the boundaries with molecular biology', *Nature* , vol. 6, October, pp. 782-792.

Spivak, G. (2015) 'Nucleotide Excision Repair in humans', *DNA repair*, vol. 36, December, pp. 13-18.

Sputova, K., Garbe, J., Pelissier, F., Chang, E., Stampfer, M. and LaBarge, M. (2013) 'Aging phenotypes in cultured normal human mammary epithelial cells are correlated with decreased telomerase activity independent of telomere length', *Genome Integrity*, vol. 4, no. 4, pp. 1-8.

Stout, G. and Blasco, M. (2013) 'Telomere length and telomerase activity impact the UV sensitivity syndrome xeroderma pigmentosum C', *Cancer Res*, vol. 73, no. 6, March, pp. 1844-1854.

Subba, R.K. (2007) 'Mechanisms of Disease: DNA repair defects and neurological disease', *Nature clinical practice neurology*, vol. 3, January, pp. 162-172.

Sung, P. and Klein, H. (2006) 'Mechanism of homologous recombination: mediators and helicases take on regulatory functions.', *Nat Rev Mol Cell Biolo*, vol. 7, no. 10, Oct, pp. 739-750.

Sway, S. (2010) *Digital Imaging Systems Ltd*, April, [Online], Available: http://www.digitalimagingsystems.co.uk/software/iplab.html.

Takai, H., Smogorzewska, A. and de Lange, T. (2003) 'DNA Damage Foci at Dysfunctional Telomeres', *Current Biology*, vol. 13, September, pp. 1549-1556.

Takata, M., Sasaki, M.S., Sonoda, E., Morrison, C., Hashimoto, M., Utsumi, H., Yamaguchi-Iwai, Y., Shinohara, A. and Takeda, S. (1998) 'Homologous

recombination and non-homologous end-joining pathways of DNA double-strand break repair have overlapping roles in the maintenance of chromosomal integrity in vertebrate cells.', *The Embo Journal*, vol. 17, no. 18, September, pp. 5497-5508.

Taylor, A. (2013) 'Report of the independent Advisory Group on Ionising Radiation', March, p. 164, Available: http://www.hpa.org.uk/webc/HPAwebFile/HPAweb_C/1317138381573.

Thomas, D., Yang, H., Alexander, K. and Hinds, P. (2003) 'Role of the retinoblastoma protein in differentiation and senescence', *Cancer Biol Ther*, vol. 2, no. 2, Mar, pp. 124-130.

Tommerup, H., Dousmanis, A. and de Lange, T. (1994) 'Unusual chromatin in human telomeres', *Mol Cell Bio*, vol. 14, no. 9, September, pp. 5777-5785.

Tzanetakou, I.P., Katsilambros, N.L., Benetos, A., Mikhaillidis, D.P. and Perrea, D.N. (2011) '"Is Obesity linked to aging?" Adipose tissue and the role of telomeres', *Ageing Research Reviews*, vol. 11, no. 2, April, pp. 220-229.

van Steensel, B. and de Lange, T. (1997) 'Control of telomere length by the human telomeric protein TRF1', *Nature*, vol. 385, no. 6618, February, pp. 740-743.

van Steensel, B., Smogorzewska, A. and de Lange, T. (1998) 'TRF2 protects human telomeres from end-to-end fusions', *Cell*, vol. 92, no. 3, February, pp. 401-413.

Venteicher, A.S., Zhaojing, M., Mason, P.J., Veenstra, T.D. and Artandi, S.E. (2008) 'Identification of ATPases pontin and reptin as telomerase components essential for holoenzyme assembly', *Cell*, vol. 132, no. 6, March, pp. 945-957.

Verdun, R.E. and Karlseder, J. (2007) 'Replication and protection of telomeres', *Nature*, vol. 447, Jun, pp. 924 -931.

Virmouni, S.A., Al-Mahdawi, S., Sandi, C., Yasaei, H., Giunti, P., Slijepcevic, P. and Pook, M. (2015) 'Identification of telomere dysfunction in Friedreich ataxia', *Molecular Neurodegeneration*, vol. 10, no. 1, June, pp. 2-11.

Volpi, E.V. and Bridger, J.M. (2008) 'FISH glossary: an overview of the fluorescence in situ hybridisation technique. ', *Biotechniques*, vol. 45, October, pp. 385-409.

Ward, J. (2000) 'Complexity of damage produced by ionising radiation', *Cold Spring Harb Symp Quant Biol*, vol. 65, pp. 377-382.

Watson, J.D. (1972) 'Origin of Concatemeric T7DNA', *Nature*, vol. 239, October, pp. 197-201.

Wege, H., Chui, M.S., le, H.T., Tran, J.M. and Zern, M.A. (2003) 'SYBR Green real-time telomeric repeat amplification protocol for the rapid quantification of telomerase activity', *Nucleic Acids Research*, vol. 31, no. 2.

Worgul BV, K.Y.S.N.C.V.V.P.M.C.B.E.J.A.K.O.M.N.S.S.V.O.X.S.X.X.S.R. (2007) 'Cataracts among Chernobyl clean-up workers: implications regarding permissible eye exposures', *Radiation Research*, vol. 167, no. 2, Febraury, pp. 233-243.

Wright, D.L., Jones, E.L., Mayer, J.F., Ochninger, S., Gibbons, W.E. and Lanzendorf, S.E. (2001) 'Characterization of telomerase activity in the human oocyte and preimplantation embryo', *Molecular Human Reproduction*, vol. 7, no. 10, pp. 947-955.

Wright, W., Piatyszek, M., Rainey, W., Byrd, W. and Shay, J. (1996) 'Telomerase activity in human germline and embryonic tissues and cells.', *Dev Genet*, vol. 18, no. 2, pp. 173-189.

Yasaei Hemad, S.P. (2010) 'Defective Artemis causes mild telomere dysfunction', *Genome integrity*, vol. 1, no. 3, May, pp. 1-12.

Yeager, T.R., Neumann, A.A., Englezou, A., Huschtcha, L.I., Noble, J.R. and Reddel, R.R. (1999) 'Telomerase-negative immortalized human cells contain a novel type of Promyelocytic Leukemia (PML) Body', *Cancer Research*, vol. 59, September, pp. 4175-4179.

Yuri E Dubrova, M.P.B.G.E.B.A.J.J. (2000) 'Genome stability: Transgenerational mutation by radiation ', *Nature*, vol. 405, no. 37, May.

Zeng, X. and Rao, M.S. (2007) 'Human embryonic stem cells: Long term stability, absence of senescence and a potential cell sourse for neural replacement', *Neuroscience*, vol. 145, no. 4, April, pp. 1348-1358.

Zhu, X.-D., Niedernhofer, L., Kuster, B., Mann, M., Hoeijmakers, J.H.J. and de Lange, T. (2003) 'ERCCA/XPF removes the 3' overhang from uncapped telomeres and represses formation of telomeric DNA-containing double minute chromosomes', *Molecular Cell*, vol. 12, December, pp. 1489-1498.

Zijlmans, J.M.J.M., Martens, U.M., Poon, S.S.S., Raap, A.K., Tanke, H.J., Ward, R.K. and Lansdorp, P.M. (1997) 'Telomere in the mouse have large inter-chromosomal variations in the number of T2AG3 repeats', *Proceedings of the National Academy of Sciences of the United States of America*, vol. 94, no. 14, July, pp. 7423-7428.